Czech Technical University in Prague
Faculty of Nuclear Sciences and Physical Engineering

DISSERTATION

Erbium-doped diode-pumped solid-state lasers generating in mid-infrared spectral range

Prague 2020 Richard Švejkar

Bibliografický záznam

Autor:	Ing. Richard Švejkar
	České vysoké učení technické v Praze
	Fakulta jaderná a fyzikálně inženýrská
	Katedra fyzikální elektroniky

Název práce:	Erbiem dopované diodově čerpané pevnolátkové lasery generující ve střední infračervené oblasti
Studijní program:	Aplikace přírodních věd
Studijní obor:	Fyzikální inženýrství

Školitel:	Ing. Jan Šulc, Ph.D.
Školitel specialista:	prof. Ing. Helena Jelínková, DrSc.
	České vysoké učení technické v Praze
	Fakulta jaderná a fyzikálně inženýrská
	Katedra fyzikální elektroniky

Akademický rok:	2020/2021
Počet stran:	79 + 54 (Apendix)
Klíčová slova:	Erbium, pevnolátkové lasery, střední infračervená oblast, diodové čerpání

Bibliographic Entry

Author:	Ing. Richard Švejkar
	Czech Technical University in Prague
	Faculty of Nuclear Sciences and Physical Engineering
	Department of Physical Electronic

Title of Dissertation:	Erbium-doped diode-pumped solid-state lasers generating in mid-infrared spectral range
Degree Programme:	Application of Natural Sciences
Field of Study:	Physical Engineering

Supervisor:	Ing. Jan Šulc, Ph.D.
Supervisor specialist:	prof. Ing. Helena Jelínková, DrSc.
	Czech Technical University in Prague
	Faculty of Nuclear Sciences and Physical Engineering
	Department of Physical Electronic

Academic Year:	2020/2021
Number of Pages:	79 + 54 (Appendix)
Keywords:	Erbium, solid-state lasers, mid-infrared lasers, diode-pumped

Abstract

Lasers based on erbium ions using the transition $^4I_{11/2} \rightarrow {}^4I_{13/2}$ allow a generation of laser radiation in the spectral range from 2.7 µm to 3 µm. Since at the 3 µm the strong absorption peak of water is located, there is an effort to develop a suitable laser source for various medical applications, e.g., dentistry, dermatology, urology, and surgery. This wavelength range can be also used in spectroscopy or as pumping sources for optical parametric oscillators as well as for excitation of new active materials emitting radiation deeper in mid-infrared spectral range.

Goal of this thesis is research of erbium doped active media (e.g., Er:YAG, Er:YAP, Er:GGG, Er:SrF_2, Er:YLF, Er:Y_2O_3, Er:KYW, etc.) for laser generation in spectral range 2.7 - 3 µm. Study can be divided into two parts, the former is dedicated to Er^{3+}-doped active media, the latter contains a summary of results and published papers related to the topic of PhD thesis.

Abstrakt

Lasery využívající ionty erbia dovolují, díky přechodu mezi energetickými hladinami $^4I_{11/2} \rightarrow {}^4I_{13/2}$, generovat laserové záření s vlnovou délkou v rozmezí 2,7 až 3 µm. Jelikož na vlnové délce 3 µm je silná absorpce ve vodě, která je obsažena v biologických tkáních, je snahou vyvinout vhodné laserové systémy pro aplikace, např.: v medicíně – stomatologii, dermatologii, urologii, a obecné chirurgii. Mimo jiné mohou být tyto vlnové délky využity ve spektroskopii nebo jako čerpací zdroje pro optické parametrické zesilovače a k buzení nových aktivních materiálů generujících záření hlouběji ve střední infračervené oblasti elektromagnetického spektra.

Cílem této práce je výzkum erbiem dopovaných aktivní prostředí (Er:YAG, Er:YAP, Er:GGG, Er:SrF_2, Er:YLF, Er:Y_2O_3, Er:KYW, etc.) pro generaci záření v oblasti vlnových délek 2,7 – 3 µm. Celá práce může být rozdělena do dvou částí, první je věnována Er^{3+}-dopovaným aktivním prostředím, druhá pak shrnuje výsledky a publikace vztahující se k tématu PhD práce.

Acknowledgement

I would like to express my special thanks of gratitude to Ing. Jan Šulc, Ph.D. for supervising this thesis and for providing guidance, support, and invaluable advice during my PhD study. Furthermore, I would like to thanks to prof. Ing. Helena Jelínková, DrSc. for consistent support during my research. I cannot forget to thank my family and friends for the unconditional support during my way to the PhD degree.

Richard Švejkar

The research was supported by the following grants:

- The Czech Technical University Grant No. SGS16/247/OHK4/3T/14.
- The Czech Technical University Grant No. SGS19/191/OHK4/3T/14.
- The Czech Science Foundation, *Temperature influence on spectral and lasing characteristics of solid-state materials covering spectral range from visible up to mid-infrared*, project, No. 15-05360S.
- The Czech Science Foundation, *Optimization of the solid-state laser active materials for spectral range from near-up to mid-infrared*, project, No.18-11954S.
- "Center of Advanced Applied Sciences", Reg. No. CZ.02.1.01/0.0/0.0/16_019/0000778, supported by the Operational Program Research, Development and Education, co-financed by the European Structural and Investment Funds and the state budget of the Czech Republic.

Declaration

I hereby declare that the thesis has been composed by myself and that the work has not been submitted for any other professional qualification. I confirm that the work submitted is my own, except where the work which has formed part of jointly authored publications has been included. My contributions to this work has been explicitly indicated below.

Prague, 28.10.2020 Richard Švejkar

"If you ask naive but relevant questions, then almost immediately the person doesn't know the answer, if he is an honest man."

Richard P. Feynman

Contents

1 Introduction

Sixty years have now passed since the invention of the first laser. It was based on ruby crystal and emitted laser radiation at 694.3 nm. Nowadays, there are various types of lasers able to generate radiation in the extremely diverse spectral range from T-rays ($\sim 5{\cdot}10^{12}$ Hz) to X-rays ($\sim 5{\cdot}10^{17}$ Hz). However, still, there is a desire to generate new wavelengths to fill the empty space in a wide spectral range or create sources of laser radiation for a particular application where, up to now, they are not solid-state laser sources. The mid-infrared (2.5 - 8 µm) spectral range is interesting and significant especially for spectroscopy (remote sensing of gases, environmental monitoring, meteorology), medicine, polymer processing, or military applications (countermeasures, rangefinders, target pointing). [1–4]

Lasers emitting in the first part of the mid-infrared spectrum (from 2.5 to 3 µm) are primarily interesting for various branches of medicine (dermatology, surgery, dentistry, ophthalmology, urology); also, they can be used as a pumping source for further wavelength conversion. To generate laser radiation in this spectral range, an optical parametric oscillators (OPO) or material based on Cr:ZnSe or Cr:ZnS pumped with Tm-fibre lasers can be used; nevertheless, these systems are complex and expensive [3]. At present, there are many coherent diode-pumped Er-doped laser active media, e.g., Er:YAG, Er:YLF, Er:CaF_2, Er:Y_2O_3, etc., for generating laser radiation in the spectral range 2.65 – 3 µm. Today, erbium is a well-known element from the lanthanide series used as an activator in various laser active media. Due to the structure of energetic levels, erbium-doped active media offer a laser transition in several spectral ranges.

Two best-known erbium laser wavelengths, i.e., $\sim$ 1.6 µm and $\sim$ 3 µm, correspond to laser transitions $^4I_{13/2} \rightarrow {}^4I_{15/2}$ and $^4I_{11/2} \rightarrow {}^4I_{13/2}$, respectively. Using direct (in-band, resonant) pumping of the laser level $^4I_{13/2}$, it is possible to generate laser radiation at 1.6 µm with high output power and slope efficiency up to 80 % [5,6]. Since this wavelength is known as "eye-safe" because $\sim$ 1.6 µm does not penetrate the eye, it can be used for rangefinders, free-spectral communication, radar, or other applications where the laser beam can collide with the human eyes [2, 7]. Moreover, this laser radiation can be used

in telecommunication for pure optical amplification of the transmitted signal in EDFA (erbium doped fibre amplifier) [2]. On the other hand, to obtain laser radiation at ~ 3 µm wavelength with the high enough slope efficiency, the pumping wavelength ~ 970 nm has to be used; nevertheless, the slope efficiency is limited by the quantum defect to a theoretical value of ~ 35 %. The latest published papers [8, 9] show that it is possible to get close to the quantum limit. Another alternative are ZBLAN fibres which allow to exceed the theoretical limit of the slope efficiency. At 2.8 µm, the maximal slope efficiency 40 % was obtained and presented in [10]. From the point of view of the spectroscopy, another interesting laser wavelength in mid-infrared spectral range is ~ 3.5 µm ($^4F_{9/2} \rightarrow {}^4I_{9/2}$). It was shown that Er:YLF crystals can generate laser radiation at 3.41 µm; however, only a few papers deal with this issue, e.g. [11]. It is also possible to generate laser emission in the visible spectral range, particularly at 551 nm [12]. Erbium doped active media can also generate radiation at 1.7 µm if the transition $^4F_{9/2} \rightarrow {}^4I_{9/2}$ is used [13]. Nevertheless, to obtain this laser wavelength from a diode-pumped laser system, a special shape of laser resonator and pumping has to be used [13]. One can see that erbium-doped active media offers many interesting laser wavelengths which can be used in various branches of research and industry. From this point of view, I believe that a further research of such active media doped with erbium ions and laser systems designed with them is important. [3, 14]

This PhD study is divided into several sections. Starting with the introduction (section 1), the second chapter (section 2) concerns itself with state of the art of erbium-doped matrices for laser generation in the spectral range 2.5 - 3 µm. In essence, the whole section 2 is based on a summarizing paper published in Progress in Quantum Electronics [RS1][1]. The summary of the thesis goals is presented in section 3. In the next part of thesis, the measurement methods (section 4) and an overview of published papers (sections 5 and 6) can be found. Finally, the summary of the reached results and contribution to progress of science are presented in conclusion (section 7); also the bibliography list and appendix with several applicant's publications are enclosed.

[1]The abbreviation RS (Richard Švejkar) refers to the author's publications related PhD thesis.

2 State of the art

Diode-pumped 3-µm Er-based lasers

For the first time, the name "erbium" was used in 1842 by C. Mosander after separation of yttrium into three fractions - terbium, erbium, and yttrium. Nevertheless, pure metal erbium was produced in 1934 by Klemm and Bommer who reduced the anhydrous chloride with potassium vapour. Nowadays, ion-exchange reactions are used to produce pure metal erbium at a reasonable price ($20/g) [15]. The pure metal is soft and malleable with silver colour; beside other erbium can be used as an activator in laser active media [15].

Erbium (Er^{3+}) ion is one of the rare-earth ions of the lanthanide series, so it has electron configuration $[Xe]4f^{N-1}5s^25p^6$, where N is equal to 12. Thus, the *4f* shell contains 11 electrons shielded by fully occupied subshells *5s5p* [16]. Therefore, the spectral lines are narrower in comparison with the transition metal ions [7]. It follows from the quantum theory that the ground state of the Er^{3+} ion is $^4I_{15/2}$ which is also the terminal level for several possible laser transitions. In Figure 1 one can see the feasible laser transition between energy levels of the erbium ion. From the point of view of laser action, the two most interesting erbium laser wavelengths are $\sim 1.6\,\mu m$ and $\sim 2.9\,\mu m$. The radiation from the spectral range 1.6 µm is so-called "eye-safe" laser radiation because this wavelength does not reach the retina since it is being absorbed in the frontal part of the eye. For this reason, radiation with 1.6 µm wavelength finds use in LIDARs, rangefinders, or free-space communication. The latter wavelength range around 2.9 µm is very close to the absorption maximum of water at $\sim 3\,\mu m$, thus it is interesting for medical applications, e.g., surgery, dentistry, dermatology, urology, etc. Besides above mentioned wavelengths, it is possible to generate laser radiation in other parts of the spectrum, i.e., $\sim 0.55\,\mu m$, $\sim 0.85\,\mu m$, $\sim 1.3\,\mu m$, $\sim 1.7\,\mu m$, $\sim 3.5\,\mu m$ [11, 16–18]. Laser emission in erbium-doped active media is strongly affected by the typical and important phenomenon – the up-conversion processes. These can cause depopulation of lower laser level and subsequently decrease the laser efficiency for $\sim$ 3 µm laser emission [2, 7, 16]. This phenomenon will be discussed in detail in section 2.1.

The possible generated laser wavelength depends, besides others, e.g., optical resonator and pumping wavelength, on the concentration of erbium ions. In the first assumption, it was supposed that for generation ∼3 µm radiation the matrix has to be heavy doped with erbium [7] to allow fast quenching of the lower laser level $^4I_{13/2}$. It was shown that even if the concentration is low, the laser emission at mid-infrared range is possible [14, 19]. The first active medium using low concentration of Er^{3+} ions (∼ 5 %) was based on fluorides [20]; now it is possible to use doping concentration 1 % and even lower; however, for such low doping cryogenic cooling has to be used [14]. Even if the cryogenic temperatures allow to obtain lasing with low erbium-doped active media, the whole cryogenic systems made laser system complex and hard to operates. On the other hand, a high doping concentration of active ion affects thermal conductivity and homogeneity of grown crystal [2,7]. This will be in detail discussed in text below, see section 2.1 and 2.2.

2.1 Up-conversion, self-termination, and quenching

The main known problems linked with Er^{3+} ions are relatively complicated up-conversion processes (energy transfer, cross-relaxation $^4I_{15/2} \rightarrow {}^4I_{13/2}+{}^4S_{3/2}+{}^4I_{9/2}$, excited state absorption), self-termination, and fluorescence quenching; all affecting the slope efficiency, the output power, and the threshold of 3 µm laser emission [2, 7, 21–23]. These three processes depend strongly on a combination of the level doping concentration of erbium and type of matrix [21].

If the Er^{3+} ions are doped into low phonon matrix, the probability of non-radiative transition is reduced and the fluorescence decay time at the upper laser level $^4I_{11/2}$ is prolonged. This fact results in a low probability of the self-termination effect typical for the situation when the upper laser level possesses significantly shorter fluorescence decay time compared with the lower laser level. Furthermore, the matrix determines the probability of a cluster forming. In SrF_2 and CaF_2 crystals, for example, the clusters are formed at a concentration of 3 - 7 % of Er^{3+}. Thus, the distance between erbium ions in the active medium could be shorter, which could be a benefit to ion-ion energy transfer.

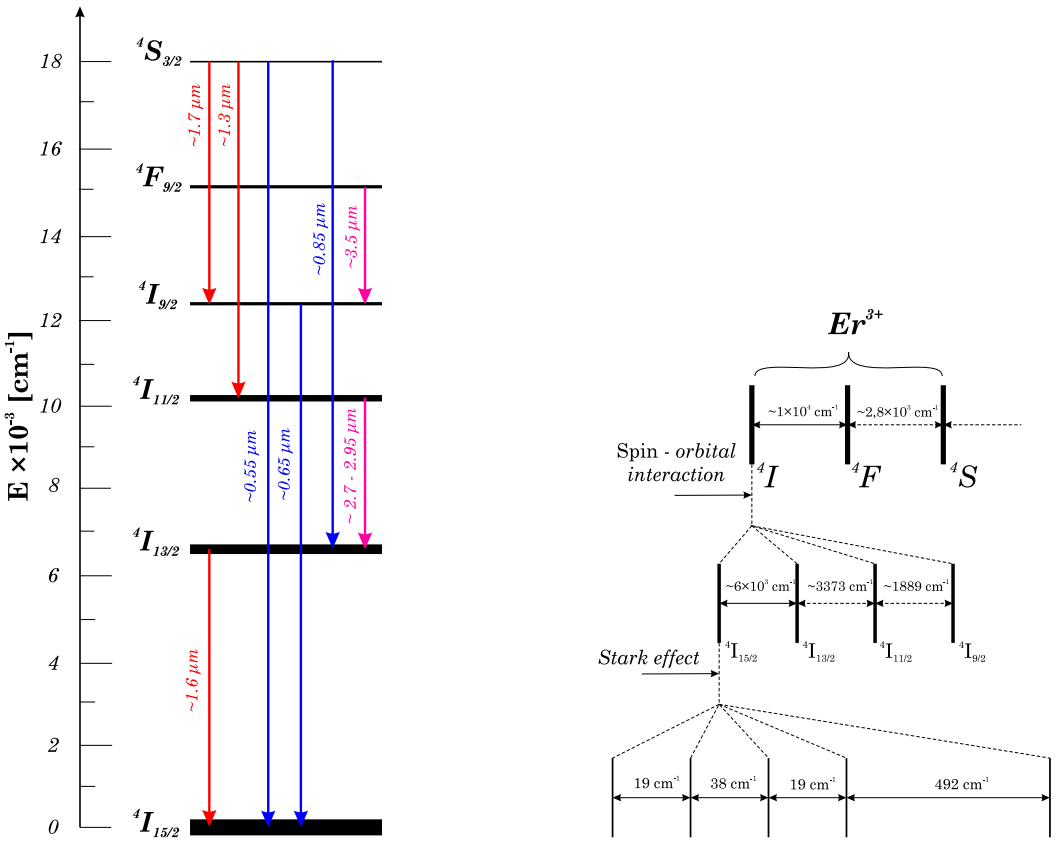

(a) Laser transition

(b) Energy level splitting

Figure 1: Energy levels of Er^{3+} ion.

For this reason, La^{3+} can be added to the active medium to control the clustering of Er^{3+} ions [RS2]. Another possibility how to reduce the self-termination effect and shorten the spacing between Er^{3+} ions is to use the high erbium doping level. The high concentration of erbium results in faster quenching of the lower laser level $^4I_{13/2}$. However, using the high doped active medium affects thermal conductivity; moreover, fabrication of a highly doped, homogeneous crystal with good optical quality can be challenging. [2, 21–25]

As mentioned above, the doping level of Er^{3+} affects the up-conversion processes illustrated in Figure 2. As one can see, there are two crucial transitions that cause the emission in the visible spectral range, particularly at green - ESA1 (excited state absorption) and ET1 (energy transfer); both depopulate the upper laser level $^4I_{11/2}$ of $\sim$ 3 µm

laser transition. The red emission is probably caused by ESA2, which is fortunately advantageous for ~ 3 µm lasing because it depopulates lower laser level $^4I_{13/2}$. The transition ET2 re-populate the $^4I_{11/2}$ level and moreover depopulate the $^4I_{13/2}$ level, so this transition probably partly suppress the self-termination process [21, 22].

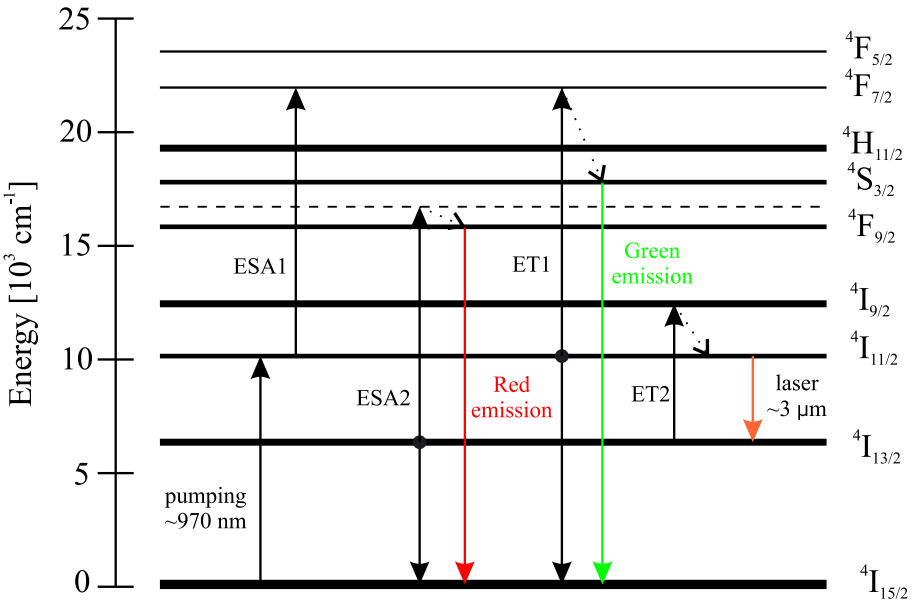

Figure 2: Up-conversion processes of Er^{3+} ion [21, 22].

In summary, to obtain the long fluorescence decay time at the upper laser level ($^4I_{11/2}$) of 3 µm laser transition simultaneously with the short fluorescence decay time at energy level $^4I_{13/2}$, the combination of matrix and concentration of erbium ions must be chosen wisely. However, this is a very complex and demanding task which will be discussed in the following section.

2.2 Erbium doped matrices

Nowadays, there are many matrices (YAG, YAP, GGG, YVO_4, Y_2O_3, KYW, etc.) doped with erbium ions which offer various material and optical parameters. In this section, several Er^{3+}-doped laser active media based on garnet, fluoride, sesquioxide, orthovanadates, tungstate, and others are discussed in detail.

To present and cite the latest results that were reached and published by the laser community, this section contains references up to the year 2020. For this reason, the state of the art also includes several references that refer to the author's results published during the work on a PhD thesis.

2.2.1 Er-doped garnet matrices

Laser matrices based on garnets are well known; the first laser working with an erbium-doped garnet matrix was the Er:YAG developed in 1975 by A.M. Prokhorov and his colleagues. The erbium concentration was ~ 50 % and this laser emitted radiation at 2940 nm and became attractive because its laser radiation is close to the absorption maximum in water [7]. Garnets are important due to their material parameters such as high thermal conductivity, chemical stability, and hardness [26, 27]. The chemical formula of garnets can be written as $C_3A_2D_3O_{12}$ [28]. In general, the C, A, and D represent ions located at dodecahedral (large ion), octahedral (medium ion), and tetrahedral (small ion) sites, respectively [28]. Usually, in laser science, the C denotes Y^{3+}, Gd^{3+}, or Lu^{3+}; A together with D can represent Ga^{3+} or Al^{3+}; separately A and D can denote $Sc^{3+}Ga^{3+}$, $Ga^{3+}Al^{3+}$, $Sc^{3+}Al^{3+}$, or $La^{3+}Ga^{3+}$ [29–33].

Er:YAG crystal $Y_3Al_5O_{12}$ is a cubic crystal with O_h^{10} (Ia3d) space group and excellent thermal conductivity, see Table 1. If Er^{3+} is doped into the crystal structure of YAG, it replaces Y^{3+} because of similar atomic radii [28]. To obtain laser action in the Er:YAG active medium, the doping level of Er^{3+} can vary from 0.5 % to 50 % [7, 14, 31, 34]. Nevertheless, with rising concentration of Er^{3+}, the structural changes and distortion of a crystal can occur [31] which can affects the final quality of the laser crystal and the laser action.

Nowadays, there are many papers dealing with Er:YAG lasers, and it is evident that based on doping level, the Er:YAG crystal can generate laser radiation at 1.6, 2.7, or 2.94 µm [3, 7, 14, 19]. In highly doped crystals, the $^4I_{11/2} \rightarrow {}^4I_{13/2}$ laser transition (2.94 µm) will be supported due to the fast quenching of the lower laser level $^4I_{13/2}$. On the other hand, low-doped YAG crystals make possible to generate cascade laser radiation at 1.6 µm

and 2.7 µm; nevertheless, cryogenic cooling has to be used for this laser action to suppress ground-state re-absorption [14]. Due to cryogenic cooling, the Stark levels are populated in a different way in comparison with the room temperature case. This probably causes that the laser emission from the energy multiplet $^4I_{11/2}$ is shifted to the lower wavelength of 2.7 µm.

Since the Er:YAG crystal is the commonly used erbium-doped active medium able to generate laser radiation directly at 2.94 µm (which is the nearest to 3 µm), it is widely used in various branches of medicine. For instance, Er:YAG laser can be used in dermatology for wrinkles removal [35], hair transplantation [36], or in dentistry for removal of natural caries lesions from dentine [37]. However, as mentioned above, Er:YAG has been known for a long time, but the pumping of this laser was mainly non-coherent by flash-lamps. Since the Er:YAG possesses short fluorescence decay time at the upper laser level ($^4I_{11/2}$), the flash-lamp pumping is the easiest way to obtain high energy laser output (hundreds of mJ). Even if the optical to optical efficiency of flash-lamp pumped laser system is very low in comparison with diode-pumping, the flash-lamps can provide a high amount of energy during hundreds of microseconds which could be beneficial for Er:YAG [38]. Due to its possible application, there has also been an effort to build a high power diode-pumped laser or a system able to generate short pulses with a high peak power at $\sim$ 3 µm wavelength. Yang et al. [38] published a paper dealing with high peak power Q-switched flash-lamp pumped Er:YAG, the 226 mJ pulse energy together with 62 ns pulse duration was achieved, which corresponds to 3.6 MW peak power. In the free-running regime, Messner's group [39] presented a laser set-up that can generate an average output power exceeding 50 W. Such powerful lasers could be used in surgery for cutting of bone [40] or in industry for cutting of various materials (glasses, wood, textile) [39].

Er:GGAG crystal Same as the YAG the GGAG matrix possesses a cubic structure with O_h^{10} (Ia3d) space group [RS3]. From the ion radius and oxidation states of the Er^{3+} one could predict that Er^{3+} will substitutes for Gd^{3+} in the GGAG crystal lattice. Due to the partial substitution of Ga^{3+} for Al^{3+} ions, the crystal field is distorted and the spectral

line-width becomes larger because of inhomogeneous broadening [33]. Contrary to the Er:YAG, the Er:GAGG has a lower melting point (2100 K), see Tables 1 and 2. As far as the low phonon energy is concerned, similar to the GGG ($Gd_3Ga_5O_{12}$) crystal (600 cm^{-1}) [41], the GGAG crystal should have a comparable value of the phonon energy. This is given by using heavier elements such as gallium and gadolinium; a similar phenomenon was observed e.g., in heavy metal glasses [2]. Moreover, the Er:GGAG can be easily grown by the Czochralski method. Since the first diode pumped Er:GGAG laser was published in 2018 in [RS3], the further details are presented in research results of this thesis in section 5.3.

Er:YSGG crystal One of the garnet matrices with a cubic structure and with O_h^{10} (Ia3d) space group symmetry is the yttrium scandium gallium garnet – YSGG ($Y_3Sc_2Ga_3O_{12}$) [31, 42]. Since the YSGG possesses lower phonon energy, the fluorescence decay time of upper laser level $^4I_{11/2}$ is longer in comparison with Er:YAG [43]. Due to the atomic radii of scandium and gallium, the distance between the dodecahedral sites is larger and thus the ion-ion interaction is reduced, which is beneficial to high power lasers [31, 43].

Using diode-pumped Er:YSGG active medium, the 10.1 W average output power with slope efficiency 6.5 % was reached. This high output power was obtained with the compensation of the thermal lens [44].

2.2.2 Er:YAP crystal

Orthoaluminate $YAlO_3$ (YAP) has an orthorhombic crystal structure with space group D_{2h}^{16} (Pnma), which means that the crystal is anisotropic (biaxial) [42, 45]. Similar to the YAG crystal, the Er^{3+} ions entering the crystal lattice as impurities substitute for Y^{3+} ions [45]. Er:YAP active medium is suitable for generating polarized laser radiation at $\sim$ 3 µm, first presented by A. A. Kaminskii [46]. Due to the polarization-dependent of laser emission, the Er:YAP laser could be interesting in spectroscopy or microsurgery [47]. Several papers dealing with highly doped Er:YAP emitting at $\sim$ 3 µm were published in [47–49]. Nevertheless, the first emission of laser radiation at 2.8 µm with the low-

doped erbium YAP crystal was published in 2018 [RS4]. In [RS4] it was proposed that a concentration around 5 % of Er^{3+} should improve the laser parameters. In [8] (published in 2020) it was confirmed that if a higher concentration of erbium (5 %) is used, it is possible to obtain laser action at 2.92 µm (output power 6.9 W) at room-temperature. This is deeply discussed in section 5.1 since it belongs to the results of the PhD thesis.

2.2.3 Er-doped fluoride matrices

For the first time a fluoride matrix was presented by Sorokin and Stevenson in 1960. It was uranium-doped calcium fluoride laser emitting radiation at 2.5 µm [50]. The first CW operation of a Er:CaF_2 laser at 2.7 µm based on a stepwise up-conversion pumping scheme under Xe-flashlamp excitation was reported by S. A. Pollack et al. [51]. A single crystal Er:CaF_2 and Er:SrF_2 lasing at 2.7 µm under diode pumping was realized by T. T. Basiev et al. [20]. Ion clustering in CaF_2 and SrF_2 matrices, which is caused by charge compensation, enables to use the active medium with a low concentration of erbium to obtain lasing [22]. The lower requirement on the doping level of erbium together with the lower melting point of fluoride (YLF – 1092 K, CaF_2 – 1630 K, SrF_2 – 1710 K) makes their fabrication easier [42].

The CaF_2 and SrF_2 matrices have a cubic structure (Fm3m) consisting of F^- and Ca^{2+} or Sr^{2+} ions. If the Er^{3+} ion enters the CaF_2 or SrF_2 structure, it is a substitute for Ca^{2+} or Sr^{2+} [52]. Thus, clearly, because of the extra positive Er^{3+} ion, the charge compensation is required to keep electrical neutrality. Probably, this is the reason for forming a multi-site structure with isolated and complex centres [53], resulting in a broadband absorption and emission spectrum [RS5] of this active medium. This clustering is probably beneficial to ion-ion energy transfer [22].

Recently, lasing in the near- and mid-infrared spectral range of Er^{3+} ions in laser-quality fluoride crystals has been successfully demonstrated under laser diode pumping [21–24], [RS5, RS6, RS7]. However, due to the thermal expansion and the conductivity coefficient, the Er:CaF_2 and Er:SrF_2 are not the best active media for high power lasers. Su et. al.

[54] presented the maximal output power 1 W and slope efficiency 26 % in CW laser regime with Er:SrF_2, which could be interesting and sufficient for some applications.

Both active media Er:CaF_2 (322 cm^{-1}) and Er:SrF_2 (280 cm^{-1}) belong to the low-phonon materials [22]. As mentioned above, the probability of non-radiative transitions for low-phonon materials is lower as against crystalline oxides; thus the fluorescence decay time at $^4I_{11/2}$ is longer and the ratio of the $^4I_{11/2}/^4I_{13/2}$ is higher which is beneficial for CW laser operation [21, 22]. Due to their broadband emission spectrum, Er:CaF_2 and Er:SrF_2 crystals are interesting for possible ultra-short pulse generation [55] and wide wavelength laser tuning.

In the YLF ($LiYF_4$) matrix, Er^{3+} substitutes for trivalent yttrium; so charge compensation is not required [56]. The YLF crystal has a tetragonal crystal structure with C_{4h}^6 ($I4_1/A$) space group, and so the crystal is anisotropic and uniaxial [42, 57]. Due to the anisotropy of the $LiYF_4$ crystal, the Er:YLF laser is able to emit linearly polarized laser radiation at 2.8 µm [23]. For this laser emission, the common doping level of erbium is $\sim$ 15 % [23, 58–60]. Using pulsed side-pumping, a high power laser can be obtained with an output average power 10 W and slope efficiency 18.7 % in the free-running regime [23]. In [61], the true CW laser regime of Er:YLF was presented with a maximum output power of 4 W and slope efficiency 16.5 %.

2.2.4 Er-doped sesquioxides

The erbium-doped sesquioxides (Er:Y_2O_3, Er:Sc_2O_3, Er:Lu_2O_3, Er:Al_2O_3) represent a very interesting sort of active media because of the material parameters, and particularly for high thermal conductivity which is required for high-power lasers [62]. For instance, the un-doped Y_2O_3, Lu_2O_3, and Sc_2O_3 possess higher thermal conductivity than the YAG [63]. The main difficulty in obtaining the high optical quality crystal is the very high melting point (2770 K), which makes the fabrication challenging [62–64]. Therefore, only a few materials such as rhenium, tungsten, osmium, tantalum, and carbon (all with their melting point exceeding 3400 K) could be used for the fabrication of a crucible. Due to the toxicity,

chemical reactivity, colouration, or corrosion by oxidic melts, only rhenium is the suitable material [63]. Using the heat-exchanger method with rhenium crucibles enables to fabricate a high-quality single crystal; however, production of sesquioxide is still expensive [62, 63], which is the main drawback of these matrices. On the other hand, it is possible to produce sesquioxide in ceramic form, which reduces the cost and offers the fabrication of active media in large dimensions and at high concentration [65].

The above-mentioned crystal hosts have a cubic bixbyite structure with space group T_H^7 (Ia3). The unit cell consists of two site symmetries, namely, C_2 and C_{3i}, and the rare-earth ions can substitute both of them. However, the optical properties are mainly given by the activator in C_2 sites [63]. Due to the cation densities of $\sim 3{\cdot}10^{22}$ cm^{-3} the doping concentration of rare-earth ions in sesquioxides is comparable with a double value in a YAG crystal [62]. Moreover, because of the low phonon energy of 600 cm^{-1}, the non-radiative transitions are reduced, and obtaining lasing in the mid-infrared range 2.7 µm is possible even with low-level doping of erbium. [62, 63]

There are three sesquioxide matrices that are commonly used with erbium ions, namely, Er:Y_2O_3, Er:Lu_2O_3, and Er:Sc_2O_3. All have very similar material and optical parameters, discussed in detail in [62]. Nevertheless, thermal conductivity is worthy of notice, because for the 5 % erbium concentration, Lu_2O_3 unlike two other sesquioxides, changes this value minimally. From 12.8 W·m^{-1}·K^{-1} (un-doped) the thermal conductivity drops down only to 11.7 W·m^{-1}·K^{-1}; for the Er:Y_2O_3 and Er:Sc_2O_3 this decline is more than two times higher [62]. For this reason, the Er:Lu_2O_3 could be more interesting for high power lasers. With Er:Lu_2O_3, the maximal output power of 2.3 W and slope efficiency 29 % in the CW regime was reached, which are the highest values obtained with the sesquioxide at 2.8 µm [66]. On the other hand, there is an active medium with higher thermal conductivity in comparison with Er:Lu_2O_3; it is the Er:α-Al_2O_3 (single crystal) [67]. Up to now, only the spectroscopic properties were published; however, according to [67], the Er:α-Al_2O_3 should possess extremely high power extraction capabilities. Moreover, Er:α-Al_2O_3 is uniaxial and it should generate polarisation dependent laser radiation [67].

2.2.5 Er-doped orthovanadates

In general, the orthovanadates formula can be written as MVO_4, where M can represent: Sc, Y, Ce, Pr, Nd, Tb, Ho, Er, Tm, Yb, Lu; nevertheless, for laser active medium doped with erbium ions mainly three matrices are used, namely $GdVO_4$, YVO_4, and $LuVO_4$ [41, 68–70]. In these matrices, erbium substitutes for Y^{3+}, Gd^{3+}, or Lu^{3+} depending on the orthovanadates structure. The orthovanadate crystal has a tetragonal crystal structure with space group symmetry D_{4h}^{19} ($I4_1/amd$); so these crystals are anisotropic and uniaxial [42, 68, 71]. Because of the anisotropy of crystals, the erbium-doped orthovanadates are able to emit linearly polarized laser radiation at 2.72 µm [41], [RSadd1][2].

Orthovanadates are interesting particularly for lasing at 1.6 µm, because the fluorescence decay time at upper laser level $^4I_{13/2}$ is much longer compared with $^4I_{11/2}$ [68]. Nevertheless, using the high doping level of erbium in YVO_4, makes it possible to lase at 2.72 µm due to the strong quenching of fluorescence decay time at $^4I_{13/2}$ [62]. To the best knowledge of the author, the only paper deals with laser emission at $\sim$ 2.7 µm using the orthovanadates Er:YVO_4 (concentration of Er^{3+} 30 %) is [41].

2.2.6 Er-doped tungstates

There are many tungstate compositions based on $(WO_4)^{-2}$; however, for the erbium doping purpose, only two groups will be mentioned. The first group possesses a monoclinic crystal structure with space group C_{2h}^6 (C2/c); so these crystals are biaxial, and the general formula could be written as $AB(WO_4)_2$ [42,72–75], where A stands for the K, Li, Na [76,77] and B denotes the Gd, Y, Lu, Yb, Tm [72,74,78]. In the second group, there are anisotropic (uniaxial) crystals with a tetragonal crystal structure, space group C_{4h}^6 ($I4_1/A$) [42] and general formula XWO_4. X can stand for Ca, Sr, Ba [79,80]. Thus, the Er^{3+} substitutes the trivalent Gd, Y, Lu, Yb, and Tm or divalent Ca, Sr, and Ba [73,79]. For the divalent ions, charge compensation is required; however, according to [79], it is long-range, and thus it

[2]The abbreviation RSadd (Richard Švejkar additional) refers to the author's publications outside topic of PhD thesis.

should not affect the undisturbed Ca^{2+} site.

There are several papers dealing with lasers that use Er-doped tungstate as an active medium [75, 81, 82]; however, most publications concern with ~ 1.6 µm lasers. Laser emission at 2.8 µm using the flashlamp pumping was obtained only with Er:KGW and Er:KYW and then published in [83] and [84], respectively. Nevertheless, both active materials are interesting for being able to emit directly polarization-dependent laser radiation, which could be important for spectroscopy applications [47].

2.2.7 Er:CALGO

Generally, the formula for CALGO crystal can be written as $ABCO_4$, where A represents Ba, Ca, or Sr, B denotes rare-earth ion, and C stands for Al or Ga [85, 86]. The CALGO ($CaGdAlO_4$) crystal possesses the D_{4h}^{17} (I4/mmm) space group and it can be grown by the Czochralski method. The activator ions Er^{3+} entering to the crystal lattice substitutes for Gd^{3+} ions [86]. Since the Er-doped CALGO is an uniaxial crystal, it is possible to generate naturally polarized laser radiation [85]. However, from spectroscopic measurements [87] it follows that the fluorescence decay times at upper and lower laser levels are very short as against the other erbium-doped active media. For the Er:CALGO at the upper $^4I_{11/2}$ and lower $^4I_{13/2}$ laser levels, the decay time is 450 µs and 982 µs, respectively [87]. Using Pr^{3+} to co-dope the Er:CALGO, it is possible to make the fluorescence decay time longer at the upper laser level; nevertheless, both fluorescence decay times are reduced to 84 µs and 74.3 µs at the upper and lower laser level, respectively [87]. To the knowledge of the author, there is no Er:CALGO laser system emitting at 3 µm wavelength region up to now.

2.2.8 Er-doped glasses

Glasses represent a special group of matrices because they can be fabricated in the form of bulk or fibres, also, glasses possess an amorphous structure, which bestows them a characteristic attribute [16]. Nowadays, there are many types of glass matrices based

on various compositions, all with different materials and optical parameters, e.g., silicate [RSadd2], potassium-lanthanum phosphate glasses [RSadd3, RSadd4], aluminoborate glasses [88], germanate glasses [89], chalcogenide glasses [90], etc. However, for laser emission in the spectral range $\sim$ 3 µm, only a few types of glasses are suitable. This is given by the presence of OH^- in glass. These groups reduce the emission intensity and efficiency because they take part in the energy transfer of Er^{3+} ions [91], [RSadd2]. To avoid or reduce this issue, glasses with a minimal content of OH^- groups, such as fluoride glasses, should be used [91]. The best known fluoride glasses for 2.8 µm laser emission are fluoro-zirco-aluminate [92], ZBYA (ZrF_4-BaF_2-AlF_3-YF_3) [91], fluoro-tellurite [93] and ZBLAN (ZrF_4-BaF_2-LaF_3-AlF_3-NaF) [94].

The main advantage of glasses is their relative easy fabrication and possibility of producing in large volumes. As mentioned above, glass has an amorphous structure, and thus the spectral lines are broader in comparison with crystals, which can be given by inhomogeneous line broadening. On the other hand, the absence of the crystal lattice reduces the thermal conductivity, which to a certain extent limits the possible thermal load. However, from [95] it follows that using the multimode-core fibre configuration and cryogenic cooling, this problem can be overcome. Paper [95] presents the Er:ZBLAN CW laser operation at $\sim$ 3 µm with maximum output power 24 W and slope efficiency 14.5 %.

2.3 Short pulse generation at wavelength of 3 µm

Short pulse generation at 3 µm is interesting, particularly for applications in medicine (ophthalmology, surgery, and dentistry) [1] or for further radiation conversion to mid-infrared spectra, e.g. pumping of active material as Fe:ZnSe, or for nonlinear conversion [96]. Basically, for bulk lasers, there are only two ways to obtain short pulses, i.e., active or passive switching [2, 7]. Systems using the former method are mostly based on Pockles cell or acousto-optic modulators, which results in a complex resonator with the requirement for high voltage if the Pockels cell is used [97]. On the other hand, many latest papers deal with passive switching using saturable absorbers such as SESAM (semiconductor saturable absorber mirror) [96, 98], black phosphorus [55, 99, 100], graphene [24, 101], or the Fe:ZnSe crystal [97, 102]. These materials make it possible to build a compact laser resonator without the need of high voltage or a special nonlinear crystal. Several of the above-mentioned laser active media were used together with a saturable absorber hence it was possible to generate the Q-switched and mode-locked pulses. This section presents a brief overview of passively Q-switched erbium lasers.

The diode-pumped mode-locked erbium laser systems with passive (SESAM, black phosphorus, and graphene) switching were also presented; however, the active medium was a fibre based on ZBLAN [103, 104].

2.3.1 SESAM, black phosphorus, and graphene

The SESAM, black phosphorus, and graphene can be used in the laser resonator as saturable absorbers to obtain short Q-switched pulses. However, the damage threshold of such saturable absorber is lower in comparison with a crystal, which can limit the output energy of Q-switched pulses [105]. Probably, the commercially most accessible solution, with saturable absorbers, is a semiconductor structure with quantum well denoted as SESAM. The damage threshold of SESAM is ~ 4 mJ/cm^2 [106], which is almost 1000 times lower in comparison with the Fe:ZnSe crystal [105]; moreover, the SESAM can be easily damaged by Q-switched mode-locked pulses [107].

The SESAM Q-switching of Er:Y_2O_3 ceramic was successfully tested and presented [96, 98]. It was shown [98] that using SESAM enables generating 29 ns pulses with pulse energy 17.4 µJ at 2.7 µm. Now, the duration of 29 ns is probably the shortest pulse generated in the $\sim$ 3 µm region reached with saturable absorber in a bulk laser system. If black phosphorus was used as Q-switcher with Er:Y_2O_3 ceramic, the shortest generated laser pulse was 4.47 µs with pulse energy 0.48 µJ [99]. The next sesquioxide tested with black phosphorus saturable absorber was Er:Lu_2O_3, which has shifted the laser emission to 2.84 µm [62]. In [100] it was shown that Q-switched pulses from this laser reach 359 ns and 7.1 µJ. Relatively new and promising material for Q-switching is graphene, which enables the generating short pulses in a wide spectral range due to its broadband properties [101]. Li et al. showed [24] that by the graphene Q-switched Er:CaF_2 laser generated a radiation with a pulse duration 1.32 µs and pulse energy 2.74 µJ. A similar active medium Er:SrF_2 was Q-switched using the black phosphorus saturable absorber, which allows to reach the pulse duration of 702 ns and pulse energy 2.34 µJ at 2.79 µm. The last mentioned is a special composite crystal GGG/Er:Pr:GGG/GGG tested together with a graphene saturable absorber mirror. With this set-up, You et al. [101] successfully obtained 360 ns laser pulses with energy 1.54 µJ.

2.3.2 Crystalline saturable absorber

Another solution how to obtain short pulses in the 3 µm wavelength region is to use crystals as a saturable absorber. These crystals are based on ZnSe or ZnS matrix, where the Fe^{2+} or Co^{2+} can be used as an activator [4, 97, 105]. The advantage of these materials is their high damage threshold. It is 3 J/cm^2 and 1.5 J/cm^2 for Co:ZnSe and Fe:ZnSe, respectively [105], and, moreover, they are commercially available.

Q-switching of a flash-lamp pumped Cr,Er:YSGG was firstly realized by Kisel et al. [105] in 2005. It was shown that using the Fe:ZnSe crystal (as a saturable absorber), 170 ns pulses with pulse energy 60 mJ at 2.8 µm can be obtained [105]. Using a different resonator design with the Fe:ZnSe crystal, pulses from flash-lamp pumped Cr,Er:YSGG were further

shortened to 65 ns [102]. The best-known erbium doped crystal – Er:YAG – was also tested. The flash-lamp pumped highly doped Er:YAG (50 % of Er^{3+}) was successfully Q-switched using the Fe:ZnSe single crystal, and the pulse duration 50 ns with energy 6 mJ were reached for the first time in [97].

If one compares the pulse duration achieved with crystal (50 ns) and SESAM (29 ns), it is obvious that they are comparable. However, there is a large gap in pulse energy. For Fe:ZnSe crystal, the energy of Q-switched pulse is approximately three orders of magnitude higher in comparison with SESAM. For crystals, the pumping power can be higher, so it is possible to extract more energy [98].

Matrix	**Formula**	**Crystal system**	T_m [K]	**c** [$\mathbf{J{\cdot}g^{-1}K^{-1}}$]	α [$\mathbf{10^{-6}}$ **K**]	κ [$\mathbf{W{\cdot}m^{-1}K^{-1}}$]	ρ [$\mathbf{g{\cdot}cm^{-3}}$]
YAG	$Y_3Al_5O_{12}$	Cubic (Ia3d)	2200	0.625	7.7	14.5	4.56
YAP	$YAlO_3$	Orthorhombic (Pnma)	2140	0.42	11 $\perp$c	11	5.35
YLF	$LiYF_4$	Tetragonal ($I4_1/a$)	1092	0.79	13.3$\perp$a	6.3	3.99
CaF_2	CaF_2	Cubic (Fm3m)	1630	0.91	18.90	9.7	3.18
SrF_2	SrF_2	Cubic (Fm3m)	1710	0.54	18.4	8.3	4.24
Y_2O_3	Y_2O_3	Cubic (Ia3)	2703	0.46	6.56	13.4	5.01
Lu_2O_3	Lu_2O_3	Cubic (Ia3)	2723	—	6.1	12.8	9.43
YVO_4	YVO_4	Tetragonal ($I4_1/amd$)	2100	0.56 4.4$\perp$c	11.4$\parallel$c 8.9$\perp$c	12.2$\parallel$c	4.23
$GdVO_4$	$GdVO_4$	Tetragonal ($I4_1/amd$)	2053	0.50 2.2$\perp$c	8.92$\parallel$c 8.6$\perp$c	10.5$\parallel$c	5.47
KYW	$KY(WO_4)_2$	Monoclinic (C2/c)	–	0.41	3.0$\parallel$b	2.7$\parallel$b	6.56
KGdW	$KGd(WO_4)_2$	Monoclinic (C2/c)	–	0.37	1.9$\parallel$b	2.6$\parallel$b	7.11

Table 1: Material parameters of several un-doped matrices, T_m - melting point, c - specific heat capacity, α - coefficient of thermal expansion , κ - thermal conductivity, ρ - density, for 300 K [42, 62, 64, 73, 74, 108].

Matrix	**Optical activity**	**n [-] @ 632.8 nm**	**dn/dt [10^{-6}/K]**	**Δn @ 632.8**	**T [µm]**
YAG	Isotropic	1.8295	9.05 @ 1064 nm	—	0.21 - 5.2
YAP	Biaxial	1.924 (n_x), 1.938 (n_y) 1.947 (n_z)	9.8 (a), 14.5 (c) @ 1064 nm	0.0235	0.2 - 7
YLF	Uniaxial	1.4762 (o) 1.4535 (e)	-0.67 (o), @ 546 nm -2.30 (e) @ 546 nm	0.0227	0.12 - 8
CaF_2	Isotropic	1.433	-11.5 @ 632.8 nm	—	0.12 - 10
SrF_2	Isotropic	1.437	-12.5 @ 632.8 nm	—	0.13 - 12
Y_2O_3	Isotropic	1.92	8.3 @ 633 nm	—	0.29 - 7.1
Lu_2O_3	Isotropic	1.9303	9.1 @ 633 nm	—	—
YVO_4	Uniaxial	1.9934 (o), 2.2148 (e)	3.9(o), 8.5(e)	0.2233	0.35 - 4.8
$GdVO_4$	Uniaxial	2.0135 (o), 2.2468 (e)	—	0.24	0.35 - 3.5
KGdW	Biaxial	2.001 (n_x), 2.042 (n_y) 2.086 (n_z)	-10.1 (n_x), -7.3 (n_y) -8.4 (n_z) @ 633nm	0.085	–
KGdW	Biaxial	2.009 (n_x), 2.028 (n_y) 2.084 (n_z)	-10.6 (n_x), -8.4 (n_y) -15.2 (n_z) @ 633nm	0.029	–

Table 2: Optical parameters of several erbium matrices; n - refractive indexes (o - ordinary axis and e - extraordinary axis), dn/dt - Thermooptic coefficient, Δn - birefringence (only anisotropic materials), T - transparency [42,64,73,74,108–113].

Active medium	**Laser regime**	λ_{laser} **[µm]**	P^{out}_{max} **[W]**	σ_{slope} **[%]**	**References**
Er:YAG	QCW	2.94	50	–	[39]
Er:YSGG	PU	2.79	10.1	6.5	[44]
Er:GGAG	CW	2.84	0.075	7.4	[RS3]
Er:YAP	CW	2.92	6.9	31	[8, 114]
Er:YLF	CW	2.8	4	16.5	[61]
Er:CaF_2-SrF_2	CW	2.74	0.7	41.4	[9]
Er:SrF_2	CW	2.74	1	26	[54]
Er:Lu_2O_3	CW	2.71	2.3	29	[66]
Er:Y_2O_3	CW	2.71	14	26	[115]

Table 3: Summary of erbium-doped laser active media with the best output obtained laser results; λ_{laser} – emitted laser wavelength, P^{out}_{max} – maximal output power, σ_{slope} – slope efficiency.

3 Goals of thesis

This thesis deals with erbium-doped lasers that generate laser radiation in mid-infrared spectral range from 2.7 µm to 3 µm. Several laser active media doped with erbium were chosen for spectroscopic measurement and laser investigation. The goals of this thesis are following:

1. Investigation of existing and newly developed gain material for Er-based diode-pumped 3 µm laser;
2. Generation of short pulses at 3 µm region using Q-switching, gain-switching, and mode-locking regime;
3. Design and investigation of Er-based microchip lasers.

4 Measurement methods

4.1 Spectroscopy measurements

The Shimadzu spectrophotometer type UV - 3600 with spectral resolution ±0.2 nm in the visible and ultraviolet regions, and ±0.8 nm in mid-infrared was used to measure the transmission spectra of the tested samples. Fluorescence spectra and laser emission in CW regime were measured by AROptix Fourier-transform spectrometer Arcspectro FT-MIR Rocket (2 – 6 µm, resolution 3 nm @ 2.8 µm). The fluorescence decay time at 1 µm and 1.5 µm was measured using the HP 5087 (Si PIN photodiode) and FGA10 (InGaAs photodiode, 800 - 1800 nm, ThorLabs) with long pass filter cut-on wavelength 1100 nm, respectively. During measurements, both photodiodes were connected to oscilloscope (Tektronix TDS 3052B, 500 MHz, 5 GS/s). For data collection from fluorescence decay time measurements, the program in LabView was written and the data was stored automatically. Afterwards the data were batch processed with MATLAB script written by author.

4.2 Pumping source

All tested crystals were longitudinally pumped by fibre-coupled (core diameter 100 µm, numerical aperture 0.22) laser diode LIMO35-F100-DL976-EX1202 (LIMO Laser System), working in the pulsed or CW regime. Radiation from this fibre-coupled laser diode was focused into the active laser material by two achromatic doublet lenses (Thorlabs, Inc., AC508-075-B and AC508-150-B) with the focal length $f_1 = 75$ mm and $f_2 = 150$ mm, thus pumping beam diameter was $\sim 200\,\mu m$. The frequency, pulse duration, pumping wavelength, and output power are discussed individually in the text below for each active medium. To control laser diode driver a LabView program was also written; this program was extended and in the final version a single program could controls the laser diode driver (current, temperature, frequency, and pulse duration), power meter, oscilloscope, and temperature of sample in cryostat. Thus, the output and absorbed power could be measured automatically which significantly save a time during all measurements.

4.3 Laser resonator

As far as the laser resonator is concerned, all samples were tested in a hemispherical resonator with a flat pumping mirror (PM) and a spherical output coupler (OC) with various reflectivity (R_{OC}) and radius of curvature (r_{OC}). The R_{OC}, r_{OC}, and length of the resonator are described for particular active media in the text below. For the tunability measurement, the birefringent MgF_2 plate was placed under Brewster's angle in a resonator within active medium and OC. The short pulse generation in Q-switching and mode-locking regime was tested with SESAM (semiconductor saturable absorber mirror, Batop GmbH) placed in resonator. Moreover, Fe:ZnSe polycrystal was also tested for passive Q-switching in Er:YLF laser system. During these measurements, the hemispherical and V-shape laser resonator were used. The setup of this measurement will be describe in detail in text below. The layout of the laser resonator can be seen in Figure 3.

4.4 Cryogenic cooling

For experiments at low temperature, the vacuum chamber and cryogenic cooling (liquid nitrogen cryostat, Janis Research, model VPF-100) was utilized. During all experiments on the side of the pumping mirror and between the active medium and the output coupler there were uncoated CaF_2 windows, see Figure 3. The tested sample was placed in a copper holder which was attached to a cold finger inside the cryostat and its temperature was being changed between 80 - 300 K by the temperature controller Lake Shore model 325. Temperature of the sample was controlled through the LabView program and during all measurements with cryogenic cooling the automatic data collection was used.

4.5 Power and space structure measurement

The output power of the laser was measured by ThorLabs power probe S401C (0.19 - 10.6 µm) connected to a power meter PM100A. Laser beam spatial structure was measured by Spiricon Pyrocam IV (camera chip $LiTaO_3$, active area 25.6×25.6 mm) with a band

pass filter 2500±250 nm. The tunability of the emitted wavelength was measured using the Oriel monochromator 77250 (grating 77300) with Thorlabs photodiode PDA20H-EC (PbSe, 1.5 – 4.8 µm) connected to Tektronix oscilloscope.

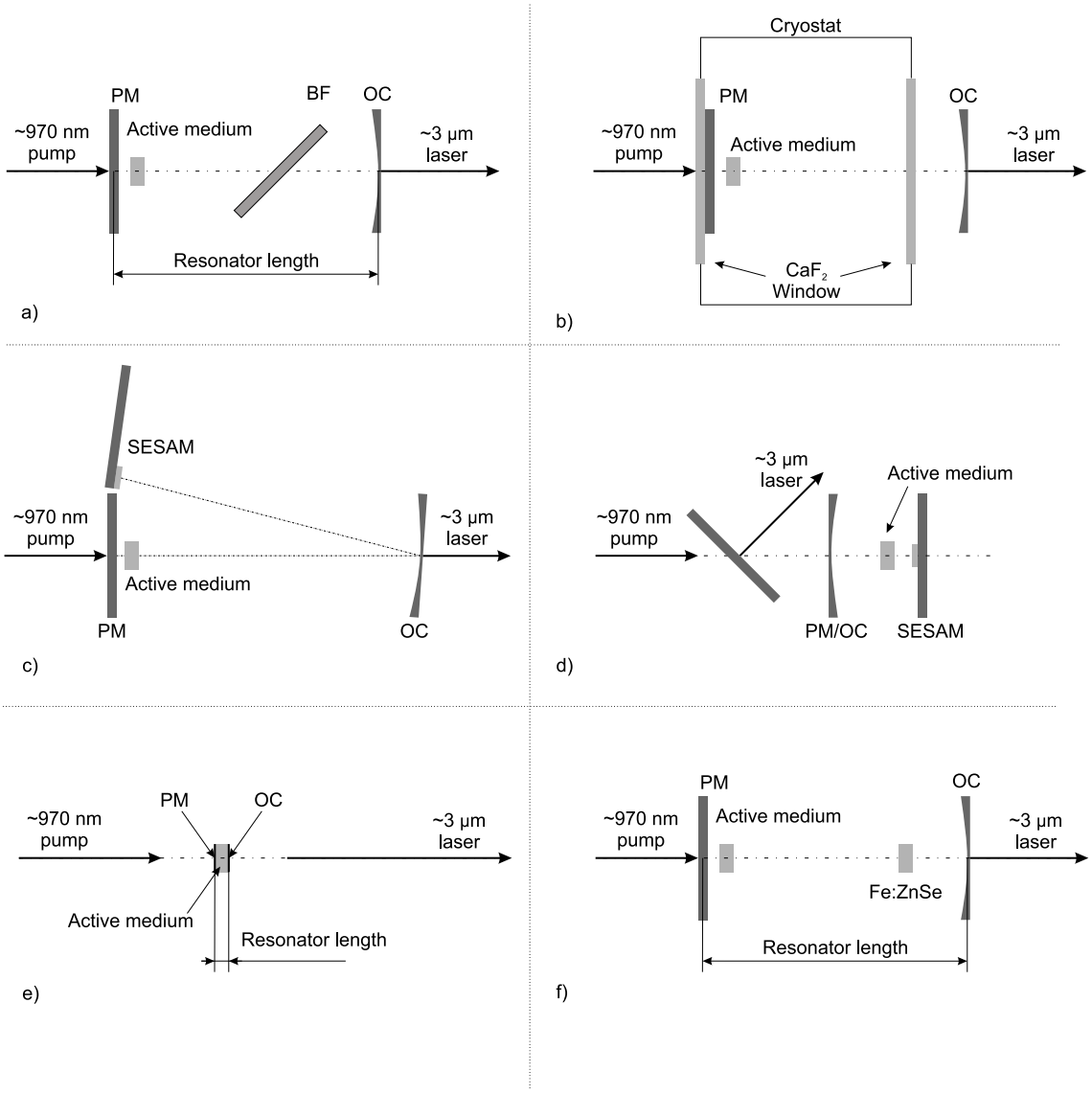

Figure 3: Layout of laser resonators; pumping mirror (PM), output coupler (OC), BF – birefringent MgF_2 plate 2 mm thick.

4.6 Short pulse characterization

The short pulses in the nanosecond range were measured using a fast detector VIGO PVI-4TE-6 (response time 0.5 ns, 2 - 6 µm, VIGO System S.A.) connected to a Tektronix oscilloscope. On the other hand, the output pulses from mode-locking laser have to be measured using an autocorrelator because there is no available photodiode able to measure picosecond pulses in the spectral range around 3 µm. The pulse duration in the picosecond range was measured by a laboratory built interferometric autocorrelator based on two-photon absorption effect in a germanium chip of Thorlabs photodiode PDA30B-EC (Ge, 800 – 1800 nm, rise time 2.5 µs) detector. The layout of the autocorrelator is presented in Figure 4 together with photograph.

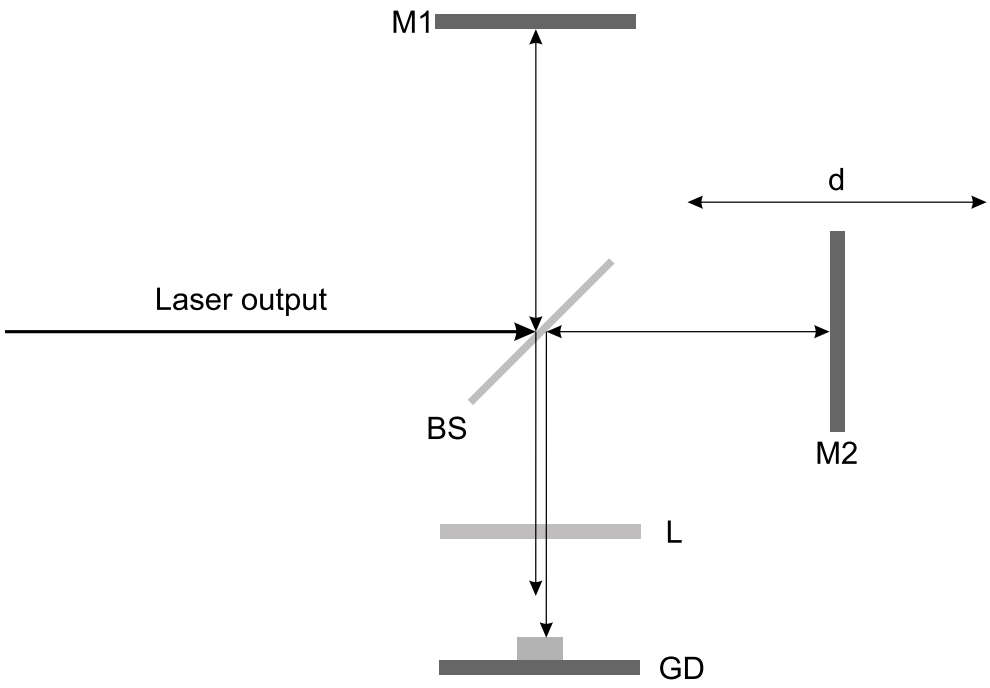

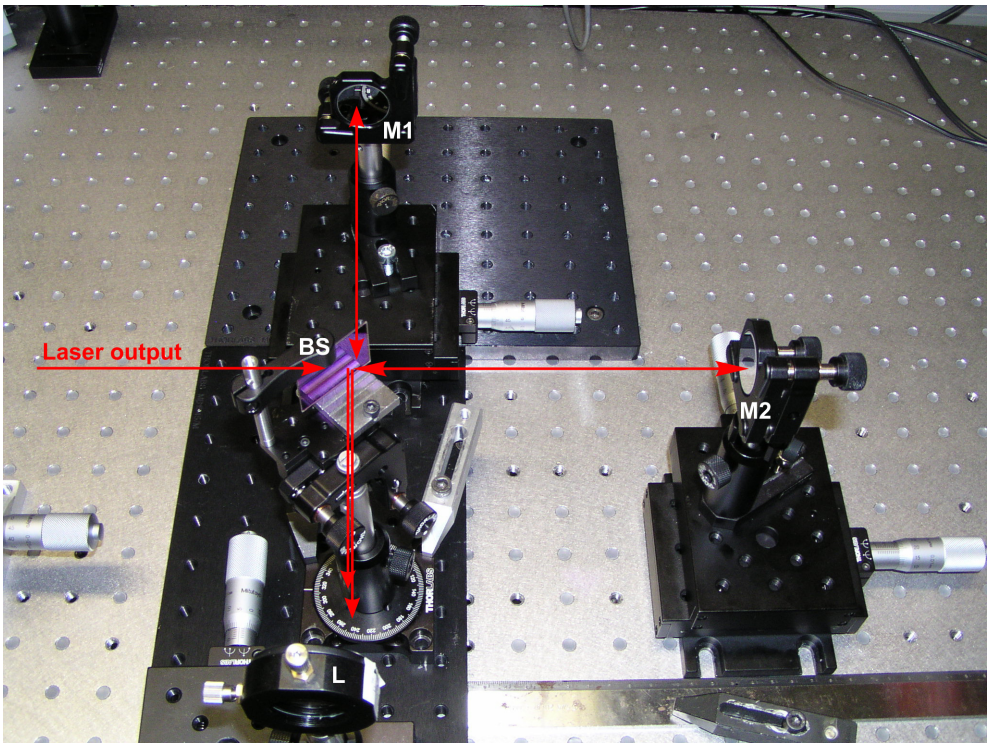

Figure 4: Layout of laboratory built autocorrelator; M1 – fixed mirror, M2 – movable mirror, BS – beam splitter, L – CaF_2 lens (f = 55 mm), GD – germanium based detector.

5 PhD research results

This PhD research work was performed at the applicant's home institution, the Laboratory of solid-state lasers (head prof. Helena Jelínková) at the Department of Physical Electronics (Faculty of Nuclear Sciences and Physical Engineering) of the Czech Technical University in Prague. The PhD research can be divided into several parts: spectroscopic and basic laser investigation of laser materials, short pulse generation in Q-switching, gain-switching, and mode-locking regime.

Overall, six crystals (Er:YAG, Er:GGAG, Er:SrF_2, Er:CaF_2, Er:YAP, Er:YLF) with various concentrations of Er^{3+} and one ceramic (Er:Y_2O_3) were tested, see Table 4; and results are summarized in text below and in Table 5. Firstly, the spectroscopic characterization (absorption and emission cross-section spectra, and fluorescence decay times at upper and lower laser levels) was performed for all samples. During the measurement of basic laser characteristics (pulsed and CW laser regimes, output energy or power, emission wavelength, beam profile, and tunability), all active media were placed in the hemispherical resonator and pumped by fibre-coupled laser diode emitting around 970 nm. It is worthy to note that not all output characteristics were measured for all active media. For example, it is not possible to reach CW lasing or wavelength tunability with Er:YAG laser due to short fluorescence decay time at upper laser level and narrow emission lines, respectively. Moreover, the Er:CaF_2 crystal cracked during CW operation thus to prevent damage of Er:SrF_2 the the CW lasing was not tested. For this reason the CW laser characteristics of Er:CaF_2 and Er:SrF_2 are not presented. From this point of view, the largest amount of data were collected for Er:YLF crystal, even if the several crystals were damage, they could be easily replaced from commercial sources. On the other hand, crystals obtained thanks to the collaboration with research institution (see Table 4) e.g., Er:SrF_2, Er:GGAG, or Er:CaF_2 cannot be easily replaced, so, they were handled with care and not pushed to the limits.

The CW laser operation was reached only with Er:GGAG, Er:YAP, and Er:YLF crystals. The Er:GGAG crystal is unique active medium based on a mixed garnet structure with relatively broad absorption and emission spectral lines and with attractive laser output characteristics. However, further research and investigation are necessary to determine an appropriate concentration of Er^{3+} ions and improve the crystal quality. On the other hand, Er:YLF lasers can be proposed for applications (e.g., polymer processing) since the CW output reaches relatively high slope efficiency 26.6 % and output power 2.9 W [RS8]. Using a birefringent plate (MgF_2) the continues wavelength tunability of the emitted laser radiation was obtained, however, only with Er:GGAG, Er:SrF_2, and Er:CaF_2 crystals. Maximal tuning range 123 nm extended from 2690 nm to 2813 nm (crossing zero) was obtained for Er:SrF_2 laser. This is one of the major results of this work since the last published result [20] presented a significantly narrower tuning range (40 nm, 2720 - 2760 nm). The Er:CaF_2 laser has an even broader tuning ranging in comparison with Er:SrF_2, it was from 2692 nm up to 2840 nm (148 nm) [RS9]. Summary of all results presented in the text above can be found in Table 5.

From the point of view of potential applications (medicine, material processing, spectroscopy, etc.), it will be interesting to generate short pulses at the spectral range around 3 µm. Using a semiconductor saturable absorber mirror (SESAM) and the laser design presented in Figure 3 the nanosecond pulses in Q-switching and picosecond pulses in mode-locking regimes were successfully generated with Er:YLF [RS10] and Er:Y_2O_3 [RS11], respectively. Even if this laser design allows to build a relatively compact resonator, the microchip design makes it possible to create a few millimetres long laser resonator. The dimensions of the resonator are given by the length of the active medium since the mirrors (dielectric layers) are deposited directly on the crystal faces. Two erbium-based microchip lasers (Er:YLF and Er:YAG) were designed and successfully tested in free-running and gain-switching regime [RS12, RS13].

In the text below, there is a summary of papers published in impacted journals (Optics Letters, Optical Material Express, Progress in Quantum Electronics, and Laser Physics Letters) and proceedings of international conferences. Since this section contains a sum-

mary of individual papers, there are not included all technical details regarding particular measurements and laser systems. Readers can trace back all information in the cited literature as well as in enclosed appendix. All results presented in the text below were measured, proceed, and evaluated by the author.

Samples	**Origin**	**Er conc.**	**Length [mm]**	**Faces [mm]**
Er:YAG	Crytur Ltd.	50 at. %	5.4	⌀ 2.96
Er:GGAG	FZU CAS	20 at. %	3.60	⌀ 12
Er:YLF	Unioriental Ltd.	6 at. %	3.00	⌀ 4
Er:Y_2O_3	Biakowski, Ltd.	5 at. %	9.00	3×3
Er:SrF_2	SIC CAS	3 at. %	9.00	3×3
Er:CaF_2	SIC CAS	3 at. %	9.00	3×3
Er:YAP	Crytur Ltd.	1 wt. %	4.47	⌀ 25.7

Table 4: Tested Er-doped active media, FZU CAS – Institute of Physics, Czech Academy of Sciences; SIC CAS – Shanghai Institute of Ceramics, Chinese Academy of Science.

Samples	conc. [%]	σ_{max}^{abs} [10^{-21}cm^2]	σ_{max}^{em} [10^{-20}cm^2]	τ_{lo} [ms]	τ_{up} [ms]	P_{CW}^{max} [mW]	E_{PU}^{max} [mJ]	σ_{CW} [%]	σ_{PU} [%]	$\Delta\lambda$ [µm]	λ [µm]	Ref.
Er:YAG	50 at.	4.25 @ 966.6 nm	10 @ 2623 nm	2.9	0.29	—	1.8	—	16.8	—	2.94	[RS13]
Er:GGAG	20 at.	8.5 @ 965.3 nm	2.5 @ 2639 nm	3.2	0.44	75.5	2.3	7.4	13.5	62	2.84	[RS3]
Er:YAP	1 wt.	9.8 @ 972.2 nm	4.2 @ 2729 nm	4.1	0.83	26.8	0.1	3.5	1.2	—	2.73	[RS4]
Er:YLF	6 at.	9.8 @ 972.2 nm	19 @ 2659 nm	10.9	4.1	2900	17.1	26.6	24.5	—	2.81	[RS8]
Er:Y_2O_3	5 at.	1.97 @ 971.2 nm	15 @ 2717 nm	15.9	2.4	—	2.6	—	4.8	—	2.75	[RS11]
Er:SrF_2	3 at.	2.67 @ 969 nm	4.5 @ 2720 nm	13.0	7.3	—	5.8	—	7.3	123	2.75	[RS14]
Er:CaF_2	3 at.	2.48 @ 968 nm	3.4 @ 2720 nm	13.1	7.7	—	2.3	—	2.8	148	2.75	[RS9]

Table 5: Summary of spectroscopic and laser results, conc. – concentration of Er^{3+}, σ_{max}^{abs} – maximal absorption cross-section, σ_{max}^{em} – maximal emission cross-section, τ_{lo} and τ_{up} fluorescence decay time at lower $^4I_{13/2}$ and upper $^4I_{11/2}$ laser level, P_{CW}^{max} – maximal output power in CW laser regime, E_{PU}^{max} – maximal output energy in pulse laser regime, σ_{CW} and σ_{PU} – slope efficiency in CW and pulsed regime, $\Delta\lambda$– maximal wavelength tunability, λ– emission laser line.

5.1 Temperature influence on spectroscopic properties and 2.7 µm lasing of Er:YAP crystal (SPIE Photonic West, 2018)

Since a few papers were dealing with Er:YAP active medium, the one of the first tested erbium-doped active media was Er:YAP (1 wt. % of Er^{3+}). Er:YAP ($Er:YAlO_3$) is a very attractive crystal, in comparison with YAG it has lower phonon energy and comparable thermal conductivity, moreover, Er:YAP laser can directly generate linearly polarized laser radiation. Unlike Er:YAG the Er:YAP can generate laser radiation in CW regime [114] [RS4]. The temperature influence on spectroscopic and laser parameters of Er:YAP active medium was presented for the first time in [RS4]. Moreover, it was shown that Er:YAP can generate laser radiation in CW regime. In the conclusion of [RS4] paper, it was suggested that the optimal concentration of Er^{3+} is around 5 %. This was confirmed in [114] and [8] where CW lasing was obtained at room-temperate with slope efficiency 31 % and output power 6.9 W, respectively. These results became interesting mainly for applications e.g., drilling, cutting, welding, etc.

It is worthy to note that the absorption coefficient at 1450 - 1600 nm is approximately 5 times higher in comparison with 960 - 1000 nm, thus the resonant pumping for laser emission at 1.6 µm is also possible. The pumping wavelength 972.5 nm, closely corresponding to the highest absorption peak at 972.1 nm (absorption coefficient 0.94 cm^{-1} at 80 K), was used and the pulsed and CW laser regime was successfully obtained. The laser slope efficiency became lower with increasing temperature; for the pulsed laser regime (duty cycle 10 %) it decreased from 1.27 % at 78 K to 0.14 % at 300 K. With the rising temperature, the population of upper energy levels became higher and the laser threshold were rising. Nevertheless, with heating the sample up to 400 K it was found, that at 380 K the laser emission at 2.73 µm was still observable. After exceeded the 310 K the output power could not be measured by power probe, the laser emission was observed only with a photodiode. At CW laser regime, the maximal output power was 27 mW at 2.4 W of absorbed power and emitted laser wavelength was 2.73 µm. The low output power in pulsed and CW regime was probably given by low Er^{3+} concentration and off-peak pumping. [RS4]

5.2 Diode-pumped Er:SrF_2 laser tunable at 2.7 µm (Optical Material Express, 2018)

In contradiction to Er:YAP crystal, fluorides materials doped by erbium ions are significant and frequently used in laser science since they possess almost three times lower phonon energy (Er:CaF_2 322 cm^{-1} and Er:SrF_2 280 cm^{-1}) which allows extracting CW lasing with Watt-level output power [22]. Moreover, a remarkably broad absorption and emission spectral lines allow a wide tunability (hundreds of nanometres) [RS2,RS14]. Since Er-doped fluorides present an important group of active media, the Er:SrF_2 (3 at. % of Er^{3+}) was grown and studied. Er:SrF_2 was prepared in collaboration with colleagues from the Shanghai Institute of Ceramics, Chinese Academy of Sciences. The most significant result published in [RS14] was prolonging a tuning curve from 40 nm (2720 - 2760 nm) published in [20] to 123 nm (2690 - 2813 nm), presented in Figure 5. Theoretically, the demonstrated broad gain bandwidth (4 THz FWHM) makes this laser potentially attractive for ultra-short pulse generation in the 2.7 µm region. For more details see [RS14] enclosed in appendix.

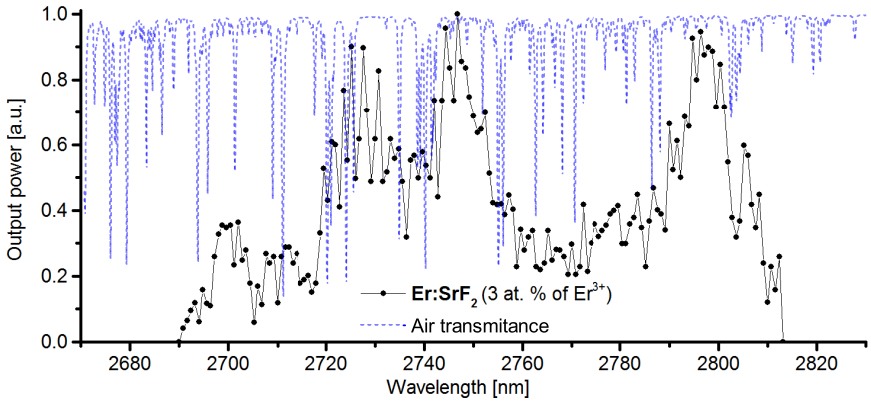

Figure 5: Tuning curve of Er:SrF_2 measured for maximal pumping shown together with air absorption lines; excitation pulse duration 5 ms, frequency 10 Hz, pumping wavelength 969 nm.

5.3 Line-tunable Er:GGAG laser (Optics Letters, 2018)

Further research was focused on the development of a new kind of active medium based on mixed garnet structure. In cooperation with the Institute of Physics of the Czech Academy of Science, the unique and entirely new mixed garnet crystalline material GGAG (gallium-gadolinium aluminium garnet) doped with high (20 %) erbium concentration was grown [RS3]. Detailed characterization of Er:GGAG is presented in section 2.2.1, however, the principal features can be summarized as follow. Due to the mixed structure with multi-structure lattice, the Er:GGAG possesses broader spectral lines (in comparison with Er:YAG, see Figure 6) which allow to tune the emission wavelength and generate short pulses. Based on the results of this paper, we recommended to modify a concentration of erbium in GGAG crystal and the Er:GGAG concentration series (from 4 % to 32 % of Er^{3+}) was successfully prepared.

During spectroscopic measurement, it was confirmed that the absorption spectra are broader in comparison with Er:YAG. This is advantageous if the diode-pumping is used because of the overlapping laser diode emission line and Er:GGAG absorption line. Fluorescence decay time 430 µs at the upper laser level ($^4I_{11/2}$) is much shorter in comparison with 3.2 ms at the lower laser level ($^4I_{13/2}$). It is obvious that Er:GGAG suffers from self-termination (bottleneck) effect [RS3], [116]. For this reason, the fabrication of Er,Pr:GGAG was proposed which leads to interesting results; if 0.09 % of Pr^{3+} is used, the Er^{3+} concentration can be decreased to 13 % which significantly shorten the fluorescence decay time at lower laser level $^4I_{13/2}$ and it allows to obtain higher slope efficiency and output power.

Er:GGAG laser works in pulsed and CW operation. In the pulsed (frequency 10 Hz and pulse duration 2 ms) laser regime, maximal output energy 4.9 mJ with slope efficiency, 13.5 % at 2.84 µm was achieved. Moreover, due to broad fluorescence lines in spectral range 2.5 - 3 µm the emission laser line was successfully tuned at 2800 - 2822 nm, 2829 - 2891 nm, and 2917 - 2942 nm. In CW regime laser emitted at 2.84 µm with slope efficiency 7.4 % and maximal output power 75.5 mW.

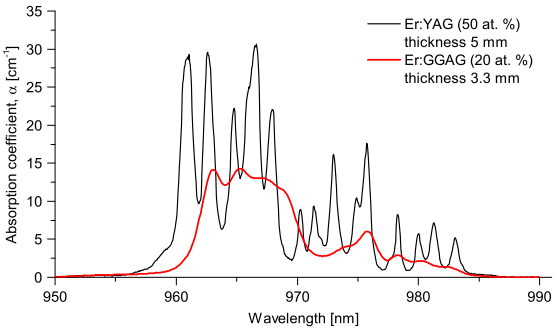

(a) Comparison of absorption spectra.

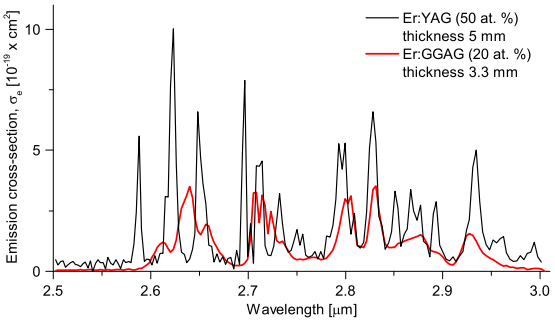

(b) Comparison of emission spectra.

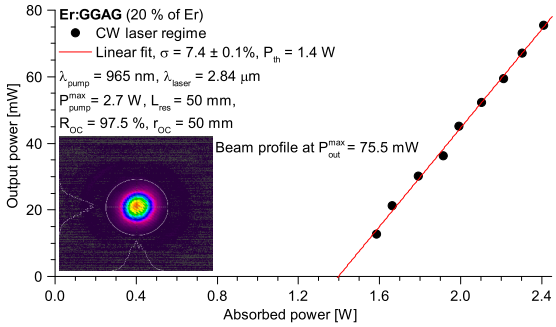

(c) Er:GGAG CW laser.

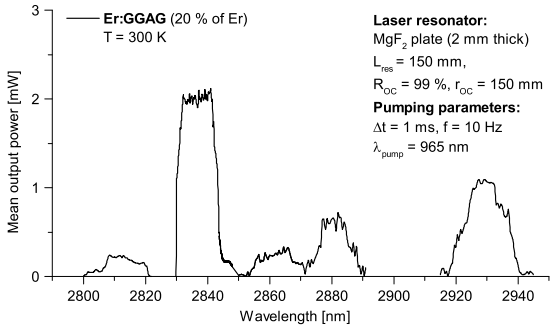

(d) Er:GGAG wavelength tuning.

Figure 6: Absorption and emission spectra of Er:YAG and Er:GGAG, CW laser characteristic and tunability of Er:GGAG laser; σ– slope efficiency, P_{th} – laser threshold, P_{out}^{max} – maximal output power, λ_{pump} – pumping wavelength, λ_{laser} – laser wavelength, P_{pump}^{max} – maximal pumping power, L_{res} – resonator length, R_{OC} and r_{OC} – output coupler reflectivity and radius.

5.4 Er:Y_2O_3 high-repetition rate picosecond 2.7 µm laser (Laser Physics Letters, 2019)

Er^{3+} can be doped into various matrix based on crystalline or glass structure, however, the ceramic matrices unify the advantages of both crystals and glasses which bring a lot of benefits, for details, see section 2.2. Since the short pulse generation in mode-locking regime at $\sim$ 3 µm was presented only in fibres it was attractive to investigate if the bulk ceramic material is able to generate in the mode-locking regime. Moreover, the main drawback of fibres is their length (several meters) because the repetition rate of the mode-locked laser system is given by the resonator length [117]. Thus, one can see that the repetition rate of the fibre system is limited to the megahertz region. [103, 117–119]. The data published in [RS11] presented the first mode-locked results reached with bulk erbium-doped active laser material with an extremely high 1.38 GHz repetition rate.

Er:Y_2O_3 was placed in a short (length 95 mm) V-shape laser resonator and end-pumped with laser diode. As a mode-locker and end-mirror, semiconductor saturable absorber mirror (SESAM, Batop GmbH) was used, see details in [RS11]. The Er:Y_2O_3 emitted laser radiation at 2.74 µm and operated in a Q-switched mode-locked regime (QML). The Q-switched pulses have 50 kHz repetition rate for maximum pumping and pulse duration at FWHM and energy was 57.9 ns and 0.3 µJ, respectively. Due to the short laser resonator, the high repetition rate 1.38 GHz of mode-locking pulses was achieved. The pulse duration of the mode-locking pulse was measured by a laboratory built autocorrelator based on two-photon absorption effect in germanium detector. At full-width half maximum, it was reached 86$\pm$4 ps pulse duration with energy per pulse equal to 3.55 nJ.

5.5 Passively mode-locked high-repetition rate Er:YLF laser at 2.81 µm generating 72 ps pulses (CLEO/Europe-EQEC 2019 Conference)

Contrary to Er:Y_2O_3 the Er:YLF crystal is uniaxial, hence a linearly polarized laser radiation can be generated. Besides, Er:YLF has longer fluorescence decay time at the upper laser level and lower phonon energy, which allows to generate laser radiation in CW regime with Watt-level output power, even if the YLF crystal has relatively low thermal conductivity, see section 5.8. Furthermore, Er:YLF possesses a broad emission spectrum which makes him an ideal candidate for generating short pulses in mode-locking regime, see Figure 7. Even though the results published in [RS10] did not reach the femtosecond range since the pulse duration was probably affected by water vapour occurring in laser resonator. The picosecond pulses could be advantageous for the medical applications [120]. It is presumable that using a hermetic chamber filled with dry air, helium or nitrogen will lead to a robust laser system with shorter pulse duration and higher repetition rate.

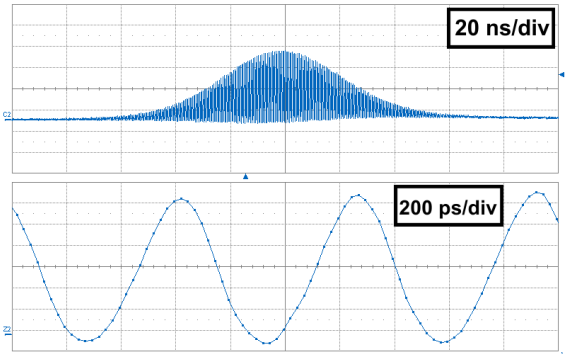

(a) Mode-locked pulse train.

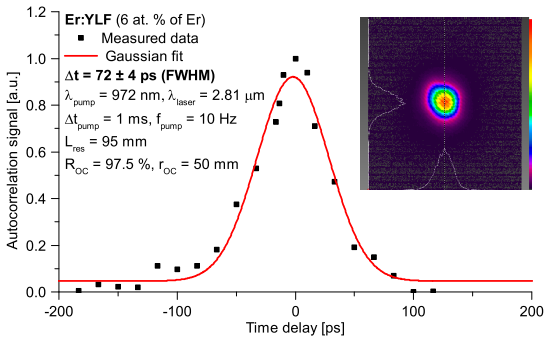

(b) Autocorrelation trace.

Figure 7: Mode-locked Er:YLF laser; Δt – mode-locked pulse duration, λ_{pump} and λ_{laser} – pumping and laser wavelength, Δt_{pump} – pumping pulse width, f_{pump} – frequency, L_{res} – resonator length, R_{OC} and r_{OC} – output coupler reflectivity and radius.

The Er:YLF laser emitted radiation at 2.81 µm in Q-switched mode-locking (QML) regime. The Q-switched pulses had the repetition rate 25 kHz, the pulse duration (FWHM) and energy of single Q-switched pulse envelope was 50.3 ns and 2.3 µJ, respectively. Using the two-photon absorption in a germanium detector the modulation inside envelop of the QML pulse and a train of mode locking pulses were observed. Due to the short laser resonator, the high repetition rate 1.41 GHz of mode-locking pulses was achieved. The mode-locked Er:YLF laser had mean energy per pulse equal to 9.9 nJ. Using a laboratory built interferometric autocorrelator based on two-photon absorption effect in germanium chip, the picosecond pulses were measured. The mode-locking pulse, presented in Figure 7, reached 72±4 ps at full-width half-maximum with the corresponding 137 W of peak power.

5.6 Er:YAG microchip for lasing in spectral range 2.94 µm and gain switching generation (2020 High-brightness Congress)

Even if the previous results present a compact laser system for generation short pulses, in principle it is possible to create a more compact and robust laser. If the dielectric layers representing a PM and OC are deposited directly to the faces of the active medium, a microchip laser can be create which brings a lot of benefits. The length of the resonator is given only by dimensions of active medium which allows to generate subnanosecond pulses (in the gain switching regime) without using special crystals or saturable absorber. Moreover, there are no more optical elements that have to be align. In cooperation with Crytur company, the Er:YAG microchip laser was prepared and for the first time the gain-switching regime was presented. It should be noted that the output energy and the slope efficiency were relatively low, it was probably given by the layers that form PM and OC mirrors. In future we would like to improve mainly these layers parametes.

The Er:YAG microchip laser emitted radiation at 2940 nm (linewidth 10 nm at FWHM) with maximal output energy 0.93 mJ and slope efficiency 8.4 ± 0.1 % in the pulsed regime. Microchip operates with repetition rate 100 Hz, duty cycle 10 % and emitted radiation close to a fundamental mode. Since using a higher duty cycle (higher pumping energy) causes a heavy thermal load of the crystal and roll-off output power the continuous wave operation cannot be obtained. During the gain switching experiments, the pumping pulse duration was set 120 µs and the repetition rate 400 Hz, using this setting, the gain switched pulse was generated 7 µs after the end of the pump pulse. The pulse duration 306±1 ns with the repetition rate 400 Hz and output energy 2.2 µJ with corresponding peak power 7.2 W was obtained [RS13].

5.7 Er:YLF microchip laser for free-running and gain-switching laser operation in spectral range 2.83 µm (Europhoton Conference 2020)

Together with Er:YAG, the dielectric layers were also deposited on Er:YLF crystal. The main advantage and properties of Er:YLF crystal was in detail discussed in sections 2.2.3 and 5.5. This paper [RS12] extended results presented in section 5.5 and shows that it is possible to prepare microchip laser emitting in spectral range 2.8 µm. Results presented in sections 5.6 and 5.7 are first successful attempt to generate short pulses in gain-switching regime and generate laser radiation from a microchip at ~ 3 µm. Even if the output presented in [RS12] is low and repetition rate of laser is limited by the capabilities of pumping laser diode, I believe that the simplicity and compactness of this laser source emitting at 2.8 µm is such beneficial that it outstrips all drawbacks. Since there are only several special fibres that can guide the wavelength in spectral range around 3 µm the microchip laser can be placed directly in laser head and only pumping radiation should be guided in fibre. This solution could simplify delivering ~ 3 µm laser radiation to a specific places during, for example, a surgery operation.

Results presented in [RS12] shows that Er:YLF microchip laser can emitted radiation in free-running regime with maximal output energy 3.21 mJ and slope efficiency 5 %. In gain-switching regime the shortest obtained pulses was 249 ± 1 ns with pulse energy 1.8 µJ and repetition rate 20 Hz. The corresponding peak power was 7.1 W.

5.8 Up to 3 W continuous power and 21 ns long pulses from 2.8 µm Er:YLF laser (ASSL 2020)

All benefits and qualities of Er:YLF were already discussed above. This paper is the result of the further research where this active medium was pushed to the bounds of possibility, hence it was possible to extract almost 3 W of in CW regime. Contrary to the results presented in [23, 61], where Er:YLF crystal was specially shaped, the [RS8] paper shows it is possible to reach Watt-level CW laser with a simple hemispherical resonator and a cylindrical plan-parallel crystal. Due to strong absorption (at 2.8 µm) and extremely short fluorescence decay time (hundreds of nanoseconds) of Fe:ZnSe polycrystal it is possible to generate high peak power in Q-switching regime which can be afterwards used in medicine or for polymer processing. In [RS8] it was shown that Er:YLF laser can operates up to 3 W of output power with slope efficiency 26.2 %, see Figure 8, which is one of the highest published results. To obtain Q-switching regime the Fe:ZnSe polycrystal was placed into laser resonator. The shortest reached pulse duration was 21 ± 1 ns (FWHM) with repetition rate 50 kHz. Laser emitted at 2.81 µm with maximal pulse energy 5.31 µJ and corresponding peak power 252 W.

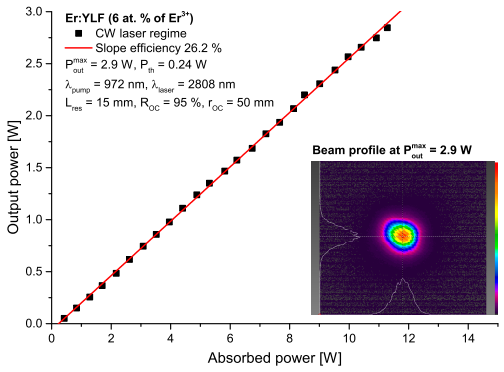

(a) Output CW laser characteristic.

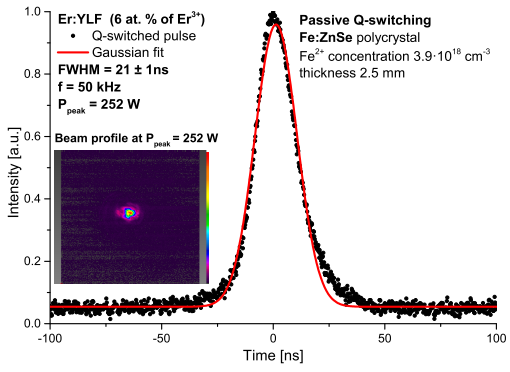

(b) Pulse duration of Q-switched pulse.

Figure 8: Characteristics of Er:YLF laser; λ_{pump} and λ_{laser} – pumping and laser wavelength, P_{out}^{max} – maximal output power, P_{th} – laser threshold, Δt – pumping pulse width, f – frequency, L_{res} – resonator length, R_{OC} and r_{OC} – output coupler reflectivity and radius.

6 Research outside topic of PhD thesis

This section contains selected results that are connected with the topic of PhD thesis, however, they are not belong to the scope of erbium-doped active media. The following results presented laser systems emitting radiation in mid-infrared spectral range, however, the active medium did not contain a Er^{3+} ion.

6.1 Compact Fe:ZnSe and Fe:ZnMnSe tunable lasers at 80 K pump with Er:YAG (Pacific Rim Conference, 2018)

One of the possible application of Er-doped lasers is converting $\sim$ 3 µm wavelength further to mid-infrared region. Fe:ZnMnSe crystals have a strong absorption peak at $\sim$ 3 µm which makes it possible to use erbium lasers as pumping sources. Depending on the concentration of manganese, the Fe:ZnMnSe lasers emitted radiation at 4.19 µm (Mn = 0 %), 4.41 µm (Mn = 0.05 %), and 4.53 µm (Mn = 0.2 %). Moreover, the wavelength of Fe:ZnMnSe laser can be tuned in the wide spectral range from 3.95 µm to 4.83 µm, see [RSadd5]. In [RSadd5], the compact laser system with direct wavelength conversion from 965 nm (laser diode) to 2.94 µm (Er:YAG laser), and to 4.5 µm (Fe:ZnMnSe laser) was proposed and successfully tested. Such a laser setup can be further reduced to a microchip system and used in various branches; medicine (non-invasive laser diagnostic), military (rangefinders, target aiming) or in spectroscopy (remote sensing of gas). Nowadays, Fe:ZnSe lasers are based on flash-lamp, hybrid (fibre-bulk laser system) or chemical (HF – Hydrogen fluoride) pumping. These setups allow to extract high output energy but on the other hand, the whole laser systems are complex with many optical components and not suitable for field application.

6.2 Diode-pumped laser and spectroscopic properties of Yb,Ho:GGAG at 2 µm and 3 µm (Laser Physics Letters, 2020)

As discussed in sections 2.2.1 and 5.3 Er:GGAG active medium possesses broad band absorption and emission spectra due to the mixed garnet structure. Similar effect should be observed if the Yb^{3+} together with Ho^{3+} is doped into GGAG matrix. From the energy levels presented in Figure 9 it is obvious that Yb,Ho:GGAG should emit laser radiation at 2.94 µm [RSadd6]. Together with colleagues from the Institute of Physics of the Czech Academy of Science, Yb,Ho:GGAG active medium was grown and from the results published in [RSadd6], it follows that using multicomponent mixed garnet structure, such as GGAG, allows the broadband tuning of emitting laser wavelength near 2.94 µm. There are several lasers (e.g., Er:YLF or Er:SrF_2) which are able to tune the emitting wavelength in a wide spectral range, however, these wavelengths are located mainly around 2840 nm. The Yb,Ho:GGAG (similarly to Er:GGAG) allows wavelength tuning around 2.94 µm which is closer to the main absorption peak of water thus it can be beneficial in potential medical applications, see details in [RSadd7]. Er:YAG also lase at 2.94 µm but due to the sharp and narrow emission spectrum, this laser wavelength cannot be tuned. We believe that with Yb,Ho:GGAG it is possible to generate 2091 nm and 2942 nm also simultaneously in the cascade laser regime.

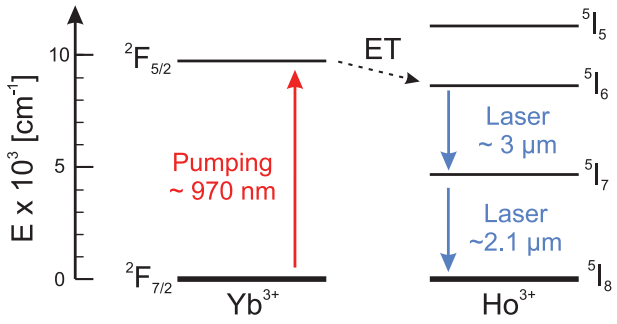

Figure 9: Simplify energy levels of Yb, Ho-doped active medium, ET - energy transfer

7 Conclusion

This PhD thesis is a summary of the applicant's research work that was focused on erbium-doped bulk active materials emitting laser radiation in the mid-infrared spectral range from 2.5 µm to 3 µm operating under diode pumping. Moreover, in section 6 readers can find a summary of selected research which were performed out of the topic of the PhD thesis.

7.1 Summary of achieved results

The material parameters and the best obtained results (maximal output power and slope efficiency, tunability range) of Er-doped laser active media are summarized in the state of the art (section 2). For several laser active media, the experimental data obtained and presented in this study represent unique results which can be further utilized in the development of new active media and laser systems. Thanks to cooling to cryogenic temperature, the laser action at 2.73 µm was for the first time obtained with the low doped Er:YAP crystal [RS4]. These results lead to testing Er(5 at. %):YAP and reach CW laser operation with output power 6.9 W and slope efficiency 30.6 % [8]. During the ongoing research of Er-doped active media, a new mixed garnet structure Er:GGAG crystal was prepared and for the first time a laser action in pulsed and CW regime was achieved with this active medium [RS3]. The multi-structure Er:GGAG possesses broad spectral lines and allows wavelength tuning, thus the Er:GGAG can be an alternative to the widely used Er:YAG crystals. The well-known Er:YLF active medium was deeply studied and it was shown that it is possible to generate up to 3 W CW output power, Q-switched pulses with duration 21 ns and peak power 252 W. In the mode-locking regime, it is possible to obtain GHz repetition rate and picosecond pulses if the short V-shape resonator is used [RS8, RS10, RS12]. It is worthy to note that from the point of view the future application (cutting, drilling, welding, material processing, and further wavelength conversion), the Er:YAP and Er:YLF are most probably candidates since they can generate a Watt-level output power directly from diode-pumped laser oscillator.

In addition, it should be mentioned that not all research work that was carried out by the applicant during PhD studies is presented in this thesis. In principle, it was not possible to include all research since the whole thesis could become extremely voluminous. At least, several papers (not included in appendix) that should be additionally mentioned and they can be downloaded from publisher's servers are the following:

- Researching of temperature influence on Er,La:SrF_2-CaF_2 [RS2], Er:YLF [RS15], and Er:GGAG [RS16] crystals in temperature range from 80 K to 300 K.
- Generating short pulses in Q-switching regime with Er,La:SrF_2-CaF_2 crystal [RS17] and Er:Y_2O_3 ceramic [RS18].
- Testing of Dy^{2+}:CaF_2 [RSadd7] and Tm:SBM [RSadd8] active media at cryogenic temperature for potential using as laser sources.
- Spectroscopy and laser properties of low doped crystals Er:GGAG [RSadd9] and Er:YAP [RSadd10] emitting around wavelength 1.6 µm.

7.2 Contributions to the progress of science and industry

As stated in the text above, the results obtained and presented in this thesis can be considered unique since it was presented for the first time. However, from the point of view of contribution to the progress of science and industry, the results of the PhD thesis can be summarized as follows:

1. Research of new active laser materials and designing of microchip lasers
    - Er:GGAG crystal was proposed, grown according to our suggestion and consequently spectroscopy and laser experiments were performed in our laboratory. Based on these results, in detail described above, the concentration series of Er:GGAG with Er^{3+} concentration from 4.4 % to 32 % was grown and comparative study is now carried out. Moreover, the co-doping of Er:GGAG with

Pr^{3+} ion was proposed to improve the ratio between fluorescence lifetimes at lower and upper laser levels and consequently gain higher laser output power and efficiency. Data from this measurement has been evaluated and writing of a paper is in process.

- After researching Er:YAP crystal it was proposed that erbium concentration around 5 % should be ideal for lasing at $\sim$ 3 µm. This was confirmed in [8] and it is obvious that 6.9 W CW output power at 2.9 µm is high enough to be used in applications.
- To design extremely compact laser system two microchip lasers Er:YAG and Er:YLF were designed and fabricated. Due to dimensions of microchip, it was possible to generate short pulses (in gain-switching regime) without using addition optics, special crystals, or high voltage.

2. Generation of short pulses in $\sim$ 3 µm spectral range

   - Several tested active media successfully generate short pulses in gain-switching, Q-switching, and mode-locking regime. Primarily mode-locking results are unique since it was the first result obtained with laser diode pumped bulk active media at a spectral range $\sim$ 3 µm with repetition rage reaching GHz region. On the other hand, high power Q-switched pulses can be used in medicine (dentistry or surgery) for drilling, cutting as well as in industry for polymer processing.
   - As mentioned above, the microchip lasers are extremely compact and it allows to generate short pulses (hundreds of nanoseconds) in the gain-switching regime. Such laser construction allows to simplify a guiding of laser radiation in some application for example in dentistry, as discussed above.

3. Laboratory and measurement improvements

   - During all experiments, it was necessary to collect and process a large amount of data. For this reason, the automatization of the measurement was a reasonable decision. During the experimental work on a PhD thesis, several programs

in LabVIEW (National Instruments) and MATLAB were written. Particularly, it was a program for controlling various instruments (Tektronix oscilloscopes, LIMO laser diode drivers, LakeShore temperature driver, Molectron and Thorlabs power meters, and linear servo motors.) In addition, several scripts in MATLAB were written for data processing. These automatizations significantly simplify collecting and processing data from experiments and can be further used in future experimental work in a laboratory.

- One of the main problem connected with measurement was the detection of picoseconds pulses at 2.8 µm. This was achieved by building an autocorrelator based on two-photon absorption in germanium chip, see details in section 4. This laboratory built device can be also used in future experiments dealing with an investigation of short pulses in the mid-infrared spectral region.

To conclude, the results presented in the PhD thesis are unique and have the potential for utilization in applications. Moreover, all results presented in this PhD thesis are well supported by papers published at international conferences and in impacted journals, which should prove that results are significant for the scientific community and research in general. Moreover, the whole theoretical part (section 2) is based on an extensive paper published in Progress in Quantum Electronics. The methodology, used apparatus and experimental arrangements, and the obtained results are in detail discussed in this papers too. Regarding the above mentioned, I believe all goals presented in section 3 were successfully done and the aims of PhD thesis were fulfilled.

List of Figures

List of Tables

Bibliography

[1] Jelínková, H., ed.: *Lasers for medical applications Diagnostics, therapy and surgery*, Woodhead Publishing Limited, 1st ed., 2013, ISBN 978-0-85709-754-5.

[2] Paschotta, R.: *Encyclopedia of Laser Physics and Technology*, Wiley-VCH, 2008, ISBN 978-3-527-40828-3.

[3] Godard, A.: Infrared (2-12 µm) solid-state laser sources: a review, *Comptes Rendus Physique*, 2007, **vol. 8(10)**, pp. 1100 – 1128, doi:10.1016/j.crhy.2007.09.010.

[4] Fedorov, V. V., Mirov, S. B., Gallian, A., Badikov, D. V., Frolov, M. P., Korostelin, Y. V., Kozlovsky, V. I., Landman, A. I., Podmar'kov, Y. P., Akimov, V. A., Voronov, A. A.: 3.77-5.05- µm tunable solid-state lasers based on Fe^{2+}-doped ZnSe crystals operating at low and room temperatures, *IEEE Journal of Quantum Electronics*, Sept 2006, **vol. 42(9)**, pp. 907–917, ISSN 0018-9197, doi:10.1109/JQE.2006.880119.

[5] Shen, D. Y., Sahu, J. K., Clarkson, W. A.: Highly efficient in-band pumped Er:YAG laser with 60 W of output at 1645 nm, *Opt. Lett.*, Mar 2006, **vol. 31(6)**, pp. 754–756, doi:10.1364/OL.31.000754.

[6] Spariosu, K., Birnbaum, M.: Room-Temperature 1.644 Micron Er:YAG Lasers, in *Advanced Solid State Lasers*, Optical Society of America, 1992 p. ML4, doi:10.1364/ASSL.1992.ML4.

[7] Koechner, W.: *Solid-State Laser Engeneering*, Springer Science+Business Media, 2006, ISBN 0-387-29338-8.

[8] Yao, W., Uehara, H., Kawase, H., Chen, H., Yasuhara, R.: Highly efficient Er:YAP laser with 6.9 W of output power at 2920 nm, *Opt. Express*, Jun 2020, **vol. 28(13)**, pp. 19000–19007, doi:10.1364/OE.395802.

[9] Liu, J., Feng, X., Fan, X., Zhang, Z., Zhang, B., Liu, J., Su, L.: Efficient continuous-wave and passive Q-switched mode-locked Er:CaF_2-SrF_2 lasers in the mid-infrared region, *Opt. Lett.*, May 2018, **vol. 43(10)**, pp. 2418–2421, doi:10.1364/OL.43.002418.

[10] Aydin, Y. O., Fortin, V., Maes, F., Jobin, F., Jackson, S. D., Vallée, R., Bernier, M.: High efficiency cascade fiber laser at 2.8 µm, in *2017 Conference on Lasers and Electro-Optics Europe European Quantum Electronics Conference (CLEO/Europe-EQEC)*, June 2017 pp. 1–1, doi:10.1109/CLEOE-EQEC.2017.8087045.

[11] Pinto, J. F., Rosenblatt, G. H., Esterowitz, L.: Continuous-wave laser action in Er^{3+}:YLF at 3.41 µm, *Electronics Letters*, Sep 1994, **vol. 30(19)**, pp. 1596–1598, ISSN 0013-5194, doi:10.1049/el:19941085.

[12] Brede, R., Danger, T., Heumann, E., Huber, G., Chai, B.: Room-temperature green laser emission of Er:$LiYF_4$, *Applied Physics Letters*, 1993, **vol. 63(6)**, pp. 729–730, doi:10.1063/1.109942.

[13] Ter-Gabrielyan, N., Fromzel, V.: Cascade generation at 1.62, 1.73 and 2.8 µm in the Er:YLF Q-switched laser, *Opt. Express*, Jul 2019, **vol. 27(15)**, pp. 20199–20210, doi:10.1364/OE.27.020199.

[14] Sanamyan, T.: Efficient cryogenic mid-IR and eye-safe Er:YAG laser, *J. Opt. Soc. Am. B*, Nov 2016, **vol. 33(11)**, pp. D1–D6, doi:10.1364/JOSAB.33.0000D1.

[15] Haynes, W. M., Lide, D. R., Bruno, T. J.: *CRC Handbook of Chemistry and Physics (2016-2017)*, CRC Press, 97th ed., 2017, ISBN 978-1-4987-5429-3.

[16] Desurvire, E.: *Erbium-Doped Fiber Amplifiers*, John Wiley and Sons, Inc., 1994, ISBN 0-471-58977-2.

[17] Kaminskii, A. A.: *Laser Crystals - Their Physics and Properties*, Springer-Verlag Berlin Heidelberg GmbH, 2nd ed., 1990, ISBN 978-3-540-70749-3.

[18] Weber, M. J., ed.: *Handbook of Laser Wavelength*, CRC press, 1996, ISBN 0-8493-3508-6.

[19] Ter-Gabrielyan, N., Dubinskii, M., Newburgh, G. A., Michael, A., Merkle, L. D.: Temperature Dependence of a Diode-Pumped Cryogenic Er:YAG laser, *Opt. Express*, Apr 2009, **vol. 17(9)**, pp. 7159–7169, doi:10.1364/OE.17.007159.

[20] Basiev, T. T., Orlovskii, Y. V., Polyachenkova, M. V., Fedorov, P. P., Kuznetsov, S. V., V. A. Konyushkin, V. A., Osiko, V. V., Alimov, O. K., Dergachev, A. Y.: Continuously tunable cw lasing near 2.75 µm in diode-pumped Er^{3+}:SrF_2 and Er^{3+}:CaF_2 crystals, *Quant. Electr.*, 2006, **vol. 36**, pp. 591–594, doi:10.1070/QE2006v036n07ABEH013178.

[21] Labbe, C., Doualan, J., Camy, P., Moncorgé, R., Thuau, M.: The 2.8 µm laser properties of Er^{3+} doped CaF_2 crystals, *Optics Communications*, 2002, **vol. 209(1)**, pp. 193 – 199, ISSN 0030-4018, doi:10.1016/S0030-4018(02)01628-0.

[22] Ma, W., Qian, X., Wang, J., Liu, J., Fan, X., Liu, J., Su, L., Xu, J.: Highly efficient dual-wavelength mid-infrared CW laser in diode end-pumped Er:SrF_2 single crystals, *Scientific Reports*, 11 2016, **vol. 6(36635)**, p. 36635, doi:10.1038/srep36635.

[23] Messner, M., Heinrich, A., Unterrainer, K.: High-energy diode side-pumped Er:$LiYF_4$ laser, *Appl. Opt.*, Feb 2018, **vol. 57(6)**, pp. 1497–1503, doi:10.1364/AO.57.001497.

[24] Li, C., Liu, J., Jiang, S., Xu, S., Ma, W., Wang, J., Xu, X., Su, L.: 2.8 µm passively Q-switched Er:CaF_2 diode-pumped laser, *Opt. Mater. Express*, May 2016, **vol. 6(5)**, pp. 1570–1575, doi:10.1364/OME.6.001570.

[25] Silversmith, A. J., Lenth, W., Macfarlane, R. M.: Green infrared pumped erbium upconversion laser, *Applied Physics Letters*, 1987, **vol. 51(24)**, pp. 1977–1979, doi:10.1063/1.98316.

[26] Vetrone, F., Boyer, J.-C., Capobianco, J. A., Speghini, A., Bettinelli, M.: Luminescence Spectroscopy and Near-Infrared to Visible Upconversion of Nanocrystalline $Gd_3Ga_5O_{12}$:Er^{3+}, *Journal of Physical Chemistry B*, 2003, **vol. 107**, pp. 10747–10752, doi:10.1021/jp030434r.

[27] Lupei, V.: RE^{3+} emission in garnets: multisites, energy transfer and quantum efficiency, *Optical Materials*, 2002, **vol. 19(1)**, pp. 95 – 107, doi:10.1016/S0925-3467(01)00206-3.

[28] Dobrzycki, L., Bulska, E., Pawlak, D. A., Frukacz, Z., Woźniak, K.: Structure of YAG Crystals Doped/Substituted with Erbium and Ytterbium, *Inorganic Chemistry*, 2004, **vol. 43**, pp. 7656–7664, doi:10.1021/ic049920z.

[29] Šulc, J., Boháček, P., Němec, M., Jelínková, H., Trunda, B., Havlák, L., Jurek, K., Nikl, M.: Tunable diode-pumped Er:GGAG laser, in *2016 International Conference Laser Optics (LO)*, June 2016 pp. R1–64–R1–64, doi:10.1109/LO.2016.7549682.

[30] You, Z., Wang, Y., Xu, J., Zhu, Z., Li, J., Tu, C.: Diode-End-Pumped Mid-infrared Multiwavelength Er:Pr:GGG laser, *IEEE Photonics Technology Letters*, April 2014, **vol. 26(7)**, pp. 667–670, ISSN 1041-1135, doi:10.1109/LPT.2014.2302837.

[31] Dinerman, B. J., Moulton, P. F.: 3-µm cw laser operations in erbium-doped YSGG, GGG, and YAG, *Opt. Lett.*, Aug 1994, **vol. 19(15)**, pp. 1143–1145, doi:10.1364/OL.19.001143.

[32] Tempus, M., Luthy, W., Weber, H. P., Ostroumov, V. G., Shcherbakov, I. A.: 2.79 µm YSGG:Cr:Er laser pumped at 790 nm, *IEEE Journal of Quantum Electronics*, Nov 1994, **vol. 30(11)**, pp. 2608–2611, ISSN 0018-9197, doi:10.1109/3.333714.

[33] Henderson, B., Bartram, R. H.: *Crystal-field engineering of solid-state laser materials*, Cambridge University Press, Cambridge, 2000, ISBN 9780511524165, doi:10.1017/CBO9780511524165.

[34] Skorczakowski, M., Swiderski, J., Pichola, W., Nyga, P., Zajac, A., Maciejewska, M., Galecki, L., Kasprzak, J., Gross, S., Heinrich, A., Bragagna, T.: Mid-infrared Q-switched Er:YAG laser for medical applications, *Laser Physics Letters*, 2010, **vol. 7(7)**, p. 498, doi:10.1002/lapl.201010019.

[35] Volkova, N. V., Glazkova, L. K., Khomchenko, V. V., Sadick, N. S.: Novel method for facial rejuvenation using Er:YAG laser equipped with a spatially modulated ablation module: An open prospective uncontrolled cohort study, *Journal of Cosmetic and Laser Therapy*, 2017, **vol. 19**, pp. 25–29, doi:10.1080/14764172.2016.1247964.

[36] Maurizio, P., Konstanze, S., Roland, K.: Er:YAG Laser–Assisted Hair Transplantation in Cicatricial Alopecia, *Dermatologic Surgery*, 2001, **vol. 26(11)**, pp. 1010–1014, doi:10.1046/j.1524-4725.2000.0260111010.x.

[37] Jew, J., Chan, K. H., Darling, C. L., Fried, D.: Selective removal of natural caries lesions from dentin and tooth occlusal surfaces using a diode-pumped Er:YAG laser, in P. Rechmann, D. Fried, eds., *SPIE Proceedings: Lasers in Dentistry XXIII*, vol. 10044, 2017 pp. 10044–10049, doi:10.1117/12.2256728.

[38] Yang, J., Wang, L., Wu, X., Cheng, T., Jiang, H.: High peak power Q-switched Er:YAG laser with two polarizers and its ablation performance for hard dental tissues, *Opt. Express*, Jun 2014, **vol. 22(13)**, pp. 15686–15696, doi:10.1364/OE.22.015686.

[39] Messner, M., Heinrich, A., Hagen, C., Unterrainer, K.: High brightness diode pumped Er:YAG laser system at 2.94 µm with nearly 1kW peak power, in W. A. Clarkson, R. K. Shori, eds., *SPIE Proceedings: Solid State Lasers XXV: Technology and Devices*, vol. 9726, 2016 pp. 9726–6, doi:10.1117/12.2209098.

[40] Stock, K., Diebolder, R., Hausladen, F., Hibst, R.: Efficient bone cutting with the novel diode pumped Er:YAG laser system: in vitro investigation and optimization of the treatment parameters, in B. Choi, et al., eds., *SPIE Proceedings:*

Photonic Therapeutics and Diagnostics X, vol. 8926, 2014 pp. 8926 – 8926 – 10, doi:10.1117/12.2039648.

[41] Wang, J., Zhang, Z., Xu, J., Xu, J., Fu, P., Liu, U., Baining Taeuber, Eichler, H. J., Dicninig, A., Huber, G., Yan, X., Wu, X., Jiang, Y.: Spectroscopic properties and 3-µm lasing of Er^{3+}:YVO_4 crystals, in S.-S. Mei, K. A. Truesdell, eds., *High-Power Lasers: Solid State, Gas, Excimer, and Other Advanced Lasers II*, vol. 3549, 1998 pp. 3549–3549, doi:10.1117/12.344113.

[42] Weber, M. J., ed.: *Handbook of Optical Materials*, CRC press, 2003, ISBN 0-8493-3512-4.

[43] Wang, S., Wu, K., Wang, Y., Yu, H., Zhang, H., Tian, X., Dai, Q., Liu, J.: Spectral and lasing investigations of Yb:YSGG crystal, *Opt. Express*, Jul 2013, **vol. 21(14)**, pp. 16305–16310, doi:10.1364/OE.21.016305.

[44] Wang, J., Cheng, T., Wang, L., Yang, J., Sun, D., Yin, S., Wu, X., Jiang, H.: Compensation of strong thermal lensing in an LD side-pumped high-power Er:YSGG laser, *Laser Physics Letters*, 2015, **vol. 12(10)**, p. 105004, doi:10.1088/1612-2011/12/10/105004.

[45] Arutyunyan, S. M., Kostanyan, R. B., Petrosyan, A. G., Sanamyan, T. V.: $YAlO_3$:Er^{3+} crystal laser, *Soviet Journal of Quantum Electronics*, 1987, **vol. 17(8)**, p. 1010.

[46] Kaminskii, A. A., Butaeva, T., Ivanov, A., Mochalov, I., Petrosyan, A., Rogov, G., Fedorov, V.: New data on stimulated emission of crystals containing Er^{3+} and Ho^{3+} ions, *Sov. Tech. Phys. Lett.*, 1976, **vol. 2(9)**, pp. 308–310.

[47] Frauchiger, J., Lüthy, W., Albers, P., Weber, H. P.: Laser properties of selectively excited $YAlO_3$:Er, *Opt. Lett.*, Nov 1988, **vol. 13(11)**, pp. 964–966, doi:10.1364/OL.13.000964.

[48] Lüthy, W., Stalder, M., Weber, K. P.: Spectroscopy of the 3 µm Laser Transitions in $YAlO_3$:Er, in W. Persson, S. Svanberg, eds., *Laser Spectroscopy VIII*, Springer Berlin Heidelberg, Berlin, Heidelberg, ISBN 978-3-540-47973-4, 1987 pp. 420–421.

[49] Stalder, M., Lüthy, W., Weber, H. P.: Five new 3-µm laser lines in $YAlO_3$:Er, *Opt. Lett.*, Aug 1987, **vol. 12(8)**, pp. 602–604, doi:10.1364/OL.12.000602.

[50] Sorokin, P. P., Stevenson, M. J.: Stimulated infrared emission from trivalent uranium, *Physical Review Letters*, 1960, **vol. 5**, pp. 557–559, doi:10.1103/PhysRevLett.5.557.

[51] Pollack, S. A., Chang, D. B., Moise, N. L.: Upconversion–pumped infrared erbium laser, *Journal of Applied Physics*, 1986, **vol. 60(12)**, pp. 4077–4086, doi:10.1063/1.337486.

[52] Baker, J., Davies, E., Hurrell, J.: Charge compensation in calcium fluoride doped with trivalent rare-earth ions at tetragonal sites, *Physics Letters A*, 1968, **vol. 26**, pp. 352–353, doi:10.1016/0375-9601(68)90368-x.

[53] Kolesnikov, N., ed.: *Modern Aspects of Bulk Crystal and Thin Film Preparation*, Intech, 2012, ISBN 978-953-307-610-2, doi:10.5772/1348.

[54] Su, L., Guo, X., Jiang, D., Wu, Q., Qin, Z., Xie, G.: Highly-efficient mid-infrared CW laser operation in a lightly-doped 3 at.% Er:SrF_2 single crystal, *Opt. Express*, Mar 2018, **vol. 26(5)**, pp. 5558–5563, doi:10.1364/OE.26.005558.

[55] Liu, J., Liu, J., Guo, Z., Zhang, H., Ma, W., Wang, J., Su, L.: Dual-wavelength Q-switched Er:SrF_2 laser with a black phosphorus absorber in the mid-infrared region, *Opt. Express*, Dec 2016, **vol. 24(26)**, pp. 30289–30295, doi:10.1364/OE.24.030289.

[56] Gao, W., Wang, R., Han, Q., Dong, J., Yan, L., Zheng, H.: Tuning Red Upconversion Emission in Single $LiYF_4$:Yb^{3+}/Ho^{3+} Microparticle, *The Journal of Physical Chemistry C*, 01 2015, pp. 2349–2355, doi:10.1021/jp511566h.

[57] Authier, A.: *International Tables for Crystallography*, Springer, 1st ed., 2003, ISBN 1-4020-0714-0.

[58] Jensen, T., Diening, A., Huber, G., Chai, B. H. T.: Investigation of diode-pumped 2.8-µm Er:$LiYF_4$ lasers with various doping levels, *Opt. Lett.*, Apr 1996, **vol. 21(8)**, pp. 585–587, doi:10.1364/OL.21.000585.

[59] Inochkin, M. V., Korostelin, Y. V., Landman, A. I., Nazarov, V. V., Sachkov, D. Y., Podmar'kov, Y. P., Frolov, M. P., Khloponin, L. V., Khramov, V. Y.: A compact Er:YLF laser with a passive Fe^{2+}:ZnSe shutter, *J. Opt. Technol.*, Jun 2012, **vol. 79(6)**, pp. 337–339, doi:10.1364/JOT.79.000337.

[60] Pollnau, M., Graf, T., Balmer, J. E., Lüthy, W., Weber, H. P.: Explanation of the cw operation of the Er^{3+} 3-µm crystal laser, *Phys. Rev. A*, May 1994, **vol. 49**, pp. 3990–3996, doi:10.1103/PhysRevA.49.3990.

[61] Dergachev, A., Moulton, P. F.: Tunable CW Er:YLF Diode-Pumped Laser, in *Advanced Solid-State Photonics*, Optical Society of America, 2003 p. 3, doi:10.1364/ASSP.2003.3.

[62] Kränkel, C.: Rare-Earth-Doped Sesquioxides for Diode-Pumped High-Power Lasers in the 1-, 2-, and 3- µm Spectral Range, *IEEE Journal of Selected Topics in Quantum Electronics*, Jan 2015, **vol. 21(1)**, pp. 250–262, ISSN 1077-260X, doi:10.1109/JSTQE.2014.2346618.

[63] Capper, P., Rudolph, P., eds.: *Crystal Growth Technology: Semiconductors and Dielectrics*, Wiley-VCH, 2010, ISBN 978-3-527-32593-1.

[64] Snetkov, I. L., Silin, D. E., Palashov, O. V., Khazanov, E. A., Yagi, H., Yanagitani, T., Yoneda, H., Shirakawa, A., Ueda, K., Kaminskii, A. A.: Study of the thermo-optical constants of Yb doped Y_2O_3, Lu_2O_3 and Sc_2O_3 ceramic materials, *Opt. Express*, Sep 2013, **vol. 21(18)**, pp. 21254–21263, doi:10.1364/OE.21.021254.

[65] Wang, L., Huang, H., Shen, D., Zhang, J., Chen, H., Tang, D.: Diode-pumped high power 2.7 µm Er:Y_2O_3 ceramic laser at room temperature, *Optical Materials*, 2017, **vol. 71**, pp. 70 – 73, doi:10.1016/j.optmat.2016.06.014.

[66] Uehara, H., Tokita, S., Kawanaka, J., Konishi, D., Murakami, M., Shimizu, S., Yasuhara, R.: Optimization of laser emission at 2.8 µm by Er:Lu_2O_3 ceramics, *Opt. Express*, Feb 2018, **vol. 26(3)**, pp. 3497–3507, doi:10.1364/OE.26.003497.

[67] Sanamyan, T., Pavlacka, R., Gilde, G., Dubinskii, M.: Spectroscopic properties of Er^{3+}-doped α-Al_2O_3, *Optical Materials*, 2013, **vol. 35(5)**, pp. 821 – 826, ISSN 0925-3467, doi:10.1016/j.optmat.2012.10.036.

[68] Ryba-Romanowski, W., Lisiecki, R., Jelínková, H., Šulc, J.: Thulium-doped vanadate crystals: Growth, spectroscopy and laser performance, *Progress in Quantum Electronics*, 2011, **vol. 35(5)**, pp. 109 – 157, ISSN 0079-6727, doi:10.1016/j.pquantelec.2011.06.001.

[69] Ter-Gabrielyan, N., Fromzel, V., Dubinskii, M.: Record-low quantum defect operation of an eye-safe Er-doped laser, *Laser Physics Letters*, 2016, **vol. 13(11)**, p. 115001, doi:10.1088/1612-2011/13/11/115001.

[70] Ter-Gabrielyan, N., Fromzel, V.: Wavelength tuning in cryogenically cooled lasers based on Er-doped orthovanadates, *Appl. Opt.*, Jan 2017, **vol. 56(3)**, pp. B70–B73, doi:10.1364/AO.56.000B70.

[71] Miller, S. A., Caspers, H. H., Rast, H. E.: Lattice Vibrations of Yttrium Vanadate, *Phys. Rev.*, Apr 1968, **vol. 168**, pp. 964–969, doi:10.1103/PhysRev.168.964.

[72] Serres, J. M., Loiko, P., Jambunathan, V., Mateos, X., Vitkin, V., Lucianetti, A., Mocek, T., Aguiló, M., Díaz, F., Griebner, U., Petrov, V.: Efficient diode-pumped Er:$KLu(WO_4)_2$ laser at $\sim$ 1.61 µm, *Opt. Lett.*, Jan 2018, **vol. 43(2)**, pp. 218–221, doi:10.1364/OL.43.000218.

[73] Pujol, M., Rico, M., Zaldo, C., Solé, R., Nikolov, V., Solans, X., Aguiló, M., Díaz, F.: Crystalline structure and optical spectroscopy of Er^{3+}-doped $KGd(WO_4)_2$ single crystals, *Applied Physics B*, Feb 1999, **vol. 68(2)**, pp. 187–197, ISSN 1432-0649, doi:10.1007/s003400050605.

[74] Aggarwal, R. L., Ripin, D. J., Ochoa, J. R., Fan, T. Y.: Measurement of thermo-optic properties of $Y_3Al_5O_{12}$, $Lu_3Al_5O_{12}$, $YAlO_3$, LiF_4, $LiLuF_4$, BaY_2F_8, $KGd(WO_4)_2$, and $KY(WO_4)_2$ laser crystals in the 80-300 K, *Journal of Applied Physics*, 2005, **vol. 98(10)**, p. 14, doi:10.1063/1.2128696.

[75] Kuleshov, N. V., Lagatsky, A. A., Podlipensky, A. V., Mikhailov, V. P., Kornienko, A. A., Dunina, E. B., Hartung, S., Huber, G.: Fluorescence dynamics, excited-state absorption, and stimulated emission of Er^{3+} in $KY(WO_4)_2$, *Journal of the Optical Society of America B*, Mar 1998, **vol. 15(3)**, pp. 1205–1212, doi:10.1364/JOSAB.15.001205.

[76] Rico, M., Liu, J., Griebner, U., Petrov, V., Serrano, M. D., Esteban-Betegón, F., Cascales, C., Zaldo, C.: Tunable laser operation of ytterbium in disordered single crystals of Yb:$NaGd(WO_4)_2$, *Optics Express*, 2004, **vol. 12**, pp. 5362–0, doi:10.1364/OPEX.12.005362.

[77] Zhang, Y., Gong, W., Yu, J., Lin, Y., Ning, G.: Tunable white-light emission via energy transfer in single-phase $LiGd(WO_4)_2$:Re^{3+}(Re=Tm, Tb, Dy, Eu) phosphors for UV-excited WLEDs, *RSC Advances*, 2015, doi:10.1039/C5RA19345A.

[78] Borowiec, M., Zayarnyuk, T., Pujol, M., Aguiló, M., Díaz, F., Zubov, E., Prokhorov, A., Berkowski, M., Domuchowski, W., Wisniewski, A., Puzniak, R., Pietosa, J., Dyakonov, V., Baranski, M., Szymczak, H.: Magnetic properties of $KRE(WO_4)_2$ (RE=Gd, Yb, Tm) single crystals, *Physica B: Condensed Matter*, 2010, **vol. 405(23)**, pp. 4886 – 4891, doi:10.1016/j.physb.2010.09.028.

[79] Enrique, B. G.: Optical Spectrum and Magnetic Properties of Er^{3+} in $CaWO_4$, *The Journal of Chemical Physics*, 1971, **vol. 55**, pp. 2538–, doi:10.1063/1.1676445.

[80] Arora, S. K., Chudasama, B.: Crystallization and optical properties of $CaWO_4$ and $SrWO_4$, *Crystal Research and Technology*, 2006, **vol. 41**, pp. 1089–1095, doi:10.1002/crat.200610727.

[81] Gorbachenya, K. N., Kisel, V. E., Yasukevich, A. S., Pavlyuk, A. A., Kuleshov, N. V.: In-band pumped room-temperature Er:$KY(WO_4)_2$ laser emitting around 1.6 µm, *Laser Physics Letters*, 2013, **vol. 23(12)**, p. 125005, doi:10.1088/1054-660X/23/12/125005.

[82] Gorbachenya, K., Kisel, V., Kurilchik, S., Yasukevich, A., Korableva, S., Semashko, V., Pavlyuk, A., Kuleshov, N.: Er:$KY(WO_4)_2$ and Er:$LiYF_4$ Crystals for Eye-Safe In-Band Pumped Lasers, in *Advanced Solid State Lasers*, Optical Society of America, 2015 p. AM5A.14, doi:10.1364/ASSL.2015.AM5A.14.

[83] Kaminskii, A. A., Pavlyuk, A. A., Butaeva, T. I., Fedorov, V. A., Balashov, I. F., Berenberg, V. A., Lyubchenko, V. V.: Stimulated emission by subsidiary transition of Ho^{3+} and Er^{3+} - ions in $KGd(WO_4)_2$, *Inorganic materials*, 1977, **vol. 13(8)**, pp. 1251–1252.

[84] Kaminskii, A. A., Pavlyuk, A. A., Balashov, I. F., et al.: Stimulated emission by $KY(WO_4)_2$-Er^{3+} crystal at 0.85, 1.73 and 2.8 µm at 300 K, *Inorganic materials*, 1978, **vol. 14(12)**, pp. 1765–1767.

[85] Di, J., Sun, X., Xu, X., Xia, C., Sai, Q., Yu, H., Wang, Y., Zhu, L., Gao, Y., Guo, X.: Growth and spectral characters of Nd:$CaGdAlO_4$ crystal, *The European Physical Journal Applied Physics*, 04 2016, **vol. 74**, doi:10.1051/epjap/2016150511.

[86] Wells, J.-P. R., Yamaga, M., Kodama, N., Han, T. P. J.: Polarized laser spectroscopy and crystal-field analysis of Er^{3+} doped $CaGdAlO_4$, *Journal of Physics: Condensed Matter*, 1999, **vol. 11(39)**, p. 7545, doi:10.1088/0953-8984/11/39/310.

[87] Zhu, Z., Li, J., You, Z., Wang, Y., Lv, S., Ma, E., Xu, J., Wang, H., Tu, C.: Benefit of Pr^{3+} ions to the spectral properties of Pr^{3+}/Er^{3+}:$CaGdAlO_4$ crystal for a 2.7 µm laser, *Opt. Lett.*, Dec 2012, **vol. 37(23)**, pp. 4838–4840, doi:10.1364/OL.37.004838.

[88] Deters, H., de Camargo, A. S. S., Santos, C. N., Ferrari, C. R., Hernandes, A. C., Ibanez, A., Rinke, M. T., Eckert, H.: Structural Characterization of Rare-Earth Doped Yttrium Aluminoborate Laser Glasses Using Solid State NMR, *The Journal of Physical Chemistry C*, 09 2009, **vol. 113**, doi:10.1021/jp9032904.

[89] Xu, R., Xu, L., Hu, L., Zhang, J.: Structural origin and laser performance of thulium-doped germanate glasses, *Journal of Physical Chemistry A*, 12 2011, **vol. 115**, doi:10.1021/jp207574m.

[90] Seddon, A.: Chalcogenide glasses: a review of their preparation, properties and applications, *Journal of Non-Crystalline Solids*, 1995, **vol. 184**, pp. 44 – 50, doi:10.1016/0022-3093(94)00686-5.

[91] Huang, F., Guo, Y., Ma, Y., Zhang, L., Zhang, J.: Highly Er^{3+}-doped ZrF_4-based fluoride glasses for 2.7 µm laser materials, *Appl. Opt.*, Mar 2013, **vol. 52(7)**, pp. 1399–1403, doi:10.1364/AO.52.001399.

[92] Yanagita, H., Toratani, H., Yamashita, T. T., Masuda, I., Righini, G. C.: Diode-pumped Er^{3+} glass laser at 2.7 µm, in G. C. Righini, ed., *SPIE Proceedings: Glasses for Optoelectronics II*, vol. 1513, 1991 pp. 386–395, doi:10.1117/12.46045.

[93] Xue, T., Li, Y., Liu, Y., Liu, Z., Dai, S., Liao, M., Hu, L.: High thermal stability and intense 2.71 µm emission in Er^{3+}-doped fluorotellurite glass modified by GaF_3, *Optical Materials*, 2018, **vol. 75**, pp. 367 – 372, ISSN 0925-3467, doi:10.1016/j.optmat.2017.10.055.

[94] Schäfer, C., Konishi, D., Murakami, M., Shimizu, S., Tokita, S.: 7 W Er:ZBLAN Fiber Laser at 2.8 µm Using a Fiber Side-Pump Combiner, in

Laser Congress 2017 (ASSL, LAC), Optical Society of America, 2017 p. JTh2A.34, doi:10.1364/ASSL.2017.JTh2A.34.

[95] Tokita, S., Murakami, M., Shimizu, S., Hashida, M., Sakabe, S.: Liquid-cooled 24 W mid-infrared Er:ZBLAN fiber laser, *Opt. Lett.*, Oct 2009, **vol. 34(20)**, pp. 3062–3064, doi:10.1364/OL.34.003062.

[96] Qin, Z., Xie, G., Zhang, J., Ma, J., Yuan, P., Qian, L.: Continuous-Wave and Passively Q-Switched Er:Y_2O_3 Ceramic Laser at 2.7 µm, *International Journal of Optics*, 2018, **vol. 2018**, p. 5, doi:10.1155/2018/3153614.

[97] Voronov, A. A., Kozlovskii, V. I., Korostelin, Y. V., Landman, A. I., Podmarkov, Y. P., Polushkin, V. G., Frolov, M. P.: Passive Fe^{2+}:ZnSe single-crystal Q switch for 3-µm lasers, *Quantum Electronics*, 2006, **vol. 36(1)**, p. 1, doi:10.1070/QE2006v036n01ABEH013097.

[98] Wang, L., Huang, H., Ren, X., Wang, J., Shen, D., Zhao, Y., Zhou, W., Liu, P., Tang, D.: Nanosecond Pulse Generation at 2.7 µm From a Passively Q-Switched Er:Y_2O_3 Ceramic Laser, *IEEE Journal of Selected Topics in Quantum Electronics*, Sept 2018, **vol. 24(5)**, pp. 1–6, ISSN 1077-260X, doi:10.1109/JSTQE.2018.2801478.

[99] Kong, L., Qin, Z., Xie, G., Guo, Z., Zhang, H., Yuan, P., Qian, L.: Black phosphorus as broadband saturable absorber for pulsed lasers from 1 µm to 2.7 µm wavelength, *Laser Physics Letters*, 2016, **vol. 13(4)**, p. 045801, doi:10.1088/1612-2011/13/4/045801.

[100] Fan, M., Li, T., Zhao, S., Li, G., Gao, X., Yang, K., Li, D., Kränkel, C.: Multilayer black phosphorus as saturable absorber for an Er:Lu_2O_3 laser at $\sim$ 3 µm, *Photon. Res.*, Oct 2016, **vol. 4(5)**, pp. 181–186, doi:10.1364/PRJ.4.000181.

[101] You, Z. Y., Wang, Y., Sun, Y. J., Xu, J. L., Zhu, Z. J., Li, J. F., Wang, H. Y., Tu, C. Y.: CW and Q-switched GGG/Er:Pr:GGG/GGG composite crystal

laser at 2.7 µm, *Laser Physics Letters*, 2017, **vol. 14(4)**, p. 045810, doi:10.1088/1612-202X/aa5fea.

[102] Gallian, A., Martinez, A., Marine, P., Fedorov, V., Mirov, S., Badikov, V., Boutoussov, D., Andriasyan, M.: Fe:ZnSe passive Q-switching of 2.8-µm Er:Cr:YSGG laser cavity, in H. J. Hoffman, R. K. Shori, N. Hodgson, eds., *Solid State Lasers XVI: Technology and Devices;*, vol. 6451, 2007 p. 9, doi:10.1117/12.701289.

[103] Hu, T., Jackson, S. D., Hudson, D. D.: Ultrafast pulses from a mid-infrared fiber laser, *Opt. Lett.*, Sep 2015, **vol. 40(18)**, pp. 4226–4228, doi:10.1364/OL.40.004226.

[104] Qin, Z., Xie, G., Zhao, C., Wen, S., Yuan, P., Qian, L.: Mid-infrared mode-locked pulse generation with multilayer black phosphorus as saturable absorber, *Opt. Lett.*, Jan 2016, **vol. 41(1)**, pp. 56–59, doi:10.1364/OL.41.000056.

[105] Kisel, V. E., Shcherbitskii, V. G., Kuleshov, N. V., Postnova, L. I., Levchenko, V. I.: Saturable absorbers for passive Q-switching of erbium lasers emitting in the region of 3 µm, *Journal of Applied Spectroscopy*, Nov 2005, **vol. 72(6)**, pp. 818–823, ISSN 1573-8647, doi:10.1007/s10812-006-0009-0.

[106] Feng, T., Yang, K., Zhao, J., Zhao, S., Qiao, W., Li, T., Dekorsy, T., He, J., Zheng, L., Wang, Q., Xu, X., Su, L., Xu, J.: 1.21 W passively mode-locked Tm:LuAG laser, *Opt. Express*, May 2015, **vol. 23(9)**, pp. 11819–11825, doi:10.1364/OE.23.011819.

[107] Ma, J., Xie, G. Q., Gao, W. L., Yuan, P., Qian, L. J., Yu, H. H., Zhang, H. J., Wang, J. Y.: Diode-pumped mode-locked femtosecond Tm:CLNGG disordered crystal laser, *Opt. Lett.*, Apr 2012, **vol. 37(8)**, pp. 1376–1378, doi:10.1364/OL.37.001376.

[108] Kasprowicz, D., Brik, M., Majchrowski, A., Michalski, E., Guchowski, P.: Spectroscopic properties of $KGd(WO_4)_2$ single crystals doped with Er^{3+},

Ho^{3+}, Tm3+ and Yb^{3+} ions: Luminescence and micro-Raman investigations, *Journal of Alloys and Compounds*, 2013, **vol. 577**, pp. 687 – 692, ISSN 0925-8388, doi:10.1016/j.jallcom.2013.06.153.

[109] Medenbach, O., Dettmar, D., Shannon, R. D., Fischer, R. X., Yen, W. M.: Refractive index and optical dispersion of rare earth oxides using a small-prism technique, *Journal of Optics A: Pure and Applied Optics*, 2001, **vol. 3(3)**, p. 174, doi:10.1088/1464-4258/3/3/303.

[110] Zelmon, D. E., Small, D. L., Page, R.: Refractive-index measurements of undoped yttrium aluminum garnet from 0.4 to 5.0 µm, *Appl. Opt.*, Jul 1998, **vol. 37(21)**, pp. 4933–4935, doi:10.1364/AO.37.004933.

[111] Studenikin, P. A., Zagumennyi, A. I., Zavartsev, Y. D., Popov, P. A., Shcherbakov, I. A.: $GdVO_4$ as a new medium for solid-state lasers: some optical and thermal properties of crystals doped with Cd^{3+} , Tm^{3+} , and Er^{3+} ions, *Quantum Electronics*, 1995, **vol. 25(12)**, p. 1162, doi:10.1070/QE1995V025N12ABEH000556.

[112] Loiko, P. A., Filippov, V. V., Yumashev, K. V., Kuleshov, N. V., Pavlyuk, A. A.: Thermo-optic coefficients study in $KGd(WO_4)_2$ and $KY(WO_4)_2$ by a modified minimum deviation method, *Appl. Opt.*, May 2012, **vol. 51(15)**, pp. 2951–2957, doi:10.1364/AO.51.002951.

[113] Loiko, P., Segonds, P., Inácio, P., na, A. P., Debray, J., Rytz, D., Filippov, V., Yumashev, K., Pujol, M. C., Mateos, X., Aguiló, M., Díaz, F., Eichhorn, M., Boulanger, B.: Refined orientation of the optical axes as a function of wavelength in three monoclinic double tungstate crystals $KRE(WO_4)_2$ (RE = Gd, Y or Lu), *Opt. Mater. Express*, Sep 2016, **vol. 6(9)**, pp. 2984–2990, doi:10.1364/OME.6.002984.

[114] Kawase, H., Yasuhara, R.: 2.92-µm high-efficiency continuous-wave laser operation of diode-pumped Er:YAP crystal at room temperature, *Opt. Express*, Apr 2019, **vol. 27(9)**, pp. 12213–12220, doi:10.1364/OE.27.012213.

[115] Sanamyan, T., Kanskar, M., Xiao, Y., Kedlaya, D., Dubinskii, M.: High power diode-pumped 2.7-µm Er^{3+}:Y_2O_3 laser with nearly quantum defect-limited efficiency, *Opt. Express*, Sep 2011, **vol. 19(S5)**, pp. A1082–A1087, doi:10.1364/OE.19.0A1082.

[116] Wang, Y., You, Z., Li, J., Zhu, Z., Ma, E., Tu, C.: Spectroscopic investigations of highly doped Er^{3+}:GGG and Er^{3+}/Pr^{3+}:GGG crystals, *Journal of Physics D: Applied Physics*, 2009, **vol. 42(21)**, p. 215406, doi:10.1088/0022-3727/42/21/215406.

[117] Diels, J.-C., Rudolph, W.: *Ultrashort Laser Pulse Phenomena, Second Edition*, Optics and Photonics Series, Academic Press, 2nd ed., 2006, ISBN 978-0-12-215493-5.

[118] Shen, Y., Wang, Y., Chen, H., Luan, K., Tao, M., Si, J.: Wavelength-tunable passively mode-locked mid-infrared Er^{3+}-doped ZBLAN fiber laser, *Scientific Reports*, 2017, **vol. 7(1)**, pp. 2045–2322, doi:10.1038/s41598-017-13089-6.

[119] Zhu, G., Zhu, X., Wang, F., Xu, S., Li, Y., Guo, X., Balakrishnan, K., Norwood, R. A., Peyghambarian, N.: Graphene Mode-Locked Fiber Laser at 2.8 µm, *IEEE Photonics Technology Letters*, Jan 2016, **vol. 28(1)**, pp. 7–10, doi:10.1109/LPT.2015.2478836.

[120] Miller, R. J. D.: Picosecond Infrared Laser (PIRL) Scalpel: Achieving Fundamental Limits to Minimally Invasive Surgery and Biodiagnostics, in *Advanced Solid State Lasers*, Optical Society of America, 2015 p. AF2A.1, doi:10.1364/ASSL.2015.AF2A.1.

List of publications related to PhD thesis

[RS1] **Švejkar, R.**, Šulc, J., Jelínková, H.: Er-doped crystalline active media for ~ 3 µm diode-pumped lasers, *Progress in Quantum Electronics*, 2020, **vol. 74**, p. 100276, ISSN 0079-6727, doi:10.1016/j.pquantelec.2020.100276.

[RS2] **Švejkar, R.**, Šulc, J., Němec, M., Jelínková, H., Doroshenko, M., Konyushkin, V., Nakladov, A., Osiko, V.: Effect of cryogenic temperature on spectroscopic and laser properties of Er,La:SrF_2-CaF_2 crystal, in *Proc. SPIE 9726, Solid State Lasers XXV: Technology and Devices*, Bellingham (stát Washington), US, ISBN 978-1-62841-961-0, ISSN 0277-786X, 2016 p. 7, doi:10.1117/12.2208569.

[RS3] **Švejkar, R.**, Šulc, J., Němec, M., Boháček, P., Jelínková, H., Trunda, B., Havlák, L., Nikl, M., Jurek, K.: Line-tunable Er:GGAG laser, *Opt. Lett.*, Jul 2018, **vol. 43(14)**, pp. 3309–3312, doi:10.1364/OL.43.003309.

[RS4] **Švejkar, R.**, Šulc, J., Němec, M., Jelínková, H., Nejezchleb, K., Čech, M.: Temperature influence on spectroscopic properties and 2.7 µm lasing of Er:YAP crystal, in *Solid State Lasers XXVII: Technology and Devices*, vol. 10511, 2018 pp. 10511 – 6, doi:10.1117/12.2287138.

[RS5] Šulc, J., Němec, M., **Švejkar, R.**, Jelínková, H., Doroshenko, M. E., Fedorov, P. P., Osiko, V. V.: Diode-pumped Er:CaF_2 ceramic 2.7 µm tunable laser, *Opt. Lett.*, Sep 2013, **vol. 38(17)**, pp. 3406–3409, doi:10.1364/OL.38.003406.

[RS6] Šulc, J., **Švejkar, R.**, Němec, M., Jelínková, H., Doroshenko, M. E., Konyushkin, V. A., Nakladov, A. N., Osiko, V. V.: Er:SrF_2; Crystal for Diode-pumped 2.7 µm Laser, *Advanced Solid State Lasers*, 2014, p. ATu2A.22, doi:10.1364/ASSL.2014.ATu2A.22.

[RS7] Šulc, J., **Švejkar, R.**, Němec, M., Jelínková, H., Doroshenko, M. E., Fedorov, P. P., Osiko, V. V.: Temperature influence on diode pumped Er:CaF_2 laser, *Proc. SPIE*, 2015, **vol. 9342**, pp. 93421S–93421S–8, doi:10.1117/12.2077454.

[RS8] **Švejkar, R.**, Šulc, J., Němec, M., Jelínková, H.: Up to 3 W continuous power and 21 ns long pulses from 2.8 µm Er:YLF laser, in *Laser Congress 2020 (ASSL, LAC, LS&C)*, Optical Society of America, 2020 .

[RS9] **Švejkar, R.**, Šulc, J., Němec, M., Jelínková, H., Kubeček, V., Ma, W., Jiang, D., Wu, Q., Su, L.: Diode-Pumped Er:CaF_2 Crystal 2.7 µm Tunable Laser, in *26th International Laser Physics Workshop*, Moscow, RU, 2017 .

[RS10] **Švejkar, R.**, Šulc, J., Němec, M., Jelínková, H.: Passively Mode-Locked High-Repetition Rate Er:YLF Laser at 2.81 µm Generating 72 ps Pulses, in *2019 Conference on Lasers and Electro-Optics Europe European Quantum Electronics Conference (CLEO/Europe-EQEC)*, 2019 pp. 1–1, doi:10.1109/CLEOE-EQEC.2019.8873182.

[RS11] **Švejkar, R.**, Šulc, J., Jelínková, H.: Er:Y_2O_3 high-repetition rate picosecond 2.7 µm laser, *Laser Physics Letters*, Jun 2019, **vol. 16(7)**, p. 075802, doi:10.1088/1612-202x/ab1918.

[RS12] **Švejkar, R.**, Šulc, J., Němec, M., Jelínková, H.: Er:YLF microchip laser for free-running and gain-switching laser operation in spectral range 2.83 µm, in *9th EPS-QEOD Europhoton*, Prague, Czech republic, 2020 pp. Tu–P1.8.

[RS13] **Švejkar, R.**, Šulc, J., Jelínková, H.: Er:YAG microchip for lasing in spectral range 2.94 µm and gain switching generation, in *High-Brightness Sources and Light-driven Interactions*, Optical Society of America, 2020 .

[RS14] **Švejkar, R.**, Šulc, J., Jelínková, H., Kubeček, V., Ma, W., Jiang, D., Wu, Q., Su, L.: Diode-pumped Er:SrF_2 laser tunable at 2.7 µm, *Opt. Mater. Express*, Apr 2018, **vol. 8(4)**, pp. 1025–1030, doi:10.1364/OME.8.001025.

[RS15] **Švejkar, R.**, Šulc, J., Jelínková, H., Čech, M.: Temperature influence on spectroscopic and laser properties of Er:YLF crystal, in *Solid State Lasers XXVIII: Technology and Devices*, vol. 10896, 2019 doi:10.1117/12.2506384.

[RS16] **Švejkar, R.**, Šulc, J., Boháček, P., Jelínková, H., Trunda, B., Hávlak, L., Nikl, M., Jurek, K.: Temperature influence on Er:GGAG crystal spectroscopic properties and lasing at 3 µm, in W. A. Clarkson, R. K. Shori, eds., *Solid State Lasers XXIX: Technology and Devices*, vol. 11259, International Society for Optics and Photonics, SPIE, 2020 pp. 330 – 335, doi:10.1117/12.2541965.

[RS17] **Švejkar, R.**, Šulc, J., Jelínková, H., Doroshenko, M. E., Konyushkin, V. A., Nakladov, A. N., Osiko, V. V.: Passively Q-switched Er,La:SrF_2-CaF_2 laser at 2.74 µm, in *High-Power, High-Energy, and High-Intensity Laser Technology IV*, vol. 11033, 2019 doi:10.1117/12.2520268.

[RS18] **Švejkar, R.**, Šulc, J., Němec, M., Jelínková, H.: Nanosecond pulses from SESAM Q-switched Er:Y_2O_3 laser at 2.7 µm, in *8th EPS-QEOD Europhoton*, Barcelona, Spain, 2018 p. ThP.31.

List of publications outside topic of PhD thesis

[RSadd1] Šulc, J., **Švejkar, R.**, Jelínková, H., Ryba-Romanowski, W., Lukasiewicz, T.: Diode Pumped Room-temperature Operating Eye-safe Er:YVO_4 and Er:$GdVO_4$ Lasers, in *22th International Laser Physics Workshop - Book of Abstracts*, Moskva, RU, 2013 p. 1.

[RSadd2] Šulc, J., **Švejkar, R.**, Jelínková, H., Nejezchleb, K., Nitsch, K., Cihlář, A., Král, R., Ledinský, M., Fejfar, A. i., Rodová, M., Zemenová, P., Nikl, M.: Phosphate content influence on structural, spectroscopic, and lasing properties of Er,Yb-doped potassium-lanthanum phosphate glasses, *Optical Engineering*, 2016, **vol. 55**, pp. 55 – 10, doi:10.1117/1.OE.55.4.047102.

[RSadd3] Šulc, J., **Švejkar, R.**, Němec, M., Jelínková, Nitsch, K., Cihlář, A., Král, R., Nejezchleb, K., Rodová, M., Nikl, M.: Er-doped ortho- and metha-phosphate glassy mixtures for 1.54 µm laser construction, in J. I. Mackenzie, et al., eds., *SPIE Proceedings: Laser Sources and Applications II*, vol. 9135, 2014 pp. 9135 – 8, doi:10.1117/12.2051209.

[RSadd4] **Švejkar, R.**, Šulc, J., Němec, M., Jelínková, Nitsch, K., Cihlář, A., Král, R., Nejezchleb, K., Nikl, M.: Effect of cryogenic temperature on spectroscopic and laser properties of Er, Yb-doped potassium-lanthanum phosphate glass, in J. Hein, ed., *SPIE Proceedings: High-Power, High-Energy, and High-Intensity Laser Technology III*, vol. 10238, 2017 p. 7, doi:10.1117/12.2264673.

[RSadd5] **Švejkar, R.**, Šulc, J., Říha, A., Jelínková, H., Doroshenko, M. E., Kovalenko, N. O., Gerasimenko, A. S.: Compact Fe:ZnSe and Fe:ZnMnSe tunable lasers at 80 K pump with Er:YAG, in *13th Pacific Rim Con-*

ference on Lasers and Electro-Optics (CLEO Pacific Rim, CLEO-PR 2018), 2018 p. W3A.55.

[RSadd6] **Švejkar, R.**, Šulc, J., Němec, M., Boháček, P., Jelínková, H., Trunda, B., Havlák, L., Nikl, M., Jurek, K.: Diode-pumped laser and spectroscopic properties of Yb,Ho:GGAG at 2 µm and 3 µm, *Laser Physics Letters*, feb 2020, **vol. 17(3)**, p. 035801, doi:10.1088/1612-202x/ab6d61.

[RSadd7] **Švejkar, R.**, Papashvili, A. G., Šulc, J., Němec, M., Jelínková, H., Doroshenko, M. E., Batygov, S. H., Osiko, V. V.: 2.4 µm diode-pumped Dy^{2+}:CaF_2 laser, *Laser Physics Letters*, 2018, **vol. 15(1)**, p. 015803, doi:10.1088/1612-202X/aa806d.

[RSadd8] **Švejkar, R.**, Šulc, J., Němec, M., Jelínková, H., Doroshenko, M.: Cryogenic-cooled Tm:SBN tunable laser, in *Photonics, Devices, and Systems VII*, vol. 10603 of *Proceedings of SPIE*, Bellingham, US, ISBN 978-1-5106-1702-5, ISSN 0277-786X, 2017 p. 6, doi:10.1117/12.2292425.

[RSadd9] Němec, M., Boháček, P., **Švejkar, R.**, Šulc, J., Jelínková, H., Trunda, B., Havlák, L., Nikl, M., Jurek, K.: Er:GGAG crystal temperature influence on spectroscopic and laser properties, *Opt. Mater. Express*, May 2020, **vol. 10(5)**, pp. 1249–1254, doi:10.1364/OME.383098.

[RSadd10] Němec, M., Šulc, J., **Švejkar, R.**, Jelínková, H.: Temperature influence on Er:$YAlO_3$ spectroscopy and diode-pumped laser properties, *Laser Physics*, 2018, **vol. 28(10)**, p. 105801, doi:10.1088/1555-6611/aacfa0.

Appendix

In Appendix, reader can find all papers that are mentioned in section 5. All papers stated below can be also found in digital library of particular publishers.

Progress in Quantum Electronics 74 (2020) 100276

Contents lists available at ScienceDirect

Progress in Quantum Electronics

journal homepage: www.elsevier.com/locate/pqe

Er-doped crystalline active media for ~ 3 μm diode-pumped lasers

Richard Švejkar *, Jan Šulc, Helena Jelínková

Faculty of Nuclear Sciences and Physical Engineering, Czech Technical University in Prague, Břehová 7, 115 19, Prague, Czech Republic

ARTICLE INFO

Keywords:
Erbium
Solid-state lasers
Mid-infrared lasers
Diode-pumped

ABSTRACT

Lasers based on erbium ions using $^4I_{11/2} \rightarrow {}^4I_{13/2}$ transition can generate laser radiation in the spectral range from 2.7 μm to 3 μm. Since the strong absorption peak of water is located at 3 μm, there has been an effort to develop a suitable laser source for various medical applications, e.g. dentistry, dermatology, urology, or surgery. Laser radiation from this wavelength range can also be used in spectroscopy, as a pumping source for optical parametric oscillators, or for further mid-infrared conversion.

This paper represents an overview of the erbium-doped active media (e.g. Er:YAG, Er:YAP, Er:GGG, Er:SrF_2, Er:YLF, Er:Y_2O_3, Er:KYW, etc.) for laser radiation generation in the spectral range 2.7–3 μm. In the first part of this paper, the particular active media are discussed in detail. On the other hand, the experimental results summarized absorption and emission cross-section spectra together with decay times at upper ($^4I_{11/2}$) and lower ($^4I_{13/2}$) laser levels of all tested Er-doped samples at room temperature. Moreover, laser results in CW and pulsed laser regime with tunability curves, achieved in recent years, are presented, too.

1. Introduction

Sixty years have now passed since the invention of the first laser. It was based on ruby crystal and emitted laser radiation at 694.3 nm. Nowadays, there are various types of lasers able to generate radiation in the extremely wide spectral range from T-rays (~ $5{\cdot}10^9$ Hz) to X-rays (~ $5{\cdot}10^{17}$ Hz). However, still, there is a desire to generate a new wavelengths to fill the empty space in wide spectral range or create sources of laser radiation for a particular application. The mid-infrared (2.5–8 μm) spectral range is interesting and significant especially for spectroscopy (remote sensing of gases, environmental monitoring, meteorology), medicine, polymer processing, or military applications (countermeasure, rangefinders, target pointing) [1–4].

Lasers emitting in the first part of the mid-infrared spectrum (from 2.5 to 3 μm) are primarily interesting for various branches in medicine (dermatology, surgery, dentistry, ophthalmology, urology); also, they can be used as a pumping source for further wavelength conversion. To generate laser radiation in this spectral range, an optical parametric oscillator (OPO) or materials based on Cr:ZnSe or Cr:ZnS pumped with Tm-fibre lasers can be used; nevertheless, these systems are complex and expensive [3,5]. At present there are many coherent diode-pumped Er-doped laser active media, e.g. Er:YAG, Er:YLF, Er:CaF_2, Er:Y_2O_3, etc., for generating laser radiation in the spectral range 2.7–3 μm. Today, erbium is a well-known element from the lanthanide series used as an activator in various laser active media. Due to the structure of energetic levels, erbium-doped active media offer a laser transition in several spectral ranges. Two best-known erbium laser wavelengths, i.e. ~ 1.6 μm and ~ 3 μm, correspond to laser transitions $^4I_{13/2} \rightarrow {}^4I_{15/2}$ and $^4I_{11/2} \rightarrow {}^4I_{13/2}$, respectively. Using direct (in-band, resonant) pumping of the laser level $^4I_{13/2}$, it is possible to generate laser radiation at 1.6 μm with high output power and slope efficiency up to 80% [6,7]. On the other hand, to obtain laser radiation at ~ 3 μm wavelength with the high

* Corresponding author.
E-mail address: richard.svejkar@fjfi.cvut.cz (R. Švejkar).

https://doi.org/10.1016/j.pquantelec.2020.100276

Available online 28 August 2020

enough slope efficiency, pumping wavelength ~ 970 nm has to be used; nevertheless, the slope efficiency is limited by quantum defect to a theoretical value of ~ 35%. From the point of view the spectroscopy, another interesting laser wavelength in mid-infrared spectral range is ~ 3.5 μm ($^4F_{9/2} \rightarrow {}^4I_{9/2}$). It was shown that Er:YLF crystal can generate laser radiation at 3.41 μm; however, only few papers deal with this issue, e.g. Ref. [8]. It is also possible to generate laser emission at visible spectral range, particularly at 551 nm [9]. Erbium doped active media can also generate radiation with the laser wavelength 1.7 μm if the transition $^4F_{9/2} \rightarrow {}^4I_{9/2}$ is used [10], Nevertheless, to obtain this laser wavelength from a diode-pumped laser system a special shape of laser resonator and pumping has to be used [10]. One can see, that erbium-doped active media offers many interesting laser wavelengths which can be used in various branches of research and industry. From this point of view, we believe that a further research of such active media doped with erbium ions and also laser systems designed with them is important [3,5,11].

This paper presents a review of the most often used Er-doped active media that are able to generate laser radiation in spectral range from 2.6 to 3 μm. After the first introductory part, the second section of this paper deals with the Er^{3+} ions in general as well as the well-known problems connected with these ions such as up-conversion, fluorescence quenching, and self-termination. The third section deals with various Er^{3+}-doped matrices that can be used as active medium for the lasers. Section 4 discusses generation of short pulses which is challenging in this spectral range. The last but one section is devoted to our experimental results obtained with several active media generating the radiation in the spectral region around 3 μm. Finally, the summary dealing with the properties of erbium lasers generated radiation in the range at ~ 3 μm is presented in section 6 together with the possibility of their application.

2. Trivalent erbium (Er^{3+}) ions

For the first time, the name "erbium" was used in 1842 by C. Mosander after separation of yttrium into three fractions - terbium, erbium, and yttrium. Nevertheless, pure metal erbium was produced in 1934 by Klemm and Bommer who reduced the anhydrous chloride with potassium vapour. Nowadays, ion-exchange reactions are used to produce pure metal erbium at a reasonable price ($20/g) [12]. The pure metal is soft and malleable with silver colour; erbium can be used as an activator in laser active media [12].

It is well known that the erbium ion is one of the rare-earth ions of the lanthanide series, so it has electron configuration [Xe] $4f^{N-1}5s^25p^6$, where N is equal to 12. Thus the *4f* shell contains 11 electrons shielded by fully occupied sub-shells *5s5p* [13]. For this reason, the spectral lines are narrower in comparison with the transition metal ions [14]. It follows from the quantum theory that the ground state of the Er^{3+} ion is $^4I_{15/2}$ which is also the terminal level for several possible laser transitions. In Fig. 1 one can see the feasible laser transition between energy levels of the erbium ion. From the point of view of laser action, the two most interesting erbium laser wavelengths are ~ 1.6 μm and ~ 2.9 μm. The radiation from the spectral range 1.6 μm is so-called "eye-safe" laser radiation because this wavelength does not reach the retina, being absorbed in the frontal part of the eye. For this reason, radiation with 1.6 μm wavelength finds use in LIDARs, rangefinders, or free-space communication. The latter wavelength range around 2.9 μm is very close to the absorption maximum of water at ~ 3 μm, thus it is interesting for medical applications, e.g. surgery, dentistry, dermatology, urology, etc. Besides above mentioned wavelengths, it is possible to generate laser radiation in other parts of the spectrum, i.e. ~ 0.55 μm, ~ 0.85 μm, ~ 1.3 μm, ~ 1.7 μm, ~ 3.5 μm [8,13,15,16]. Laser emission in erbium-doped active media is strongly affected by the typical and

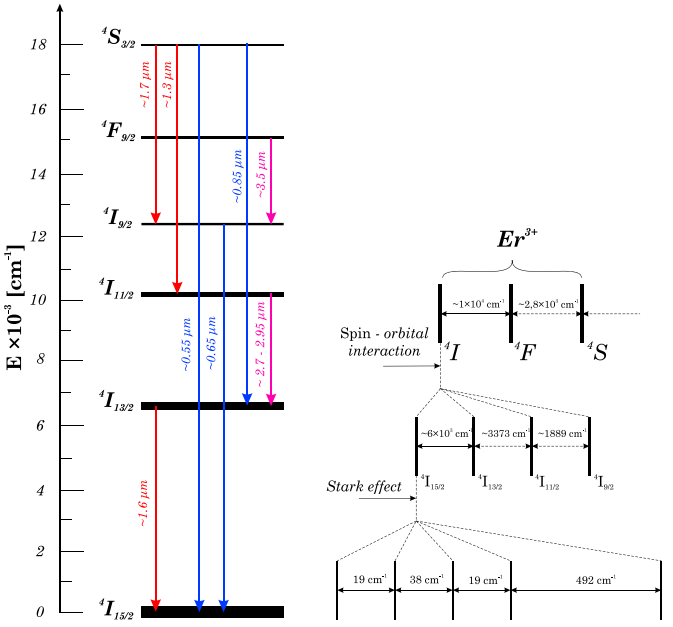

(a) Laser transition (b) Energy level splitting

Fig. 1. Energy levels of Er^{3+} ion.

important phenomenon – the up-conversion processes. It can cause depopulation of lower laser level and subsequently decrease the laser efficiency for 3 μm emission [2,13,14]. This phenomenon will be discussed in detail in section 2.1.

The possible generated laser wavelength depends, besides others, e.g. optical resonator and pumping wavelength, on the concentration of erbium ions. In the first assumption it was supposed that for generation 3 μm radiation the matrix has to be heavy doped with erbium [14] to allow fast quenching of the lower laser level $^4I_{13/2}$. Nevertheless, it was shown that even if the concentration is low, the laser emission at mid-infrared range is possible [5,11,17,18]. The first active medium using low concentration of Er^{3+} ions (~ 5%) was based on fluorides [19]; now it is possible to use doping concentration 1% and even lower; however, for such low doping cryogenic cooling has to be used [11,18]. Even if the cryogenic temperatures allow to obtain lasing with low erbium-doped active media, the whole cryogenic systems made laser system complex and hard to operates. On the other hand, a high doping concentration of active ion in an active medium affects thermal conductivity and homogeneity of grown crystal [2,14]. This will be in detail discussed in text below, see section 2.1. Section 3 presents various active media and this issue is discussed there in detail.

2.1. Up-conversion, self-termination, quenching

The main known problems linked with Er^{3+} ions are relatively complicated up-conversion processes (energy transfer, excited state absorption, cross-relaxation $^4I_{15/2}\rightarrow{}^4I_{13/2}+{}^4S_{3/2}+{}^4I_{9/2}$), self-termination, and fluorescence quenching affecting the slope efficiency, the output power, and the threshold of 3 μm laser emission [2,14,20–22]. These three processes depend strongly on a combination of the level doping concentration of erbium and type of matrix [18,20].

If the Er^{3+} ions are doped into low phonon matrix, the probability of non-radiative transition is reduced and the fluorescence decay time at the upper laser level $^4I_{11/2}$ is prolonged. This fact results in a low probability of the self-termination effect typical for the situation when the upper laser level possesses significantly shorter fluorescence decay time compared with the lower laser level. Furthermore, the matrix determines the probability of a cluster forming. In SrF_2 and CaF_2 crystals, for example, the clusters are formed at erbium concentration of 3–7% of Er^{3+}. So, a distance between erbium ions in active medium could be shorter which could be benefit to ion-ion energy transfer. For this reason La^{3+} can be added to the active medium to control clustering of Er^{3+} ions [23]. Another possibility how to reduce the self-termination effect and shorten the spacing between Er^{3+} ions is to use the high erbium doping level. Also, high concentration of erbium results in faster quenching of the lower laser level $^4I_{13/2}$. However, using the high doped active medium affects thermal conductivity; moreover, fabrication of a highly doped, homogeneous crystal with good optical quality can be challenging [2,5,18,20–22,24,25].

As mentioned above, the doping level of Er^{3+} affects the up-conversion processes illustrated in Fig. 2. As one can see, there are two crucial transitions that cause the emission in visible spectral range, particularly at green - ESA1 (excited state absorption) and ET1 (energy transfer); both depopulate upper laser level $^4I_{11/2}$ of ~ 3 μm laser transition. The red emission is probably caused by ESA2, which is fortunately advantageous for ~ 3 μm lasing because it depopulates lower laser level $^4I_{13/2}$. The transition ET2 re-populate the $^4I_{11/2}$ level and moreover depopulate the $^4I_{13/2}$ level, so this transition probably partly suppress the self-termination process [20,21].

In summary, to obtain the long fluorescence decay time at upper laser level ($^4I_{11/2}$) of 3 μm laser transition simultaneously with the short fluorescence decay time at energy level $^4I_{13/2}$, the combination of matrix and concentration of erbium ions must be chosen wisely. However, this is a very complex and demanding task which will be discussed in the following section.

3. Erbium doped matrices

Nowadays, there are many matrices (YAG, YAP, GGG, YVO_4, Y_2O_3, KYW, etc.) doped with erbium ions which offer various material and optical parameters. In this section, several Er^{3+}-doped laser active media based on garnet, fluoride, sesquioxide, orthovanadates, tungstate, and others are discussed in details. The best output power characteristics for several Er-doped active media are presented in

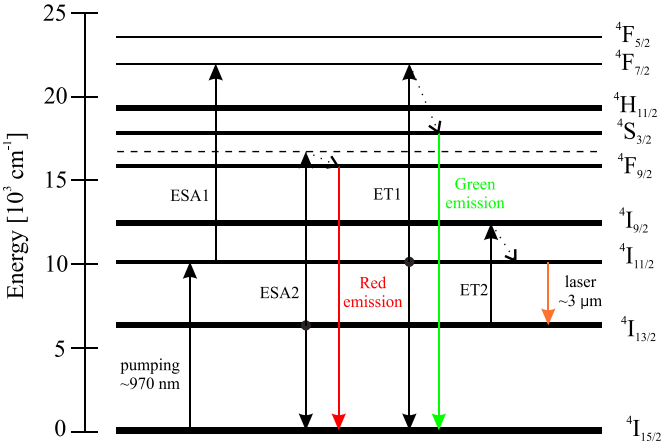

Fig. 2. Up-conversion of Er^{3+} ion [5,20,21].

Table 3.

3.1. Er-doped garnet matrices

Laser matrices based on garnets are well known; the first laser working with an erbium-doped garnet matrix was the Er:YAG developed in 1975 by A.M. Prokhorov and his colleagues [14]. The erbium concentration was ~ 50% and this laser emitted radiation at 2940 nm and became attractive because its laser radiation is close to the absorption maximum in water [14]. Garnets are important due to their material parameters such as high thermal conductivity, chemical stability, and hardness [26,27]. The chemical formula of garnets can be written as $C_3A_2D_3O_{12}$ [28]. In general, the C, A, and D represent ions located at dodecahedral (large ion), octahedral (medium ion), and tetrahedral (small ion) sites, respectively [28]. Usually, in laser science the C denotes Y^{3+}, Gd^{3+}, or Lu^{3+}; A together with D can represent Ga^{3+} or Al^{3+}; separately A and D can denote $Sc^{3+}Ga^{3+}$, $Ga^{3+}Al^{3+}$, $Sc^{3+}Al^{3+}$, or $La^{3+}Ga^{3+}$ [29–33].

3.1.1. Er:YAG

$Y_3Al_5O_{12}$ is a cubic crystal with O_h^{10} (Ia3d) space group and excellent thermal conductivity, see Table 1. If Er^{3+} is doped into the crystal structure of YAG, it replaces Y^{3+} because of similar atomic radii [28]. To obtain laser action in the Er:YAG active medium, the doping level of Er^{3+} can vary from 0.5% to 50% [11,14,31,34]. Nevertheless, with rising concentration of Er^{3+}, the structural changes and distortion of a crystal can occur [31] which can affect the final quality of the laser crystal and also the laser action.

Nowadays, there are many papers dealing with Er:YAG lasers, and it is evident that based on doping level the Er:YAG crystal can generate laser radiation at 1.6, 2.7, or 2.94 μm [3,11,14,17]. Using highly doped crystals, the $^4I_{11/2} \rightarrow {}^4I_{13/2}$ laser transition (2.94 μm) will be supported due to the fast quenching of the lower laser level $^4I_{13/2}$. On the other hand, low-doped YAG crystals make possible to generate cascade laser radiation at 1.6 μm and 2.7 μm; nevertheless, cryogenic cooling has to be used for this laser action to suppress ground-state re-absorption [11]. Due to cryogenic cooling, the Stark levels are populated in a different way in comparison with the room temperature case. This probably causes that laser emission from energy multiplet $^4I_{11/2}$ is shifted to the lower wavelength of 2.7 μm.

Since the Er:YAG crystal is the only commonly used erbium-doped active medium able to generate laser radiation directly at 2.94 μm (which is the nearest to 3 μm), it is widely used in various branches of medicine. For instance Er:YAG with a low output power can be used in dermatology for rejuvenation [35] and hair transplantation [36] or in dentistry for removal of the natural caries lesions from dentine [37]. However, as mentioned above, Er:YAG has been known for a long time, but the pumping of this laser was mainly non-coherent by flash-lamps. Since the Er:YAG possesses short fluorescence decay time at upper laser level ($^4I_{11/2}$) the flash-lamp pumping is the easiest way how to obtain high energy laser output (hundreds of mJ). Even if the optical to optical efficiency of flash-lamp pumped laser system is very low in comparison with diode-pumping, the flash-lamps can provide a high amount of energy during hundreds of microseconds which could be beneficial for Er:YAG [38]. Due to its possible application, there has also been an effort to build a high power diode-pumped laser or a system able to generate short pulses with a high peak power at ~ 3 μm wavelength. Yang et al. [38] published a paper dealing with high peak power Q-switched flash-lamp pumped Er:YAG, the 226 mJ pulse energy together with 62 ns pulse duration was achieved, which corresponds to 3.6 MW peak power. In the free-running regime, Messner's group [39] presented a laser set-up that can generate an average output power exceeding 50 W. Such powerful lasers could be used in surgery for cutting of bones [40] or in industry for cutting of various materials (glasses, wood, textile) [39].

3.1.2. Er:GGAG

Same as the YAG the GGAG matrix possesses a cubic structure with O_h^{10} (Ia3d) space group [30,41]. From the ion radius and oxidation states of the Er^{3+} one could predict that Er^{3+} will substitutes for Gd^{3+} in the GGAG crystal lattice. Due to the partial substitution of Ga^{3+} for Al^{3+} ions, the crystal field is distorted and the spectral line-width becomes larger because of inhomogeneous broadening [33]. Contrary to the Er:YAG, the Er:GAGG has a lower melting point (2100 K), see Tables 1 and 2. As far as the low phonon energy is concerned, similar to the GGG ($Gd_3Ga_5O_{12}$) crystal (600 cm^{-1}) [42], the GGAG crystal should have a comparable value of the

Table 1
Material parameters of several un-doped matrices, T_m - melting point, c - specific heat capacity, α - coefficient of thermal expansion, κ - thermal conductivity, ρ - density, for 300 K [43,67,69,79,80,118].

Matrix	Formula	Crystal system	T_m [K]	c [$J \cdot g^{-1}K^{-1}$]	α [10^{-6} K]	κ [$W \cdot m^{-1}K^{-1}$]	ρ [$g \cdot cm^{-3}$]
YAG	$Y_3Al_5O_{12}$	Cubic (Ia3d)	2200	0.625	7.7	14.5	4.56
YAP	$YAlO_3$	Orthorhombic (*Pnma*)	2140	0.42	11 ⊥c	11	5.35
YLF	$LiYF_4$	Tetragonal ($I4_1/a$)	1092	0.79	13.3⊥a	6.3	3.99
CaF_2	CaF_2	Cubic (Fm3m)	1630	0.91	18.90	9.7	3.18
SrF_2	SrF_2	Cubic (Fm3m)	1710	0.54	18.4	1.42	4.24
Y_2O_3	Y_2O_3	Cubic (Ia3)	2703	0.46	6.56	13.4	5.01
Lu_2O_3	Lu_2O_3	Cubic (Ia3)	2723	–	6.1	12.8	9.43
YVO_4	YVO_4	Tetragonal ($I4_1/amd$)	2100	0.56 4.4⊥c	11.4‖c 8.9⊥c	12.2‖c	4.23
$GdVO_4$	$GdVO_4$	Tetragonal ($I4_1/amd$)	2053	0.50 2.2⊥c	8.92‖c 8.6⊥c	10.5‖c	5.47
KYW	$KY(WO_4)_2$	Monoclinic ($C2/c$)	–	0.41	3.0‖b	2.7‖b	6.56
KGdW	$KGd(WO_4)_2$	Monoclinic ($C2/c$)	–	0.37	1.9‖b	2.6‖b	7.11

phonon energy. This is given by using heavier elements such as gallium and gadolinium; a similar phenomenon was observed e.g. in heavy metal glasses [2]. Moreover, the Er:GGAG can be easily grown by the Czochralski method [41].

The first diode-pumped Er:GGAG laser was introduced in Ref. [41], by reporting that this active medium can emit laser radiation in CW regime with maximum output power 75.5 mW with slope efficiency 7.4%. Also, a line tuning was present in spectral ranges 2800–2822 nm, 2829–2891 nm, and 2917–2942 nm [41].

3.1.3. Er:YSGG

One of garnet matrices with a cubic structure and with O_h^{10} (Ia3d) space group symmetry is the yttrium scandium gallium garnet – YSGG ($Y_3Sc_2Ga_3O_{12}$) [31,43]. Since the YSGG possesses lower phonon energy the fluorescence decay time of upper laser level $^4I_{11/2}$ is longer compared with Er:YAG [44]. Moreover, due to the atomic radii of scandium and gallium, the distance between dodecahedral site is larger and thus the ion-ion interaction is reduced which is beneficial to the high power lasers [31,44].

Using diode-pumped Er:YSGG active medium the 10.1 W average output power with slope efficiency 6.5% was reached. This high output power was obtained with the compensation of thermal lens [45].

3.2. Er:YAP

Orthoaluminate $YAlO_3$ (YAP) has an orthorhombic crystal structure with space group D_{2h}^{16} (*Pnma*) which means that the crystal is anisotropic (biaxial) [43,46]. Similar to the YAG crystal, the Er^{3+} ions entering the crystal lattice as impurities substitute for Y^{3+} ions [46]. The Er:YAP active medium is suitable for generating polarized laser radiation at ~ 3 μm, first presented by A. A. Kaminskii [47]. Several papers dealing with highly doped Er:YAP emitting at ~ 3 μm were published in Ref. [48–50]. Nevertheless, the first emission of laser radiation at 2.8 μm of the low-doped erbium YAP crystal was published in Ref. [18].

In [18] we reported the temperature influence on spectroscopic properties and lasing characteristics of a Er:YAP crystal. Among others it was shown that using the 972 nm pumping wavelength the CW Er:YAP (1% of Er^{3+}) laser can work at cryogenic temperature (78 K). In the CW regime the slope efficiency up to 3.5% and maximal output power 27 mW at 2.73 μm were reached. Due to polarization-dependent laser emission the Er:YAP laser could be interesting in spectroscopy or microsurgery [18,50]. If higher concentration of erbium (5%) is used, it is possible to obtain laser action at 2.92 μm (output power 0.65 W) at room-temperature, as presented in Ref. [51].

3.3. Er-doped fluoride matrices

The first laser using a fluoride matrix was presented by Sorokin and Stevenson in 1960. It was an uranium-doped calcium fluoride laser emitting radiation at 2.5 μm [52]. The first CW operation of a Er:CaF_2 laser at 2.7 μm based on a stepwise up-conversion pumping scheme under Xe-flashlamp excitation was reported by S. A. Pollack et al. [53]. A single crystal Er:CaF_2 and Er:SrF_2 lasing at 2.7 μm under diode pumping was realized by T. T. Basiev et al. [19]. Ion clustering in CaF_2 and SrF_2 matrices, which is caused by charge compensation, enables to use the active medium with a low concentration of erbium to obtain lasing [5,21]. The lower requirement on the doping level of erbium together with the lower melting point of fluoride (YLF – 1092 K, CaF_2 – 1630 K, SrF_2 – 1710 K) makes their fabrication easier [5,43].

The CaF_2 and SrF_2 matrices have a cubic structure (Fm3m) consisting of F^- and Ca^{2+} or Sr^{2+} ions. If the Er^{3+} ion enters the CaF_2 or SrF_2 structure, it substitutes for Ca^{2+} or Sr^{2+} [54]. So, obviously, because of the extra positive Er^{3+} ion the charge compensation is required to keep electrical neutrality. Probably, this is the reason for forming a multi-site structure with isolated and complex centres [55], resulting in broadband absorption and emission spectrum [5] of this active medium. This clustering is probably beneficial to ion-ion energy transfer [5,21].

Table 2
Optical parameters of several erbium matrices; n - refractive indexes (o - ordinary axis and e – extraordinary axis), dn/dt - Thermooptic coefficient, Δ n - birefringence, T - transparency [43,69,79,80,118–123].

Matrix	Optical activity	n [–] @ 632.8 nm	dn/dt [10^{-6}/K]	Δ n @ 632.8	T [μm]
YAG	Isotropic	1.8295	9.05 @ 1064 nm	–	0.21–5.2
YAP	Biaxial	1.924 (n_x), 1.938 (n_y) 1.947 (n_z)	9.8 (a), 14.5 (c) @ 1064 nm	0.0235	0.2–7
YLF	Uniaxial	1.4762 (o) 1.4535 (e)	−0.67 (o), @ 546 nm −2.30 (e) @ 546 nm	0.0227	0.12–8
CaF_2	Isotropic	1.433	−11.5 @ 632.8 nm	–	0.12–10
SrF_2	Isotropic	1.437	−12.5 @ 632.8 nm	–	0.13–12
Y_2O_3	Isotropic	1.92	8.3 @ 633 nm	–	0.29–7.1
Lu_2O_3	Isotropic	1.9303	9.1 @ 633 nm	–	–
YVO_4	Uniaxial	1.9934 (o), 2.2148 (e)	3.9(o), 8.5(e)	0.2233	0.35–4.8
$GdVO_4$	Uniaxial	2.0135 (o), 2.2468 (e)	–	0.24	0.35–3.5
KGdW	Biaxial	2.001 (n_x), 2.042 (n_y) 2.086 (n_z)	−10.1 (n_x), −7.3 (n_y) −8.4 (n_z) @ 633 nm	0.085	–
KGdW	Biaxial	2.009 (n_x), 2.028 (n_y) 2.084 (n_z)	−10.6 (n_x), −8.4 (n_y) −15.2 (n_z) @ 633 nm	0.029	–

Recently, lasing in the near- and mid-infrared spectral range of Er^{3+} ions in laser-quality fluoride crystal has been successfully demonstrated under laser diode pumping [20,21,24,56–58]. However, due to thermal expansion and the conductivity coefficient, the Er:CaF_2 and Er:SrF_2 are not the best active media for high power lasers. Su et al. [59]. presented the maximal output power 1 W and slope efficiency 26% in CW laser regime with Er:SrF_2. This characteristics could be sufficient for some applications.

Both active media Er:CaF_2 (322 cm^{-1}) and Er:SrF_2 (280 cm^{-1}) belong to the low-phonon materials [21]. As mentioned above, the probability of non-radiative transitions for low-phonon materials is lower as against crystalline oxides; thus the fluorescence decay time at $^4I_{11/2}$ is longer and the ratio of the $^4I_{11/2}/^4I_{13/2}$ is higher which is beneficial for CW laser operation [20,21]. Due to their broadband emission spectrum, Er:CaF_2 and Er:SrF_2 crystals are interesting for possible ultra-short pulse generation [60] and a wide wavelength laser tuning. Our group has shown that using a birefringent element in laser resonator makes it possible to tune the output laser wavelength for 123 nm (2690–2813 nm) [5] and 118 nm (2687–2805 nm) [58] for Er:SrF_2 and Er:CaF_2, respectively.

In the YLF ($LiYF_4$) matrix, Er^{3+} substitutes for trivalent yttrium; so charge compensation is not required [61]. The YLF crystal has a tetragonal crystal structure with C_{4h}^6 ($I4_1/A$) space group, and so the crystal is anisotropic and uniaxial [43,62]. Due to the anisotropy of the $LiYF_4$ crystal, the Er:YLF laser is able to emit linearly polarized laser radiation at 2.8 μm [22]. For this laser emission the common doping level of erbium is ~ 15% [22,63–65]. Using pulsed side-pumping, a high power laser can be obtained with an output average power 10 W and slope efficiency 18.7% in the free-running regime [22]. In Ref. [66], the true CW laser regime of Er:YLF was presented with a maximum output power of 4 W and slope efficiency 16.5%.

3.4. Er-doped sesquioxides

The erbium-doped sesquioxides (Er:Y_2O_3, Er:Sc_2O_3, Er:Lu_2O_3, Er:Al_2O_3) represent a very interesting sort of active media because of the material parameters, and particularly for high thermal conductivity which is required for high-power lasers [67]. For instance, the un-doped Y_2O_3, Lu_2O_3, and Sc_2O_3 possess higher thermal conductivity than the YAG [68]. The main difficulty in obtaining the high optical quality crystal is very high melting point (2770 K) which makes the fabrication challenging [67–69]. So, only a few materials such as rhenium, tungsten, osmium, tantalum, and carbon, (all with their melting point exceeding 3400 K) could be used for the fabrication of a crucible. Due to the toxicity, chemical reactivity, colouration, or corrosion by oxidic melts only rhenium is suitable material [68]. Using the heat-exchanger method with rhenium crucibles enables to fabricate a high-quality single crystal; however, production of a sesquioxide is still expensive [67,68], which is the main drawback of these matrices. On the other hand, it is possible to produce the sesquioxide in ceramic form, which reduces the cost and offers fabrication of active media in large dimensions and at high concentration [70].

The above-mentioned crystal hosts have a cubic bixbyite structure with space group T_H^7 (Ia3). The unit cell consists of two site symmetries, namely C_2 and C_{3i}, and the rare-earth ions can substitute both of them. However, the optical properties are mainly given by the activator in C_2 sites [68]. Due to the cation densities of ~ $3{\cdot}10^{22}$ cm^{-3} the doping concentration of rare-earth ions in sesquioxides is comparable with a double value in a YAG crystal [67]. Moreover, because of the low phonon energy of 600 cm^{-1}, the non-radiative transitions are reduced, and obtaining lasing in the mid-infrared range 2.7 μm is possible even with low-level doping of erbium [67,68]

There are three sesquioxide matrices that are commonly used with erbium ions namely Er:Y_2O_3, Er:Lu_2O_3, and Er:Sc_2O_3. All have very similar material and optical parameters, discussed in detail in Ref. [67]. Nevertheless, thermal conductivity is worthy of notice, because for the 5% concentration Lu_2O_3 unlike two other sesquioxides changes this value minimally. From 12.8 W m^{-1} K^{-1} (un-doped) thermal conductivity drops down only to 11.7 W m^{-1} K^{-1}; for the Er:Y_2O_3 and Er:Sc_2O_3 this decline is more than two-times higher [67]. For this reason, the Er:Lu_2O_3 could be more interesting for high power laser. With Er:Lu_2O_3, the maximal output power of 2.3 W and slope efficiency 29% in the CW regime was reached, which are the highest values obtained with the sesquioxide at 2.8 μm [71]. On the other hand, there is an active medium with higher thermal conductivity in comparison with Er:Lu_2O_3; it is the Er:α-Al_2O_3 (single crystal) [72]. So far, only the spectroscopic properties were published; however, according to Ref. [72], the Er:α-Al_2O_3 should possess extremely high power extraction capabilities. Moreover, Er:α-Al_2O_3 is uniaxial and it should generate polarization dependent laser radiation [72].

3.5. Er-doped orthovanadates

In general, the orthovanadates formula can be written as MVO_4, where M can represent: Sc, Y, Ce, Pr, Nd, Tb, Ho, Er, Tm, Yb, Lu; nevertheless, for laser active medium doped with erbium ions mainly three matrices are used, namely $GdVO_4$, YVO_4, and $LuVO_4$ [43,73–75]. In these matrices erbium substitutes for Y^{3+}, Gd^{3+}, or Lu^{3+} depending on the orthovanadates structure. The orthovanadate crystal has a tetragonal crystal structure with space group symmetry D_{4h}^{19} ($I4_1/amd$); so these crystals are anisotropic and uniaxial [43,73,76]. Because of the anisotropy crystals, the erbium-doped orthovanadates are able to emit linearly polarized laser radiation at 2.72 μm [42,77].

Orthovanadates are interesting particularly for lasing at 1.6 μm because the fluorescence decay time at upper laser level $^4I_{13/2}$ is much longer compared with $^4I_{11/2}$ [73]. Nevertheless, using the high doping level of erbium in YVO_4, makes it possible to lase at 2.72 μm due to the strong quenching of fluorescence decay time at $^4I_{13/2}$ [67]. To the best knowledge of the authors, the only paper deals with laser emission at ~ 2.7 μm using the orthovanadates Er:YVO_4 (concentration of Er^{3+} 30%) is [42].

3.6. Er-doped tungstates

There are many tungstate compositions based on $(WO_4)^{-2}$; however, for the erbium doping purpose, only two groups are interesting.

The first group possesses a monoclinic crystal structure with space group C_{2h}^6 ($C2/c$); so these crystals are biaxial and the general formula could be written as $AB(WO_4)_2$ [43,78–81], where A stands for the K, Li, Na [82,83] and B denotes the Gd, Y, Lu, Yb, Tm [78,80,84]. In the second group there are anisotropic (uniaxial) crystals with a tetragonal crystal structure, space group C_{4h}^6 ($I4_1/A$) [43] and general formula XWO_4. X can stand for Ca, Sr, Ba [85,86]. So, the Er^{3+} substitute the trivalent Gd, Y, Lu, Yb, and Tm or divalent Ca, Sr, and Ba [79,85]. For the divalent ions charge compensation is required; however, according to Ref. [85], it is a long-range, and thus it should not affect the undisturbed Ca^{2+} site.

There are several papers dealing with lasers that use Er-doped tungstate as an active medium [81,87,88]; however, most publications concern with ~ 1.6 μm lasers. Laser emission at 2.8 μm using the flashlamp pumping was obtained only with Er:KGW and Er:KYW and then published in Ref. [89,90], respectively. Nevertheless, both active materials are interesting for being able to emit directly polarization-dependent laser radiation which could be important for spectroscopy applications [50].

3.7. Er:CALGO

Generally, the formula for CALGO crystal can be written as $ABCO_4$, where A represents Ba, Ca, or Sr, B denotes rare-earth ion, and C stands for Al or Ga [91,92]. The CALGO ($CaGdAlO_4$) crystal possesses the D_{4h}^{17} ($I4/mmm$) space group and it can be grown by the Czochralski method. The activator ions Er^{3+} entering to crystal lattice substitute for Gd^{3+} ions [92]. Since the Er-doped CALGO is a uniaxial crystal, it is possible to generate naturally polarized laser radiation [91]. However, from spectroscopic measurements [93] it follows that the fluorescence decay times at upper and lower laser levels are very short as against the other erbium-doped active media. For the Er:CALGO at the upper $^4I_{11/2}$ and lower $^4I_{13/2}$ laser levels, the decay time is 450 μs and 982 μs, respectively [93]. Using Pr^{3+} to co-dope the Er:CALGO, it is possible to make the fluorescence decay time longer at the upper laser level; nevertheless, both fluorescence decay times are reduced to 84 μs and 74.3 μs at upper and lower laser level, respectively [93]. To the knowledge of the authors, there is no Er:CALGO laser system emitting at 3 μm wavelength region up to now.

3.8. Er-doped glasses

Glasses represent a special group of matrices because they can be fabricated in the form of bulk or fibres, also, glasses possess an amorphous structure, which bestows them a characteristic attribute [13,94]. Nowadays, there are many types of glass matrices based on various compositions, all with different material and optical parameters, e.g. silicate [94], potassium-lanthanum phosphate glasses [95,96], aluminoborate glasses [97], germanate glasses [98], chalcogenide glasses [99], etc. However, for laser emission in the spectral range ~ 3 μm only a few types of glasses are suitable. This is given by the presence of OH^- in glass. These groups reduce emission intensity and efficiency because they take part in energy transfer of Er^{3+} ions [94,100]. To avoid or reduce this issue, glasses with a minimal content of OH^- groups, such as fluoride glasses, should be used [100]. The best known fluoride glasses for 2.8 μm laser emission are fluoro-zirco-aluminate [101], ZBYA (ZrF_4-BaF_2-AlF_3-YF_3) [100], fluoro-tellurite [102], and ZBLAN (ZrF_4-BaF_2-LaF_3-AlF_3-NaF) [103].

The main advantage of glasses is their relative easy fabrication and possibility of producing in large volumes. As mentioned above, glass has an amorphous structure, and thus the spectral lines are broader in comparison with crystals which can be given by inhomogeneous line broadening. On the other hand, the absence of the crystal lattice reduces thermal conductivity, which to a certain extent limits the possible thermal load. However, from Refs. [104] it follows that using the multimode-core fibre configuration and cryogenic cooling, this problem can be overcome. Paper [104] presents the Er:ZBLAN CW laser operation at ~ 3 μm with maximum output power 24 W and slope efficiency 14.5% [13,96].

4. Short pulse generation at wavelength of 3 μm

Short pulse generation in the spectral range 3 μm is interesting particularly for applications in medicine (ophthalmology, surgery and dentistry) [1] or for further radiation conversion to mid-infrared spectrum, e.g. pumping of the active material as Fe:ZnSe, or for non-linear conversion [5,105]. Basically, for bulk lasers, there are only two ways how to obtain short pulses, i.e. the active or passive switching [2,14]. Systems using the former method are mostly based on Pockles cell or acousto-optic modulators which results in a complex resonator with the requirement for high voltage if the Pockels cell is used [106]. On the other hand, many latest papers deal with passive switching using saturable absorber such with SESAM (semiconductor saturable absorber mirror) [105,107], black phosphorus [60,108,109], graphene [24,110], or the Fe:ZnSe crystal [106,111]. These materials make it possible to build a compact laser resonator without the need of high voltage or a special non-linear crystal. Several of the above-mentioned laser active media were used together with a saturable absorber and the Q-switched or mode-locked pulses were generated. This section, presents a brief overview of passively Q-switched erbium lasers.

The diode-pumped mode-locked erbium laser systems with passive (SESAM, black phosphorus, and graphene) switching were also presented; however, the active medium was a fibre based on ZBLAN [112,113]. Up to now, the only paper deals with diode-pumped mode-locking erbium bulk laser was presented in Ref. [114], where the passively Q-switched mode-locked $Er:Y_2O_3$ laser was mentioned.

4.1. SESAM, black phosphorus, and graphene

The SESAM, black phosphorus, and graphene can be used in the laser resonator as saturable absorbers to obtain short Q-switched

pulses. However, the damage threshold of such saturable absorber is lower in comparison with a crystal, which can limit the output energy of Q-switched pulses [115]. Probably, the commercially most accessible solution saturable absorbers is a semiconductor structure with quantum well denotes as SESAM. The damage threshold of SESAM is ~ 4 mJ/cm^2 [116], which is almost 1000 times lower in comparison with the Fe:ZnSe crystal [115]; moreover, the SESAM can be damaged by Q-switched mode-locked pulses [117].

The SESAM Q-switching of Er:Y_2O_3 ceramic was successfully tested and presented [105,107]. It was shown [107] that using SESAM enables generating 29 ns pulses with pulse energy 17.4 μJ at 2.7 μm. Now, duration of 29 ns is probably the shortest pulse generated in the ~ 3 μm region reached with saturable absorber in a bulk laser system. If black phosphorus was used as Q-switcher with Er:Y_2O_3 ceramic, the shortest generated laser pulse was 4.47 μs with pulse energy 0.48 μJ [108]. The next sesquioxide tested with black phosphorus saturable absorber was Er:Lu_2O_3, which has shifted laser emission to 2.84 μm [67]. In Ref. [109] it was shown that Q-switched pulses reach 359 ns and 7.1 μJ. The relatively new and promising material for Q-switching is graphene, which enables the generating short pulses in a wide spectral range due to its broadband properties [110]. Li et al. showed [24] that by the graphene Q-switched Er:CaF_2 laser generated a radiation with a pulse duration 1.32 μs and pulse energy 2.74 μJ. A similar active medium Er:SrF_2 was Q-switched using the black phosphorus saturable absorber, which allows to reach the pulse duration of 702 ns and pulse energy 2.34 μJ at 2.79 μm. The last mentioned is special composite crystal GGG/Er:Pr:GGG/GGG tested together with a graphene saturable absorber mirror. With this set-up You et al. [110] successfully obtained 360 ns laser pulses with energy 1.54 μJ.

4.2. Crystalline saturable absorbers

Another solution how to obtain short pulses in the 3 μm wavelength region is to use crystals as saturable absorber. These crystals are based on ZnSe or ZnS matrix, where the Fe^{2+} or Co^{2+} can be used as an activator [4,106,115]. The advantage of these materials is their high damage threshold. It is 3 J/cm^2 and 1.5 J/cm^2 for Co:ZnSe and Fe:ZnSe, respectively [115], and, moreover, they are commercially available.

Q-switching of a flash-lamp pumped Cr,Er:YSGG was firstly realized by Kisel et al. [115] in 2005. It was shown that using the Fe:ZnSe crystal (as a saturable absorber) the 170 ns pulses with pulse energy 60 mJ at 2.8 μm can be obtained [115]. Using a different resonator design with the Fe:ZnSe Q-switcher the pulses from flash-lamp pumped Cr,Er:YSGG were further shortened to 65 ns [111]. The best-known erbium doped crystal – Er:YAG – was also tested. The diode-pumped highly doped Er:YAG (50% of Er^{3+}) was successfully Q-switched using the Fe:ZnSe single crystal, and pulse duration 50 ns with energy 6 mJ was reached [106].

If one compares the pulse duration achieved with crystal (50 ns) and SESAM (29 ns) Q-switchers, it is obvious that they are comparable. However, there is a huge gap in obtained pulse energy. With Fe:ZnSe crystal the energy of Q-switched pulse is approximately three order of magnitude higher in comparison with SESAM. For crystals, the pumping power can be higher, so it is possible to extract more energy [107].

5. Generation of radiation in the range 2.7–3 μm

The previous sections summarize the properties and laser results measured with various active media doped with erbium ions in the past years. In this section, the spectroscopic and laser results obtained in our laboratory with samples shown in Table 4 are presented. All samples were tested under similar conditions, which are discussed in detail in the text below. Also, all active media were plan-parallel polished and had no anti-reflection coating. All samples were pumped in the wavelength region ~ 970 nm by a fibre coupled laser diode and the data presented are for room-temperature. The only exception is made for Er:YAP laser, which was cooled to 80 K. For cryogenic cooling, the vacuum chamber of a liquid nitrogen cryostat (Janis Research, model VPF-100) was used. As far as the laser resonator (longitudinal pumping scheme) is concerned, all samples were tested in a hemispherical resonator with a flat pumping mirror (PM) and a spherical output coupler (OC) with various reflectivity (R_{OC}) and radius of curvature (r_{OC}). The R_{OC}, r_{OC}, and length of the resonator for particular active media are described in the text below. To measure the tunability, a birefringent MgF_2 plate was placed (under Brewster's angle) in a resonator between active medium and OC. The layout of the laser resonator can be seen in Fig. 3, the summary of laser results is presented in Table 6.

Table 3
Summary of erbium-doped laser active media with the best output laser results obtained; λ_{laser} – emitted laser wavelength, P^{out}_{max} – maximal output power, σ_{slope} – slope efficiency.

Active medium	Laser regime	λ_{laser} [μm]	P^{out}_{max} [W]	σ_{slope} [%]	References
Er:YAG	QCW	2.94	50	–	[39]
Er:YSGG	PU	2.79	10.1	6.5	[45]
Er:GGAG	CW	2.84	0.075	7.4	[41]
Er:YAP	CW	2.92	0.95	31	[51]
Er:YLF	CW	2.8	4	16.5	[66]
Er:CaF_2-SrF_2	CW	2.74	0.7	41.4	[124]
Er:SrF_2	CW	2.74	1	26	[59]
Er:Lu_2O_3	CW	2.71	2.3	29	[71]
Er:Y_2O_3	CW	2.71	14	26	[125]

Table 4
Tested Er-doped active media, FZU CAS – Institute of Physics, Czech Academy of Sciences; SIC CAS – Shanghai Institute of Ceramics, Chinese Academy of Science; INTiBS PAS – Institute of Low Temperature and Structure Research, Polish Academy of Sciences.

Samples	Origin	Er conc.	Length [mm]	Faces [mm]
Er:YAG	Crytur Ltd.	50 at. %	5.4	⌀ 2.96
Er:GGAG	FZU CAS	20 at. %	3.60	⌀ 12
Er:YLF	Unioriental Ltd.	6 at. %	3.00	⌀ 4
Er:Y_2O_3	Biakowski	5 at. %	9.00	3 × 3
Er:SrF_2	SIC CAS	3 at. %	9.00	3 × 3
Er:CaF_2	SIC CAS	3 at. %	9.00	3 × 3
Er:YAP	Crytur Ltd.	1 wt %	4.47	⌀ 25.7
Er:$GdVO_4$	INTiBS PAS	0.7 at. %	4.00	3 × 3
Er:GGAG	FZU CAS	0.5 at. %	9.50	⌀ 12
Er:YVO_4	INTiBS PAS	0.5 at. %	3.10	3 × 3

5.1. Methods and characterization

Transmission spectra of all samples were measured using Shimadzu spectrophotometer type UV – 3600 with spectral resolution ±0.2 nm in the visible and ultraviolet spectral band, and ±0.8 nm in the mid-infrared spectral band. Firstly, the absorption coefficient α [cm^{-1}] was calculated using the Lambert-Beer law and then the absorption cross-section σ [cm^{-2}] was derived. To avoid the inaccuracy in lifetime caused by radiation trapping or re-absorption, a confocal method [126] was used to measure the lifetimes at upper ($^4I_{11/2}$) and lower laser levels ($^4I_{13/2}$). The lifetime at $^4I_{11/2}$ was measured, using HP 4220 (Si PIN photodiode), and at $^4I_{13/2}$ using Thorlabs photodiode FGA10 (InGaAs, 800–1800 nm) with a long pass filter (cut-on wavelength 1400 nm). During these measurements, both photodiodes were connected to Tektronix oscilloscope TDS 3052B (500 MHz, 5 GS/s). The fluorescence spectra in the laser emission spectral range were measured using AROptix Fourier-transform spectrometer Arcspectro FT-MIR Rocket (FTIR, 2–6 μm, resolution 4 cm^{-1}). From the knowledge of the lifetimes at $^4I_{11/2}$ and fluorescence spectra it is possible to calculate the emission cross-section in the spectral range from 2.5 μm to 3 μm. In this spectral range there are no absorption lines, and therefore the reciprocity (McCumber relation) method cannot be utilised. Thus to obtain emission spectra the Füchtbauer–Ladenburg equation [2,21]:

$$\sigma_{em}(\lambda) = \frac{\lambda^5 \cdot I(\lambda)}{8\pi n(\lambda)^2 c \tau_{rad} \int I(\lambda) \cdot \lambda d\lambda}, \quad (1)$$

was used, where λ is the wavelength, $I(\lambda)$ fluorescence intensity, c speed of light, $n(\lambda)$ refractive index, and τ_{rad} corresponds to the radiative lifetime from Table 5. The emitted laser wavelength was measured using the Arcspectro FT-MIR Rocket Fourier-transform spectrometer and Oriel monochromator 77250 (grating 77300) with Thorlabs photodiode PDA20H-EC for CW and pulsed laser regimes, respectively. To evaluate the laser wavelength during the tunability measurement Oriel monochromator 77250 with Thorlabs photodiode PDA20H-EC was used. The setup with the monochromator was chosen because these measurements were carried out at a low repetition rate. The output power of the lasers was measured by Thorlabs power probe S401C (0.19–10.6 μm) connected to power meter PM100A. The laser beam spatial structure was evaluated by Spiricon Pyrocam III (camera chip $LiTaO_3$, active area 12.4 × 12.4 mm) with Thorlabs bandpass filter FB2500-500 (2500 ± 250 nm).

5.2. Er:YAG

The Er:YAG (50% of Er^{3+}, thickness 5.4 mm) crystal was grown in Crytur company by using the Czochralski method. For this crystal, the absorption and emission cross-section spectra were calculated and they are shown in Fig. 4 (PU in this and all other figures means pulsed regime). From Fig. 4a follows that the maximal absorption cross-section $0.97 \cdot 10^{-21}$ cm^2 corresponds to the wavelength 966 nm. Therefore, the pumping wavelength 966 nm was chosen for further experiments. The emission cross-section spectrum shown in Fig. 4b was obtained using FTIR spectrometer. As one can see, there are several peaks corresponding to possible emission laser lines. From the

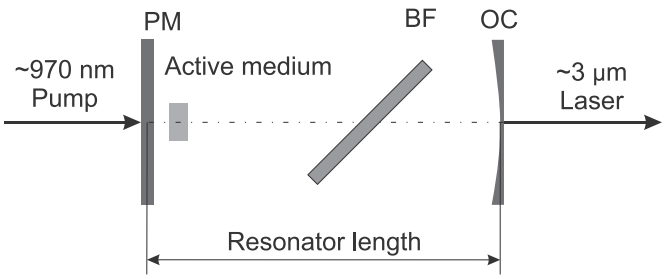

Fig. 3. Layout of laser resonator; pumping mirror (PM) – HT @ 660 – 980 nm, HR @ 2.65 – 3 μ m, output coupler – OC, BF – birefringent MgF_2 plate 2 mm thick.

Table 5
Fluorescence decay time at lower $^4I_{13/2}$ and upper $^4I_{11/2}$ laser level and σ_{max} – maximum of absorption cross-section for tested samples.

Samples	Fluorescence decay time		σ_{max} [10^{-21}cm^2]
	τ at $^4I_{13/2}$ [ms]	τ at $^4I_{11/2}$ [ms]	
Er:YAG	2.9	0.294	4.25 @ 966.6 nm
Er:GGAG	3.2	0.440	8.5 @ 965.3 nm
Er:YLF	10.9	4.1	9.8 @ 972.2 nm
Er:Y_2O_3	15.9	2.4	1.97 @ 971.2 nm
Er:SrF_2	13	7.3	2.67 @ 969 nm
Er:CaF_2	13.1	7.7	2.48 @ 968 nm
Er:YAP	4.1	0.83	9.8 @ 972.2 nm
Er:$GdVO_4$	4.2	–	25 @ 978.1 nm
Er:YVO_4	3.3	0.024	24.7 @ 977.4 nm

Table 6
Laser results for tested laser active media, L_{res} – resonator length, R_{OC} – output coupler reflectivity, f – frequency, P_{max} – maximal output power, σ – slope efficiency.

Sample	L_{res} [mm]	R_{OC} [%]	f [Hz]	P_{max} [mW]	σ [%]
Pulsed laser regime					
Er:YAG	40	97.5	50	105	16.8
Er(20%):GGAG	50	97.5	10	23	13.5
Er:YLF	45	95	10	171	24.5
Er:Y_2O_3	10	97.5	10	26	4.8
Er:SrF_2	145	95	10	58	7.3
Er:CaF_2	145	95	10	23	2.8
CW laser regime					
Er:YAP	145	95	–	26.8	3.5
Er(20%):GGAG	50	97.5	–	75.5	7.4
Er:YLF	45	95	–	1100	30.0

lifetime of the upper $^4I_{11/2}$ (294 μs) and lower $^4I_{13/2}$ (2.9 ms) laser levels presented in Table 5, it can be seen that the ratio between decay times is almost 1:10. So, the self-termination effect will probably affect the laser action.

The laser output characteristics for the highly doped Er:YAG is presented in Fig. 4c. The Er:YAG was placed in a copper holder in a hemispherical laser resonator with $R_{OC} = 97.5\%$ @ 2.94 μm, $r_{OC} = 50$ mm and resonator length 10 mm. The pulsed pumping radiation (frequency 10 Hz, pulse duration 2 ms) from LIMO laser diode (LIMO35-F100-DL976-EX1202) was focused into the tested crystal by two achromatic doublet lenses with a focal length of $f_1 = 75$ mm and $f_2 = 150$ mm, thus the pumping beam diameter was ~200 μm. The maximal output energy 1.8 mJ at 2.94 μm with slope efficiency 16.8% was reached. The theoretical limit for slope efficiency is ~ 32%, thus with respect to this fact, almost half of the possible efficiency was reached. Moreover, from the beam profile shown in Fig. 4c, one can see that the laser emitted radiation close to the fundamental mode TEM_{00}.

5.3. Er:GGAG

The Er:GGAG (20% of Er^{3+}, thickness 3.6 mm) active medium was grown by the Czochralski method in the Institute of Physics of the Czech Academy of Sciences. In Fig. 5a one can see the absorption spectrum which is broader compared with the Er:YAG. This is beneficial for laser diode pumping because of overlapping the laser diode spectral line and absorption line of the crystal. The maximum of the absorption cross-section ($8.5 \cdot 10^{-21}$ cm^2) is located at 965.3 nm, so during experiments, the pumping wavelength 965 nm was chosen. On the other hand, from the emission cross-section spectrum in Fig. 5b one can assume that the Er:GGAG is appropriate for generating short pulses, since its spectrum is broader in comparison with Er:YAG. Even if the ratio between lifetimes (at lower and upper laser level) is smaller, in comparison with Er:YAG; the Er:GGAG is probably affected by the bottleneck effect, too.

The laser results are presented in Fig. 5c–d. To reduce the losses caused by absorption on water molecules in air a short 50 mm hemispherical resonator ($R_{OC} = 97.5\%$, $r_{OC} = 50$ mm) was used. In the pulsed regime, the maximal output energy 4.9 mJ, slope efficiency 13.5%, and emitted laser wavelength 2839 nm were reached. In the CW laser regime the slope efficiency was smaller (7.4%); however, the maximal output power was increased to a value of 75.5 mW. From the tunability measurements it follows that the Er:GGAG can be line-tuned in several spectral ranges: 2800–2822 nm, 2829–2891 nm, and 2917–2942 nm, see Fig. 5e. A detailed study of Er:GGAG active medium was first published in Ref. [41].

5.4. Er:SrF_2 and Er:CaF_2

Both active media, i.e. Er:SrF_2 and Er:CaF_2 (3% of Er^{3+}, thickness 9 mm) was grown at the Chinese Academy of Science. From the absorption spectra of both samples shown in Fig. 6a it can be seen that the maximal absorption cross-section of active media is similar, being $2.48 \cdot 10^{-21}$ cm^2 @ 968 nm and $2.67 \cdot 10^{-21}$ cm^2 @ 969 nm for Er:CaF_2 and Er:SrF_2, respectively. As far as the emission cross-section

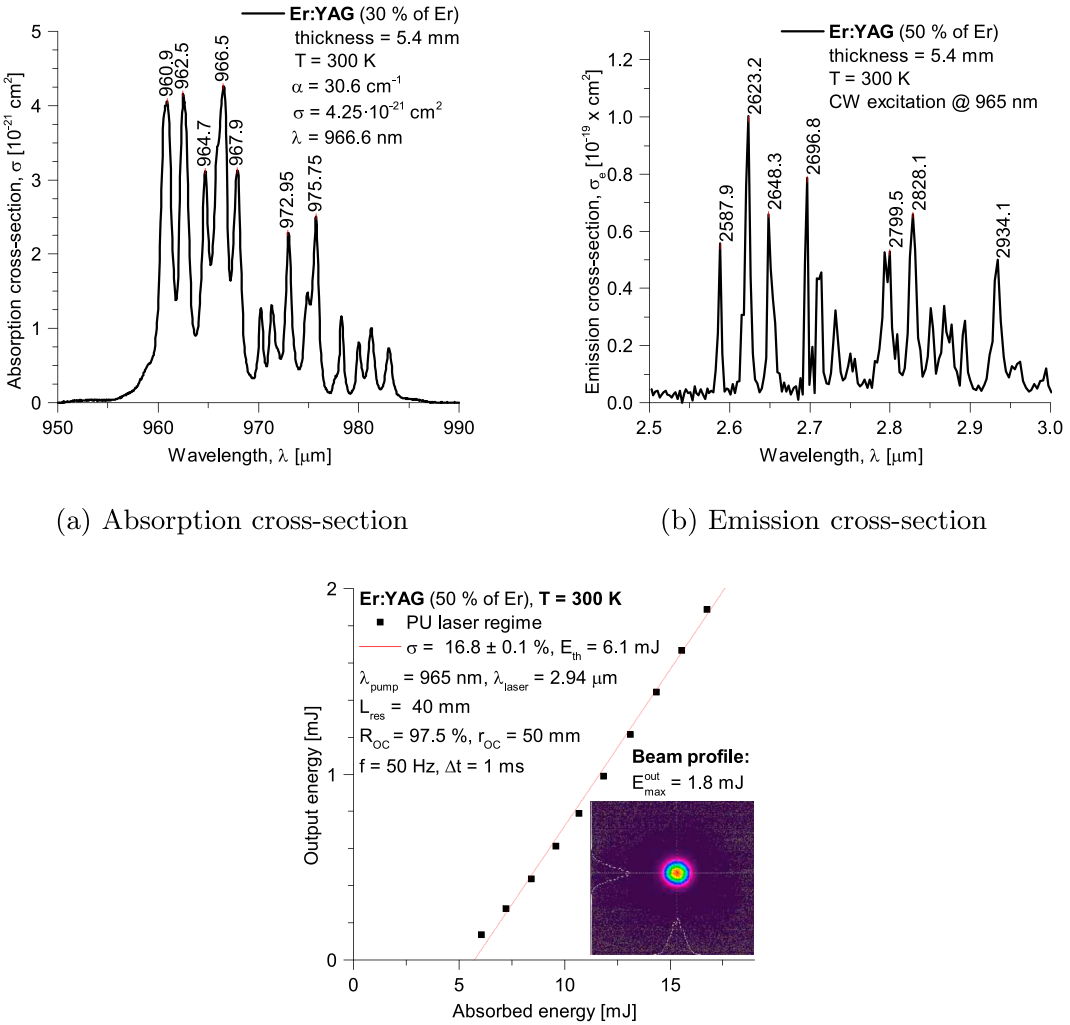

(a) Absorption cross-section

(b) Emission cross-section

(c) Laser output characteristic; inset: beam profile

Fig. 4. Spectroscopic and laser characteristic of Er:YAG active medium.

spectrum is concerned, it is obvious that the broad emission spectrum shown in Fig. 6b should be advantageous for generating a short pulses in the mode-locked regime. Due to the crystal structure of these active media, which was analysed above, both crystals are suitable for CW laser application; however, the low thermal conductivity limits the obtainable output power [5].

As in the previous measurements, both samples were attached to a copper holder and placed in the laser resonator. The hemispherical laser resonator 145 mm long with $R_{OC} = 95\%$ and $r_{OC} = 150$ mm was used for both active media. To reduce the thermal load, the laser was tested in pulsed laser regime with low repetition rate 10 Hz. The maximal output energy 5.8 mJ, 2.3 mJ and slope efficiency 7.3%, 2.8% for Er:SrF_2 and Er:CaF_2 were reached, respectively. Since both crystals posses broadband emission spectra, the laser tuning was also tested. It was found that the Er:SrF_2 can be tuned in the spectral range from 2690 nm to 2813 nm, which was published in Ref. [5]. Also, the Er:CaF_2 active medium has a broad tuning ranging curve from 2692 nm up to 2840 nm [127]. Both tunning curves are presented in Fig. 6e.

5.5. Er:YAP

The Er:YAP crystal was grown in the Crytur company, using the Czochralski method. The tested sample of Er:YAP (thickness 4.47 mm) contained 1 wt % of Er^{3+}. Since the Er:YAP is a biaxial crystal, the absorption spectra presented in Fig. 7a are for σ - and π - polarization. However, the fluorescence and laser measurements were executed in un-polarized light. The pumping wavelength 972.2 nm was chosen because it corresponds with the maximum of absorption cross-section $9.8 \cdot 10^{-21}$ cm^2 at 972.2 nm. The emission cross-

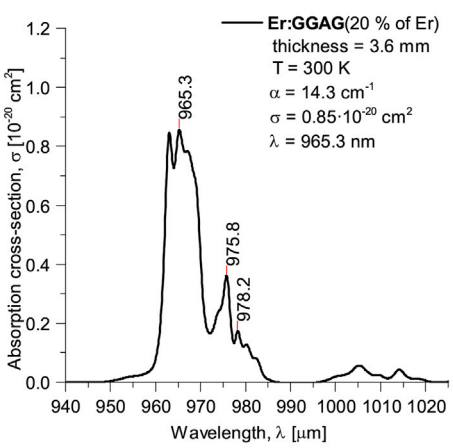

(a) Absorption cross-section

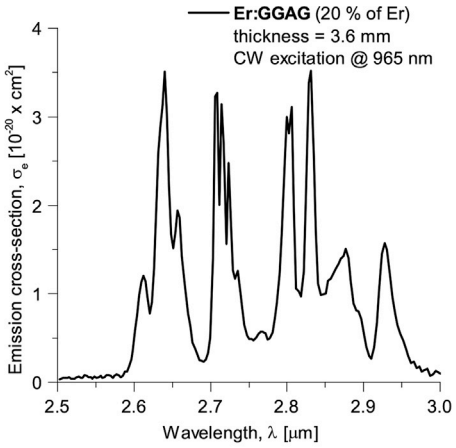

(b) Emission cross-section

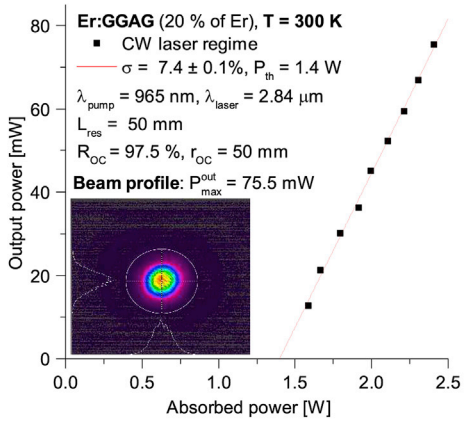

(c) CW laser output characteristic; inset: beam profile

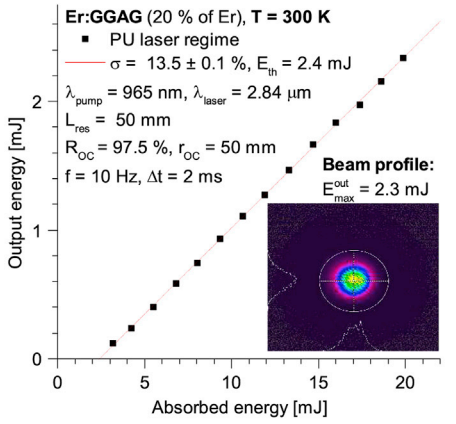

(d) Pulsed laser output characteristic; inset: beam profile

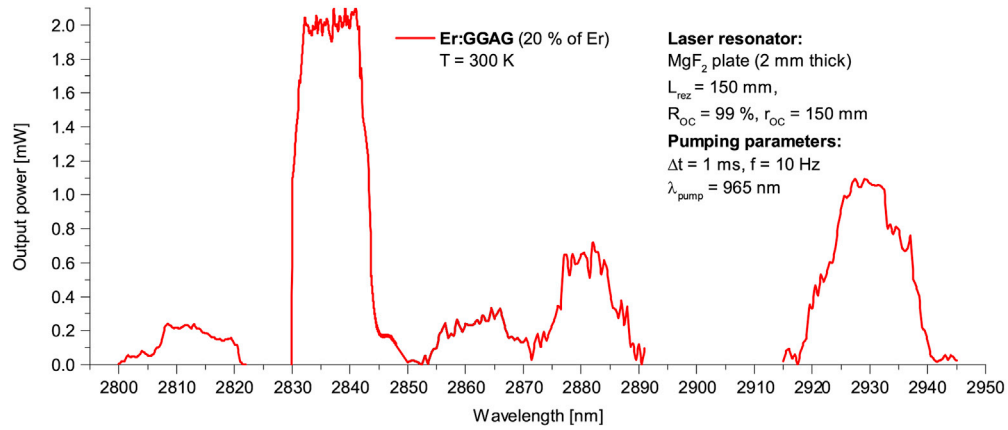

(e) Tuning curve of Er:GGAG laser measured for maximal pumping

Fig. 5. Spectroscopic and laser characteristic of Er:GGAG active medium.

section spectrum shown in Fig. 7b has narrow lines compared with Er:CaF_2, Er:GGAG, or Er:SrF_2, so it was not possible to tune the output laser wavelength. The lifetime at upper laser level (830 μs) is much shorter in comparison with the lower laser level (4.2 ms), so the laser action is affected by the self-termination effect [18].

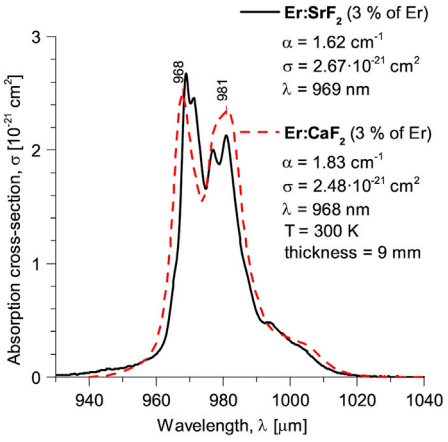

(a) Absorption cross-section

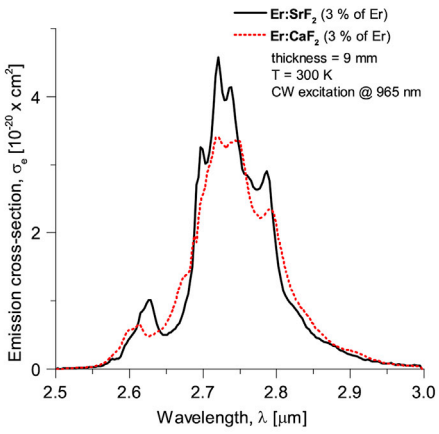

(b) Emission cross-section

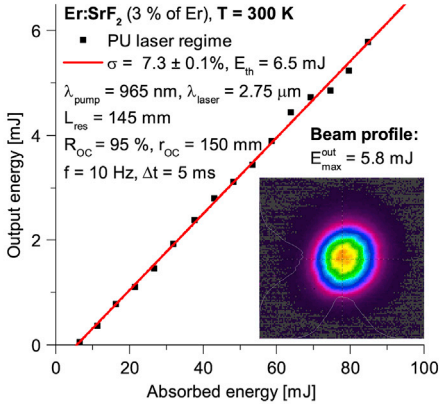

(c) $Er:SrF_2$ laser output characteristic; inset: beam profile

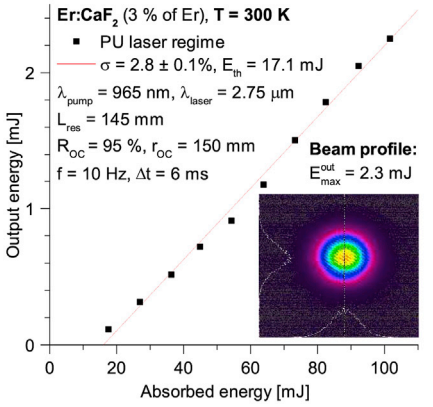

(d) $Er:CaF_2$ laser output characteristic; inset: beam profile

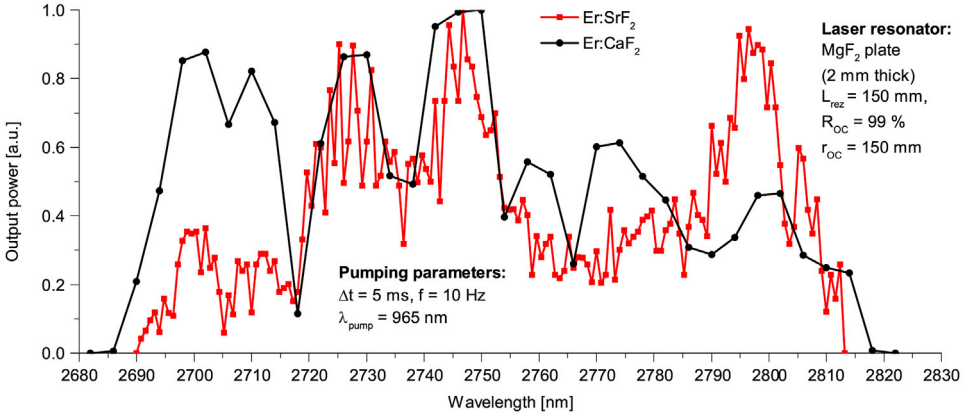

(e) Tuning curve of $Er:SrF_2$ and $Er:CaF_2$ measured for maximal pumping shown together with air absorption lines

Fig. 6. Spectroscopic and laser characteristic of $Er:CaF_2$ and $Er:SrF_2$ active media.

For the Er:YAP laser, a 145 mm hemispherical laser resonator with output coupler $R_{OC} = 95\%$ and $r_{OC} = 150$ mm was built. To obtain laser action at 2.73 μm in the CW laser regime the active medium had to be cooled down to 77 K. Detailed description of the measurement can be found in Ref. [18]. The maximal output power and slope efficiency were 26.8 mW and 3.5%, respectively. These values were reached at 77 K for a CW laser regime (see Fig. 7c–d). From Fig. 7c it can be seen that in case of pulsed regime the laser radiation space structure was close to the fundamental mode.

5.6. Er:YLF

The uniaxial a-cut Er:YLF crystal (6 at. % of Er^{3+}) was fabricated in Unioriental Ltd. The tested sample was cylindrical rod (length 9 mm, diameter 4 mm). The absorption spectra were measured for both π - and σ - polarization and it can be seen in Fig. 8a. The maximal absorption cross-section is located at 972.4 nm ($3.8 \cdot 10^{-21}$ cm^2). The following measurements were carried out with non-polarized laser radiation.

The short laser resonator (45 mm) with $R_{OC} = 95\%$ and $r_{OC} = 50$ mm was used to obtain the laser radiation in pulsed and CW laser regimes. In both regimes, the laser emitted radiation at 2809 nm. The maximal slope efficiency 30% and output power 1.1 W together with laser threshold 0.8 W were reached in the CW laser regime. The results are presented in Fig. 8c and d. As the sample was not actively cooled, higher pumping power was not used to prevent the destruction of the crystal. From all tested laser crystals, the Er:YLF provides the maximal output power and slope efficiency.

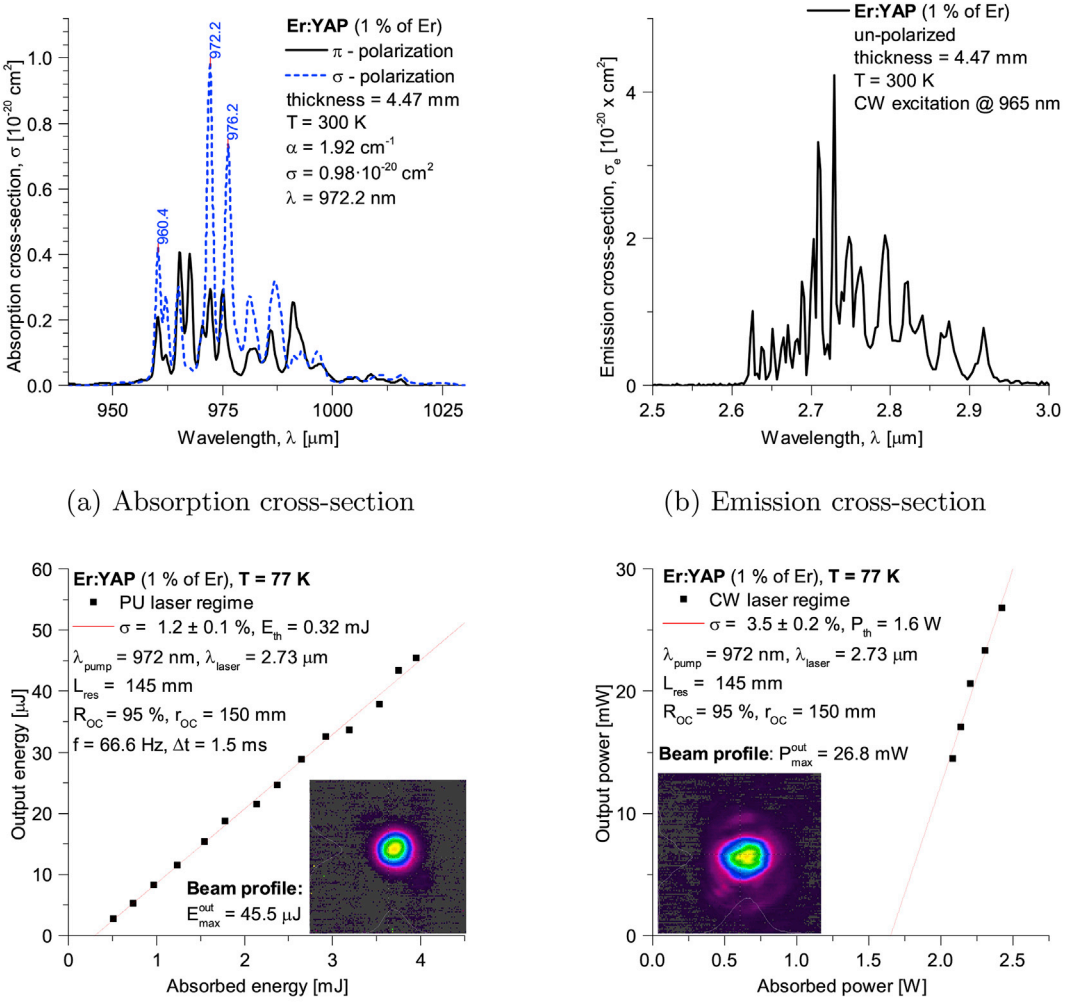

(a) Absorption cross-section

(b) Emission cross-section

(c) Pulsed laser output characteristic; inset: beam profile

(d) CW laser output characteristic; inset: beam profile

Fig. 7. Spectroscopic and laser characteristics of Er:YAP active medium.

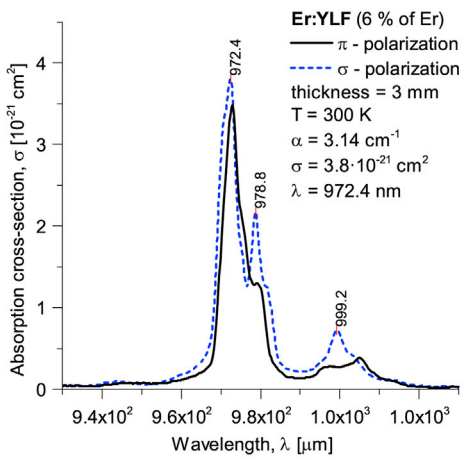

(a) Absorption cross-section

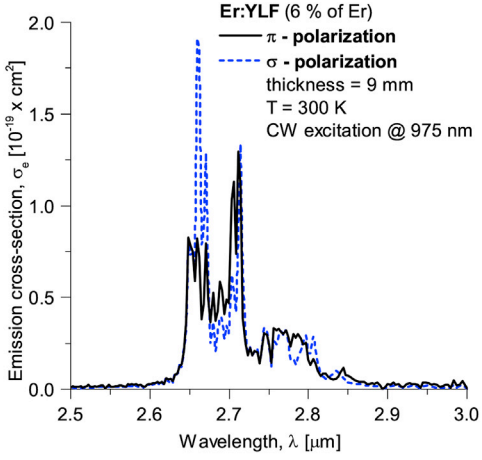

(b) Emission cross-section

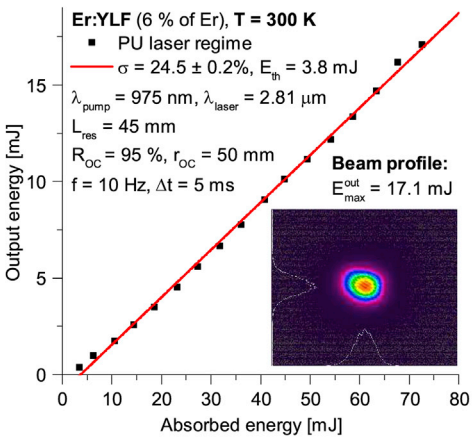

(c) Pulsed laser output characteristic; inset: beam profile

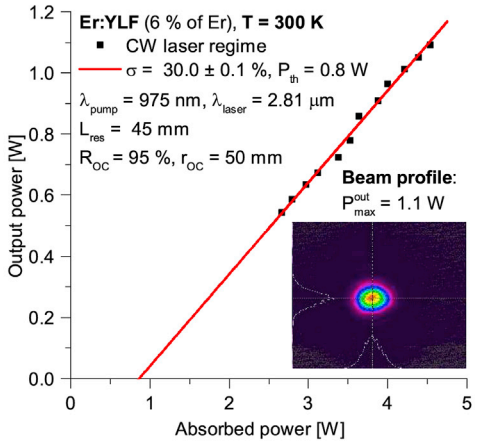

(d) CW laser output characteristic; inset: beam profile

Fig. 8. Spectroscopic and laser characteristics of Er:YLF active medium.

5.7. *Er:Y_2O_3*

The Er:Y_2O_3 ceramic from Biakowski Ltd. has the form of a brick (length 9 mm, faces 3 × 3 mm) and 5 at. % concentration of erbium. In Fig. 9a one can see the absorption spectrum of Er:Y_2O_3, it shows that the maximal absorption cross-section ($1.97{\cdot}10^{-21}$ cm^2) corresponds with wavelength 971.2 nm. So, for the laser experiments and fluorescence measurements (presented in Fig. 9b), the chosen pumping wavelength was 971 nm.

Using a short laser resonator (10 mm) with output coupler $R_{OC} = 97.5\%$ ($r_{OC} = 50$ mm) the Er:Y_2O_3 ceramic was tested in the pulsed laser regime. The maximal output energy achieved was 2.6 mJ with 4.8% slope efficiency; the output laser characteristic is presented in Fig. 9c. The low output energy was probably affected by sample quality. The laser emitted at wavelength 2.75 μm, the tunability was tested, however, the tuning was not reached.

5.8. *Summary of experimental results*

In this comprehensive study, a spectroscopic and laser properties of erbium-doped active media under laser diode pumping were investigated. Overall six crystals (Er:YAG, Er:GGAG, Er:SrF_2, Er:CaF_2, Er:YAP, Er:YLF) with various concentration of Er^{3+} and one ceramic (Er:Y_2O_3) were tested and results are presented in text above and summarized in Table 7. All active media were pumped with fibre-coupled laser diode emitting around 970 nm. From results follow that all active media emitted laser radiation in pulsed laser

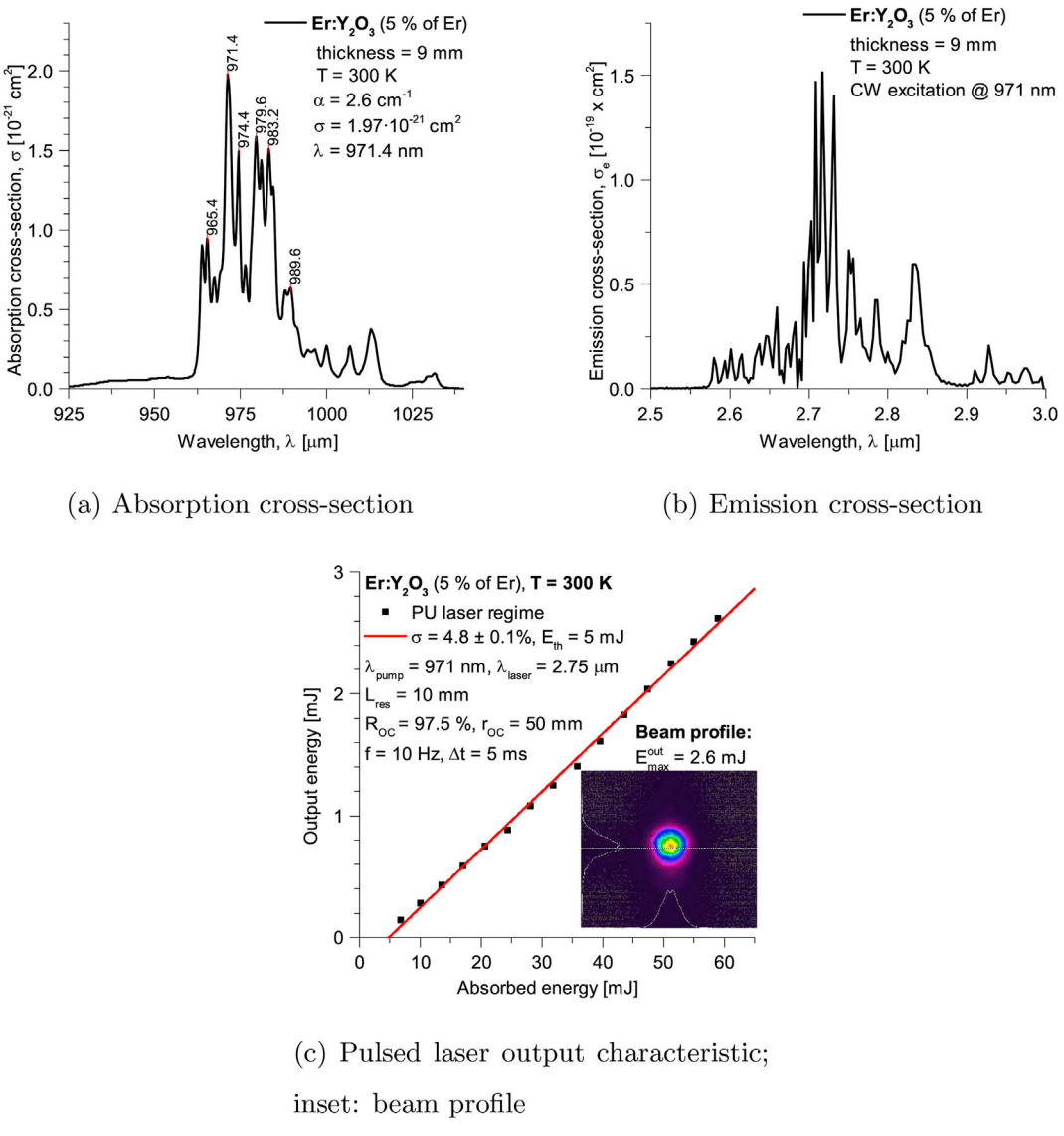

Fig. 9. Spectroscopic and laser characteristics of Er:Y_2O_3 active medium.

regime, however, the CW laser operation was reached with Er:GGAG, Er:YAP, and Er:YLF crystals. The Er:GGAG crystal is a unique active medium based on a mixed garnet structure with relatively broad absorption and emission spectral lines and with attractive laser

Table 7
Summary of spectroscopic and laser results, conc. – at. concentration of Er^{3+}, σ_{max}^{abs} – maximal absorption cross-section, σ_{max}^{em} – maximal emission cross-section, τ_{lo} and τ_{up} fluorescence decay time at lower $^4I_{13/2}$ and upper $I_{11/2}$ laser level, $P_J^J CW^{max}$ – maximal output power in CW laser regime, $E_J^J PU^{max}$ – maximal output energy in pulse laser regime, σ_{CW} and σ_{PU} – slope efficiency in CW and pulsed regime, $\Delta\lambda$ – maximal wavelength tunability, λ – emission laser line, Ref. – author's literature references, * – presented for the first time in this work.

Samples	conc.	σ_{max}^{abs}	σ_{max}^{em}	τ_{lo}	τ_{up}	P_{CW}^{max}	E_{PU}^{max}	σ_{CW}	σ_{PU}	$\Delta\lambda$	λ	Ref.
	[%]	[10^{-21}cm^2]	[10^{-20}cm^2]	[ms]	[ms]	[mW]	[mJ]	[%]	[%]	[nm]	[μm]	
Er:YAG	50 at.	4.25 @ 966.6 nm	10 @ 2623 nm	2.9	0.29	–	1.8	–	16.8	–	2.94	*
Er:GGAG	20 at.	8.5 @ 965.3 nm	2.5 @ 2639 nm	3.2	0.44	75.5	2.3	7.4	13.5	62	2.84	[41]
Er:YAP	1 wt	9.8 @ 972.2 nm	4.2 @ 2729 nm	4.1	0.83	26.8	0.1	3.5	1.2	–	2.73	[18]
Er:YLF	6 at.	9.8 @ 972.2 nm	19 @ 2659 nm	10.9	4.1	1100	17.1	30	24.5	–	2.81	*
Er:Y_2O_3	5 at.	1.97 @ 971.2 nm	15 @ 2717 nm	15.9	2.4	–	2.6	–	4.8	–	2.75	[114]
Er:SrF_2	3 at.	2.67 @ 969 nm	4.5 @ 2720 nm	13.0	7.3	–	5.8	–	7.3	123	2.75	[5]
Er:CaF_2	3 at.	2.48 @ 968 nm	3.4 @ 2720 nm	13.1	7.7	–	2.3	–	2.8	148	2.75	[127]

output characteristics. However, further research and investigation is necessary to determine an appropriate concentration of Er^{3+} ions and improve crystal quality. On the other hand, Er:YLF lasers can be proposed for application (e.g. polymer processing) since the CW output reached relatively high slope efficiencies 30% and output powers 1.1 W. Using a birefringent plate (MgF_2) the tunability of emitted laser wavelength was obtained, however, only with Er:GGAG, Er:SrF_2, and Er:CaF_2 crystals. Maximal tuning range 123 nm extended from 2690 nm to 2813 nm (crossing zero) was obtained for Er:SrF_2 laser. This is one of the major results of this work since the last published result [19] presented significantly narrower tuning range only (40 nm, 2720–2760 nm). Moreover, for Er:CaF_2 laser has an even broad tuning ranging in comparison with Er:SrF_2, it was from 2692 nm up to 2840 nm (148 nm) [127]. Summary of all results presented in the text above can be found in Table 7.

6. Conclusion

This paper summarizes the erbium-doped bulk active materials the majority of which are used in laser science. It is an overview work of the Er-doped matrices, it contents the various materials optical parameters and spectroscopic properties as well as the best laser radiation outputs (the highest output power, slope efficiency, laser wavelength tunability, and short pulse generation) obtained with these active media. Our main goals were investigation and research of new active media such as Er:GGAG and their comparison with commonly used erbium-doped crystals or ceramic. We have focused on spectroscopy of erbium-doped active media as well as on tunning of emitting laser wavelength. The summary of all results obtained in our laboratory can be found in section 5.8 and in Table 7. From the point of view of authors the most significant results that are shown in text above are summary of emission cross-section spectra for particular active media together with fluorescence decay times, spectroscopy and laser results of Er:GGAG crystal [41], and tuning curves of Er:SrF_2 [5] and Er:CaF_2 [127] lasers which significantly exceeded results published in literature. If the emitted wavelength of Er:SrF_2 laser is tuned (using birefringent plate) it is possible to reach a continuous tuning range 123 nm (2690–2813 nm), moreover, for Er:CaF_2 laser this range can be even wider 148 nm (2692–2840 nm). This tuning range was broadened to 2942 nm when new active laser medium Er:GGAG was used. As stated above, Er:GGAG crystal is unique since it is based on mixed garnet structure and possesses broad spectral lines which beside other things allow to tune emitted laser wavelength contrary to Er:YAG.

In comparison with OPO, sum frequency generation or other non-linear conversions which are able to cover the wavelength range of 3 μm, the erbium lasers offer a compact and cheaper way how to generate laser radiation in this spectral range. The solid-state bulk lasers based on erbium ions enable to extract the output power exceeding the watts in CW regime (Er:YLF, Er:Y_2O_3,Er:Lu_2O_3, Er:SrF_2) and reaching 50 W in free-running regime (Er:YAG). Moreover, with a new saturable absorber it is possible to generate short pulses that reach the nanoseconds level with a peak power of 3.6 MW. Therefore, we believe that intense and further research of the existing and new laser active media containing Er^{3+} ions is desirable to push the limits of erbium lasers further beyond the contemporary results.

Acknowledgment

The Research has been supported by the “Center of Advanced Applied Sciences”, Reg. No. CZ.02.1.01/0.0/0.0/16_019/0000778 - the Operational Program Research, Development and Education, co-financed by the European Structural and Investment Funds and the goverment budget of the Czech Republic.

Authors would like to express special thanks to prof. Liangbi Su from Key Laboratory of Transparent and Opto-functional Inorganic Materials, Shanghai Institute of Ceramics, Chinese Academy of Science for providing Er:SrF_2 and Er:CaF_2 crystals; as well as our colleagues from Institute of Physics of the Czech Academy of Sciences for growing, cutting and polishing Er:GGAG crystal.

References

[1] H. Jelínková (Ed.), Lasers for Medical Applications Diagnostics, Therapy and Surgery, first ed., Woodhead Publishing Limited, 2013.
[2] R. Paschotta, Encyclopedia of Laser Physics and Technology, Wiley-VCH, 2008.
[3] A. Godard, Infrared (2-12 μm) solid-state laser sources: a review, Compt. Rendus Phys. 8 (10) (2007) 1100–1128, https://doi.org/10.1016/j.crhy.2007.09.010.
[4] V.V. Fedorov, S.B. Mirov, A. Gallian, D.V. Badikov, M.P. Frolov, Y.V. Korostelin, V.I. Kozlovsky, A.I. Landman, Y.P. Podmar'kov, V.A. Akimov, A.A. Voronov, 3.77-5.05- μm tunable solid-state lasers based on Fe^{2+}-doped ZnSe crystals operating at low and room temperatures, IEEE J. Quant. Electron. 42 (9) (2006) 907–917, https://doi.org/10.1109/JQE.2006.880119.
[5] R. Švejkar, J. Šulc, H. Jelínková, V. Kubeček, W. Ma, D. Jiang, Q. Wu, L. Su, Diode-pumped Er:SrF_2 laser tunable at 2.7 μm, Opt. Mater. Express 8 (4) (2018) 1025–1030, https://doi.org/10.1364/OME.8.001025.
[6] D.Y. Shen, J.K. Sahu, W.A. Clarkson, Highly efficient in-band pumped Er:YAG laser with 60 W of output at 1645 nm, Opt. Lett. 31 (6) (2006) 754–756, https://doi.org/10.1364/OL.31.000754.
[7] K. Spariosu, M. Birnbaum, Room-temperature 1.644 micron Er:YAG lasers, in: Advanced Solid State Lasers, Optical Society of America, 1992, p. ML4, https://doi.org/10.1364/ASSL.1992.ML4.
[8] J.F. Pinto, G.H. Rosenblatt, L. Esterowitz, Continuous-wave laser action in Er^{3+}:YLF at 3.41 μm, Electron. Lett. 30 (19) (1994) 1596–1598, https://doi.org/10.1049/el:19941085.
[9] R. Brede, T. Danger, E. Heumann, G. Huber, B. Chai, Room temperature green laser emission of Er:$LiYF_4$, Appl. Phys. Lett. 63 (6) (1993) 729–730, https://doi.org/10.1063/1.109942.
[10] N. Ter-Gabrielyan, V. Fromzel, Cascade generation at 1.62, 1.73 and 2.8 μm in the Er:YLF Q-switched laser, Optic Express 27 (15) (2019) 20199–20210, https://doi.org/10.1364/OE.27.020199.
[11] T. Sanamyan, Efficient cryogenic mid-IR and eye-safe Er:YAG laser, J. Opt. Soc. Am. B 33 (11) (2016) D1–D6, https://doi.org/10.1364/JOSAB.33.0000D1.
[12] W.M. Haynes, D.R. Lide, T.J. Bruno, CRC Handbook of Chemistry and Physics (2016-2017), 97th Edition, CRC Press, 2017.
[13] E. Desurvire, Erbium-Doped Fiber Amplifiers, John Wiley and Sons, Inc., 1994.
[14] W. Koechner, Solid-State Laser Engeneering, Springer Science Business Media, 2006.
[15] A.A. Kaminskii, Laser Crystals - Their Physics and Properties, second ed., Springer-Verlag Berlin Heidelberg GmbH, 1990.
[16] M.J. Weber (Ed.), Handbook of Laser Wavelength, CRC press, 1996.

[17] N. Ter-Gabrielyan, M. Dubinskii, G.A. Newburgh, A. Michael, L.D. Merkle, Temperature dependence of a diode-pumped cryogenic Er:YAG laser, Optic Express 17 (9) (2009) 7159–7169, https://doi.org/10.1364/OE.17.007159.

[18] R. Švejkar, J. Šulc, M. Němec, H. Jelínková, K. Nejezchleb, M. Čech, Temperature influence on spectroscopic properties and 2.7 μm lasing of Er:YAP crystal, in: Solid State Lasers XXVII: Technology and Devices, vol. 10511, 2018, pp. 10511–10516, https://doi.org/10.1117/12.2287138.

[19] T.T. Basiev, Y.V. Orlovskii, M.V. Polyachenkova, P.P. Fedorov, S.V. Kuznetsov, V.A.V.A. Konyushkin, V.V. Osiko, O.K. Alimov, A.Y. Dergachev, Continuously tunable cw lasing near 2.75 μm in diode-pumped Er^{3+}:SrF_2 and Er^{3+}:CaF_2 crystals, Quant. Electron. 36 (2006) 591–594, https://doi.org/10.1070/QE2006v036n07ABEH013178.

[20] C. Labbe, J. Doualan, P. Camy, R. Moncorgé, M. Thuau, The 2.8 μm laser properties of Er^{3+} doped CaF_2 crystals, Optic Commun. 209 (1) (2002) 193–199, https://doi.org/10.1016/S0030-4018(02)01628-0.

[21] W. Ma, X. Qian, J. Wang, J. Liu, X. Fan, J. Liu, L. Su, J. Xu, Highly efficient dual-wavelength mid-infrared CW laser in diode end-pumped Er:SrF_2 single crystals, Sci. Rep. 6 (36635) (2016) 36635, https://doi.org/10.1038/srep36635.

[22] M. Messner, A. Heinrich, K. Unterrainer, High-energy diode side-pumped Er:$LiYF_4$ laser, Appl. Optic. 57 (6) (2018) 1497–1503, https://doi.org/10.1364/AO.57.001497.

[23] R. Švejkar, J. Šulc, M. Němec, Jelínková, M.E. Doroshenko, A.N. Nakladov, V.V. Osiko, Effect of cryogenic temperature on spectroscopic and laser properties of Er,La:SrF_2-CaF_2 crystal, Proc. SPIE 9726 (2016), https://doi.org/10.1117/12.2208569, 97261C–7.

[24] C. Li, J. Liu, S. Jiang, S. Xu, W. Ma, J. Wang, X. Xu, L. Su, 2.8 μm passively Q-switched Er:CaF_2 diode-pumped laser, Opt. Mater. Express 6 (5) (2016) 1570–1575, https://doi.org/10.1364/OME.6.001570.

[25] A.J. Silversmith, W. Lenth, R.M. Macfarlane, Green infrared pumped erbium upconversion laser, Appl. Phys. Lett. 51 (24) (1987) 1977–1979, https://doi.org/10.1063/1.98316.

[26] F. Vetrone, J.-C. Boyer, J.A. Capobianco, A. Speghini, M. Bettinelli, Luminescence spectroscopy and near-infrared to visible upconversion of nanocrystalline $Gd_3Ga_5O_{12}$:Er^{3+}, J. Phys. Chem. B 107 (2003) 10747–10752, https://doi.org/10.1021/jp030434r.

[27] V. Lupei, RE^{3+} emission in garnets: multisites, energy transfer and quantum efficiency, Opt. Mater. 19 (1) (2002) 95–107, https://doi.org/10.1016/S0925-3467(01)00206-3, photonic Materials for the 21st Century. Proceedings of the 2nd International Symposium on Laser, Scintillator and Nonlinear Optical Materials.

[28] L. Dobrzycki, E. Bulska, D.A. Pawlak, Z. Frukacz, K. Woźniak, Structure of YAG crystals doped/substituted with erbium and ytterbium, Inorg. Chem. 43 (2004) 7656–7664, https://doi.org/10.1021/ic049920z.

[29] J. Šulc, P. Boháček, M. Němec, H. Jelínková, B. Trunda, L. Havlák, K. Jurek, M. Nikl, Tunable diode-pumped Er:GGAG laser, in: 2016 International Conference Laser Optics (LO), 2016, https://doi.org/10.1109/LO.2016.7549682. R1–64–R1–64.

[30] Z. You, Y. Wang, J. Xu, Z. Zhu, J. Li, C. Tu, Diode-End-pumped midinfrared multiwavelength Er:Pr:GGG laser, IEEE Photon. Technol. Lett. 26 (7) (2014) 667–670, https://doi.org/10.1109/LPT.2014.2302837.

[31] B.J. Dinerman, P.F. Moulton, 3-μm cw laser operations in erbium-doped YSGG, GGG, and YAG, Opt. Lett. 19 (15) (1994) 1143–1145, https://doi.org/10.1364/OL.19.001143.

[32] M. Tempus, W. Luthy, H.P. Weber, V.G. Ostroumov, I.A. Shcherbakov, 2.79 μm YSGG:Cr:Er laser pumped at 790 nm, IEEE J. Quant. Electron. 30 (11) (1994) 2608–2611, https://doi.org/10.1109/3.333714.

[33] B. Henderson, R.H. Bartram, Crystal-field Engineering of Solid-State Laser Materials, Cambridge Studies in Modern Optics, Cambridge University Press, Cambridge, 2000.

[34] M. Skorczakowski, J. Swiderski, W. Pichola, P. Nyga, A. Zajac, M. Maciejewska, L. Galecki, J. Kasprzak, S. Gross, A. Heinrich, T. Bragagna, Mid-infrared Q-switched Er:YAG laser for medical applications, Laser Phys. Lett. 7 (7) (2010) 498, https://doi.org/10.1002/lapl.201010019.

[35] N.V. Volkova, L.K. Glazkova, V.V. Khomchenko, N.S. Sadick, Novel method for facial rejuvenation using Er:YAG laser equipped with a spatially modulated ablation module: an open prospective uncontrolled cohort study, J. Cosmet. Laser Ther. 19 (2017) 25–29, https://doi.org/10.1080/14764172.2016.1247964.

[36] P. Maurizio, S. Konstanze, K. Roland, Er:YAG laser assisted hair transplantation in cicatricial alopecia, Dermatol. Surg. 26 (11) (2001) 1010–1014, https://doi.org/10.1046/j.1524-4725.2000.0260111010.x.

[37] J. Jew, K.H. Chan, C.L. Darling, D. Fried, Selective removal of natural caries lesions from dentin and tooth occlusal surfaces using a diode-pumped Er:YAG laser, in: P. Rechmann, D. Fried (Eds.), SPIE Proceedings: Lasers in Dentistry XXIII, vol. 10044, 2017, pp. 10044–10049, https://doi.org/10.1117/12.2256728.

[38] J. Yang, L. Wang, X. Wu, T. Cheng, H. Jiang, High peak power Q-switched Er:YAG laser with two polarizers and its ablation performance for hard dental tissues, Optic Express 22 (13) (2014) 15686–15696, https://doi.org/10.1364/OE.22.015686.

[39] M. Messner, A. Heinrich, C. Hagen, K. Unterrainer, High brightness diode pumped Er:YAG laser system at 2.94 μm with nearly 1kW peak power, in: W.A. Clarkson, R.K. Shori (Eds.), SPIE Proceedings: Solid State Lasers XXV: Technology and Devices, vol. 9726, 2016, https://doi.org/10.1117/12.2209098, 9726–6.

[40] K. Stock, R. Diebolder, F. Hausladen, R. Hibst, Efficient bone cutting with the novel diode pumped Er:YAG laser system: in vitro investigation and optimization of the treatment parameters, in: B. Choi, et al. (Eds.), SPIE Proceedings: Photonic Therapeutics and Diagnostics X, vol. 8926, 2014, https://doi.org/10.1117/12.2039648, 8926 – 8926 – 10.

[41] R. Švejkar, J. Šulc, M. Němec, P. Boháček, H. Jelínková, B. Trunda, L. Havlák, M. Nikl, K. Jurek, Line-tunable Er:GGAG laser, Opt. Lett. 43 (14) (2018) 3309–3312, https://doi.org/10.1364/OL.43.003309.

[42] J. Wang, Z. Zhang, J. Xu, J. Xu, P. Fu, U. Liu, Baining Taeuber, H.J. Eichler, A. Dicninig, G. Huber, X. Yan, X. Wu, Y. Jiang, Spectroscopic properties and 3-μ m lasing of Er^{3+}:YVO_4 crystals, in: S.-S. Mei, K.A. Truesdell (Eds.), High-Power Lasers: Solid State, Gas, Excimer, and Other Advanced Lasers II, vol. 3549, 1998, https://doi.org/10.1117/12.344113, 3549–3549.

[43] M.J. Weber (Ed.), Handbook of Optical Materials, CRC press, 2003.

[44] S. Wang, K. Wu, Y. Wang, H. Yu, H. Zhang, X. Tian, Q. Dai, J. Liu, Spectral and lasing investigations of Yb:YSGG crystal, Optic Express 21 (14) (2013) 16305–16310, https://doi.org/10.1364/OE.21.016305.

[45] J. Wang, T. Cheng, L. Wang, J. Yang, D. Sun, S. Yin, X. Wu, H. Jiang, Compensation of strong thermal lensing in an LD side-pumped high-power Er:YSGG laser, Laser Phys. Lett. 12 (10) (2015) 105004, https://doi.org/10.1088/1612-2011/12/10/105004.

[46] S.M. Arutyunyan, R.B. Kostanyan, A.G. Petrosyan, T.V. Sanamyan, $YAlO_3$:Er^{3+} crystal laser, Sov. J. Quant. Electron. 17 (8) (1987) 1010.

[47] A.A. Kaminskii, T. Butaeva, A. Ivanov, I. Mochalov, A. Petrosyan, G. Rogov, V. Fedorov, New data on stimulated emission of crystals containing Er^{3+} and Ho^{3+} ions, Sov. Tech. Phys. Lett. 2 (9) (1976) 308–310.

[48] W. Lüthy, M. Stalder, K.P. Weber, Spectroscopy of the 3 μm laser transitions in $YAlO_3$:Er, in: W. Persson, S. Svanberg (Eds.), Laser Spectroscopy VIII, Springer Berlin Heidelberg, Berlin, Heidelberg, 1987, pp. 420–421.

[49] M. Stalder, W. Lüthy, H.P. Weber, Five new 3-μm laser lines in $YAlO_3$:Er, Opt. Lett. 12 (8) (1987) 602–604, https://doi.org/10.1364/OL.12.000602.

[50] J. Frauchiger, W. Lüthy, P. Albers, H.P. Weber, Laser properties of selectively excited $YAlO_3$:Er, Opt. Lett. 13 (11) (1988) 964–966, https://doi.org/10.1364/OL.13.000964.

[51] H. Kawase, R. Yasuhara, 2.92-μm high-efficiency continuous-wave laser operation of diode-pumped Er:YAP crystal at room temperature, Optic Express 27 (9) (2019) 12213–12220, https://doi.org/10.1364/OE.27.012213.

[52] P.P. Sorokin, M.J. Stevenson, Stimulated infrared emission from trivalent uranium, Phys. Rev. Lett. 5 (1960) 557–559, https://doi.org/10.1103/PhysRevLett.5.557.

[53] S.A. Pollack, D.B. Chang, N.L. Moise, Upconversion pumped infrared erbium laser, J. Appl. Phys. 60 (12) (1986) 4077–4086, https://doi.org/10.1063/1.337486.

[54] J. Baker, E. Davies, J. Hurrell, Charge compensation in calcium fluoride doped with trivalent rare-earth ions at tetragonal sites, Phys. Lett. 26 (1968) 352–353, https://doi.org/10.1016/0375-9601(68)90368-x.

[55] N. Kolesnikov (Ed.), Modern Aspects of Bulk Crystal and Thin Film Preparation, Intech, 2012, https://doi.org/10.5772/1348.

[56] J. Šulc, R. Švejkar, M. Němec, H. Jelínková, M.E. Doroshenko, V.A. Konyushkin, A.N. Nakladov, V.V. Osiko, Er:SrF_2 crystal for diode-pumped 2.7 μm laser, Adv. Solid State Lasers 22 (2014), https://doi.org/10.1364/ASSL.2014.ATu2A.22. ATu2A.

[57] J. Šulc, R. Švejkar, M. Němec, H. Jelínková, M.E. Doroshenko, P.P. Fedorov, V.V. Osiko, Temperature influence on diode pumped Er:CaF_2 laser, Proc. SPIE 9342 (2015), https://doi.org/10.1117/12.2077454, 93421S–93421S–8.

[58] J. Šulc, M. Němec, R. Švejkar, H. Jelínková, M.E. Doroshenko, P.P. Fedorov, V.V. Osiko, Diode-pumped Er:CaF_2 ceramic 2.7 μm tunable laser, Opt. Lett. 38 (17) (2013) 3406–3409, https://doi.org/10.1364/OL.38.003406.

[59] L. Su, X. Guo, D. Jiang, Q. Wu, Z. Qin, G. Xie, Highly-efficient mid-infrared CW laser operation in a lightly-doped 3 at.% Er:SrF_2 single crystal, Optic Express 26 (5) (2018) 5558–5563, https://doi.org/10.1364/OE.26.005558.

[60] J. Liu, J. Liu, Z. Guo, H. Zhang, W. Ma, J. Wang, L. Su, Dual-wavelength Q-switched Er:SrF_2 laser with a black phosphorus absorber in the mid-infrared region, Optic Express 24 (26) (2016) 30289–30295, https://doi.org/10.1364/OE.24.030289.

[61] W. Gao, R. Wang, Q. Han, J. Dong, L. Yan, H. Zheng, Tuning red upconversion emission in single $LiYF_4$:Yb^{3+}/Ho^{3+} microparticle, J. Phys. Chem. C (2015) 2349–2355, https://doi.org/10.1021/jp511566h.

[62] A. Authier, International Tables for Crystallography, first ed., Springer, 2003.

[63] T. Jensen, A. Diening, G. Huber, B.H.T. Chai, Investigation of diode-pumped 2.8-μm Er:$LiYF_4$ lasers with various doping levels, Opt. Lett. 21 (8) (1996) 585–587, https://doi.org/10.1364/OL.21.000585.

[64] M.V. Inochkin, Y.V. Korostelin, A.I. Landman, V.V. Nazarov, D.Y. Sachkov, Y.P. Podmar'kov, M.P. Frolov, L.V. Khloponin, V.Y. Khramov, A compact Er:YLF laser with a passive Fe^{2+}:ZnSe shutter, J. Opt. Technol. 79 (6) (2012) 337–339, https://doi.org/10.1364/JOT.79.000337.

[65] M. Pollnau, T. Graf, J.E. Balmer, W. Lüthy, H.P. Weber, Explanation of the cw operation of the Er^{3+} 3-μm crystal laser, Phys. Rev. A 49 (1994) 3990–3996, https://doi.org/10.1103/PhysRevA.49.3990.

[66] A. Dergachev, P.F. Moulton, Tunable CW Er:YLF diode-pumped laser, in: Advanced Solid-State Photonics, Optical Society of America, 2003, p. 3, https://doi.org/10.1364/ASSP.2003.3.

[67] C. Kränkel, Rare-earth-doped sesquioxides for diode-pumped high-power lasers in the 1-, 2-, and 3 μm spectral range, IEEE J. Sel. Top. Quant. Electron. 21 (1) (2015) 250–262, https://doi.org/10.1109/JSTQE.2014.2346618.

[68] P. Capper, P. Rudolph (Eds.), Crystal Growth Technology: Semiconductors and Dielectrics, Wiley-VCH, 2010.

[69] I.L. Snetkov, D.E. Silin, O.V. Palashov, E.A. Khazanov, H. Yagi, T. Yanagitani, H. Yoneda, A. Shirakawa, K. Ueda, A.A. Kaminskii, Study of the thermo-optical constants of Yb doped Y_2O_3, Lu_2O_3 and Sc_2O_3 ceramic materials, Optic Express 21 (18) (2013) 21254–21263, https://doi.org/10.1364/OE.21.021254.

[70] L. Wang, H. Huang, D. Shen, J. Zhang, H. Chen, D. Tang, Diode-pumped high power 2.7 μm Er:$Y2_O3$ ceramic laser at room temperature, Opt. Mater. 71 (2017) 70–73, https://doi.org/10.1016/j.optmat.2016.06.014, 11th Laser Ceramics Symposium: International Symposium on Transparent Ceramics for Photonic Applications (11th LCS), Xuzhou, China, November 30-December 4, 2015.

[71] H. Uehara, S. Tokita, J. Kawanaka, D. Konishi, M. Murakami, S. Shimizu, R. Yasuhara, Optimization of laser emission at 2.8 μm by Er:Lu_2O_3 ceramics, Optic Express 26 (3) (2018) 3497–3507, https://doi.org/10.1364/OE.26.003497.

[72] T. Sanamyan, R. Pavlacka, G. Gilde, M. Dubinskii, Spectroscopic properties of Er^{3+}-doped α-Al_2O_3, Opt. Mater. 35 (5) (2013) 821–826, https://doi.org/10.1016/j.optmat.2012.10.036.

[73] W. Ryba-Romanowski, R. Lisiecki, H. Jelínková, J. Šulc, Thulium-doped vanadate crystals: growth, spectroscopy and laser performance, Prog. Quant. Electron. 35 (5) (2011) 109–157, https://doi.org/10.1016/j.pquantelec.2011.06.001.

[74] N. Ter-Gabrielyan, V. Fromzel, M. Dubinskii, Record-low quantum defect operation of an eye-safe Er-doped laser, Laser Phys. Lett. 13 (11) (2016) 115001, https://doi.org/10.1088/1612-2011/13/11/115001.

[75] N. Ter-Gabrielyan, V. Fromzel, Wavelength tuning in cryogenically cooled lasers based on Er-doped orthovanadates, Appl. Optic. 56 (3) (2017), https://doi.org/10.1364/AO.56.000B70. B70–B73.

[76] S.A. Miller, H.H. Caspers, H.E. Rast, Lattice vibrations of yttrium vanadate, Phys. Rev. 168 (1968) 964–969, https://doi.org/10.1103/PhysRev.168.964.

[77] J. Šulc, R. Švejkar, H. Jelínková, W. Ryba-Romanowski, T. Lukasiewicz, Diode pumped room-temperature operating eye-safe Er:YVO_4 and Er:$GdVO_4$ lasers, in: 22th International Laser Physics Workshop - Book of Abstracts, RU, Moscow, 2013.

[78] J.M. Serres, P. Loiko, V. Jambunathan, X. Mateos, V. Vitkin, A. Lucianetti, T. Mocek, M. Aguiló, F. Díaz, U. Griebner, V. Petrov, Efficient diode-pumped Er:$KLu(WO_4)_2$laser at ~ 1.61 μm, Opt. Lett. 43 (2) (2018) 218–221, https://doi.org/10.1364/OL.43.000218.

[79] M. Pujol, M. Rico, C. Zaldo, R. Solé, V. Nikolov, X. Solans, M. Aguiló, F. Díaz, Crystalline structure and optical spectroscopy of Er^{3+}-doped $KGd(WO_4)_2$ single crystals, Appl. Phys. B 68 (2) (1999) 187–197, https://doi.org/10.1007/s003400050605.

[80] R.L. Aggarwal, D.J. Ripin, J.R. Ochoa, T.Y. Fan, Measurement of thermo-optic properties of $Y_3Al_5O_{12}$, $Lu_3Al_5O_{12}$, $YAlO_3$, LiF_4, $LiLuF_4$, BaY_2F_8, $KGd(WO_4)_2$, and $KY(WO_4)_2$ laser crystals in the 80-300 K, J. Appl. Phys. 98 (10) (2005) 14, https://doi.org/10.1063/1.2128696.

[81] N.V. Kuleshov, A.A. Lagatsky, A.V. Podlipensky, V.P. Mikhailov, A.A. Kornienko, E.B. Dunina, S. Hartung, G. Huber, Fluorescence dynamics, excited-state absorption, and stimulated emission of Er^{3+} in $KY(WO_4)_2$, J. Opt. Soc. Am. B 15 (3) (1998) 1205–1212, https://doi.org/10.1364/JOSAB.15.001205.

[82] M. Rico, J. Liu, U. Griebner, V. Petrov, M.D. Serrano, F. Esteban-Betegn, C. Cascales, C. Zaldo, Tunable laser operation of ytterbium in disordered single crystals of Yb:$NaGd(WO_4)_2$, Optic Express 12 (2004), https://doi.org/10.1364/OPEX.12.005362, 5362–0.

[83] Y. Zhang, W. Gong, J. Yu, Y. Lin, G. Ning, Tunable white-light emission via energy transfer in single-phase $LiGd(WO_4)_2$:Re^{3+}(Re=Tm, Tb, Dy, Eu) phosphors for UV-excited WLEDs, RSC Adv. doi: 10.1039/C5RA19345A.

[84] M. Borowiec, T. Zayarnyuk, M. Pujol, M. Aguil, F. Daz, E. Zubov, A. Prokhorov, M. Berkowski, W. Domuchowski, A. Wisniewski, R. Puzniak, J. Pietosa, V. Dyakonov, M. Baranski, H. Szymczak, Magnetic properties of $KRE(WO_4)_2$ (RE=Gd, Yb, Tm) single crystals, Phys. B Condens. Matter 405 (23) (2010) 4886–4891, https://doi.org/10.1016/j.physb.2010.09.028.

[85] B.G. Enrique, Optical spectrum and magnetic properties of Er^{3+} in $CaWO_4$, J. Chem. Phys. 55 (1971) 2538, https://doi.org/10.1063/1.1676445.

[86] S.K. Arora, B. Chudasama, Crystallization and optical properties of $CaWO_4$ and $SrWO_4$, Cryst. Res. Technol. 41 (2006) 1089–1095, https://doi.org/10.1002/crat.200610727.

[87] K.N. Gorbachenya, V.E. Kisel, A.S. Yasukevich, A.A. Pavlyuk, N.V. Kuleshov, In-band pumped room-temperature Er:$KY(WO_4)_2$ laser emitting around 1.6 μm, Laser Phys. Lett. 23 (12) (2013) 125005, https://doi.org/10.1088/1054-660X/23/12/125005.

[88] K. Gorbachenya, V. Kisel, S. Kurilchik, A. Yasukevich, S. Korableva, V. Semashko, A. Pavlyuk, N. Kuleshov, Er:$KY(WO_4)_2$ and Er:$LiYF_4$ crystals for eye-safe in-band pumped lasers, in: Advanced Solid State Lasers, Optical Society of America vol. 14, 2015, https://doi.org/10.1364/ASSL.2015.AM5A.14. AM5A.

[89] A.A. Kaminskii, A.A. Pavlyuk, T.I. Butaeva, V.A. Fedorov, I.F. Balashov, V.A. Berenberg, V.V. Lyubchenko, Stimulated emission by subsidiary transition of Ho^{3+} and Er^{3+} - ions in $KGd(WO_4)_2$, Inorg. Mater. 13 (8) (1977) 1251–1252.

[90] A.A. Kaminskii, A.A. Pavlyuk, I.F. Balashov, et al., Stimulated emission by $KY(WO_4)_2$-Er^{3+} crystal at 0.85, 1.73 and 2.8 μm at 300 K, Inorg. Mater. 14 (12) (1978) 1765–1767.

[91] J. Di, X. Sun, X. Xu, C. Xia, Q. Sai, H. Yu, Y. Wang, L. Zhu, Y. Gao, X. Guo, Growth and spectral characters of Nd:$CaGdAlO_4$ crystal, Eur. Phys. J. Appl. Phys. 74. doi: 10.1051/epjap/2016150511.

[92] J.-P.R. Wells, M. Yamaga, N. Kodama, T.P.J. Han, Polarized laser spectroscopy and crystal-field analysis of Er^{3+} doped $CaGdAlO_4$, J. Phys. Condens. Matter 11 (39) (1999) 7545.

[93] Z. Zhu, J. Li, Z. You, Y. Wang, S. Lv, E. Ma, J. Xu, H. Wang, C. Tu, Benefit of Pr^{3+} ions to the spectral properties of Pr^{3+}/Er^{3+}:$CaGdAlO_4$ crystal for a 2.7 μm laser, Opt. Lett. 37 (23) (2012) 4838–4840, https://doi.org/10.1364/OL.37.004838.

[94] J. Šulc, R. Švejkar, H. Jelínková, K. Nejezchleb, K. Nitsch, A. Cihlář, R. Král, M. Ledinský, A.i. Fejfar, M. Rodová, P. Zemenová, M. Nikl, Phosphate content influence on structural, spectroscopic, and lasing properties of Er,Yb-doped potassium-lanthanum phosphate glasses, Opt. Eng. 55 (2016) 55, https://doi.org/10.1117/1.OE.55.4.047102.

[95] J. Šulc, R. Švejkar, M. Němec, Jelínková, K. Nitsch, A. Cihlář, R. Král, K. Nejezchleb, M. Rodová, M. Nikl, Er-doped ortho- and metha-phosphate glassy mixtures for 1.54 μm laser construction, in: J.I. Mackenzie, et al. (Eds.), SPIE Proceedings: Laser Sources and Applications II, vol. 9135, 2014, pp. 9135–9138, https://doi.org/10.1117/12.2051209.

[96] R. Švejkar, J. Šulc, M. Němec, Jelínková, K. Nitsch, A. Cihlář, R. Král, K. Nejezchleb, M. Nikl, Effect of cryogenic temperature on spectroscopic and laser properties of Er, Yb-doped potassium-lanthanum phosphate glass, in: J. Hein (Ed.), SPIE Proceedings: High-Power, High-Energy, and High-Intensity Laser Technology III, vol. 10238, 2017, p. 7, https://doi.org/10.1117/12.2264673.

[97] H. Deters, A. S. S. de Camargo, C. N. Santos, C. R. Ferrari, A. C. Hernandes, A. Ibanez, M. T. Rinke, H. Eckert, Structural characterization of rare-earth doped yttrium aluminoborate laser glasses using solid state NMR, J. Phys. Chem. C 113 (36). doi: 10.1021/jp9032904.

[98] R. Xu, L. Xu, L. Hu, J. Zhang, Structural origin and laser performance of thulium-doped germanate glasses, J. Phys. Chem. 115 (49). doi: 10.1021/jp207574m.

[99] A. Seddon, Chalcogenide glasses: a review of their preparation, properties and applications, J. Non-Cryst. Solids 184 (1995) 44–50, https://doi.org/10.1016/0022-3093(94)00686-5.

[100] F. Huang, Y. Guo, Y. Ma, L. Zhang, J. Zhang, Highly Er^{3+}-doped ZrF_4-based fluoride glasses for 2.7 μm laser materials, Appl. Optic. 52 (7) (2013) 1399–1403, https://doi.org/10.1364/AO.52.001399.

[101] H. Yanagita, H. Toratani, T.T. Yamashita, I. Masuda, G.C. Righini, Diode-pumped Er^{3+} glass laser at 2.7 μm, in: G.C. Righini (Ed.), SPIE Proceedings: Glasses for Optoelectronics II, vol. 1513, 1991, pp. 386–395, https://doi.org/10.1117/12.46045.

[102] T. Xue, Y. Li, Y. Liu, Z. Liu, S. Dai, M. Liao, L. Hu, High thermal stability and intense 2.71 μm emission in Er^{3+}doped fluorotellurite glass modified by GaF_3, Opt. Mater. 75 (2018) 367–372, https://doi.org/10.1016/j.optmat.2017.10.055.

[103] C. Schäfer, D. Konishi, M. Murakami, S. Shimizu, S. Tokita, 7 w Er:ZBLAN fiber laser at 2.8 μm using a fiber side-pump combiner, in: Laser Congress 2017 (ASSL, LAC), Optical Society of America, 2017. JTh2A.34.

[104] S. Tokita, M. Murakami, S. Shimizu, M. Hashida, S. Sakabe, Liquid-cooled 24 W mid-infrared Er:ZBLAN fiber laser, Opt. Lett. 34 (20) (2009) 3062–3064, https://doi.org/10.1364/OL.34.003062.

[105] Z. Qin, G. Xie, J. Zhang, J. Ma, P. Yuan, L. Qian, Continuous-Wave and passively Q-switched Er:Y_2O_3 ceramic laser at 2.7μm, Int. J. Optics 2018 (2018) 5, https://doi.org/10.1155/2018/3153614.

[106] A.A. Voronov, V.I. Kozlovskii, Y.V. Korostelin, A.I. Landman, Y.P. Podmarkov, V.G. Polushkin, M.P. Frolov, Passive Fe^{2+}:ZnSe single-crystal Q-switch for 3-μm lasers, Quant. Electron. 36 (1) (2006) 1, https://doi.org/10.1070/QE2006v036n01ABEH013097.

[107] L. Wang, H. Huang, X. Ren, J. Wang, D. Shen, Y. Zhao, W. Zhou, P. Liu, D. Tang, Nanosecond pulse generation at 2.7 μm from a passively Q-switched Er:Y_2O_3 ceramic laser, IEEE J. Sel. Top. Quant. Electron. 24 (5) (2018) 1–6, https://doi.org/10.1109/JSTQE.2018.2801478.

[108] L. Kong, Z. Qin, G. Xie, Z. Guo, H. Zhang, P. Yuan, L. Qian, Black phosphorus as broadband saturable absorber for pulsed lasers from 1 μm to 2.7 μm wavelength, Laser Phys. Lett. 13 (4) (2016), 045801, https://doi.org/10.1088/1612-2011/13/4/045801.

[109] M. Fan, T. Li, S. Zhao, G. Li, X. Gao, K. Yang, D. Li, C. Kränkel, Multilayer black phosphorus as saturable absorber for an Er:Lu_2O_3 laser at μm, Photon. Res. 4 (5) (2016) 181–186, https://doi.org/10.1364/PRJ.4.000181.

[110] Z.Y. You, Y. Wang, Y.J. Sun, J.L. Xu, Z.J. Zhu, J.F. Li, H.Y. Wang, C.Y. Tu, CW and Q-switched GGG/Er:Pr:GGG/GGG composite crystal laser at 2.7 μm, Laser Phys. Lett. 14 (4) (2017), 045810, https://doi.org/10.1088/1612-202X/aa5fea.

[111] A. Gallian, A. Martinez, P. Marine, V. Fedorov, S. Mirov, V. Badikov, D. Boutoussov, M. Andriasyan, Fe:ZnSe passive Q-switching of 2.8-μm Er:Cr:YSGG laser cavity, 2007, https://doi.org/10.1117/12.701289.

[112] T. Hu, S.D. Jackson, D.D. Hudson, Ultrafast pulses from a mid-infrared fiber laser, Opt. Lett. 40 (18) (2015) 4226–4228, https://doi.org/10.1364/OL.40.004226.

[113] Z. Qin, G. Xie, C. Zhao, S. Wen, P. Yuan, L. Qian, Mid-infrared mode-locked pulse generation with multilayer black phosphorus as saturable absorber, Opt. Lett. 41 (1) (2016) 56–59, https://doi.org/10.1364/OL.41.000056.

[114] R. Švejkar, J. Šulc, H. Jelínková, Er:Y_2O_3 high-repetition rate picosecond 2.7 μm laser, Laser Phys. Lett. 16 (7) (2019), 075802, https://doi.org/10.1088/1612-202x/ab1918.

[115] V.E. Kisel, V.G. Shcherbitskii, N.V. Kuleshov, L.I. Postnova, V.I. Levchenko, Saturable absorbers for passive Q-switching of erbium lasers emitting in the region of 3 μm, J. Appl. Spectrosc. 72 (6) (2005) 818–823, https://doi.org/10.1007/s10812-006-0009-0.

[116] T. Feng, K. Yang, J. Zhao, S. Zhao, W. Qiao, T. Li, T. Dekorsy, J. He, L. Zheng, Q. Wang, X. Xu, L. Su, J. Xu, 1.21 W passively mode-locked Tm:LuAG laser, Optic Express 23 (9) (2015) 11819–11825, https://doi.org/10.1364/OE.23.011819.

[117] J. Ma, G.Q. Xie, W.L. Gao, P. Yuan, L.J. Qian, H.H. Yu, H.J. Zhang, J.Y. Wang, Diode-pumped mode-locked femtosecond Tm:CLNGG disordered crystal laser, Opt. Lett. 37 (8) (2012) 1376–1378, https://doi.org/10.1364/OL.37.001376.

[118] D. Kasprowicz, M. Brik, A. Majchrowski, E. Michalski, P. Głuchowski, Spectroscopic properties of $KGd(WO_4)_2$ single crystals doped with Er^{3+}, Ho^{3+}, Tm^{3+} and Yb^{3+} ions: luminescence and micro-Raman investigations, J. Alloys Compd. 577 (2013) 687–692, https://doi.org/10.1016/j.jallcom.2013.06.153.

[119] O. Medenbach, D. Dettmar, R.D. Shannon, R.X. Fischer, W.M. Yen, Refractive index and optical dispersion of rare earth oxides using a small-prism technique, J. Optic. Pure Appl. Optic. 3 (3) (2001) 174.

[120] D.E. Zelmon, D.L. Small, R. Page, Refractive-index measurements of undoped yttrium aluminum garnet from 0.4 to 5.0 μm, Appl. Optic. 37 (21) (1998) 4933–4935, https://doi.org/10.1364/AO.37.004933.

[121] P.A. Studenikin, A.I. Zagumennyi, Y.D. Zavartsev, P.A. Popov, I.A. Shcherbakov, $GdVO_4$ as a new medium for solid-state lasers: some optical and thermal properties of crystals doped with Cd^{3+}, Tm^{3+} , and Er^{3+} ions, Quant. Electron. 25 (12) (1995) 1162.

[122] P.A. Loiko, V.V. Filippov, K.V. Yumashev, N.V. Kuleshov, A.A. Pavlyuk, Thermo-optic coefficients study in $KGd(WO_4)_2$ and $KY(WO_4)_2$ by a modified minimum deviation method, Appl. Optic. 51 (15) (2012) 2951–2957, https://doi.org/10.1364/AO.51.002951.

[123] P. Loiko, P. Segonds, P. Inácio, A.P. na, J. Debray, D. Rytz, V. Filippov, K. Yumashev, M.C. Pujol, X. Mateos, M. Aguiló, F. Díaz, M. Eichhorn, B. Boulanger, Refined orientation of the optical axes as a function of wavelength in three monoclinic double tungstate crystals $KRE(WO_4)_2$ (RE = Gd, Y or Lu), Opt. Mater. Express 6 (9) (2016) 2984–2990, https://doi.org/10.1364/OME.6.002984.

[124] J. Liu, X. Feng, X. Fan, Z. Zhang, B. Zhang, J. Liu, L. Su, Efficient continuous-wave and passive Q-switched mode-locked Er:CaF_2-SrF_2 lasers in the mid-infrared region, Opt. Lett. 43 (10) (2018) 2418–2421, https://doi.org/10.1364/OL.43.002418.

[125] T. Sanamyan, M. Kanskar, Y. Xiao, D. Kedlaya, M. Dubinskii, High power diode-pumped 2.7-μm Er^{3+}:Y_2O_3 laser with nearly quantum defect-limited efficiency, Optic Express 19 (S5) (2011) A1082–A1087, https://doi.org/10.1364/OE.19.0A1082.

[126] K. Nejezchleb, J. Kubát, J. Šulc, H. Jelínková, Yb:YAG disc for high energy laser systems, in: W.A. Clarkson, R.K. Shori (Eds.), Solid State Lasers XXVI: Technology and Devices, vol. 10082, International Society for Optics and Photonics, SPIE, 2017, pp. 79–87, https://doi.org/10.1117/12.2249039.

[127] R. Švejkar, J. Šulc, M. Němec, H. Jelínková, V. Kubeček, W. Ma, D. Jiang, Q. Wu, L. Su, Diode-pumped Er:CaF_2 crystal 2.7 μm tunable laser, in: 26th International Laser Physics Workshop, RU, Moscow, 2017.

Temperature influence on spectroscopic properties and 2.7 μm lasing of Er:YAP crystal

Richard Švejkar[a], Jan Šulc[a], Michal Němec[a], Helena Jelínková[a], Karel Nejezchleb[b], Miroslav Čech[a]

[a]Czech Technical University in Prague, Faculty of Nuclear Sciences and Physical Engineering Břehová 7, 115 19 Prague 1, Czech Republic
[b]Crytur, Ltd., Palackého 175, 511 01 Turnov, Czech Republic

ABSTRACT

The spectroscopic and laser properties of Er:YAP crystal, that is appropriate for generation at 2.7 μm, in temperature range 78 - 400 K are presented. The sample of Er:YAP (1 at. % of Er^{3+}) had face-polished plan-parallel faces without anti-reflection coatings (thickness 4.47 mm). During experiments the Er:YAP was attached to temperature controlled copper holder and it was placed in vacuum chamber. The transmission and emission spectra together with the fluorescence decay time were measured depending on temperature. The Er:YAP crystal was longitudinally pumped by radiation from laser diode that works in pulse regime (repetition rate 66.6 Hz, pulse duration 1.5 ms, pump wavelength 972.5 nm) or in CW regime. Laser resonator was hemispherical, 145 mm in length with flat pumping mirror (HR @ 2.7 μm) and spherical output coupler (r = 150 mm, R = 95 % @ 2.5 - 2.8 μm). The fluorescence decay time of manifold $^4I_{11/2}$ (upper laser level) became shorter and intensity of up-conversion radiation was increasing with decreasing temperature. In pulsed regime, the highest slope efficiency with respect to absorbed mean power was 1.27 % at 78 K. The maximum output of mean power was 3.5 mW at 78 K, i.e. 8.7 times higher than measured this value at 300 K. The maximal output power 27 mW with slope efficiency up to 3.5 % was achieved in CW. The radiation generated by Er:YAP laser (2.73 μm) is close to absorption peak of water (3 μm) thus this wavelength can be use in medicine and spectroscopy.

Keywords: Erbium, Er:YAP, $YAlO_3$, cryogenic cooling, 2.7 μm laser, CW laser

1. INTRODUCTION

The Er^{3+} ions provide two significant laser transitions, the first one $^4I_{13/2} \rightarrow ^4I_{15/2}$ corresponds with laser emission at 1.6 μm and the second one $^4I_{11/2} \rightarrow ^4I_{13/2}$ which corresponds with laser emission at wavelength range of 2.65 - 3 μm.[1] The former mentioned laser emission is interesting for LIDAR and rangefinders, the latter wavelength range is suitable for medical and spectroscopic applications.[2] In recent time, coherently pumped laser with active media doped by Er^{3+} ions are well known and many papers were published, e.g. Er:YAG,[3] Er:YSGG,[4] Er:YLF,[5] Er:SrF_2,[6] Er:Y_2O_3,[7] etc. On the other hand, there are few publications deal with the anisotropic, uniaxial, crystalline yttrium orthoaluminate doped by erbium ions.[8] The highly doped incoherently pumped Er:YAP was successfully tested as source of laser radiation at 2.73 μm at room-temperature.[9–12] Nevertheless diode pumping can be more compact, in longitudinal set-up provides better beam quality and is more effective then flash pumping.[13] Thus, in this paper, we present the first low-doped longitudinally diode-pumped Er:YAP as pulsed and CW laser source of 2.73 μm laser radiation at cryogenic and room temperature.

Further author information: (Send correspondence to R.Š.)
R.Š.: E-mail: richard.svejkar@fjfi.cvut.cz, Tel.: +420 224 358 672
J.Š.: E-mail: jan.sulc@fjfi.cvut.cz, Tel.: +420 224 358 672
M.N.: E-mail: michal.nemec@fjfi.cvut.cz, Tel.: +420 224 358 672
H.J.: E-mail: helena.jelinkova@fjfi.cvut.cz, Tel.: +420 224 358 538
K.N.: E-mail: nejezchleb@crytur.cz, Tel.: +420 481 319 511
M.Č.: E-mail: miroslav.cech@fjfi.cvut.cz, Tel.: +420 224 358 536

Solid State Lasers XXVII: Technology and Devices, edited by W. Andrew Clarkson, Ramesh K. Shori, Proc. of SPIE Vol. 10511, 1051121 · © 2018 SPIE · CCC code: 0277-786X/18/$18 · doi: 10.1117/12.2287138

2. MATERIALS AND METHODS

The tested sample of Er:YAP ($Er:YAlO_3$) contained 1 wt. % of Er^{3+}. The thickness of sample was 4.47 mm, it had face-polished plan-parallel faces without anti-reflection coating; the photograph of the Er:YAP crystal can be seen in Figure 1.

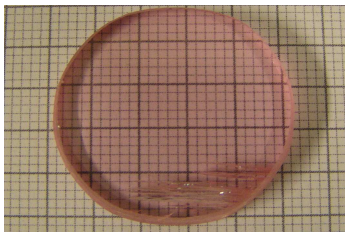

Figure 1. Photograph of Er:YAP tested sample.

For cryogenic cooling the vacuum chamber of liquid nitrogen cryostat (Janis Research, model VPF-100) was used. During all experiments on the side of pumping mirror there was a uncoated CaF_2 windows and between Er:YAP sample and output coupler there was CaF_2 windows with AR coating @1.65 - 3 μm, see Figure 2. The tested sample of Er:YAP was attached to a copper holder inside this cryostat and its temperature was being changed between 78 - 400 K by temperature controller Lake Shore model 325.

2.1 Pumping and laser setup

The Er:YAP crystal was longitudinally pumped by fibre-coupled (core diameter 100 μm, numerical aperture 0.22) laser diode LIMO35-F100-DL976-EX1202 (LIMO Laser System), working in pulse and CW regime. Radiation from this fibre-coupled laser diode was focused into the active laser material Er:YAP by two achromatic doublet lenses (Thorlabs, Inc., AC508-075-B and AC508-150-B) with the focal length $f_1 = 75$ mm and $f_2 = 150$ mm, thus the pumping beam diameter was $\sim 200\,\mu$m. During spectroscopic measurements (fluorescence intensity and decay time) the parameters of pumping pulse were: frequency 5 Hz, pulse duration 1 ms, pumping wavelength 972.5 nm. In laser experiments the pulse duration and frequency were changed to 1.5 ms and 66.6 Hz, respectively.

The hemispherical laser resonator (length 145 mm) with flat pumping mirror (PM, HR @ 2.65 − 2.85 μm, HT @ 960 − 980 nm) and spherical output coupler (OC, r = 150 mm, R = 95 % @ 2.65 − 2.85 μm) was used. The PM was placed inside the cryostat together with the laser active medium, and OC was placed outside the chamber. The experimental laser resonator setup can be seen in Figure 2.

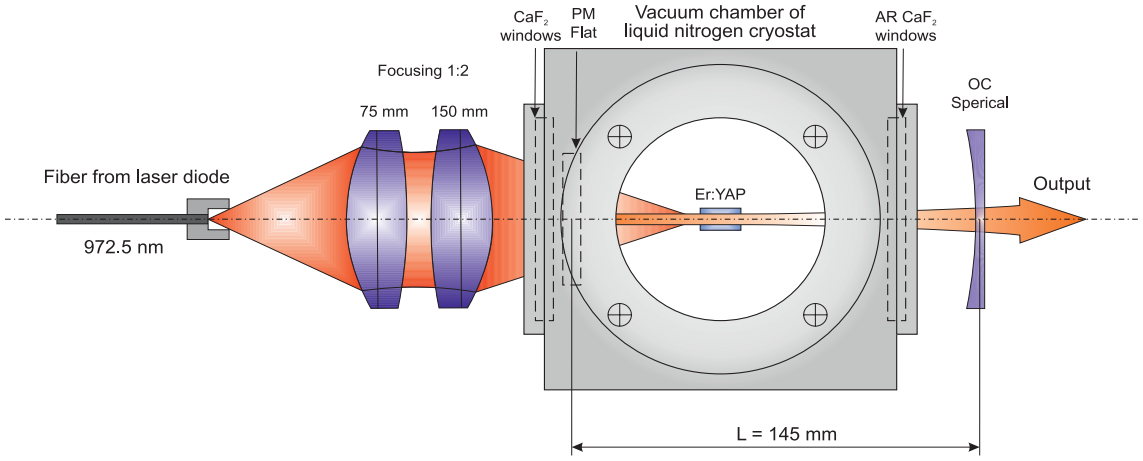

Figure 2. Layout of diode pumped Er:YAP laser; hemispherical resonator formed by flat pumping mirror (PM) placed in vacuum chamber and spherical output coupler (OC) in the air.

2.2 Methods of characterization

The Shimadzu spectrophotometer type UV - 3600 with spectral resolution ±0.2 nm in visible and ultraviolet region, and ±0.8 nm in mid-infrared was used for measuring the transmission spectra of Er:YAP. Fluorescence spectra and laser emission were measured by Oriel monochromator 77250 with ThorLab photodiode PDA 30G-EC (PbS, 1.0 - 2.9 μm), the resolution of the measurement was 10 nm. The fluorescence decay time at 1 μm was measured using HP 4220 (Si PIN photodiode) and at 1.5 μm using FGA10 (InGaAs photodiode, 800 - 1800 nm, ThorLabs) with long pass filter cut-on wavelength 1400 nm. During this measurement, both photodiodes were connected to oscilloscope (Tektronix TDS 3052B, 500 MHz, 5 GS/s). The output power of the Er:YAP laser was measured by ThorLabs power probe S401C (0.19 - 10.6 μm) connected to power meter PM100A. Laser beam spatial structure was measured by Spiricon Pyrocam III (camera chip $LiTaO_3$, active area 12.4×12.4 mm) with band pass filter 2500±250 nm.

3. RESULTS AND DISCUSSION

3.1 Spectroscopy measurement

The Er:YAP transmission spectra were measured with Shimadzu spectrophotometer UV-3600 and investigated at a temperature range of 80 - 300 K. From these measurements corrected to Fresnel losses, the absorption spectra were calculated, as shown in Figure 3. It could be noted that the absorption coefficients at 1450 - 1600 nm are approximately 5 times higher than at 960 - 1000 nm, thus the resonant pumping for laser emission at 1.6 μm is also possible. The 972.5 nm wavelength, closely corresponding to the highest absorption peak at 972.1 nm (absorption coefficient 0.94 cm^{-1} at 80 K), was chosen. Figure 3 also shows unpolarize fluorescence spectra of the Er^{3+} ions in YAP crystal for 78 K and 300 K. Fluorescence decay time at upper laser level $^4I_{11/2}$ is rising together with decreasing temperature; at 78 K it is 1.20±0.01 ms and at 300 K it is 0.83±0.01 ms, results are presented in Figure 4.

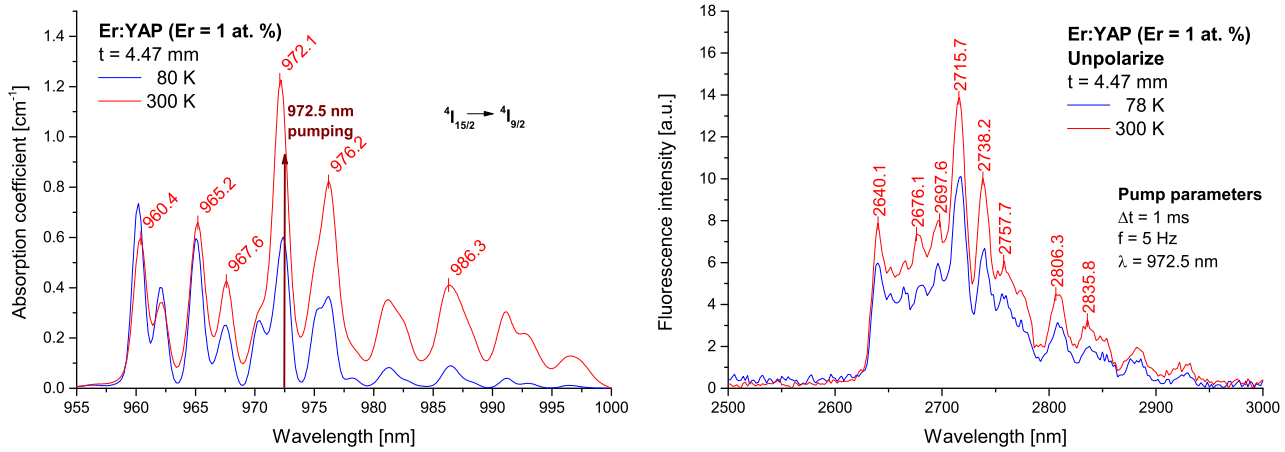

Figure 3. Absorption spectra of Er:YAP crystal depending on temperature, absorption spectra for $^4I_{15/2} \rightarrow ^4I_{9/2}$ transition - left, unpolarize fluorescence spectrum of Er:YAP crystal at 78 K - right; sample thickness – t, pumping pulse width – Δt, frequency – f, pumping wavelength – λ.

3.2 Laser experiments

The Er:YAP active medium was longitudinally pumped by laser diode radiation (pulse regime - frequency 66.6 Hz, pulse duration 1.5 ms, temperature of diode 18° C, wavelength 972.5 nm). The temperature of the sample was changed from 78 K to 400 K. From Figure 5 it can be seen that with increasing temperature the slope efficiency became lower; for duty cycle 10 % it decreased from 1.27 % at 78 K to 0.14 % at 300 K. With the rising temperature a population of upper energy levels become higher and the threshold of lasing was rising. Nevertheless, with heating the sample up to 400 K it was found, that laser emission at 2.73 μm was observable at 380 K. After exceeded the 310 K the output power could not be measured by power probe, the laser emission

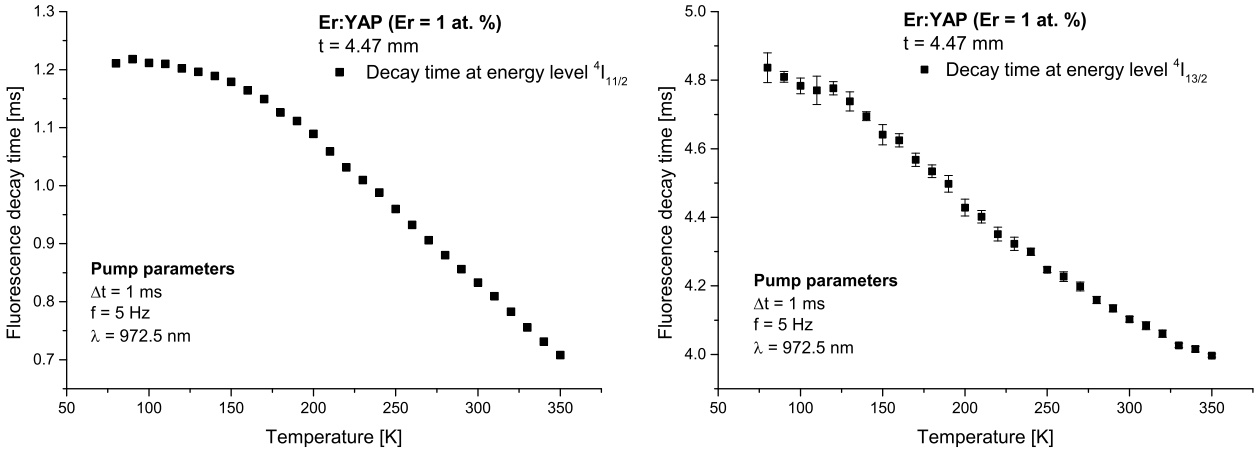

Figure 4. Fluorescence decay time of Er:YAP crystal depending on temperature, upper laser level $^4I_{11/2}$ - right and lower laser level $^4I_{13/2}$ depending on temperature - left; sample thickness – t, pumping pulse width – Δt, frequency – f, pumping wavelength – λ.

was observed with photodiode PDA 30G-EC connected to oscilloscope. In Figure 6 there are profiles of laser beam for different temperatures, it can be seen that laser emitted radiation in fundamental mode TEM_{00}. The emitted wavelength 2.73 μm is affected by series of up-conversion processes, the excited state absorption (ESA) $^4I_{13/2} \rightarrow {}^4F_{9/2}$ and energy transfer (ET) $^4I_{13/2} \rightarrow {}^4I_{15/2}$ and $^4I_{13/2} \rightarrow {}^4I_{9/2}$ that reduce population of lower laser level $^4I_{13/2}$, moreover the latter mentioned fractionally repopulate the upper laser level, which brings benefits for 2.73 μm lasing.[1,3,14] Nevertheless, there are two more transition that affect laser action the $^4I_{11/2} \rightarrow {}^4F_{7/2}$ and $^4I_{13/2} \rightarrow {}^4F_{9/2}$, both transition are cause of the emission in visible spectral range $\sim$ 553 nm and $\sim$ 670 nm, respectively, and the former mentioned transition depopulate the upper laser level $^4I_{11/2}$.[14] Moreover, the population of the energy levels depend on temperature,[13] it follows that mentioned transition are also affected by temperature. Thus for a potential laser application the optimal temperature of active medium has to be established. The laser emission at 2.73 μm is strongly affected above mentioned transition and sample temperature that both impair the laser properties.

The CW laser regime at 78 K was also successfully tested and the results are presented in Figure 5. Maximum output power at CW was 27 mW at 2.4 W of absorbed power, emitted laser wavelength was 2.73 μm. The steep

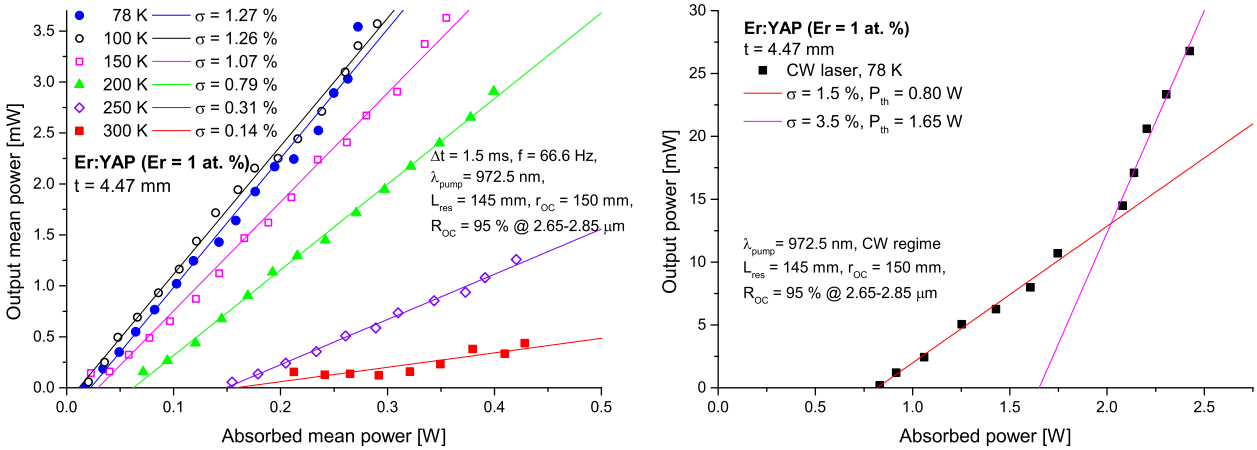

Figure 5. Output characteristic of Er:YAP laser, output pulse laser parameters depending on temperature - left, CW laser at 78 K - right; sample thickness – t, pumping pulse width – Δt, slope efficiency with respect to absorbed power – σ, laser threshold – P_{th}, pumping wavelength – λ_{pump}, resonator length – L_{res}, output coupler reflexivity and radius – R_{OC} and r_{OC}.

change of the slope efficiency and output power during CW measurement that can be seen in Figure 5 was probably caused by change of laser mode or stability of resonator. The low output power in pulsed and CW regime is probably given by low absorption coefficient and off-peak pumping. The doping concentration of Er^{3+} ions was probably not optimal, with slightly higher concentration of erbium (2 - 5 wt. %) and pumping radiation corresponding with absorption peak the output power and slope efficiency should be improve.

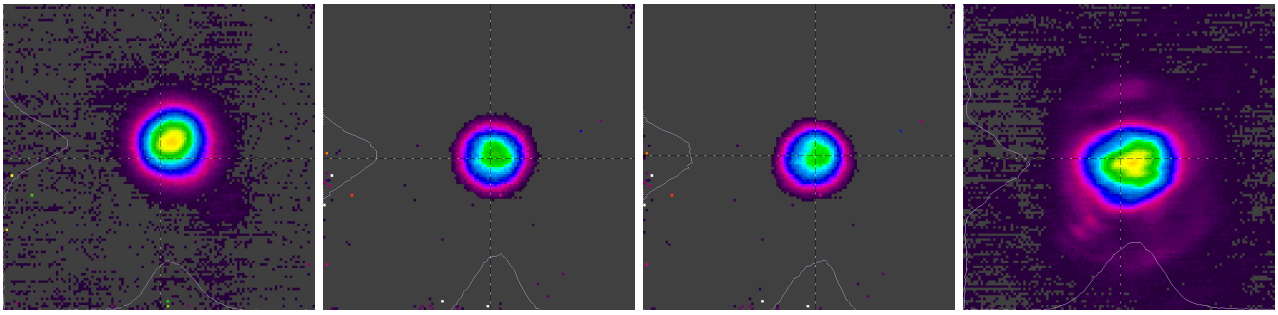

a) b) c) d)

Figure 6. Beam profiles of Er:YAP pulsed laser radiation for maximal output power a) at 78 K, b) at 200 K and c) at 300 K; d) beam profile at CW regime

4. CONCLUSION

In this work the temperature dependence of spectroscopic and laser properties of Er:YAP crystal are presented. The calculated absorption coefficient at chosen pumping wavelength range 970 - 975 nm was decreasing with decreasing temperature. The optimum pumping wavelength was chosen to be 972.5 nm. The fluorescence decay time at upper laser level $^4I_{11/2}$ was rising with decreasing temperature; it was 1.20±0.01 ms and 0.71±0.01 ms at 78 and 350 K, respectively. Due to cooling from 300 K to 78 K, the maximum obtained output mean power was 8.7 times higher. During CW laser operation at 78 K the maximum output power 27 mW, slope efficiency up to 3.5 % and laser threshold 1.65 W were obtained. The Er:YAP is promising candidate for medial and spectroscopic applications or for further non-linear conversion deeper to infra-red region.

ACKNOWLEDGEMENT

This research has been supported by the Czech Science Foundation, project No. 15-05360S and by the CTU Grant No. SGS16/247/OHK4/3T/14.

REFERENCES

[1] Koechner, W., [*Solid-State Laser Engeneering*], Springer Science+Business Media (2006).

[2] Sorokina, I. and Vodopyanov, K. L., eds., [*Solid-state mid-infrared laser sources*], vol. 89 of *Topics in Applied Physics*, Springer-Verlag, Berlin (2003).

[3] Sanamyan, T., "Efficient cryogenic mid-IR and eye-safe Er:YAG laser," *J. Opt. Soc. Am. B* **33**, D1–D6 (Nov 2016).

[4] Dinerman, B. J. and Moulton, P. F., "3-μm cw laser operations in erbium-doped YSGG, GGG, and YAG," *Opt. Lett.* **19**, 1143–1145 (Aug 1994).

[5] Stoneman, R. C., Lynn, J. G., and Esterowitz, L., "Direct Upper-State Pumping of the 2.8 μm Er^{3+}:YLF Laser," *JOURNAL OF QUANTUM ELECTRONICS* **28**(4), 1041–1045 (1992).

[6] Šulc, J., Švejkar, R., Němec, M., Jelínková, H., Doroshenko, M. E., Konyushkin, V. A., Nakladov, A. N., and Osiko, V. V., "Er:SrF_2; Crystal for Diode-pumped 2.7 μm Laser," *Advanced Solid State Lasers* , ATu2A.22 (2014).

[7] Sanamyan, T., "Diode pumped cascade Er:Y_2O_3 laser," *Laser Physics Letters* **12**(12), 125804 (2015).

[8] Epstein, R. I., Brown, J. J., Edwards, B. C., and Gibbs, A., "Measurements of optical refrigeration in ytterbium-doped crystals," *Journal of Applied Physics* **90**(9), 4815–4819 (2001).

[9] Arutyunyan, S. M., Kostanyan, R. B., Petrosyan, A. G., and Sanamyan, T. V., "$YAlO_3:Er^{3+}$ crystal laser," *Soviet Journal of Quantum Electronics* **17**(8), 1010 (1987).

[10] Frauchiger, J., Lüthy, W., Albers, P., and Weber, H. P., "Laser properties of selectively excited $YAlO_3$:Er," *Opt. Lett.* **13**, 964–966 (Nov 1988).

[11] Lüthy, W., Stalder, M., and Weber, K. P., [*Spectroscopy of the 3 μm Laser Transitions in $YAlO_3$:Er*], 420–421, Springer Berlin Heidelberg, Berlin, Heidelberg (1987).

[12] Stalder, M., Lüthy, W., and Weber, H. P., "Five new 3-μm laser lines in $YAlO_3$:Er," *Opt. Lett.* **12**, 602–604 (Aug 1987).

[13] Paschotta, R., [*Encyclopedia of Laser Physics and Technology*], Wiley-VCH (2008).

[14] Ma, W., Qian, X., Wang, J., Liu, J., Fan, X., Liu, J., Su, L., and Xu, J., "Highly efficient dual-wavelength mid-infrared CW laser in diode end-pumped Er:SrF_2 single crystals," *Scientific Reports* **6** (11 2016).

Research Article | Vol. 8, No. 4 | 1 Apr 2018 | OPTICAL MATERIALS EXPRESS 1025
Optical Materials EXPRESS

Diode-pumped Er:SrF_2 laser tunable at 2.7 μm

Richard Švejkar,[1,*] Jan Šulc,[1] Helena Jelínková,[1] Václav Kubeček,[1] Weiwei Ma,[2] Dapeng Jiang,[2] Qinghui Wu,[2] and Liangbi Su[2]

[1] *Czech Technical University in Prague, Faculty of Nuclear Sciences and Physical Engineering, Břehová 7, Prague 11519, Czech Republic*
[2] *Key Laboratory of Transparent and Opto-functional Inorganic Materials, Shanghai Institute of Ceramics, Chinese Academy of Sciences, No. 588 Heshuo Road, Shanghai 201899, China*
[*] *richard.svejkar@fjfi.cvut.cz*

Abstract: The tunability of Er:SrF_2 lasers was investigated at room temperature. Under pulsed laser diode pumping, the mid-infrared (2.75 μm) radiation was obtained with a maximal reached output power amplitude of 1.3 W and a slope efficiency up to 9.2 %. Laser tunability was reached using a MgF_2 birefringent filter and the tuning range of 123 nm (2690 nm - 2813 nm) with Er:SrF_2 was obtained.

OCIS codes: (140.3580) Lasers, solid-state; (140.5680) Rare earth and transition metal solid-state lasers; (140.3480) Lasers, diode-pumped; (140.3070) Infrared and far-infrared lasers; (160.3380) Laser materials; (300.6280) Spectroscopy, fluorescence and luminescence.

References and links

1. I. Sorokina and K. L. Vodopyanov, eds., *Solid-state Mid-infrared Laser Sources*, vol. 89 of Topics in Applied Physics (Springer-Verlag, Berlin, 2003).
2. M. Skorczakowski, J. Swiderski, W. Pichola, P. Nyga, A. Zajac, M. Maciejewska, L. Galecki, J. Kasprzak, S. Gross, A. Heinrich, and T. Bragagna, "Mid-infrared Q-switched Er:YAG laser for medical applications," Laser Phys. Lett. **7**, 498 (2010).
3. H. Jelínková, ed., *Lasers for Medical Applications Diagnostics, Therapy and Surgery* (Woodhead Publishing Limited, 2013), 1st ed.
4. T. Sanamyan, J. Simmons, and M. Dubinskii, "Efficient cryo-cooled 2.7-μm Er^{3+}:Y_2O_3 ceramic laser with direct diode pumping of the upper laser level," Laser Phys. Lett. **7**, 569–572 (2010).
5. B. J. Dinerman and P. F. Moulton, "3-μm cw laser operations in erbium-doped YSGG, GGG, and YAG," Opt. Lett. **19**, 1143–1145 (1994).
6. C. E. Hamilton, R. J. Beach, S. B. Sutton, L. H. Furu, and W. F. Krupke, "1-w average power levels and tunability from a diode-pumped 2.94-μm Er:YAG oscillator," Opt. Lett. **19**, 1627–1629 (1994).
7. C. Ziolek, H. Ernst, G. F. Will, H. Lubatschowski, H. Welling, and W. Ertmer, "High-repetition-rate, high-average-power, diode-pumped 2.94-μm Er:YAG laser," Opt. Lett. **26**, 599–601 (2001).
8. T. Sanamyan, "Efficient cryogenic mid-IR and eye-safe Er:YAG laser," J. Opt. Soc. Am. B **33**, D1–D6 (2016).
9. J. Wang, Z. Zhang, J. Xu, J. Xu, P. Fu, B. Liu, U. Taeuber, H. J. Eichler, A. Dicninig, G. Huber, X. Yan, X. Wu, and Y. Jiang, "Spectroscopic properties and 3-μm lasing of Er^{3+}:YVO_4 crystals," Proceeding SPIE **3549**, 3549 (1998).
10. W. Ma, L. Su, X. Xu, J. Wang, D. Jiang, L. Zheng, X. Fan, C. Li, J. Liu, and J. Xu, "Effect of erbium concentration on spectroscopic properties and 2.79 μm laser performance of Er:CaF_2 crystals," Opt. Mater. Express **6**, 409–415 (2016).
11. C. Labbe, J. Doualan, P. Camy, R. Moncorg, and M. Thuau, "The 2.8 μm laser properties of Er^{3+} doped CaF_2 crystals," Opt. Commun. **209**, 193–199 (2002).
12. J. Šulc, R. Švejkar, M. Němec, H. Jelínková, M. E. Doroshenko, P. P. Fedorov, and V. V. Osiko, "Temperature influence on diode pumped Er:CaF_2 laser," Proceeding SPIE **9342**, 93421S–8 (2015).
13. W. Ma, X. Qian, J. Wang, J. Liu, X. Fan, J. Liu, L. Su, and J. Xu, "Highly efficient dual-wavelength mid-infrared CW laser in diode end-pumped Er:SrF_2 single crystals," Sci. Reports **6**, 36635 (2016).
14. T. Sanamyan, "Diode pumped cascade Er:Y_2O_3 laser," Laser Phys. Lett. **12**, 125804 (2015).
15. L. Wang, H. Huang, D. Shen, J. Zhang, H. Chen, and D. Tang, "Highly stable self-pulsed operation of an Er:Lu_2O_3 ceramic laser at 2.7 μm," Laser Phys. Lett. **14**, 045803 (2017).
16. H. Uehara, R. Yasuhara, S. Tokita, J. Kawanaka, M. Murakami, and S. Shimizu, "Efficient continuous wave and quasi-continuous wave operation of a 2.8 μm Er:Lu_2O_3 ceramic laser," Opt. Express **25**, 18677–18684 (2017).
17. M. J. Weber, "Radiative and Multiphonon Relaxation of Rare-Earth Ions in Y_2O_3," Phys. Rev. **171**, 283–291 (1968).

#319168 https://doi.org/10.1364/OME.8.001025
Journal © 2018 Received 9 Jan 2018; revised 13 Feb 2018; accepted 28 Feb 2018; published 23 Mar 2018

Optical Materials EXPRESS

18. M. Tikerpae, S. D. Jackson, and T. A. King, "2.8 μm Er:YLF laser transversely pumped with a CW diode laser bar," Opt. Commun. **167**, 283 – 290 (1999).
19. A. Dergachev and P. F. Moulton, "Tunable CW Er:YLF Diode-Pumped Laser," in "Advanced Solid-State Photonics," , vol. 83 of 2003 OSA Trends in Optics and Photonics (Optical Society of America, 2003), p. 3.
20. M. V. Inochkin, V. V. Nazarov, D. Y. Sachkov, L. V. Khloponin, and V. Y. Khramov, "Dynamics of the lasing spectrum of a 3-μm Er:YLF laser with semiconductor pumping," J. Opt. Technol. **76**, 720–724 (2009).
21. V. Petit, J. Doualan, P. Camy, V. Ménard, and R. Moncorgé, "CW and tunable laser operation of Yb^{3+} doped CaF_2," Appl. Phys. B **78**, 681–684 (2004).
22. T. T. Basiev, Y. V. Orlovskii, M. V. Polyachenkova, P. P. Fedorov, S. V. Kuznetsov, V. A. V. A. Konyushkin, V. V. Osiko, O. K. Alimov, and A. Y. Dergachev, "Continuously tunable cw lasing near 2.75 μm in diode-pumped Er^{3+}:SrF_2 and Er^{3+}:CaF_2 crystals," Quant. Electr. **36**, 591–594 (2006).
23. S. A. Pollack, D. B. Chang, and N. L. Moise, "Upconversion-pumped infrared erbium laser," J. Appl. Phys. **60**, 4077–4086 (1986).
24. J. Šulc, R. Švejkar, M. Němec, H. Jelínková, M. E. Doroshenko, V. A. Konyushkin, A. N. Nakladov, and V. V. Osiko, "Er:SrF_2 Crystal for Diode-pumped 2.7 μm Laser," in "Advanced Solid State Lasers, 2014 OSA Technical Digest (online)," (Optical Society of America, 2014), p. ATu2A.22.
25. C. Li, J. Liu, S. Jiang, S. Xu, W. Ma, J. Wang, X. Xu, and L. Su, "2.8 μm passively Q-switched Er:CaF_2 diode-pumped laser," Opt. Mater. Express **6**, 1570–1575 (2016).
26. J. Šulc, M. Němec, R. Švejkar, H. Jelínková, M. E. Doroshenko, P. P. Fedorov, and V. V. Osiko, "Diode-pumped Er:CaF_2 ceramic 2.7 μm tunable laser," Opt. Lett. **38**, 3406–3409 (2013).
27. P. F. Moulton, "Tunable solid-state lasers," in "Proceedings of the IEEE," , vol. 80 (IEEE, 1992), pp. 348–364.
28. R. Švejkar, J. Šulc, M. Němec, Jelínková, M. E. Doroshenko, A. N. Nakladov, and V. V. Osiko, "Effect of cryogenic temperature on spectroscopic and laser properties of Er,La:SrF_2-CaF_2 crystal," Proceeding SPIE **9726**, 97261C–7 (2016).
29. S. D. Lord, "A New software tool for computing earth's atmospheric transmission of near- and far-infrared radiation," NASA Technical Memorandum 103957, NASA (1992).
30. A. Godard, "Infrared (2-12 μm) solid-state laser sources: a review," Comptes Rendus Physique **8**, 1100 –1128 (2007). Optical parametric sources for the infrared.

1. Introduction

The erbium (Er^{3+}) ion-based lasers, operating on the transition $^4I_{11/2} \rightarrow {}^4I_{13/2}$, allow to generate radiation directly in the mid-IR spectral region close to 3 μm. This wavelength is attractive for many medical applications, e.g. dentistry, dermatology, urology, and bone surgery [1–3]. Except medical applications, these lasers can be used in spectroscopy or as pumping sources for optical parametric oscillators [1, 4]. Nowadays, coherently pumped systems based on Er-doped crystalline oxides (Er:YAG, Er:YSGG, Er:YVO_4, Er:GGG) [5–9] are well known. Nevertheless, these materials have high phonon energy, thus fluorescence decay time at upper laser level ($^4I_{11/2}$) is very short (up to 60 times shorter) in comparison with lower laser level ($^4I_{13/2}$) [10, 11]. As consequence the self-termination phenomenon occurs in these laser systems. However, this effect could be suppressed by using high concentration of Er^{3+} ions or using cascade lasing. The 0.5 % Er:YAG used in cascade laser was successfully tested and the laser action was obtained at 2.7 μm at liquid nitrogen (78 K) temperature [8]. So, the laser action in Er^{3+} doped crystalline oxides matrix is limited by the non-radiative transition [5, 8, 11–13]. On the other hand, there are the sesquioxides doped by erbium, e.g. Er:Y_2O_3 and Er:Lu_2O_3 that possess the low-phonon energy and their material parameters outstrip commonly used crystals (YAG,YSGG, GGG, YVO_4, etc.). Nevertheless, the fabrication of these active laser materials is complicated and expensive mainly due to high melting temperature [14–17]. From this reason the low-phonon energy fluoride matrices such as Er:YLF and also the Er:CaF_2 and Er:SrF_2 crystals or ceramics were tested [11, 18–20]. The CaF_2 and SrF_2 crystals and ceramics doped by Er^{3+} ions are very promising materials, possessing low phonon energy ~322 cm^{-1} and ~280 cm^{-1}, respectively [13], and their fabrication is not so complex as sesquioxides [21]. In such materials the probability of non-radiative transitions is lower than in crystalline oxides, therefore fluorescence decay time at $^4I_{11/2}$ is higher which brings benefits for CW laser operation [11, 13, 22].

The first lasing operation of Er:CaF_2 laser at 2.7 μm based on a stepwise up-conversion pumping scheme under Xe-flashlamp excitation was reported by S. A. Pollack et al [23]. Single

Optical Materials EXPRESS

crystal Er:SrF_2 lasing at 2.7 μm under diode pumping was realized by T.T. Basiev et al [22]. Recently, lasing in the near- and mid-infrared spectral range of Er^{3+} ions in laser quality fluoride crystal has been successfully demonstrated under laser diode pumping [11–13, 24–26]. It was found, that for laser generation in mid-infrared region (2.7 - 3 μm) it is not necessary to use matrix with high amount of Er^{3+} ions for room temperature lasing [12, 13, 26]. Due to broadband emission spectrum the Er:SrF_2 crystal is interesting for possible ultra-short pulse generation [13] and laser tuning. The laser tunability depends on several aspects - the laser linewidth, gain cross-section, fluorescence decay time and broadband emission spectrum [21, 27]. According to Moulton [27] the tunable laser systems with large gain cross-section and linewidth demand short fluorescence decay time. The broadband absorption and emission spectra of Er:SrF_2 are given by crystal structure [13, 21, 22]. The SrF_2 doped with Er^{3+} ions requires charge compensation if the trivalent rare-earth ions are used for doping [21, 22], and it should be also noted that the Er^{3+} ions form clusters, which is advantageous for energy transfer [13]. The Er:SrF_2 comply with all necessary requirements for tunable laser confirmed by results mentioned below and in literature [13, 22, 24, 28]. Thus the aim of this paper is to present tunable crystalline Er:SrF_2 active medium for the first time tuned over 100 nm at room temperature.

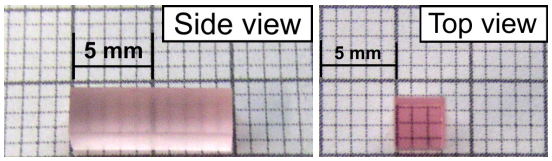

Fig. 1. Er:SrF_2 crystal sample photographs.

2. Experimental setup

The tested Er:SrF_2 crystal had a form of rectangular block, it was plane-parallel (10 mm long), face-polished (3 × 3 mm), see Fig. 1. The crystal does not have anti-reflection coatings. Since the tested sample was placed close to the pumping mirror (distance 2 mm) and the faces of the sample was plan-parallel the Fresnel losses could be neglected. The Er:SrF_2 contained 3 at. % of Er^{3+}. During all measurement, the tested sample was placed in cooper holder without active cooling. The Shimadzu spectrophotometer type UV - 3600 with spectral resolution ±0.2 nm in visible and ultraviolet region, and ±0.8 nm in mid-infrared was used for measuring the transmission spectra. Fluorescence spectra and laser emission were measured by Oriel monochromator 77250 (grating 77300) with Thorlab photodiode PDA 30G-EC (PbS, 1.0 - 2.9 μm).

The fiber-coupled (core diameter 100 μm, NA = 0.22) laser diode (LIMO35-F100-DL970-EX2082, LIMO) was used for longitudinal pumping of the crystal sample. The laser diode operated in the pulsed regime (frequency 10 Hz, pulse duration 5 ms). The pumping pulse duration was chosen to be close to fluorescence decay time at the upper laser level. Because of possible problems with a thermal lens and the overheating of the tested sample the duty cycle of 5 % was chosen, from this reason the pumping frequency of 10 Hz was used. Using temperature tuning, the emission wavelength of the laser diode was set at 969 nm. The Er:SrF_2 was placed inside the hemispherical optical resonator 145 mm long formed by a flat pumping dichroic mirror (PM) and a concave output coupler (OC, radius of curvature – 150 mm). The PM was highly transparent (T ~ 94 %) in pumping range at 960 - 980 nm and at the same time highly reflective (R = 99 %) within the spectral range of 2.65 – 2.95 μm. The output coupler (OC) with reflectivity 95 % @ 2.65 – 2.95 μm was used. The pumping radiation was focused into the tested crystal by two achromatic doublet lenses with a focal length of f_1 = 75 mm and f_2 = 150 mm, thus the pumping beam diameter was ~ 200 μm. The wavelength tuning of the

Optical Materials EXPRESS

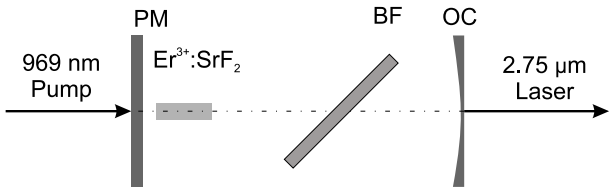

Fig. 2. Diode-pumped Er:SrF_2 laser: PM – HT @ 969 nm, HR @ 2.65 – 2.95 μm; OC – R = 95 % @ 2.65 – 2.95 μm, r = 150 mm, BF – birefringent MgF_2 plate 2 mm thick.

erbium laser was obtained by using a birefringent filter (single MgF_2 plate 2 mm thick) placed at the Brewster angle inside the optical resonator between the output coupler and laser active medium. The laser layout is shown in Fig. 2. The mean output power of the laser was measured using a broadband high-sensitivity thermopile probe PM19 (Molectron) with a germanium plate as a filter (to separate pumping radiation). The temporal structure of the generated radiation was observed by an InAs/InAsSbP photodiode (model PD36-05, peak wavelength sensitivity 2.55 – 3.45 μm, IBSG Co, Ltd.) connected to the oscilloscope (Tektronix TDS 3052B, 500 MHz, 5 GS/s). The IR sensitive camera Pyrocam III (Spiricon) was used to investigate the laser beam spatial structure.

3. Results and discussion

The absorption spectrum of the Er:SrF_2 in laser pumping spectral region is shown in Fig. 3(a). The maximum in absorption spectrum from Fig. 3(a) corresponds with wavelength of 969 nm and absorption coefficient is 1.62 cm^{-1}, the FWHM of absorption band is 17 nm (967 - 984 nm). During laser experiments, the ~74 % of pumped power was absorbed in laser active medium. From the fluorescence spectrum shown in Fig. 3(b) it can be seen that Er:SrF_2 possesses broadband emission spectra. As evident, the mid-IR fluorescence of Er^{3+} ions corresponding to laser transition $^4I_{11/2} \rightarrow {}^4I_{13/2}$ has a maximum at region 2.71 μm. The fluorescence decay curves of Er^{3+} ions in SrF_2 crystal are presented in Fig. 4, the transition $^4I_{11/2} \rightarrow {}^4I_{13/2}$ is self-terminated since the fluorescence decay time of the lower $^4I_{13/2}$ level (13 ms) is approximately 1.7 times longer than that for the upper $^4I_{11/2}$ level (7.3 ms).

The described laser system based on the Er-doped SrF_2 crystal was tested without the birefringent filter at first. The generated pulse energy and power amplitude were estimated from the mean output power, using the known pulse repetition rate and duration. Dependence of the laser output power amplitude on the absorbed power amplitude is presented in Fig. 5. From the results it is seen that in the described configuration with Er:SrF_2 it is possible to generate

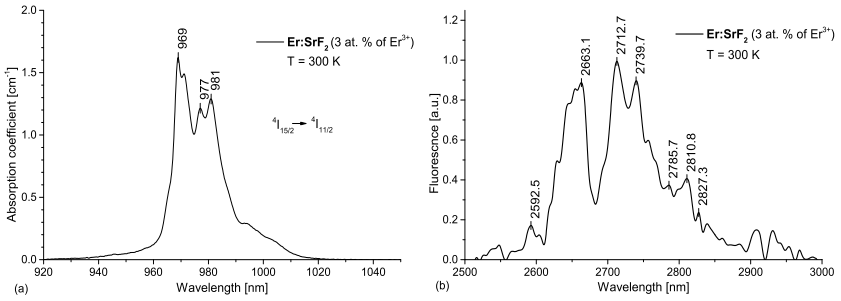

Fig. 3. Absorption spectrum of Er:SrF_2 crystal (a) and fluorescence spectrum of Er:SrF_2 crystal (b).

Optical Materials EXPRESS

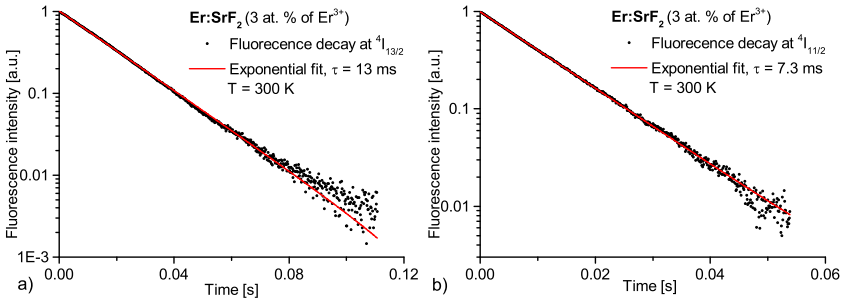

Fig. 4. Fluroescence decay time at lower $^4I_{13/2}$ (a) and at upper $^4I_{11/2}$ (b) laser level .

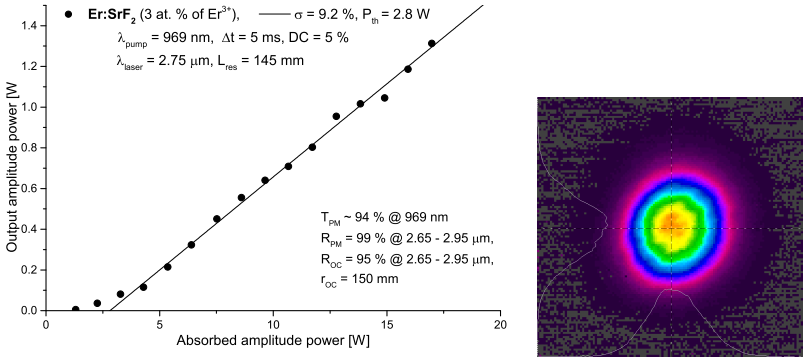

Fig. 5. Output characteristic of diode-pumped Er:SrF_2 pulsed laser with beam profile for maximum laser output power; duty cycle – DC, pumping pulse length – Δt, slope efficiency with respect to absorbed energy – σ, laser threshold – P_{th}, pumping wavelength – λ_{pump}, emission wavelength λ_{laser}, resonator length – L_{res}, pumping mirror transmission and reflectivity – T_{PM} and R_{PM}, output coupler reflectivity and radius – R_{OC} and r_{OC}.

power amplitude up to 1.3 W with slope efficiency of 9.2 % with respect to the absorbed power amplitude. This result was reached for duty cycle 5 % and the corresponding mean output power was 58 mW. The generated laser beam profile for maximum output power is shown in Fig. 5, it can be seen that the beam profile is not clear fundamental mode TEM_{00}. The M^2 of the laser beam in x- and y-axis was calculated to be 1.9 and 1.8, respectively. This data was obtained as a ratio of measured and calculated laser beam divergence. The emitted laser radiation line was 2.75 μm with linewidth 9 nm (FWHM). The emitted wavelength is affected by series of up-conversion processes, the excited state absorption and energy transfer, that are described in detail in [13].

Using the MgF_2 intra-cavity birefringent filter inside the resonator, a continuously tunable output was achieved. The tuning curve of the laser is shown in Fig. 6. The birefringent filter causes the additional losses in resonator, so the laser threshold rose and maximal output power was decreased, particular values are mentioned in text below. The obtained tuning curves were not smooth due to numerous water absorption lines [29] contained in the air in this spectral region. The slow modulation of measured tuning curve correlates well with observed fluorescence spectrum (Fig. 3(b)). The fast modulation could be mostly explained by strong absorption on the atmosphere in the laser resonator. Also water or other substance adsorption on any optical surface present in the laser resonator could influence the laser tuning significantly and in different way that the air. Tuning range of 123 nm extended from 2690 nm to 2813 nm (crossing zero) was obtained for Er:SrF_2. The maximum output mean power obtained with MgF_2 intra-cavity

Optical Materials EXPRESS

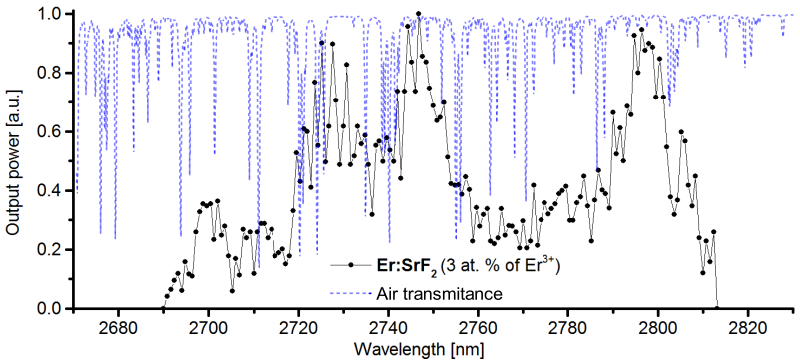

Fig. 6. Tuning curve of Er:SrF_2 measured for maximal pumping shown together with air absorption lines, excitation pulse length 5 ms, frequency 10 Hz, pumping wavelength 969 nm.

birefringent filter was 21 mW @ 2.75 µm.

4. Conclusion

The SrF_2 crystal doped with 3 at. % of Er^{3+} was tested and the spectroscopic and laser properties were investigated at room temperature. Under pulsed 969 nm laser diode pumping the mid infrared radiation at 2.75 µm was obtained with slope efficiency up to 9.2 %. The Er:SrF_2 laser emitted radiation with maximal output power amplitude of 1.3 W. Using the MgF_2 birefringent filter the new maximal tunability from 2690 nm to 2813 nm was reached. The obtained tunability range significantly exceed results (2720 - 2760 nm, tuning range 40 nm, tuning element quartz plate) on Er:SrF_2 published in [22].The broader tuning range was probably reached due to using MgF_2 instead of the quartz plate. Also, the lower laser threshold and lower losses in laser resonator helped to obtain the broader tuning range in comparison with [22]. The demonstrated broad gain bandwidth of ~ 4 THz (FWHM) makes this laser potentially attractive for ultra-short pulse generation in the 2.7 µm region (corresponding Fourier limited Gaussian pulse width ~ 110 fs). Regarding the tuning curve width, our results can be compared with data obtained using lasers based on transition metals, like Cr:ZnSe, Cr:ZnS or Cr:CdSe. These materials possess significantly broader tuning range (2100 -3100 [30]) covering also the Er:SrF_2 laser emission. On the contrary, an efficient and powerful pumping of these lasers is usually based on systems like Er- or Tm-fiber lasers witch increase the overall price and complexity of final laser. In such a case Er:SrF_2 laser could be a good option if the desired emission wavelength corresponds to its tuning range. Moreover, the lifetime of Cr^{2+} upper laser level is much shorter (~4 μs) comparing to Er^{3+} in SrF_2 (~7.3 ms), so the Q-switch pulse generation or laser radiation amplification will be much more difficult with Cr-doped materials.

As was mentioned above the Er:SrF_2 is interesting active medium because of low phonon energy that strongly affected self-termination process and improve the laser action. Moreover, the fabrication of this laser material is not so complex and expensive as the low phonon sesquioxide. All these features makes from Er:SrF_2 promising candidate for medical and spectroscopic applications or for further non-linear conversion deeper to infra-red region.

Funding

Czech Science Foundation (No. 18-11954S); National Natural Science Foundation of China (61422511).

Optics Letters

Line-tunable Er:GGAG laser

Richard Švejkar,[1,*] Jan Šulc,[1] Michal Němec,[1] Pavel Boháček,[2] Helena Jelínková,[1] Bohumil Trunda,[2] Lubomír Havlák,[2] Martin Nikl,[3] and Karel Jurek[3]

[1]Faculty of Nuclear Sciences and Physical Engineering, Czech Technical University in Prague, Prague, Czech Republic
[2]Institute of Physics of the Czech Academy of Sciences, Division of Condensed Matter Physics, Prague, Czech Republic
[3]Institute of Physics of the Czech Academy of Sciences, Division of Solid State Physics, Prague, Czech Republic
*Corresponding author: richard.svejkar@fjfi.cvut.cz

Received 28 May 2018; revised 14 June 2018; accepted 14 June 2018; posted 14 June 2018 (Doc. ID 332843); published 9 July 2018

In this Letter, for the first time, to the best of our knowledge, a pulse and CW laser based on an Er-doped $Gd_3Ga_{2.7}Al_{2.3}O_{12}$ (Er:GGAG) active medium emitting laser radiation at 2.8 μm are presented. With the longitudinal diode pumping, the maximal output energy of 4.9 mJ and slope efficiency of 13.5% in the pulse regime were reached. Using the birefringent MgF_2 plate, the line tunability of Er:GGAG at several spectral bands of 2800–2822 nm, 2829–2891 nm, and 2917–2942 nm were obtained.

OCIS codes: (140.3580) Lasers, solid-state; (140.5680) Rare earth and transition metal solid-state lasers; (140.3480) Lasers, diode-pumped; (140.3070) Infrared and far-infrared lasers; (160.3380) Laser materials; (300.6280) Spectroscopy, fluorescence and luminescence.

https://doi.org/10.1364/OL.43.003309

Lasers based on Er ions using transition $^4I_{11/2} \rightarrow {}^4I_{13/2}$ enable the generation of laser radiation in the spectral range from 2.7 to 2.94 μm. Since at 3 μm a strong absorption peak of water is located, there has been considerable effort to develop a suitable laser source for various medical applications, e.g., stomatology, dermatology, urology, and surgery [1–3]. To generate a laser wavelength in this spectral range, it is possible to use the optical parametric oscillator (OPO) or materials based on Cr:ZnSe or Cr:ZnS pumped with Tm fibers; nevertheless, these systems are complex and expensive [4,5]. Nowadays, there are many coherently pumped Er-doped laser active media based on various matrices for generating laser radiation in the spectral range of 2.7–2.94 μm. The Er-doped $Y_3Al_5O_{12}$ (Er:YAG), Er:$Y_3Sc_2Ga_3O_{12}$ (Er:YSGG), Er:$YAlO_3$ (Er:YAP), Er:YVO_4, etc. are well-known laser materials; however, these laser active media possess high phonon energy resulting in a self-termination effect, which affects laser efficiency and output energy [4,6,7]. On the other hand, the Er:Y_2O_3 and Er:Lu_2O_3 sesquioxides have a low-phonon energy and possess excellent material parameters contrary to, e.g., Er:YAG, Er:YSGG, Er:$LiYF_4$ (Er:YLF), Er:CaF_2, Er:SrF_2; however, due to their high melting point, their fabrication is complicated and expensive [4,5,8–12]. The other options are mixture matrices based on garnets with a multi-structure crystal lattice, which offers attractive material parameters [13–15]. The $Gd_3Ga_5O_{12}$ (GGG) crystal possesses a relatively low-phonon energy (600 cm^{-1}) [6,16], which is given by using heavier elements, such as Ga and Gd, a similar phenomenon was observed, e.g., in heavy metal glasses [17]. So, it could be expected that the Er:$Gd_3Ga_{2.7}Al_{2.3}O_{12}$ (Er:GGAG) crystal will have a comparable value of the phonon energy. Moreover, the Er:GGAG has a lower melting point (2100 K) than YAG, YAP, YSGG, or sesquioxides [18], and it can be easily grown by the Czochralski method. Of course, there are active media based on fluorides, e.g., Er:CaF_2, Er:SrF_2, or Er:YLF [4,10,11], that have a lower melting point (below 1700 K) compared with Er:GGAG [18]. Nevertheless, their crystalline structure is fragile and has a low hardness [13,18]. On the other hand, one could expect that the hardness of the GGAG should be similar to that of the GGG (6.5–7 Mohs) matrix due to their resembling crystal structure. Moreover, the Er:GGAG has a broader emission spectrum and longer fluorescence decay time at the upper laser level compared with Er:YAG or Er:YVO_4 [6,12]. A combination of the above features offers the possibility of wide tuning of the laser wavelength contrary to Er:YAG, Er:YSGG, or sesquioxides, and also generation of short pulses [4,9,12–14,19].

In this work, to the best of our knowledge, we present the first laser results with Er:GGAG emitting laser radiation at ~2.8 μm. Also, the line tunability at 2800–2822 nm, 2829–2891 nm, and 2917–2942 nm was tested, and the results are presented.

The Er:GGAG crystal was grown by the Czochralski method in a slightly oxidative atmosphere using an Ir crucible. The tested sample was cut from the grown crystal boule perpendicularly to the growth direction (c axis). From the X-ray measurements, it follows that the GGAG crystal has a cubic structure (lattice constant $a = 12.231$ Å) with space group O_h^{10} (Ia3d), which is the same as YAG, GGG, and YSGG [14,18]. From the ion radius and oxidation states of the Er^{3+}, one could predict that Er^{3+} substitutes Gd^{3+} in the GGAG crystal lattice. Because of partial substitution of Ga^{3+} by Al^{3+} ions, the crystal field is distorted, and the spectral line width becomes larger due to the inhomogeneous broadening [20].

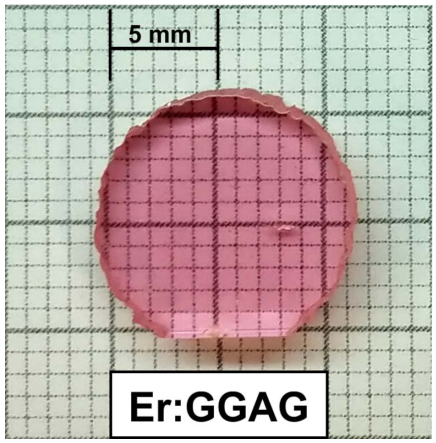

Fig. 1. Photograph of the tested Er:GGAG sample.

The tested Er:GGAG crystal (20% of Gd^{3+} replaced by Er^{3+} in melt) had a form of a cylinder (3.6 mm in length, 12 mm in diameter) with plane-parallel polished faces without anti-reflection coatings. The tested sample can be seen in Fig. 1. During all measurements, the investigated Er:GGAG was attached to a copper holder without active cooling.

The transmission spectrum of Er:GGAG was measured using a Shimadzu spectrophotometer type UV—3600 with spectral resolution ±0.2 nm in the visible and ultraviolet spectral ranges and ±0.8 nm in the mid-infrared spectral range. The fluorescence spectrum in the laser emission spectral range and emitted laser wavelength in the CW regime were measured using AROptix Fourier-transform spectrometer Arcspectro FT-MIR Rocket (2–6 μm, resolution 4 cm^{-1}). The Oriel monochromator 77250 (grating 77300) with a Thorlabs photodiode PDA20H-EC (PbSe, 1.5–4.8 μm) connected to a Tektronix oscilloscope TDS3052B (5 GS/s, 500 MHz) was utilized to evaluate the emitted laser wavelength in the pulse regime and during tunability measurements. The setup with the monochromator was chosen because this measurement was carried out at low repetition rate of the pulse Er:GGAG laser.

The fiber-coupled (core diameter 100 μm, NA = 0.22) laser diode (LIMO35-F100-DL976-EX1202, LIMO) was used for longitudinal pumping of the crystal sample. The laser diode operated in the pulsed (frequency 10 Hz, pulse duration 2 ms) and CW regimes. Using temperature tuning, the emission wavelength of the laser diode was set at 965 nm. The Er:GGAG was placed inside the hemispherical optical resonator 50 mm long, formed by a flat pumping mirror (PM) and a spherical output coupler (OC, radius of curvature 50 mm). The PM was highly transparent ($T > 94\%$) in the pumping range of 960–980 nm and at the same time highly reflective ($R > 99\%$) within the spectral range of 2.65–2.95 μm. An OC with reflectivity of 97.5% at 2.65–2.95 μm was used. The pumping radiation was focused into the tested crystal by two achromatic doublet lenses with a focal length of $f_1 = 75$ mm and $f_2 = 150$ mm, thus, the pumping beam diameter was ~200 μm. The wavelength tuning of the laser radiation was obtained using a birefringent filter (single MgF_2 plate, 2 mm thick) placed at the Brewster angle inside the optical resonator between the OC and laser active medium. To fit the birefringent plate between the crystal and the OC, a longer laser resonator (150 mm) with a different OC ($R = 99\%$ at 2.65–2.95 μm, radius of curvature 150 mm) was used. The laser layout is shown in Fig. 2. The output power of the Er:GGAG laser was measured by Thorlabs power probe S401 C (0.19–10.6 μm) connected to a Thorlabs power meter (PM100A).

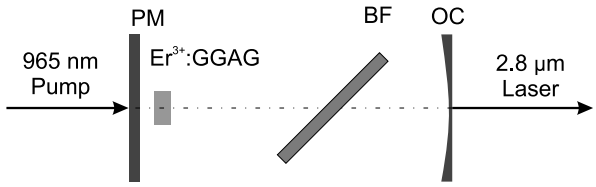

Fig. 2. Diode-pumped Er:GGAG laser; PM, pumping mirror; HT, high transmittance at 965 nm; HR, high reflectivity at 2.65–2.95 μm; OC, output coupler; $R = 97.5\%$ at 2.65–2.95 μm with $r = 50$ mm, or $R = 99\%$ at 2.65–2.95 μm with $r = 150$ mm; BF, birefringent MgF_2 plate 2 mm thick.

The absorption spectrum of Er:GGAG in the pumping spectral range, shown in Fig. 3, corresponds with the above-mentioned contention that the absorption lines are broad in comparison with Er:YAG [12]. This is advantageous for pumping because of the overlapping of the laser diode spectral line and absorption curve of the laser crystal. From Fig. 3, it can be seen that the maximum absorption coefficient of 14.3 cm^{-1} corresponds with the wavelength of 965.3 nm. Thus, for ideal absorption of pumping radiation, the chosen excitation wavelength was 965 nm, and approximately 91% of the pump power was absorbed in the crystal. As stated above, the Er:GGAG laser possesses broadband fluorescence spectral lines in the spectral range of 2.6–3 μm, which was successfully confirmed, and the fluorescence curve is presented in Fig. 4. Due to the broad fluorescence spectrum, the Er:GGAG crystal is potentially interesting for generating short pulses; moreover, the broadband emission spectrum enables laser wavelength tuning in a wide spectral range, which was confirmed in our laser experiments. Fluorescence decay at the upper ($^4I_{11/2}$) and lower ($^4I_{13/2}$) laser levels was measured, see Fig. 5. The ladder-like data grouping in Fig. 5 was caused by digitization of a low signal by a digital oscilloscope. Using the logarithmic scale, this effect was emphasized. Using an exponential fit, the fluorescence decay time was evaluated to be 430 ± 7 μs ($^4I_{11/2}$) and 3.2 ± 0.1 ms ($^4I_{13/2}$), respectively. It has to be noted that because of the ratio between fluorescence decay time at the

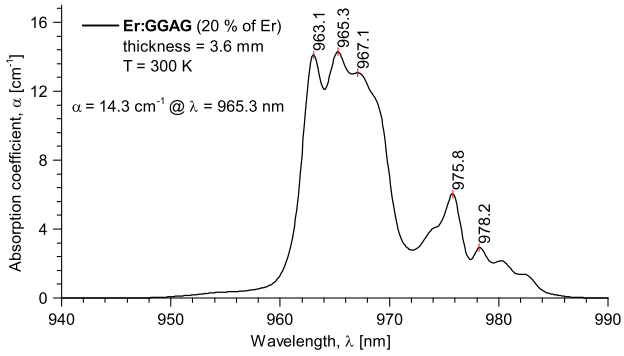

Fig. 3. Absorption spectrum of Er:GGAG.

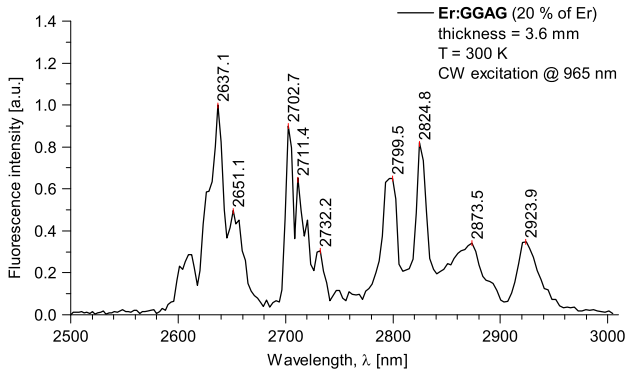

Fig. 4. Fluorescence spectrum of Er:GGAG.

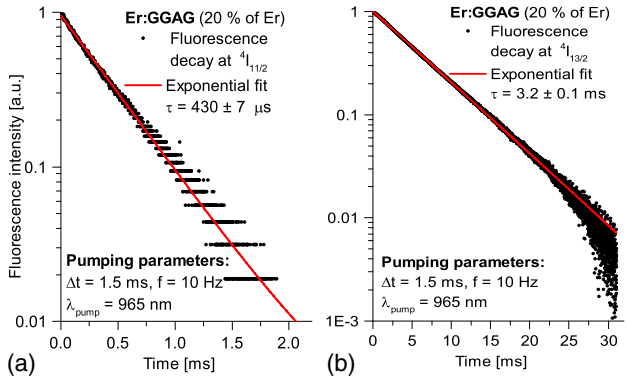

Fig. 5. (a) Fluorescence decay at upper laser level $^4I_{11/2}$ and (b) lower laser level $^4I_{13/2}$; τ, decay time; Δt, pumping pulse width; f, frequency; λ_{pump}, pumping wavelength.

upper (430 μs) and lower (3.2 ms) laser levels, the Er:GGAG can suffer by the self-termination (bottleneck) effect [4,14]. Nonetheless, this phenomenon is probably, to a certain extent, suppressed by high concentration of Er and the low-phonon matrix [4,10,16]. However, according to the results in Ref. [15], using co-doping ions, e.g., Pr^{3+} in Er:GGG, this

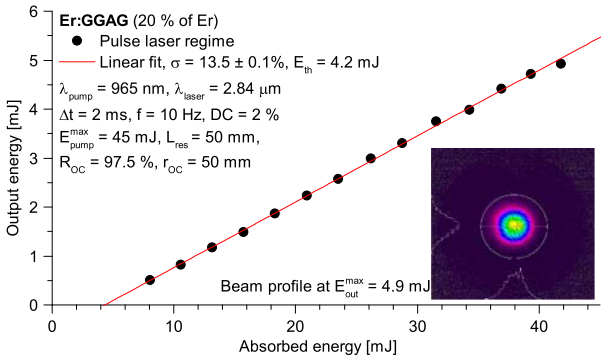

Fig. 6. Output characteristic of the Er:GGAG pulse laser; σ, slope efficiency; E_{th}, laser threshold; λ_{pump}, pumping wavelength; λ_{laser}, laser wavelength; Δt, pumping pulse width; f, frequency; DC, duty cycle; E_{pump}^{max}, maximal pumping energy; L_{res}, resonator length; R_{OC} and r_{OC}, output coupler reflectivity and radius; E_{out}^{max}, maximal output energy.

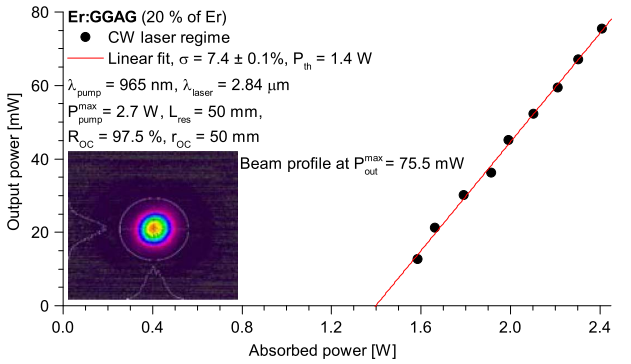

Fig. 7. Output characteristic of the Er:GGAG CW laser; σ, slope efficiency; P_{th}, laser threshold; λ_{pump}, pumping wavelength; λ_{laser}, laser wavelength; P_{pump}^{max}, maximal pumping power; L_{res}, resonator length; R_{OC} and r_{OC}, output coupler reflectivity and radius; P_{out}^{max}, maximal output power.

undesirable effect of self-termination can be further reduced. So, we believe that in Er:GGAG the Pr^{3+} ions can also be used, and the bottleneck effect could be decreased.

At first, the Er:GGAG laser system was tested without a birefringent plate. The results for the pulse and CW lasers are presented in Figs. 6 and 7, respectively. In both cases, a short laser resonator was used to reduce the losses caused by absorption on the water molecules in the air. Using a 50 mm hemisperical resonator with OC $R_{OC} = 97.5\%$, the maximal output energy of 4.9 mJ, slope efficiency of 13.5% ± 0.1%, and laser threshold of 4.2 mJ with respect to absorbed energy were reached for the pulse Er:GGAG laser. The emitted laser wavelength was 2839 nm with a linewidth 5 nm at FWHM. The CW laser regime was also tested, and the maximal output power of 75.5 mW, slope efficiency of 7.4% ± 0.1%, emission laser wavelength of 2839 nm (linewidth 5 nm at FWHM), and laser threshold of 1.4 W with respect to the absorbed power were reached. Since the laser beam profile was close to the fundamental transverse electromagnetic (TEM_{00}) mode, the quality of the laser beam presented in Figs. 6 and 7 for the pulse and CW laser regimes was evaluated, respectively. From the ratio of the measured and calculated laser beam divergence the M^2 of the laser beam in both the x and y axis was calculated to be $M_{x,y}^2 = 2.0$ in the pulse and $M_{x,y}^2 = 1.9$ in the CW regime. Both of the presented beam profiles in Figs. 6 and 7 were measured at maximal output energy and power, respectively. After placing the MgF_2 birefringent plate into the laser resonator (150 mm long) between the OC ($R = 99\%$) and the Er:GGAG crystal, the tunability of the laser wavelength was tested. By rotating the birefringent plate along the horizontal axis, the conditions in the laser resonator were changed, and the emitted laser wavelength was shifted. In Fig. 8, the results for the laser wavelength tuning are presented. As can be seen, the laser is tunable in three wavelength bands: 2800–2822 nm, 2829–2891 nm, and 2917–2942 nm (measured at zero of the output power). Since the emission spectral lines of the Er:GGAG are broader in comparison with the Er:YAG, but they are narrower contrary to the Er:SrF_2 or the Er:CaF_2, only the line tunability of the Er:GGAG presented in Fig. 8 was possible [4,10,12]. Due to the crystalline structure of Er:GGAG, the emission laser lines are shifted further to the

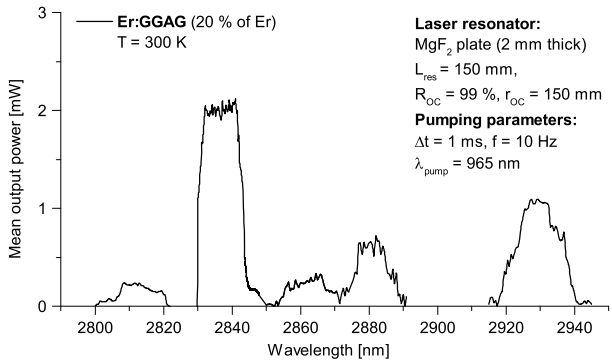

Fig. 8. Tuning curve of Er:GGAG measured for maximal pumping; λ_{pump}, pumping wavelength; Δt, pumping pulse width; f, frequency; L_{res}, resonator length; R_{OC} and r_{OC}, output coupler reflectivity and radius.

mid-infrared spectrum, as against, e.g., Er:SrF_2, Er:CaF_2, Er:Y_2O_3, and Er:Lu_2O_3 laser active media [8–10], and, thus, the Er:GGAG crystal should not be neglected as a possible tunable source of laser radiation at 2.8–3 μm.

From the results presented above, it can be seen that the Er:GGAG crystal is able to work in the pulse and CW laser regimes without active cooling. The lower slope efficiency and output power are probably due to the non-optimized laser resonator and overlapping of the pumping beam and laser mode in the resonator. In our opinion, a higher output power and slope efficiency could be reached by active (water or cryogenic) cooling and with an optimized laser resonator. Moreover, cascade lasing can be used, as from Ref. [8], it is clear that this should also increase the slope efficiency.

In conclusion, we presented the spectroscopic and laser properties of Er:GGAG, a new laser active medium. In the pulse regime, the Er:GGAG laser emitted laser radiation at 2839 nm with maximal output energy of 4.9 mJ and slope efficiency of 13.5%. Also, the CW laser regime with maximal output power of 75.5 mW and slope efficiency of 7.4% was successfully tested. From the tunability measurements, it follows that the Er:GGAG laser was line-tunable at 2800–2822 nm, 2829–2891 nm, and 2917–2942 nm. We believe that laser matrices based on garnet mixtures, such as GGAG with broadband absorption and emission spectral lines, and lower self-termination effects are one of the options to reach widely tunable and efficient lasers at ∼3 μm.

Funding. Grantová Agentura České Republiky (GACR) (18-11954S).

REFERENCES

1. I. Sorokina and K. L. Vodopyanov, eds., *Solid-State Mid-Infrared Laser Sources*, Vol. **89** of Topics in Applied Physics (Springer-Verlag, 2003).
2. M. Skorczakowski, J. Swiderski, W. Pichola, P. Nyga, A. Zajac, M. Maciejewska, L. Galecki, J. Kasprzak, S. Gross, A. Heinrich, and T. Bragagna, Laser Phys. Lett. **7**, 498 (2010).
3. H. Jelínková, ed., *Lasers for Medical Applications Diagnostics, Therapy and Surgery*, 1st ed. (Woodhead, 2013).
4. R. Švejkar, J. Šulc, H. Jelínková, V. Kubeček, W. Ma, D. Jiang, Q. Wu, and L. Su, Opt. Mater. Express **8**, 1025 (2018).
5. A. Godard, C. R. Physique **8**, 1100 (2007).
6. J. Wang, Z. Zhang, J. Xu, J. Xu, P. Fu, B. Liu, U. Taeuber, H. J. Eichler, A. Dicninig, G. Huber, X. Yan, X. Wu, and Y. Jiang, Proc. SPIE **3549**, 4 (1998).
7. J. Frauchiger, W. Lüthy, P. Albers, and H. P. Weber, Opt. Lett. **13**, 964 (1988).
8. T. Sanamyan, Laser Phys. Lett. **12**, 125804 (2015).
9. H. Uehara, R. Yasuhara, S. Tokita, J. Kawanaka, M. Murakami, and S. Shimizu, Opt. Express **25**, 18677 (2017).
10. W. Ma, X. Qian, J. Wang, J. Liu, X. Fan, J. Liu, L. Su, and J. Xu, Sci. Rep. **6**, 36635 (2016).
11. M. Messner, A. Heinrich, and K. Unterrainer, Appl. Opt. **57**, 1497 (2018).
12. B. J. Dinerman and P. F. Moulton, Opt. Lett. **19**, 1143 (1994).
13. J. Šulc, P. Bohček, M. Němec, H. Jelínková, B. Trunda, L. Havlák, K. Jurek, and M. Nikl, "Tunable diode-pumped Er:GGAG laser," in *2016 International Conference Laser Optics (LO)* (2016), paper R1-64.
14. Z. You, Y. Wang, J. Xu, Z. Zhu, J. Li, and C. Tu, IEEE Photon. Technol. Lett. **26**, 667 (2014).
15. Y. Wang, Z. You, J. Li, Z. Zhu, E. Ma, and C. Tu, J. Phys. D **42**, 215406 (2009).
16. Y. Wang, J. Li, Z. Zhu, Z. You, J. Xu, and C. Tu, Opt. Lett. **38**, 3988 (2013).
17. R. Paschotta, *Encyclopedia of Laser Physics and Technology* (Wiley-VCH, 2008).
18. M. J. Weber, ed., *Handbook of Optical Materials* (CRC Press, 2003).
19. P. F. Moulton, "Tunable solid-state lasers," in *Proceedings of the IEEE* (IEEE, 1992), Vol. **80**, pp. 348–364.
20. B. Henderson and R. H. Bartram, *Crystal-Field Engineering of Solid-State Laser Materials*, Cambridge Studies in Modern Optics (Cambridge University, 2000).

IOP Publishing | Astro Ltd
Laser Physics Letters
Laser Phys. Lett. **16** (2019) 075802 (4pp)
https://doi.org/10.1088/1612-202X/ab1918

Letter

Er:Y_2O_3 high-repetition rate picosecond 2.7 μm laser

Richard Švejkar, Jan Šulc and Helena Jelínková

Czech Technical University in Prague, Faculty of Nuclear Sciences and Physical Engineering Břehová 7, 115 19 Prague, Czech Republic

E-mail: richard.svejkar@fjfi.cvut.cz

Received 30 January 2019
Accepted for publication 12 April 2019
Published 4 June 2019

Abstract

In this paper, we present results obtained with a compact passively Q-switched mode-locked high-repetition rate Er:Y_2O_3 generating radiation in mid-infrared region. The Er:Y_2O_3 active medium was tested in a short V-shape laser resonator and the mode-locked pulses with repetition rate 1.38 GHz were obtained. With the Er:Y_2O_3 ceramic the shortest 86 $\pm$ 4 ps mode-locked pulses with pulse energy 3.55 nJ, corresponding peak power 12 W, and laser wavelength 2.74 μm were generated.

Keywords: infrared and far-infrared lasers, lasers, solid-state, erbium, mode-locked lasers, diode-pumped

(Some figures may appear in colour only in the online journal)

1. Introduction

The erbium lasers are well known due to the possibility of generating laser radiation close to 3 μm, where the absorption peak of water is located [1, 2]. The laser transition between $^4I_{11/2} \rightarrow {}^4I_{13/2}$ allows us to generate laser wavelength in a spectral range from 2.65 μm to 2.94 μm, depending on the matrix of active medium [3–6]. This spectral range is interesting mainly for applications in medicine due to the high absorption coefficient of biological tissue at 3 μm [1]. Also, the erbium $\sim$3 μm lasers can be used as a pumping source for optical parametric oscillators or for Fe:ZnSe active media [5, 7–9]. For these applications the various laser radiation characteristics following from laser regimes (free-running, Q-switching, or mode-locking) are required. Up to now, there are many papers that deal with free-running [4–6] and Q-switched [10–12] bulk erbium lasers. However, still, there is a lack of the compact passively mode-locked bulk erbium lasers generating picoseconds or sub-picoseconds pulses. The mode-locked pulses with erbium-doped active media can be generated using active or passive switching; nowadays, the most of the latest papers deals with passive mode-locking were as saturable absorber the graphene [13, 14], black phosphorus [10, 12], or semiconductor saturable absorber mirror (SESAM) [11, 15] are placed into the laser resonator. These saturable absorbers allow building compact and simple laser resonator to generate the mode-locking pulses. Since the pulse duration of the mode-locked laser is independent on the length of a laser resonator [16] many systems deal with erbium-doped fibres [10, 11, 13]. The fibre setup prevents the absorption of laser radiation on water molecules that occur in air, which can also influence the pulse duration. However, the length of resonator affects the repetition rate of the mode-locked laser system [16], thus the length of the erbium-doped fibre limits the repetition rate to the megahertz region [10, 11, 13, 16–18]. Also, the durability and long-term stability of Er-doped fibres is still limited. If the erbium bulk active medium is used, the laser resonator can be more compact and the repetition rate reaches frequency of the 10^9 Hz, which is presented in the results below. Nowadays, the generation of the high harmonics has a limit in a repetition rate up to hundreds of MHz if the femtosecond pulses from Tm:fibre are used [2, 19].

Up to now, the shortest laser pulses generated using the passive switching with erbium bulk laser (Er:CaF_2–SrF_2) were

obtained in Q-switched mode-locked regime and presented in [15]. The pulse duration in this Q-switched mode-locking (QML) regime was estimated to 1.78 ns with repetition rate 136.3 MHz [15]. To the authors' best knowledge, the [15] is only paper deals with short pulse generation with erbium-doped bulk active laser material.

In this paper, the sesquioxide ceramic Er:Y_2O_3 that generate laser radiation at 2.74 μm with SESAM were used to build the compact high-repetition-rate passively mode-locked laser system. As we believe, we report the first passively mode-locked bulk active laser material based on erbium and generating a picoseconds pulses with gigahertz repetition rate in 2.7 μm spectral range.

The Er:Y_2O_3 ceramic (5 at. % of Er^{3+}, Baikowski Co. Ltd.) had a form of a brick (thickness 9 mm, faces 3 × 3 mm), the faces of this sample were anti-parallel (1°) polished with anti-reflection coatings @ 2.7 μm. The tested sample is presented in figure 1.

2. Materials and methods

The transmission spectrum of the tested sample was measured using a Shimadzu spectrophotometer-type UV–3600 with spectral resolution ±0.2 nm in the visible and ultraviolet spectral range, and ±0.8 nm in the mid-infrared spectral range. The fluorescence spectrum in the laser emission spectral range was measured using ARCoptix Fourier-transform spectrometer Arcspectro FT-MIR Rocket (2–6 μm, resolution 4 cm^{-1}). The Oriel monochromator 77 250 (grating 77 300) with Thorlabs photodiode PDA20H-EC (PbSe, 1.5–4.8 μm) connected to a Tektronix oscilloscope TDS3052B (5 GS s^{-1}, 500 MHz) was utilized to evaluate the emitted laser wavelength. The fast detector VIGO PVI-4TE-6 (HgCdTe, 2–6 μm, rise time 1.1 ns) with Tektronix oscilloscope was used to record the Q-switched pulse train. The mode-locking pulse train was measured by the EOT photodetector ET-3000 (InGaAs, 800–1700 nm, rise time 175 ps) operating in a two-photon absorption regime and connected to the LeCroy oscilloscope SDA9000 (40 GS s^{-1}, 9 GHz). The laser pulse duration in the picosecond range was measured by a laboratory-built interferometric autocorrelator based on the two-photon absorption effect in germanium chip of Thorlabs photodiode PDA30B-EC (Ge, 800–1800 nm, rise time 2.5 μs) detector. The output energy and beam spatial structure were measured by a coherent energy probe J10-MB-LE (energy range 300 nJ–600 μJ, wavelength range 0.19–12.0 μm) and Spiricon Pyrocam IV (camera chip $LiTaO_3$, active area 25.6 × 25.6 mm) with Thorlabs bandpass filter FB2500-500 (spectral range 2500 ± 250 nm), respectively.

To reduce the attenuation of laser signal on water vapours in the air, as short as possible laser resonator was chosen, see figure 2. The simple 95 mm long V-shape optical resonator was formed by a flat pumping mirror (PM), a spherical concave output coupler (OC, radius of curvature 50 mm), and the SESAM (SAM-2800-4-10ps-4.0-25.0g-e, Batop GmbH). The

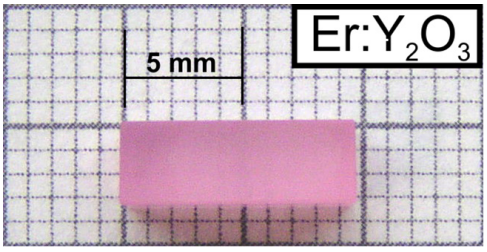

Figure 1. Photograph of tested Er:Y_2O_3 ceramic.

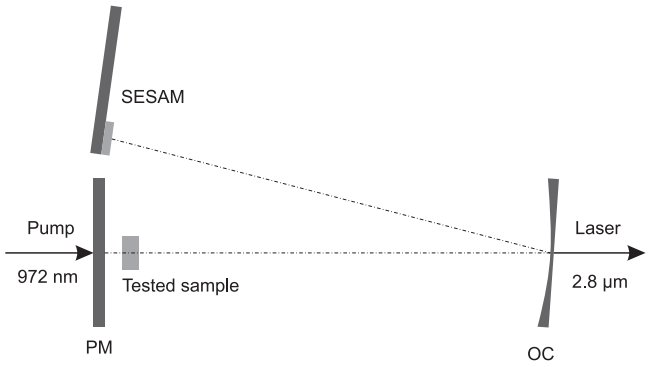

Figure 2. Layout of the V-shape laser resonator for mode-locking; PM—pumping mirror, OC—Output coupler, SESAM—semiconductor saturable absorber mirror.

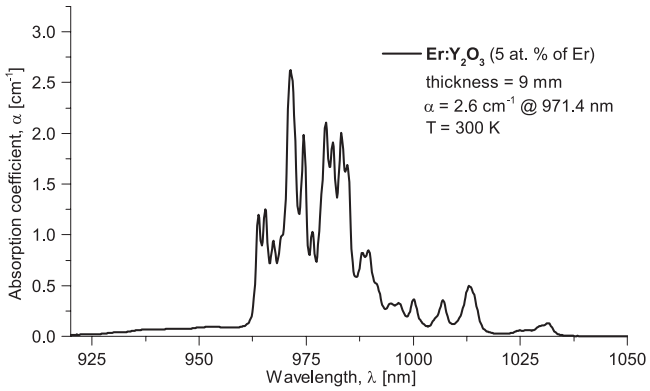

Figure 3. Absorption spectrum of tested Er:Y_2O_3 ceramic.

PM was highly transparent ($T > 94\%$) in the pumping range 960–980 nm and at the same time highly reflective ($R > 99\%$) within the spectral range 2.65–2.95 μm. OCs with reflectivity 95% @ 2.65–2.95 μm was used. The SESAM has a relaxation time of 10 ps, absorbance of 4% @ 2.8 μm, damage threshold of 2 mJ · cm^{-2}, and chip size of 4 × 4 mm. The Er:Y_2O_3 gain medium was placed close to the PM. For its longitudinal pumping the fibre-coupled (core diameter 100 μm, NA = 0.22) laser diode (LIMO35-F100-DL976-EX1202, LIMO) was used. The laser diode operated in the pulsed regime (frequency 10 Hz, pulse duration 1 ms, maximal incident mean pump 120 mW). Utilizing the temperature tuning, the emission wavelength was set at 972 nm. The pumping radiation was focused into the tested ceramic by two achromatic doublet lenses with a focal length of $f_1 = 75$ mm and $f_2 = 150$ mm, thus the pumping beam diameter was ~200 μm.

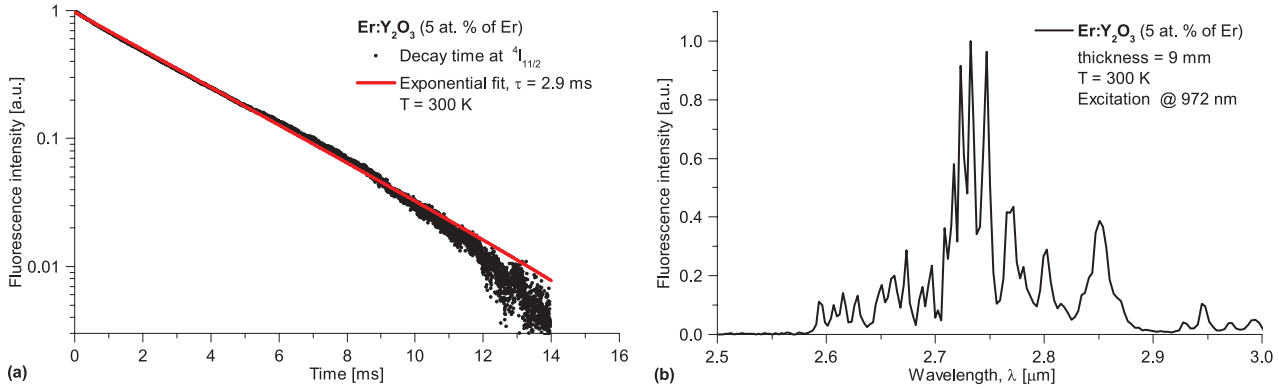

Figure 4. Fluorescence decay time at the upper laser level—(a) and fluorescence spectrum—(b) of tested Er:Y_2O_3 ceramic.

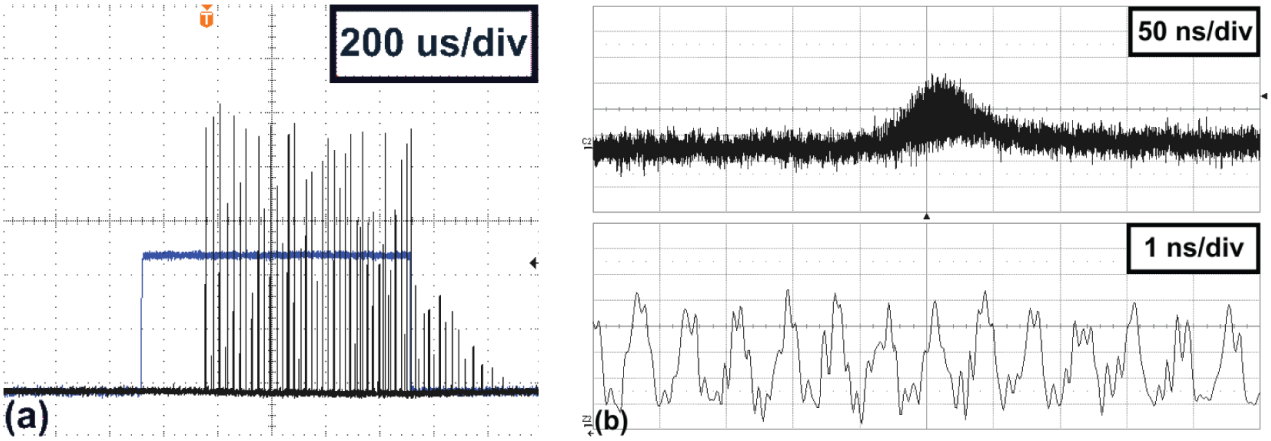

Figure 5. Train of Q-switched mode-locked pulses—(a) and mode-locked pulse train of Er:Y_2O_3 laser—(b).

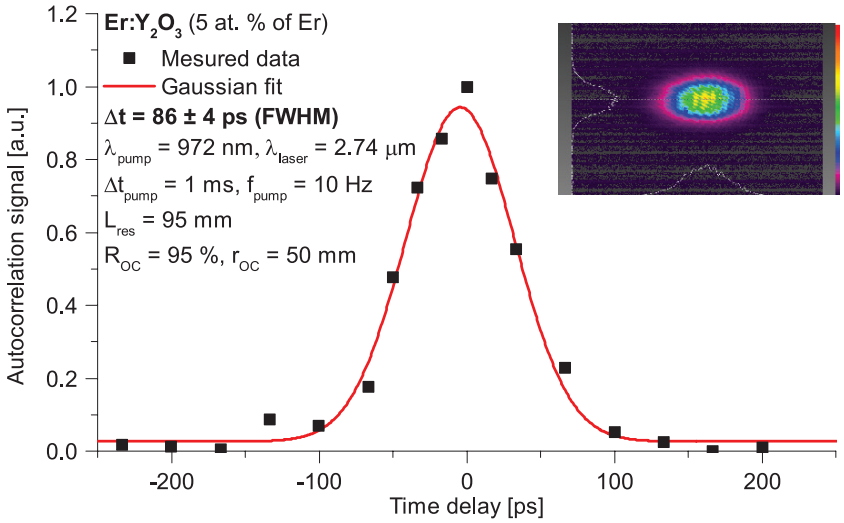

Figure 6. Autocorrelation trace of mode-locked Er:Y_2O_3; Δ t—mode-locked pulse duration, λ_{pump}—pumping wavelength, λ_{laser}—laser wavelength, Δ t_{pump}—pumping pulse width, f_{pump}—frequency, L_{res}—resonator length, R_{OC} and r_{OC}—output coupler reflectivity and radius.

3. Results and discussion

The absorption spectrum of tested Er:Y_2O_3 is presented in figure 3. As one can see the maximal absorption coefficient is 2.6 cm^{-1} @ 971.4 nm. Thus the pumping wavelength 972 nm was chosen. Using the exponential fit, the fluorescence decay time at the upper laser level ($^4I_{11/2}$) was evaluated to be 2.9 ms, result is shown in figure 4(a). The low repetition rate (10 Hz) and short pulse duration (1 ms) of pumping pulse were chosen to prevent overheating and damage of the Er:Y_2O_3 ceramic. The fluorescence spectrum of Er:Y_2O_3 in the emission spectral range is presented in figure 4(b) to illustrate the bandwidth

of the spectrum. The Er:Y_2O_3 ceramic is a well-investigated laser active medium and further spectroscopy details can be found in literature [3, 6, 20].

The Er:Y_2O_3 laser emitted radiation at 2.74 μm and operated in a QML regime in all ranges of used pumping power. Firstly, the pulse trains of Q-switched pulses, presented in figure 5(a), were recorded. The repetition rate of these pulses was 50 kHz for maximum pumping. The Q-switched pulse duration at FWHM was 57.9 ns. The energy inside this envelope was estimated from mean output power (138 μW) and the number of Q-switched pulses per second ($\sim$490) and it is equal to 0.3 μJ.

To present the modulation inside the envelop of the QML pulse and a train of mode-locking pulses (see figure 5(b)) the two-photon absorption in fast InGaAs detector connected to LeCroy oscilloscope was used. Due to the short laser resonator, the high repetition rate 1.38 GHz of mode-locking pulses was achieved. The final pulse duration of the mode-locking pulse, measured by a laboratory built autocorrelator, was 86 $\pm$ 4 ps at full-width half maximum. The autocorrelation trace is presented in figure 6. The mean energy of one mode-locked pulse was estimated from the number of pulses inside the pulse envelope ($\sim$80) and energy of these pulses. The mode-locked Er:Y_2O_3 laser had mean energy per pulse equal to 3.55 nJ.

Since the bandwidth of the fluorescence spectrum at laser line 2.74 μm is 10 nm the theoretical limit of mode-locked pulse duration is 1.1 ps. The obtained pulse duration (86 $\pm$ 4 ps) is probably affected by the losses in the laser resonator caused by water vapour and OC reflectivity 95%. From the mode-locking theory [16] follows that the pulse duration depends on the resonator losses which are, besides other things, given by OC reflexivity. With lower transparency for laser wavelength a large number of modes from spectrum will be synchronized, thus the pulse duration should be shorter. So, using the OC with e.g. $R = 99\%$ the mode-locking pulses could be shorter, however, this will limit the output energy and peak power. The losses caused by water vapour could be eliminated using the hermetic chamber filled with helium, argon, etc. We hope that the shorter pulses with the above-mentioned changes can be obtained. However, it was shown in [21] that in comparison with the unit of picosecond or femtosecond pulses the pulse duration in order of hundreds ps can be an advantage for medical application. Due to the picoseconds pulses being shorter than time for nucleation growth [21] and simultaneously the pulse duration together with energy exceed the peak power required for dielectric breakdown, the multi-photon ionization effect is suppressed [21].

4. Conclusion

In conclusion, in this work, for the first time, the results from a compact passively Q-switched mode-locked Er:Y_2O_3 laser are presented. The pulse duration of 86 $\pm$ 4 ps with a repetition rate of 1.38 GHz, pulse energy of 3.55 nJ and the corresponding peak power at 2.74 μm of 12 W were achieved. We believe that in future experiments more a compact laser resonator in a hermetic chamber filled with dry air will lead to a robust laser system with shorter pulse duration and higher repetition rate. As it was discussed above, if the picosecond pulses will be amplified it could be used in medicine or for a high-harmonic generation with high repetition rates.

Acknowledgments

This research was supported by the 'Center of Advanced Applied Sciences', Reg. No. CZ.02.1.01/0.0/0.0/16_019/0000778, supported by the Operational Program Research, Development and Education, co-financed by the European Structural and Investment Funds and the state budget of the Czech Republic.

References

[1] Jelínková H (ed) 2013 *Lasers for Medical Applications Diagnostics, Therapy and Surgery* 1st (Philadelphia, PA: Woodhead)
[2] Paschotta R 2008 *Encyclopedia of Laser Physics and Technology* (New York: Wiley)
[3] Kaminskii A A 1990 *Laser Crystals: their Physics and Properties* (New York: Springer)
[4] Švejkar R, Šulc J, Jelínková H, Kubeček V, Ma W, Jiang D, Wu Q and Su L 2018 *Opt. Mater. Express* **8** 1025–30
[5] Švejkar R, Šulc J, Němec M, Boháček P, Jelínková H, Trunda B, Havlák L, Nikl M and Jurek K 2018 *Opt. Lett.* **43** 3309–12
[6] Krankel C 2015 *IEEE J. Sel. Top. Quantum Electron.* **21** 250–62
[7] Doroshenko M E, Osiko V V, Jelínková H, Jelínek M, Šulc J, Němec M, Vyhlídal D, Čech M, Kovalenko N O and Gerasimenko A S 2016 *Opt. Express* **24** 19824–34
[8] Fedorov V V *et al* 2006 *IEEE J. Quantum Electron.* **42** 907–17
[9] Godard A 2007 *C. R. Phys.* **8** 1100–28
[10] Qin Z, Xie G, Zhang H, Zhao C, Yuan P, Wen S and Qian L 2015 *Opt. Express* **23** 24713–8
[11] Li J F, Luo H Y, He Y L, Liu Y, Zhang L, Zhou K M, Rozhin A G and Turistyn S K 2014 *Laser Phys. Lett.* **11** 065102
[12] Liu J, Liu J, Guo Z, Zhang H, Ma W, Wang J and Su L 2016 *Opt. Express* **24** 30289–95
[13] Zhu G, Zhu X, Wang F, Xu S, Li Y, Guo X, Balakrishnan K, Norwood R A and Peyghambarian N 2016 *IEEE Photonics Technol. Lett.* **28** 7–10
[14] Xu J, Liu J, Wu S, Yang Q H and Wang P 2012 *Opt. Express* **20** 15474–80
[15] Liu J, Feng X, Fan X, Zhang Z, Zhang B, Liu J and Su L 2018 *Opt. Lett.* **43** 2418–21
[16] Diels J C and Rudolph W 2006 *Ultrashort Laser Pulse Phenomena, Second Edition* (*Optics and Photonics Series*) 2nd edn (New York: Academic)
[17] Shen Y, Wang Y, Chen H, Luan K, Tao M and Si J 2017 *Sci. Rep.* **7** 2045–322
[18] Hu T, Jackson S D and Hudson D D 2015 *Opt. Lett.* **40** 4226–8
[19] Lee K F, Ding X, Hammond T J, Fermann M E, Vampa G and Corkum P B 2017 *Opt. Lett.* **42** 1113–6
[20] Sanamyan T 2015 *Laser Phys. Lett.* **12** 125804
[21] Miller R J D 2018 *8th EPS-QEOD Europhoton (Barcelona, Spain)* pEPS1

Passively mode-locked high-repetition rate Er:YLF laser at 2.81 μm generating 72 ps pulses

Richard Švejkar, Jan Šulc, Michal Němec, Helena Jelínková
Faculty of Nuclear Sciences and Physical Engineering, Czech Technical University in Prague, Břehová 7, 115 19 Prague, Czech Republic

The erbium-doped active media allow to generate laser radiation in spectral range 2.7 - 2.94 μm if the laser transition $^4I_{11/2} \rightarrow {}^4I_{13/2}$ is used [1]. Since the laser radiation in this spectral range is strongly absorbed in the water these lasers can be used in medicine (surgery, ophthalmology, urology) [1]. Nowadays, there are many papers deal with erbium-doped bulk active media operating in free-running or Q-switched regime, nevertheless, the passively mode-locked lasers are mainly built with Er-doped fibres. However, the compact passively mode-locked erbium-doped bulk lasers could offer a higher repetition rate and smaller dimensions. To date, the shortest laser pulses (1.78 ns) generated with erbium bulk laser (Er:CaF_2-SrF_2) was obtained in Q-switched mode-locked regime [2].In this paper, the SESAM mode-locked compact Er:YLF laser with the picosecond pulses and GHz repetition rate for the first time, according to the author's knowledge, is presented.

The tested Er:YLF crystal (6 % of Er^{3+}) had a form of a rod (length 9 mm, diameter 4 mm) with plane-parallel polished faces without anti-reflection coatings. The Er:YLF was placed inside the V-shape resonator (length 95 mm) consisted of a flat pumping mirror (PM, HT > 94 % and HR > 99 % @ 960 - 980 nm), a spherical output coupler (OC, radius 50 mm, R = 97.5 % @ 2.8 μm), and a SESAM (SAM-2800-4-10ps-4.0-25.0g-e, Batop GmbH, relaxation time 10 ps, absorbance 4 % @ 2.8 μm, damage threshold 2 mJ/cm^2, chip size 4×4 mm). For longitudinal pumping, the fibre-coupled (core diameter 100 μm, *NA* = 0.22) laser diode (LIMO35-F100-DL976-EX1202, LIMO) was used. The laser diode operated in the pulsed regime (pulse duration 1 ms, frequency 10 Hz, maximal mean pump power 120 mW, emitted wavelength 972 nm, focusing optic 1:2, beam diameter 200 μm).

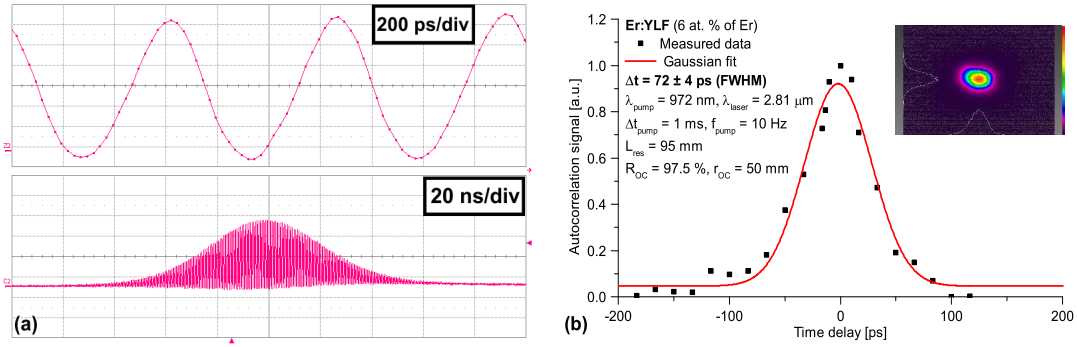

Fig. 1 Mode-locked Er:YLF laser (Δt – mode-locked pulse duration, λ_{pump} – pumping wavelength, λ_{laser} - laser wavelength, Δt_{pump} – pumping pulse width, f_{pump} – frequency, L_{res} – resonator length, R_{OC} and r_{OC}): (a) – mode-locked pulse train (b) – autocorrelation trace of mode-locked Er:YLF laser.

The Er:YLF laser emitted radiation at 2.81 μm in Q-switched mode-locking (QML) regime. The Q-switched pulses had the repetition rate 25 kHz, the pulse duration (FWHM) and energy of single Q-switched pulse envelope was 50.3 ns and 2.3 μJ, respectively. Using the two-photon absorption in EOT InGaAs photodetector ET-3000 connected to LeCroy oscilloscope SDA9000 the modulation inside envelop of the QML pulse and a train of mode-locking pulses were recorded, see Fig. 1(a). Due to the short laser resonator, the high repetition rate 1.41 GHz of mode-locking pulses was achieved. The mode-locked Er:YLF laser had mean energy per pulse equal to 9.9 nJ. Using a laboratory built interferometric autocorrelator based on two-photon absorption effect in germanium chip the picosecond pulses were measured. The mode-locking pulse, presented in Fig. 1(b), reached 72±4 ps at full-width half-maximum with the corresponding 137 W of peak power. Even though the pulse duration did not reach the femtosecond range, it was shown [3], that the picoseconds pulses could be advantageous for the medical applications. Since the pulse duration is probably affected by water vapour occurring in laser resonator future experiments will be carried out in a hermetic chamber filled with dry air, helium, etc. We believe that this improvement will lead to a robust laser system with shorter pulse duration and higher repetition rate. Moreover, if the picosecond pulses will be amplified it could be used in medicine or for a high-harmonic generation with high repetition rates.

References

[1] R. Paschotta, *Encyclopedia of Laser Physics and Technology* (Wiley-VCH, 2008).

[2] J. Liu, X. Feng, X. Fan, Z. Zhang, B. Zhang, J. Liu, and L. Su, "Efficient continuous-wave and passive Q-switched mode-locked Er^{3+}:CaF_2-SrF_2 lasers in the mid-infrared region," Opt. Lett. **43**, 2418–2421 (2018).

[3] R. J. D. Miller, "Picosecond Infrared Laser (PIRL) Scalpel: Achieving Fundamental (Single Cell) Limits to Minimally Invasive Surgery and Biodiagnostics," in "8th EPS-QEOD Europhoton," (Barcelona, Spain, 2018), p. EPS1.

978-1-7281-0469-0/19/$31.00 ©2019 IEEE

Er:YAG microchip for lasing in spectral range 2.94 µm and gain switching generation

Richard Švejkar*, **Jan Šulc, Helena Jelínková**

Czech Technical University in Prague, Faculty of Nuclear Sciences and Physical Engineering, Czech Republic

**richard.svejkar@fjfi.cvut.cz*

Abstract: Highly doped Er:YAG microchip was prepared to make laser resonator compact and generate short pulses in gain switching regime. Pulse duration 306 ns with peak power 7 W and repetition rate 400 Hz were reached.

OCIS codes: (140.3580) Lasers, solid-state; (140.5680) Rare earth and transition metal solid-state lasers; (140.3480) Lasers, diode-pumped; (140.3070) Infrared and far-infrared lasers; (160.3380) Laser materials.

1. Introduction

Nowadays, the lasers emitting radiation near the $\sim$ 3 µm are desired for various applications (spectroscopy, material processing, pumping source for further mid-infrared conversion) [1, 2]. The strong absorption peak of water is located at 3 µm so these lasers can be also used in medicine, e.g. stomatology, dermatology, urology, and surgery [3]. In medical applications it is crucial to guide laser radiation to specific spot which can be challenging since the radiation above 2.5 µm requires a special type of fibres (fluoride, germanium, sapphire, or hollow-core) [2]. This problem may be solved by using small Er:YAG microchip lasers placed into the head; thus instead of guiding the mid-infrared radiation in fibre only the pumping radiation from a laser diode can be guided into Er:YAG crystal. Moreover, microchip laser is able to generate in gain switching regime, which is beneficial for short pulse generation since the special crystal or modulator for Q-switching is not required [2].

The main purpose of this paper is to present the Er:YAG microchip laser for short pulse generation in gain switching regime at 2.94 µm.

2. Materials and methods

The Er:YAG crystal of a cubic (O_h^{10}) structure was grown in Crytur by the Czochralski method and the concentration of erbium was 50 at. %. During all measurement the Er:YAG was placed in the water-cooled copper holder. The measured sample had a form of a cylinder (5 mm in length, 3 mm in diameter) with plan-parallel polished faces. On the one side of microchip there was a pumping mirror (PM) highly transparent (T $>$ 94 %) in pumping range 960 – 980 nm and at the same time highly reflective (R $>$ 99 %) within the spectral range 2.6 $-$ 3 µm. On the second side of the microchip, there was output coupler (OC) with reflectivity 98 % @ 2.6 $-$ 3 µm was used $\sim$ 3 µm. The pumping laser diode was LIMO35-F100-DL976-EX1202 working in pulse regime (emission wavelength 965 nm, frequency 100 Hz or 400 Hz, pulse duration 1 ms or 120 µs). The output power of the Er:YAG laser was measured by Thorlabs power probe (S401C, 0.19 – 10.6 µm) connected to Thorlabs power meter (PM100A). The pulse duration of gain switched pulses were detected by a fast detector (VIGO PVI-4TE-6, HgCdTe, 2 - 6 µm, rise time 1.1 ns) with Tektronix oscilloscope (TDS3052B, 5 GS/s, 500 MHz).

3. Results and discussion

Firstly, the transmission spectrum of Er:YAG crystal (without mirrors lasers) was used and the absorption spectrum was calculated, see Fig. 1a. At 966 nm the maximal absorption coefficient 6.76 cm^{-1} is located thus for pumping the emission wavelength of the laser diode was temperature tuned to 965 nm. The Er:YAG crystal possesses a narrow fluorescence spectrum and very short fluorescence decay time ($\sim$300 µs) at $^4I_{11/2}$ energy level [4].

The Er:YAG microchip laser emitted radiation at 2940 nm with linewidth 10 nm at FWHM. The maximal output energy 0.93 mJ, slope efficiency 8.4 $\pm$ 0.1 % and laser threshold 6.6 mJ with respect to absorbed energy were reached in the pulsed regime. The laser output characteristic is presented in Fig. 1b. Microchip operates with repetition rate 100 Hz, duty cycle 10 % and emitted radiation close to a fundamental mode. However, using a higher duty cycle (higher pumping energy) caused a heavy thermal load of the crystal and roll-off output power. From this reason, the continuous wave operation cannot be obtained. During gain switching experiments the pumping pulse duration was set 120 µs and repetition rate 400 Hz, using this setting the gain switched pulse was generated 7 µs after the end of pump pulse which is presented in Fig. 1c. The gain switched pulse was recorded with VIGO detector and the data was fitted by Gaussian curve to obtain the pulse duration which is illustrated in

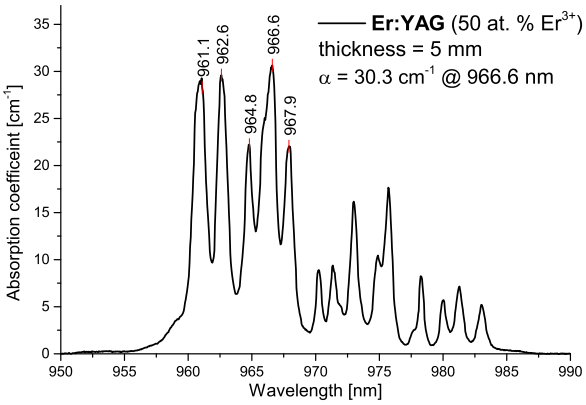

(a) Absorption spectrum of Er:YAG

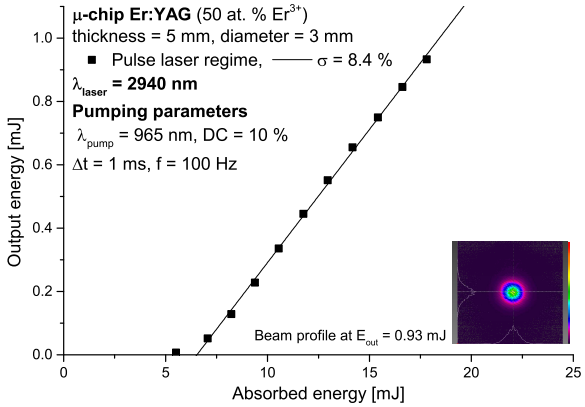

(b) Laser output characteristic of Er:YAG microchip

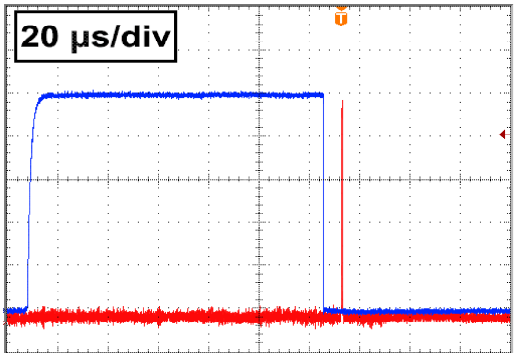

(c) Generation of gain switched pulse (red)

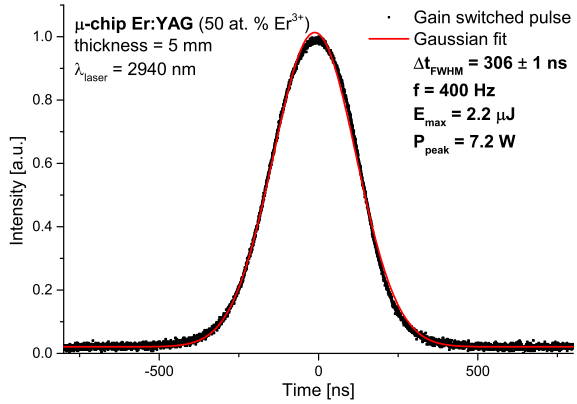

(d) Pulse duration of gain switched pulse

Fig. 1: Characteristics of Er:YAG microchip, α – absorption coefficient, λ_{laser} – laser wavelength, λ_{pump} – pumping wavelength $\triangle$t – pumping pulse duration,f – frequency, $\triangle t_{FWHM}$ – pulse duration of gain switched pulse at FWHM, P_{peak} – peak power, E_{max} – maximal output energy, σ – slope efficiency

Fig. 1d. The pulse duration 306 ns with repetition rate 400 Hz and output energy 2.2 μJ with corresponding peak power 7.2 W was obtained.

4. Conclusion

In conclusion, we presented the microchip Er:YAG laser and short pulse generation in gain switching regime. In the free-running regime the Er:YAG laser emitted laser radiation at 2940 nm with maximal output energy 0.93 mJ and slope efficiency 8.4 %. In the gain switching mode the shortest pulse duration 306 ns with repetition rate 400 Hz, energy 2.2 μJ and corresponding peak power 7.2 W was reached. The lower output energy and the slope efficiency are probably given by layers that form PM and OC mirrors on the faces of the crystal. We would like to improve mainly these layers to obtain better output results. We believe that the laser based on Er:YAG microchip is a compact solution for laser emission in the mid-infrared spectral range.

References

1. I. Sorokina and K. L. Vodopyanov, eds., *Solid-state mid-infrared laser sources*, vol. 89 of *Topics in Applied Physics* (Springer-Verlag, Berlin, 2003).
2. R. Paschotta, *Encyclopedia of Laser Physics and Technology* (Wiley-VCH, 2008).
3. R. Švejkar, J. Šulc, M. Němec, P. Boháček, H. Jelínková, B. Trunda, L. Havlák, M. Nikl, and K. Jurek, "Line-tunable Er:GGAG laser," Opt. Lett. **43**, 3309–3312 (2018).
4. Y. Yu, Z. Wu, and S. Zhang, "Concentration effects of Er^{3+} ion in YAG:Er laser crystals," Journal of Alloys and Compounds **302**, 204 – 208 (2000).

Er:YLF microchip laser for free-running and gain-switching laser operation in spectral range 2.83 µm

Richard Švejkar*, Jan Šulc, Michal Němec, Helena Jelínková

Czech Technical University in Prague, Faculty of Nuclear Sciences and Physical Engineering, Břehová 7, Prague, Czech Republic, 11519

**richard.svejkar@fjfi.cvut.cz*

Compact mid-infrared laser sources (2 – 8 µm) can be utilized in various branches (spectroscopy, remote sensing, polymer processing, medicine, etc.) [1]. For a generation of laser radiation at spectral range ~ 3 µm the active medium doped with erbium ions can be used. For medical application, there is particularly a desire for compact system generating short pulses with high peak power, that can be obtained either a Q-switching (passive or active) or gain-switching method. The gain-switching operation can be easily reached in microchip lasers. It is a compact and simple method to obtain the short pulses at ~ 3 µm wavelength. Moreover, the benefit of the microchip lasers is that the pulse duration of the gain-switched pulse is mainly determined by a resonator length which corresponds with the length of active media if the pumping pulse will be sufficiently short. This allows building a very compact laser system. [1-3] The goal of this contribusion was investigated of Er:YLF microchip working in gain-switched regime.

The tested crystal Er:YLF (6 % of Er^{3+}, a – cut, Unioriental Co., Ltd.) had a form of rectangular block, it was plane-parallel (9 mm long) and face-polished (3 × 3 mm). On the one side of the crystal there was deposited a pumping mirror (PM) highly transparent (T > 94 %) in range 960 – 980 nm and at the same time highly reflective (R > 99 %) within the spectral range 2.6 − 3 µm. Second side of microchip formed an output coupler (OC) with reflectivity 98 % @ 2.6 − 3 µm done by dielectric layers. The fibre-coupled (core diameter 100 µm, *NA* = 0.22) laser diode (LIMO35-F100-DL976-EX1202, LIMO) was used for longitudinal pumping of the crystal sample. The laser diode operated in the pulsed regime (frequency 20 Hz, pulse duration 5 ms, duty cycle 10 %, wavelength 972 nm). The energy probe (J10-MB-LE, Coherent) was utilized for output energy measurement of the Q-switched pulses. The pulse duration was measured using a photodiode (PVI-4TE-6, time constant 0.5 ns, VIGO System S.A.) connected to an oscilloscope (TDS3052B, 500 MHz, 5GS/s, Tektronix).

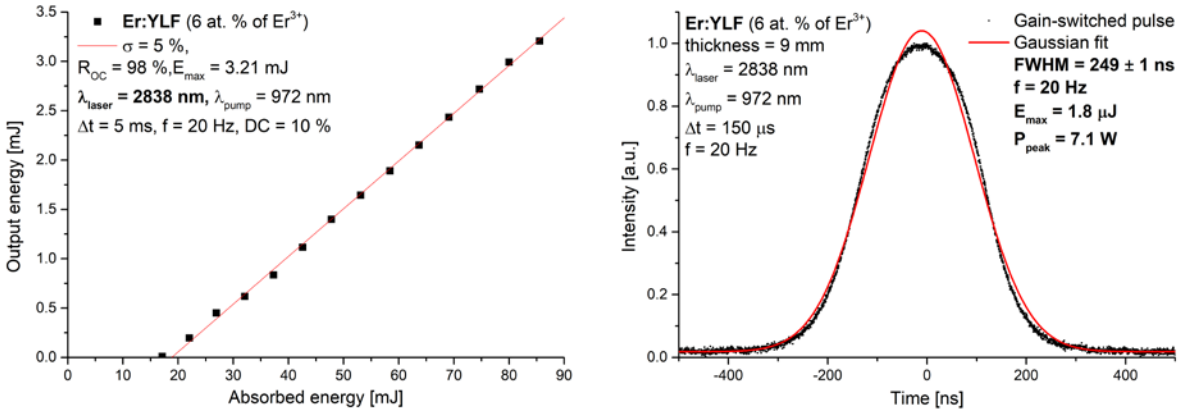

Fig. 1 Laser output energy (a) and gain-switched pulse duration (b); Δt – pumping pulse duration, f – frequency, λ_{pump} – pumping wavelength, λ_{laser} – emission wavelength, σ – slope efficiency, P_{peak} – peak power, E_{max} – maximal energy.

Firstly, the Er:YLF microchip laser was tested in free-running regime to characterize the output laser parameters. In a free-running laser regime, (Fig. 1a.), the slope efficiency, maximal output energy, and laser threshold with respect to the absorbed energy, of 5 %, 3.21 mJ, and 19 mJ were reached, respectively. The gain-switched laser system based on Er:YLF microchip was also successfully tested and the results are presented in Fig. 1b. The pulse duration of 249 ± 1 ns with a corresponding peak power of 7.1 W, pulse energy of 1.8 µJ, and a repetition rate of 20 Hz were obtained. The lower output energy and the slope efficiency are probably given by layers that form PM and OC mirrors on the flat faces of the crystal. The negative thermal lens of YLF could than destabilize the laser resonator. We would like to improve mainly these layers to obtain better output results. We believe that the laser-based on Er:YLF microchip is a compact solution for laser emission in the mid-infrared spectral range.

References

[1] Rüdiger Paschotta, *Encyclopedia of Laser Physics and Technology*, 1. Edition (Wiley-VCH, Berlin, 2008)

[2] R. Švejkar, J. Šulc, H. Jelínková, and M. Čech, "Temperature influence on spectroscopic and laser properties of Er:YLF crystal," in Solid State Lasers XXVIII: Technology and Devices, vol. 10896W. A. Clarkson and R. K. Shori, eds., International Society for Optics and Photonics (SPIE, 2019), pp. 246 – 251.

[3] Messner, M., Heinrich, A., and Unterrainer, K., "High-energy diode side-pumped Er:LiYF4 laser," Appl. Opt. 57, 1497–1503 (2018).

Up to 3 W continuous power and 21 ns long pulses from 2.8 µm Er:YLF laser

Richard Švejkar*, Jan Šulc, Michal Němec, Helena Jelínková

Czech Technical University in Prague, Faculty of Nuclear Sciences and Physical Engineering, Czech Republic

richard.svejkar@fjfi.cvut.cz

Abstract: Compact CW Er:YLF laser with output power 2.9 W and slope efficiency 26 % is presented. Using Fe:ZnSe crystal the passive Q-switching was achieved with pulse duration 21 ns, repetition rate 50 kHz, and peak power 252 W.

OCIS codes: (140.3580) Lasers, solid-state; (140.5680) Rare earth and transition metal solid-state lasers; (140.3480) Lasers, diode-pumped; (140.3500) Lasers, erbium; (140.3540) Lasers, Q-switched.

1. Introduction

Erbium-doped active media (Er:YLF, Er:YAG, Er:Y_2O_3, Er:GGAG, etc.) allow to generate a laser radiation close to the 3 µm which is interesting for many applications, e.g. medicine, spectroscopy, polymer processing, or for further mid-infrared conversion [1, 2]. The Er:YLF (Er:$LiYF_4$) is one of the interesting active medium due to several reasons: Er:YLF is uniaxial crystal, it can generate a naturally polarized laser radiation at 2.8 µm and the birefringent can eliminate thermally induced depolarization losses [1]. Moreover, the Er:YLF is a low phonon energy crystal ($\hbar\omega_{ph} = 490\,\mathrm{cm}^{-1}$), so the self-termination effect is partly suppressed and the CW laser regime can be easily reached [2]. On the other hand, Fe:ZnSe crystal possesses a strong absorption close to 3 µm and short lifetime (hundreds of nanoseconds) at room temperature thus it can be used for passive Q-switching at wavelengths around 3 µm [3]. This method of Q-switching allows to build a compact laser resonator without requirements on additional power sources or special crystals in comparison with an active Q-switching. In this paper, to the best author's knowledge, the passively Q-switched compact Er:YLF laser is reported for the first time and nanosecond pulses were successfully generated.

2. Materials and methods

The tested Er:YLF crystal (6 % of Er^{3+}, Unioriental Co., Ltd.) had a form of a brick (length 9 mm, cross-section 3×3 mm, a-cut) with plane-parallel polished faces without anti-reflection coatings. The Er:YLF was placed in water-cooled copper holder inside the optical resonator (length 15 mm) consisted of flat pumping mirror (PM, HT > 94 % and HR > 99 % @ 960 - 980 nm) and spherical output coupler (OC, radius 50 mm, R = 95 % @ 2.8 µm). During Q-switching experiments the laser resonator was prolonged to 25 mm to fit the Fe:ZnSe polycrystal ($3.9{\cdot}10^{18}$ cm^{-3} of Fe^{2+}, thickness 2.5 mm, uncoated, IPG Photonics) between Er:YLF crystal and output coupler. For longitudinal pumping, the fibre-coupled (core diameter 100 µm, $NA = 0.22$) laser diode (LIMO35-F100-DL976-EX1202, LIMO) was used. The laser diode operated in the pulsed and CW regime (maximal pump power 15.4 W, emitted wavelength 972 nm, focusing optic 2:5, beam waist diameter 250 µm). The energy probe (S401C, Thorlabs) was used for measuring the output power of the Q-switched pulses. The pulse duration was measured using a fast detector (PVI-4TE-6, τ_c = 0.5 ns, 2 - 6 µm, VIGO System S.A.) connected to an oscilloscope (TDS3052B, 5 GS/s, 500 MHz, Tektronix).

3. Results and discussion

Firstly, the spectroscopy characterization of Er:YLF was carried out. At wavelength of 972 nm the maximal absorption coefficient 3 cm^{-1} is located thus for pumping the emission wavelength of the laser diode was temperature tuned to 972 nm. The Er:YLF crystal possesses relatively broad fluorescence spectrum and long fluorescence decay time (∼4.1 ms) at upper laser level ($^4I_{11/2}$).

The Er:YLF laser emitted radiation at 2808 nm with linewidth 10 nm at FWHM in CW laser regime. The maximal output power 2.9 W with slope efficiency 26.2 % and laser threshold 0.24 W with respect to absorbed power were reached in the CW regime. The laser output characteristic is presented in Fig. 1a. Beam profile of Er:YLF laser radiation was also recorded and it can be seen as inset in Fig. 1a. During Q-switching regime the Fe:ZnSe polycrystal was placed into laser resonator. The Er:YLF passively Q-switched laser was successfully tested and the results are presented in Fig. 1. The Q-switched pulse was fitted by Gaussian curve to obtain the pulse duration which is illustrated in Fig. 1b. For maximal pumping, the pulses with repetition rate 50 kHz and duration

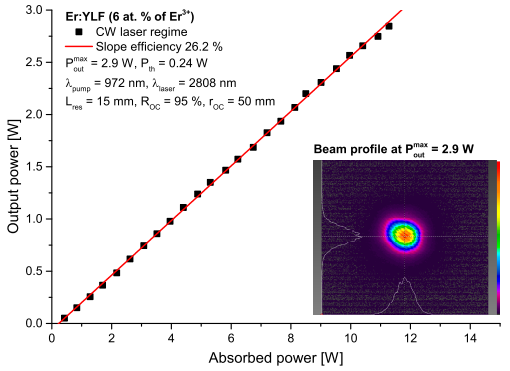

(a) Output CW laser characteristic.

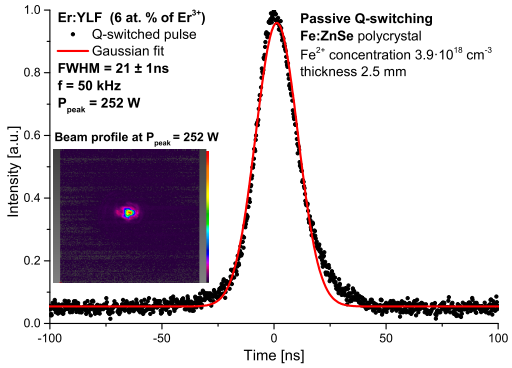

(b) Pulse duration of Q-switched pulse.

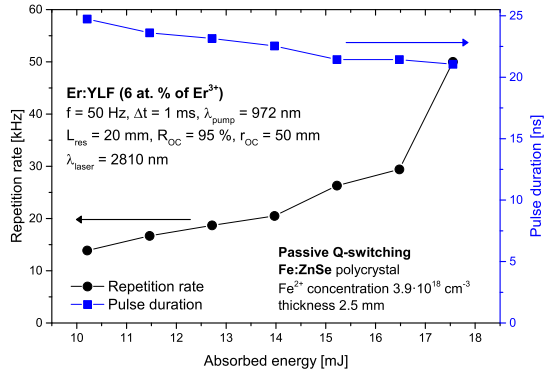

(c) Q-switched regime – repetition rate and pulse duration.

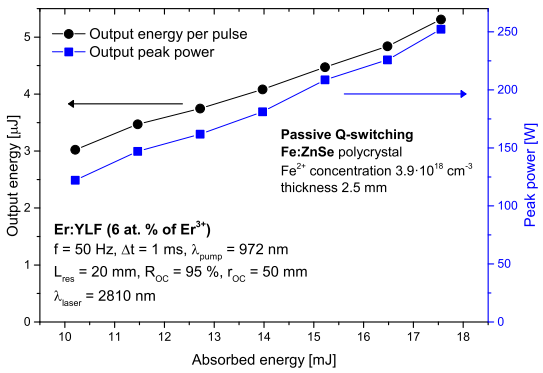

(d) Q-switched regime – output energy and peak power.

Fig. 1: Output laser characteristics for CW and Q-switch laser operation; λ_{pump} – pumping wavelength, λ_{laser} – laser wavelength, P_{out}^{max} – maximal output power, P_{th} – laser threshold, Δt – pumping pulse width, f – frequency, L_{res} – resonator length, R_{OC} and r_{OC} – output coupler reflectivity and radius.

21 ns were generated. The single pulse energy was estimated to be 5.31 μJ which corresponds to peak power 252 W. During the Q-switching regime, the laser emitted radiation at wavelength 2810 nm close to fundamental mode TEM_{00} which can be seen in inset in Fig. 1b. As one can see from Fig. 1c the repetition rate was increasing and the pulse duration was decreasing together with increasing absorbed energy. The dependence of output energy and peak power for Q-switched regime is shown in Fig. 1d.

4. Conclusion

In this work, the Er:YLF was tested in CW laser regime and the passively Q-switched operation was successfully demonstrated, too. Even if the fluoride matrix (with lower thermal conductivity) is used the CW laser regime with high output power was reached. The maximal output power 2.9 W, slope efficiency with respect to absorbed power 26.2 %, and emitted laser wavelength 2808 nm in CW laser regime were achieved. Using the Fe:ZnSe polycrystal in the laser resonator the Q-switching regime was obtained. The shortest pulse duration 21 ns with pulse energy 5.31 μJ corresponding to peak power 252 W and repetition rate 50 kHz were obtained. Such compact laser source generating high power nanosecond pulses could be afterwards used in medicine (surgery, or dentistry) or for polymer processing.

References

1. R. Paschotta, *Encyclopedia of Laser Physics and Technology* (Wiley-VCH, 2008).
2. R. Švejkar, J. Šulc, H. Jelínková, and M. Čech, "Temperature influence on spectroscopic and laser properties of Er:YLF crystal," in *Solid State Lasers XXVIII: Technology and Devices*, , vol. 10896 W. A. Clarkson and R. K. Shori, eds., International Society for Optics and Photonics (SPIE, 2019), pp. 246 – 251.
3. V. V. Fedorov, S. B. Mirov, A. Gallian, D. V. Badikov, M. P. Frolov, Y. V. Korostelin, V. I. Kozlovsky, A. I. Landman, Y. P. Podmar'kov, V. A. Akimov, and A. A. Voronov, "3.77-5.05- μm tunable solid-state lasers based on Fe^{2+}-doped ZnSe crystals operating at low and room temperatures," IEEE Journal of Quantum Electronics **42**, 907–917 (2006).

Compact Fe:ZnSe and Fe:ZnMnSe tunable lasers at 80 K pump with Er:YAG

Richard Švejkar*, Jan Šulc*, Helena Jelínková*, Maxim E. Doroshenko**, Nazar O. Kovalenko***, and Andrey S. Gerasimenko***

* Czech Technical University in Prague, Faculty of Nuclear Sciences and Physical Engineering, Břehová 7, Prague, Czech Republic, 11519

** AM Prokhorov General Physics Institute of RAS, Laser Materials and Technology Research Center, Vavilova 38-D, Moscow, Russian Federation, 119991

*** National Academy of Sciences of Ukraine, Institute for Single Crystals, 60 Lenin Ave, Kharkov, Ukraine, 61001

Abstract

The influence of manganese concentration in compact Er:YAG pumped Fe:ZnMnSe tunable lasers at 80 K were investigated. Using a birefringent plate, the wavelength range of 3950 – 4830 nm (880 nm) was covered.

I. Introduction

Nowadays, the compact laser sources for mid-infrared (3 – 8 μm) spectral range are required. This wavelength range could be utilized in spectroscopy (remote sensing), medicine (non-invasive laser diagnostic), or military applications (counter measure, rangefinders) [1,2]. The laser radiation in this spectral region can be generated with quantum cascade lasers, OPA, OPCPA, or different frequency generation. Nevertheless, the quantum cascade lasers have limited tuning range, output power and they have to operate at cryogenic temperature [3]. The OPCPA systems are able to operate at room-temperature, however, they are complex and consist of many optical components [1,3]. On the other hand, the Fe:ZnSe laser active medium possesses broad and strong emission bands in mid-infrared region and the tuning in the wide spectral range is achievable. [2]

The Er:YAG laser radiation well fits the absorption band of Fe^{2+} ions and can be used to pump Fe:ZnSe active medium. Thanks to longitudinally diode-pumped Er:YAG laser that emits laser radiation at 2.94 μm the whole Fe:ZnSe laser system for generation of laser radiation in mid-infrared spectral range could be more compact. Moreover, the fluorescence spectrum is shifted further to mid-infrared compared to ZnSe crystal if the active medium as solid-solution with a manganese is used [1]. The presence of the Mn ions influence the fluorescence decay time at upper laser level. With rising the Mn concentration the fluorescence decay time become shorter [1]. In case of a long (free-running) pulse excitation the liquid nitrogen temperature has to be used due to a short fluorescence decay time at room temperature caused by strong non-radiative quenching [1]. In this paper, to our best knowledge, we present first compact tunable Fe:ZnMnSe liquid nitrogen cooled laser pumped with diode-pumped Er:YAG laser system.

II. Materials and Methods

The tested samples Fe:ZnMnSe (Iron-Manganese Selenium, Fe:$Zn_{1-x}Mn_xSe$, x = 0, 0.05, 0.2) had a form of a plate (thickness 4.38 mm) with plan-parallel polished faces without anti-reflection coatings. The tested crystals were placed in a copper holder in the LN cryostat (Janis Research, model VPF-100), and the temperature was maintained at 80 K by a temperature controller (Lake Shore model 325). The Fe:ZnMnSe was longitudinally pumped by laboratory build diode-pumped Er:YAG laser (50 % of Er^{3+}, λ = 2.94 μm, f = 50 Hz, Δt = 980 μs, E_{max} = 0.6 mJ). The pumping laser diode was LIMO35-F100-DL976-EX1202 working in pulse regime (λ = 965 nm, f = 50 Hz, Δt = 1 ms, E_{max} = 20 mJ). The laser resonator (length 200 mm) of Fe:ZnMnSe laser shown in Figure 1 was hemispherical with the flat pumping mirror (PM, HR @ 4 – 5 μm, HT @ 2.94 μm) and spherical output coupler (OC, r_{OC} = 200 mm, R_{OC} = 95 % @ 4 - 5 μm). During tunability measurement, the OC with higher reflectivity (R_{OC} = 99 % @ 4 - 5 μm) was used for a decrease of threshold and reducing losses in the laser resonator. The tunability was tested using a MgF_2 birefringent plate, that was placed at Brewster's angle between cryostat and OC (R_{OC} = 99 %) mirror. The PM together with laser active medium was placed inside the cryostat.

The output power of the Fe:ZnMnSe lasers was measured by Thorlabs power probe S401C (0.19 - 10.6 μm) with power meter PM100A. The output laser wavelength was measured by monochromator Oriel 77250 (grating 77301) with Thorlab photodiode PDA20H-EC (PbSe, 1.5 – 4.8 μm).

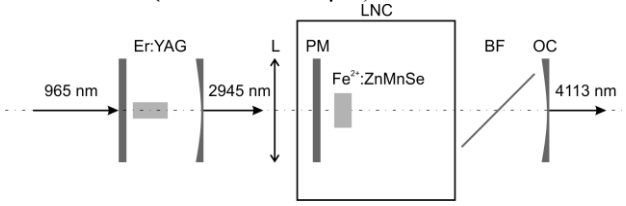

Figure 1 Layout of diode pumped Fe:ZnSe laser; L - CaF2 lens with focal length 55 mm, hemispherical resonator formed by flat pumping mirror (PM) and output coupler (OC), BF - birefringent plate, liquid nitrogen cryostat vacuum chamber (LNC).

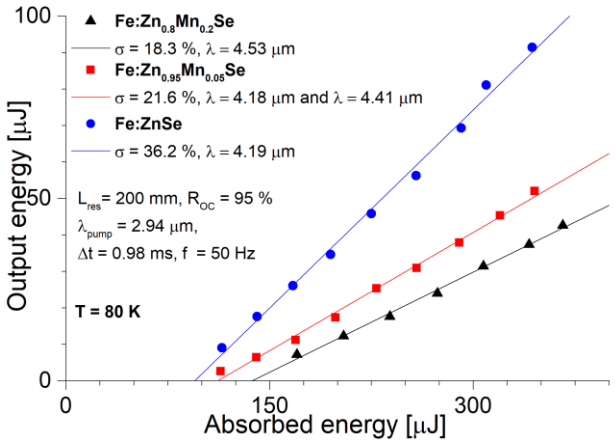

Figure 2 Output characteristic of Fe-doped active medium, σ – slope efficiency, λ – laser emission wavelength, L_{res} – laser resonator length, R_{OC} – output coupler reflectivity, λ_{pump}, Δt, f – pumping wavelength, pulse width, and frequency, T – sample temperature

III. Results and Discussion

The described laser system based on the Fe:ZnMnSe crystal was tested without the birefringent filter at first. The output energy was estimated from mean output power using the known pulse repetition rate. From Figure 2 it can be seen that the maximum output energy of 91.7 μJ, the slope efficiency of 36.2 %, the laser wavelength 4.19 μm, and the lowest threshold of 93.2 μJ with respect to absorbed energy were obtained for Mn concentration x = 0. With the highest tested concentration of Mn (x = 0.2) the wavelength 4.53 μm was reached, nevertheless, the slope efficiency and maximal output energy were decreased to the 18.3 % and the 42.5 μJ, respectively. The generated laser beams for individual Mn concentration had clear TEM_{00} transversal profile. From the laser results, one can see that with rising Mn concentration the output energy is decreasing and the laser central wavelength emission is shifted to longer wavelength. Moreover, for the Mn concentration x = 0.05 the two laser lines (4.18 nm and 4.41 nm) were observed. In Figure 3, the tuning curves for all tested samples are depicted and it can be seen that all curves well correspond with absorption lines of air. The three samples together cover the spectral range of 880 nm, from 3950 nm to 4830 nm. From these results, it is obvious that with increasing Mn concentration the wavelength emission is shifted further to mid-infrared. For concentration x = 0, x = 0.05, and x = 0.2 the wavelength tuning range of the 4.0 – 4.22 μm, 3.95 – 4.5 μm, and 4.36 – 4.83 μm were obtained, respectively. Presumably, with rising Mn concentration the tuning curve could be shifted further to mid-infrared, however the laser threshold will be higher and fluorescence decay time shorter.

IV. Conclusion

The Fe:ZnMnSe ($Fe:Zn_{1-x}Mn_xSe$, x = 0, 0.05, 0.2) laser active media were tested and in this work, the laser tuning curves together with laser output characteristics are presented. The compact Er:YAG pumped compact Fe:ZnMnSe laser system with low output energy that emits laser radiation in mid-infrared spectral range can be used in molecule spectroscopy or in gas composition measurement.

Acknowledgment

This research has been supported by the Czech Science Foundation project, No. 18-11954S.

References

[1] M.E. Doroshenko, H. Jelínková, V.V. Osiko, M. Jelínek, D. Vyhlídal, J. Šulc, M. Němec, N.O. Kovalenko, A.S. Gerasimenko, Fe:ZnMnSe laser active material at 78–300K: Spectroscopic properties and laser generation at 4.2–5.0μm, Journal of Luminescence, Volume 192, 2017, Pages 1300-1307, ISSN 0022-2313, doi: 10.1016/j.jlumin.2017.09.014.

[2] V. V. Fedorov et al., "3.77-5.05-μm tunable solid-state lasers based on Fe^{2+}-doped ZnSe crystals operating at low and room temperatures," in IEEE Journal of Quantum Electronics, vol. 42, no. 9, pp. 907-917, Sept. 2006, doi: 10.1109/JQE.2006.880119.

[3] R. Paschotta, Encyclopedia of Laser Physics and Technology (Wiley-VCH, 2008).

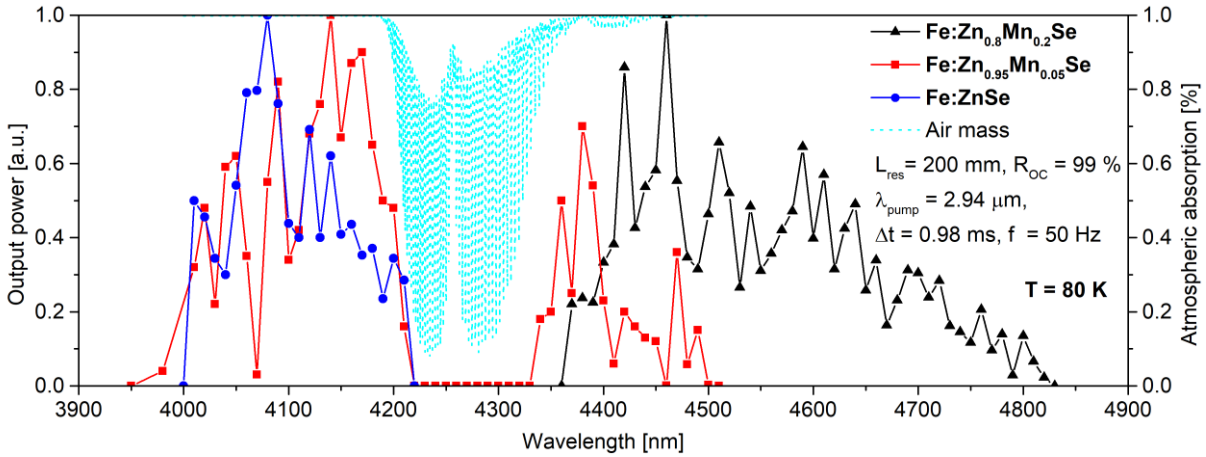

Figure 3 Tuning curves of Fe:ZnSe and Fe:ZnMnSe lasers for maximal output power

IOP Publishing | Astro Ltd
Laser Physics Letters
Laser Phys. Lett. **17** (2020) 035801 (6pp)
https://doi.org/10.1088/1612-202X/ab6d61

Letter

Diode-pumped laser and spectroscopic properties of Yb,Ho:GGAG at 2 μm and 3 μm

Richard Švejkar[1], Jan Šulc[1], Michal Němec[1], Pavel Boháček[2], Helena Jelínková[1], Bohumil Trunda[2], Lubomír Havlák[2], Martin Nikl[3] and Karel Jurek[3]

[1] Faculty of Nuclear Sciences and Physical Engineering Břehová 7, Czech Technical University in Prague, 115 19 Prague, Czech Republic
[2] Institute of Physics of the Czech Academy of Sciences, Division of Condensed Matter Physics, Prague, Czech Republic
[3] Institute of Physics of the Czech Academy of Sciences, Division of Solid State Physics, Prague, Czech Republic

E-mail: richard.svejkar@fjfi.cvut.cz

Received 22 October 2019
Accepted for publication 9 January 2020
Published 12 February 2020

Abstract

In this paper, spectroscopy and laser results obtained with new active medium Yb,Ho:GGAG (gadolinium–gallium–aluminum–garnet) emitting laser radiation at 2.09 μm and 2.94 μm are shown. The absorption, emission cross-section, and radiative decay time for several energy levels Yb^{3+} ($^2F_{5/2}$), Ho^{3+} ($^5I_6$ and $^5I_7$) are presented. Using longitudinal diode pumping the laser action at 2 μm and 3 μm together with the wavelength tunability at several spectral bands 2063–2113 nm, 2860 nm, and 2912–2942 nm were reached.

Keywords: infrared lasers, lasers, solid-state, holmium, ytterbium, diode-pumped

(Some figures may appear in colour only in the online journal)

1. Introduction

Nowadays, lasers able to emit radiation in a spectral range near 3 μm are demanded since they have utilization in various applications. At 3 μm a strong absorption peak of water is located, thus these lasers can be used in medicine (e.g. stomatology, dermatology, urology, and surgery [1]) for tissue ablation. The ~3 μm lasers can also be used as a pumping source for Fe^{2+}-doped ZnSe or ZnS which possess a strong absorption cross-section near 3 μm [2, 3]. Using direct diode pumping of the upper laser level $^4I_{11/2}$ in erbium-doped materials (YAG, YSGG, YLF, GGAG, etc) it is possible to obtain lasing between the $^4I_{11/2} \rightarrow {}^4I_{13/2}$ energy levels, which corresponds with laser radiation from 2.7 μm to 2.94 μm [4]. Aside from erbium ions, only dysprosium (Dy^{3+}, $^6H_{11/2} \rightarrow {}^6H_{15/2}$) and holmium ($Ho^{3+}$, $^5I_6 \rightarrow {}^5I_7$) allow the generation of laser radiation close to 3 μm [5, 6] if diode pumping is used. Unlike Er^{3+}-doped media, pure Ho^{3+}-doped materials cannot be directly pumped by a commercial high-power laser diode to obtain laser action in the 3 μm region. This problem can be solved by co-doping this material with Yb^{3+} [6–8]; the first proposal and lasing with Yb,Ho-doped YSGG crystal were achieved in 1993 [9]. If Yb^{3+} together with Ho^{3+} are doped into a matrix it is possible to use a laser diode emitting near 970 nm as a pumping source. The upper laser level ($^5I_6$) of holmium is pumped via ytterbium ($^2F_{7/2} \rightarrow {}^2F_{5/2}$) as a consequence of the energy transfer between ytterbium and holmium ions [6]. The difference between the $^2F_{5/2}$ (Yb^{3+}) and $^5I_6$ (Ho^{3+}) energy levels is ~1500 cm^{-1}, which can be easily crossed over by phonon energy [7]. For illustration, in figure 1 the simplified energy levels of Yb,Ho-doped active media are presented. Similarly to erbium, the Ho-doped active media suffer from the self-termination (bottleneck) effect since the fluorescence decay time at the upper laser level $^5I_6$ is shorter

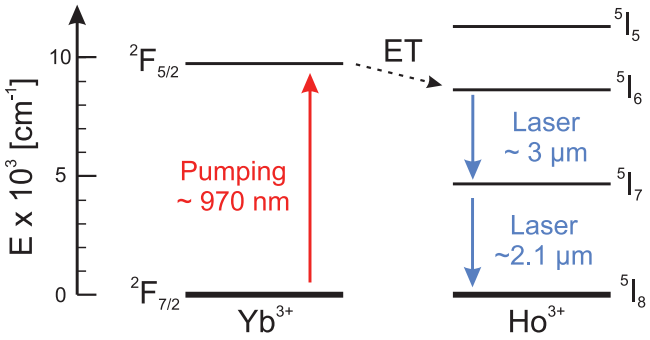

Figure 1. Simplified energy levels of Yb,Ho-doped active medium, ET—energy transfer [6].

in comparison with the lower laser level $^5I_7$ [4]. Even though there is a self-termination effect at ~3 μm the lasing from diode-pumped Yb,Ho-doped bulk crystal (YSGG) was successfully presented in [6]. The laser wavelength was 2844 nm with maximal output energy 10.5 mJ and slope efficiency 3.9% [6]. In [7], Yb,Ho:GGG crystal was proposed for a 2.84 μm laser; however, lasing was not achieved, and also it was shown that the emission cross-section is higher in comparison with pure Ho:GGG crystal [7]. The well-known YAG crystal doped by Yb and Ho was also tested; however, only 2.1 μm laser emission was presented [8]. As shown in [4] we believe the main benefit of GGAG crystal is the relatively broad tuning range and shifting the emission wavelength closer to 3 μm, which can be advantageous for potential applications.

In this work, to our best knowledge, we present the first laser results with Ho-doped and Yb-co-doped GGAG (gadolinium–gallium–aluminium–garnet) active medium which emits laser radiation at 2091 nm and 2942 nm. Also, the continuous tunability from 2063 nm to 2113 nm and the line tunability in the spectral range 2860–2942 nm were successfully tested and the results are presented below.

2. Materials and methods

The Yb,Ho:GGAG crystal was grown by the Czochralski method in a slightly oxidative atmosphere using an iridium crucible. From the x-ray measurements it follows that the GGAG crystal has a cubic structure (lattice constant $a = 12.231$ Å) with space group O_h^{10} (Ia3d), which is the same as YAG, GGG, and YSGG [10, 11]. From the ion radius and oxidation states of the Yb^{3+} and Ho^{3+} one could predict that both ions were substitutes of Gd^{3+} in the GGAG crystal lattice. Because of the partial substitution of Ga^{3+} by Al^{3+} ions the crystal field is distorted and the spectral line width becomes larger due to the inhomogeneous broadening [12].

The tested crystal Yb,Ho:GGAG was grown from the melt of starting composition $Gd_{2.775}Yb_{0.195}Ho_{0.03}Ga_{2.7}Al_{2.3}O_{12}$. In the melt, 6.5% of Gd^{3+} was substituted by Yb^{3+} and 1% by Ho^{3+}. In the measured sample these concentrations increased to 7.41% in the case of Yb^{3+} and to 1.14% for Ho^{3+}. The measured sample (figure 2) was cut from the grown crystal perpendicularly to the growth direction (*c*-axis). It had the form of a cylinder (3.2 mm in length, 14 mm in diameter), with

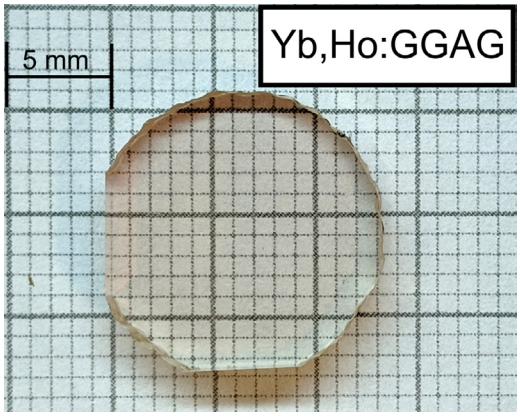

Figure 2. Photograph of tested Yb,Ho:GGAG sample.

plan-parallel polished faces without anti-reflection coatings. During laser and fluorescence measurements the investigated Yb,Ho:GGAG was attached to a copper holder with active water cooling (18 °C).

The transmission spectrum of Yb,Ho:GGAG was measured using a Shimadzu spectrophotometer type UV-3600 with spectral resolution ±0.2 nm in the visible and ultraviolet spectral range, and ±0.8 nm in the mid-infrared spectral range. The fluorescence decay times at $^2F_{5/2}$, $^5I_6$, and $^5I_7$ were measured using a confocal method (for details see [13]) with HP 4220 (Si, PIN photodiode), Thorlabs FGA10 (InGaAs, 800–1800 nm μm), and IBSG PD36-05 (InAsSbP/InAs, 1.5–3.8 nm) photodiodes, respectively, all connected to Tektronix oscilloscope TDS3052B (5 GS s^{-1}, 500 MHz). The fluorescence spectrum was measured using ARCoptix Fourier-transform spectrometer Arcspectro FT-MIR Rocket (2–6 μm, resolution 3 nm). The StellarNet RedWave spectrometer (1.5–2.2 μm, resolution 2.8 nm) was used to measure the emission laser line and tunability in the ~2 μm wavelength region. The Oriel monochromator 77 250 (grating 77 300) with Thorlabs photodiode PDA20H-EC (PbSe, 1.5–4.8 μm) connected to the Tektronix oscilloscope was utilized to evaluate the emitted laser wavelength and during tunability measurements in the ~3 μm wavelength region. The setup with the monochromator was chosen because the measurement was carried out at a low repetition rate of the laser. The output power of the Yb,Ho:GGAG laser was measured by Thorlabs power probe S401C (0.19–10.6 μm) connected to a Thorlabs power meter (PM100A).

A fiber-coupled (core diameter 100 μm, $NA = 0.22$) laser diode (LIMO35-F100-DL970-EX2082, LIMO) was used for longitudinal pumping of the crystal sample. The laser diode operated in the pulsed regime with frequency 10 Hz or 25 Hz and pulse duration 5 ms or 2 ms for pumping the $^5I_7$ and $^5I_6$ energy level, respectively. Using temperature tuning, the emission wavelength of the laser diode was set at 971 nm (linewidth 0.3 nm at full width at half maximum (FWHM)). The Yb,Ho:GGAG was placed inside the 149 mm long hemispherical resonator formed by a flat pumping mirror (PM) and spherical output coupler (OC, radius of curvature 150 mm). The PM was highly transparent (T > 94%) in the pumping range 960–980 nm and at the same time highly reflective (R > 99%) within the spectral range 2.0–2.2 μm or

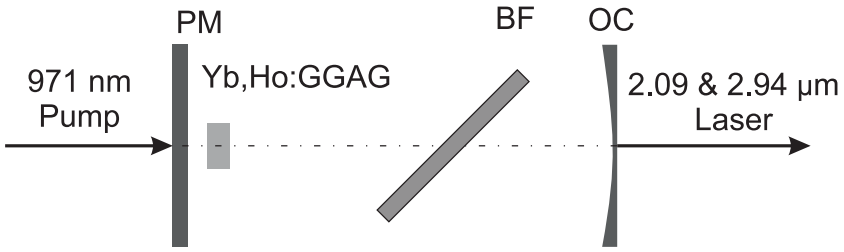

Figure 3. Diode-pumped Yb,Ho:GGAG laser; pumping mirror (PM)—HT @ 971 nm, HR @ 2.0–2.2 μm or 2.65–2.95 μm, output coupler (OC)—$R = 97\%$ @ 2.0–2.2 μm or $R = 99\%$ @ 2.65–2.95 μm both with $r_{OC} = 150$ mm, BF—birefringent MgF_2 plate 2 mm thick.

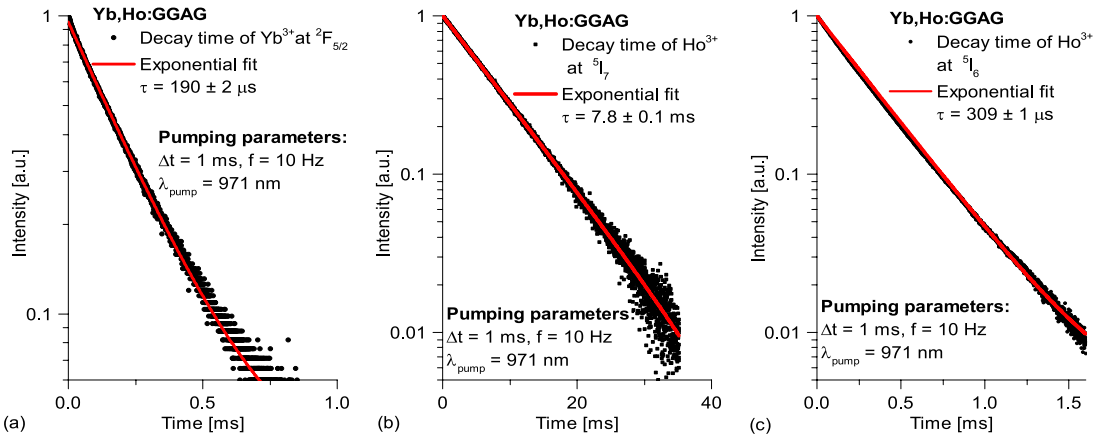

Figure 4. Lifetimes of Yb^{3+} at $^2F_{5/2}$ (a) and Ho^{3+} at $^5I_7$ laser level (b) and $^5I_6$ laser level (c), τ—decay time, Δt—pumping pulse width, f—frequency, λ_{pump}—pumping wavelength.

Table 1. Fluorescence decay times for Yb,Ho:GGAG in comparison with other Yb,Ho-doped garnet-based active media.

	Yb^{3+} ($^2F_{5/2}$)	Ho^{3+} ($^5I_7$)	Ho^{3+} ($^5I_6$)	Ref.
	τ_{fl} (μs)	τ_{fl} (ms)	τ_{fl} (μs)	
Yb(7.41%),Ho(1.14%):GGAG	190	7.8	309	[a]
	τ_{rad} (μs)	τ_{rad} (ms)	τ_{rad} (μs)	
Yb(10%),Ho(1%):YSGG	150	10.4	643	[6]
Yb(15%),Ho(2%):GGG	55	10.5	390	[7]

[a] This work.

2.65–2.95 μm. Two different OCs were used for lasing; one with R = 97% @ 2.0–2.2 μm and a second with R = 99% @ 2.65–2.95 μm were used for ~2 μm and ~3 μm lasing, respectively. The pumping radiation was focused into the tested crystal by two achromatic doublet lenses with a focal length of $f_1 = 75$ mm and $f_2 = 150$ mm, thus the pumping beam diameter was ~200 μm. The wavelength tuning of the laser radiation was obtained using a birefringent filter (single MgF_2 plate 2 mm thick) placed at the Brewster angle inside the optical resonator between the OC and laser active medium. The laser layout is shown in figure 3.

3. Results and discussion

Using a 971 nm excitation wavelength and 1 ms pulse duration the decay time at $^2F_{5/2}$ (upper energy level of Yb^{3+}), $^5I_6$ (upper laser level of ~3 μm transition), and $^5I_7$ (lower ~3 μm and upper ~2 μm laser level transition) were measured; see figure 4. Since the laser diode has a much shorter fall time in comparison with the measured fluorescence decay time and the measurements were carried out after the excitation pulse falling edge, the pulse duration should not affect the measured fluorescence decay time. Moreover, the direct influence of the excitation pulse duration on the decay time was not observed. Using a single exponential fit, the fluorescence decay time was evaluated and the results are summarized in table 1. Because of the high variation of lifetime in Ho^{3+} energy levels two different pump pulse durations of 5 ms ($^5I_7$) and 2 ms ($^5I_6$) were used during laser experiments. It has to be noted that because of the ratio between the fluorescence decay times at the upper $^5I_6$ (309 μs) and lower $^5I_7$ (7.8 ms) energy levels, the Yb,Ho:GGAG can suffer from a self-termination (bottleneck) effect at the ~3 μm transition, similarly to erbium-doped active media [4, 11]. It is also interesting to compare the measured decay time of Yb^{3+} ($^2F_{5/2}$ level) in the GGAG crystal with (190 μs) and without Ho^{3+} (917 μs) co-doping [14], which proves the efficiency of the $Yb^{3+} \rightarrow Ho^{3+}$ energy transfer.

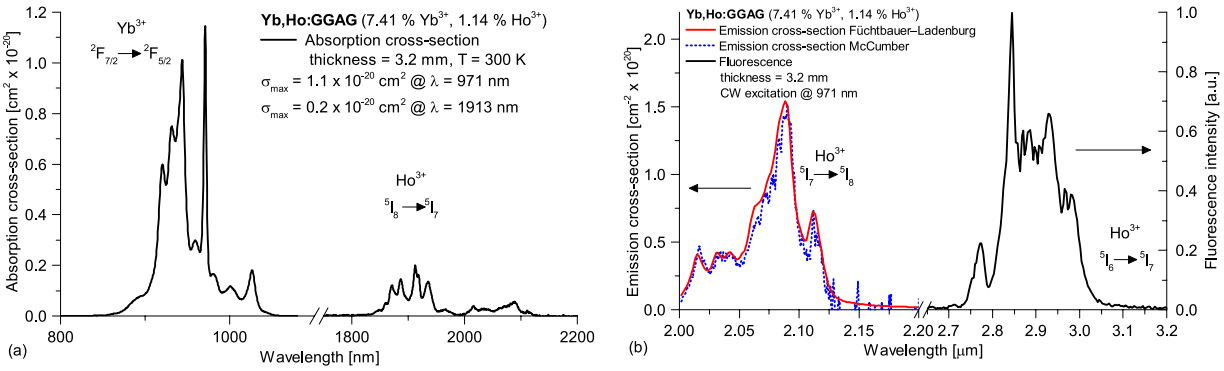

Figure 5. Absorption and emission cross-section spectra of Yb,Ho:GGAG, σ_{max}—maximal absorption cross-section.

From the measured transmission spectrum the absorption cross-section of Yb,Ho:GGAG was calculated. This spectrum is presented in figure 5(a) and shows that Yb,Ho:GGAG possesses broad absorption lines from 900 nm to 1030 nm. One can see a strong and narrow (4 nm at FWHM) absorption peak (zero-phonon line of Yb^{3+}) located at 971 nm (maximum absorption cross-section $1.1 \cdot 10^{-20}$ cm^2) which is a result of co-doping by ytterbium. This absorption peak is advantageous for laser diode pumping, because of the good overlapping of the laser diode spectral line and absorption line of the crystal. So, for ideal absorption of pumping radiation the excitation wavelength of 971 nm was chosen. Also, several weaker absorption peaks can be seen around 1913 nm ($0.2 \cdot 10^{-20}$ cm^2) which correspond to a $^5I_8 \rightarrow {}^5I_7$ transition in holmium. From figures 1 and 5 it is obvious that the lasing in the 2.1 μm region can be obtained if the active medium is pumped at 1.9 μm, which is typical for pure Ho-doped active media [15]. To obtain the emission cross-section spectra we use the reciprocity method (McCumber relation) [6]

$$\sigma_{em}^{MC}(\lambda) = \sigma_{abs}(\lambda) \cdot \exp\left[\frac{hc}{k_B \cdot T} \cdot \left(\frac{1}{\lambda_0} - \frac{1}{\lambda}\right)\right] \quad (1)$$

and Füchtbauer–Ladenburg (F–L) equation [6, 7]

$$\sigma_{em}^{F-L}(\lambda) = \frac{\beta\lambda^5 \cdot I_\lambda(\lambda)}{8\pi n^2 c \tau_{rad} \int I_\lambda(\lambda) \cdot \lambda d\lambda} \quad (2)$$

where λ_0 is a particular Ho^{3+} zero-phonon line (1945 nm), λ is the wavelength, T is the temperature, c is the speed of light, n is the refractive index, β is the branching ratio, τ_{rad} corresponds to the radiative lifetime from table 1, and k_B and h are the Boltzmann and Planck constants, respectively. Since we believe that using the confocal method should eliminate the effect of re-absorption on the fluorescence decay time [13], the value of 7.8 ms was used to evaluate the emission cross-section in the spectral range 2.0–2.2 μm. The branching ratio $\beta = 0.95$ was used for the $^5I_7 \rightarrow {}^5I_8$ transition since this value of beta should be close to one [6]. Both methods (reciprocity and F–L) were used to calculate the emission cross-section and one can see from figure 5(b) that these results are in good agreement. The emission cross-section in the spectral range around 3 μm was not calculated because the values of branching ratio and radiative lifetime for this laser transition in Yb,Ho:GGAG are not known. Moreover, at 3 μm the results from the F–L method cannot be confirmed by the McCumber relation so accurate values of β and τ_{rad} are necessary for correct evaluation of the emission cross-section. For these reasons, only the measured emission spectra intensity is presented in figure 5(b) for the $^5I_6 \rightarrow {}^5I_7$ transition. In future work we would like to focus on spectroscopy and Judd–Ofelt analysis of Yb,Ho:GGAG to obtain detailed spectroscopy information about this material.

As stated above, the Yb,Ho:GGAG active media possesses broadband spectral lines in the ranges 2.0–2.15 μm and 2.8–3.05 μm, which can be seen from the spectra presented in figure 5(b). Due to the broad emission spectrum, the Yb,Ho:GGAG crystal is potentially interesting for generating short pulses in the mode-locking regime. Also, the broadband emission spectrum allows laser wavelength tuning in a wide spectral range [16], which was obtained in laser experiments.

First, the Yb,Ho:GGAG laser system was tested without a birefringent plate. The results for ~2 μm and ~3 μm lasers are presented in figure 6. In both cases, a hemispherical laser resonator (length 149 mm) was used since during tunability measurement the birefringent plate had to fit into the resonator between the crystal and OC. For ~2 μm ($^5I_7 \rightarrow {}^5I_8$) lasing the output coupler $R_{OC} = 97\%$ was used and the maximal output energy 1 mJ, slope efficiency 2%, and laser threshold 34 mJ with respect to the absorbed energy were reached for the pulsed Yb,Ho:GGAG laser. The emitted laser wavelength was 2091 nm with linewidth 10 nm at FWHM. On the other hand, to obtain lasing near ~3 μm ($^5I_6 \rightarrow {}^5I_7$) the OC with $R_{OC} = 99\%$ has to be used. In this configuration, the laser emitted radiation at 2942 nm (linewidth 2 nm at FWHM) with maximal output energy 45 μJ and slope efficiency 0.4%. Since the laser beam profile was close to the fundamental TEM_{00} mode, from the ratio of the measured and calculated laser beam divergence the M^2 of the laser beam for both the x- and the y-axis was estimated. For ~2 μm and ~3 μm lasers $M^2_{x,y} = 1.9$ and $M^2_{x,y} = 1.4$ were obtained, respectively. The beam profiles were measured for maximal output energy and the results are presented in figure 6.

After placing the MgF_2 birefringent plate into the laser resonator between the OC and Yb,Ho:GGAG crystal the tunability of the laser wavelength was tested. By rotating the birefringent plate along the horizontal axis, the conditions in the laser resonator were changed and the emitted laser wavelength

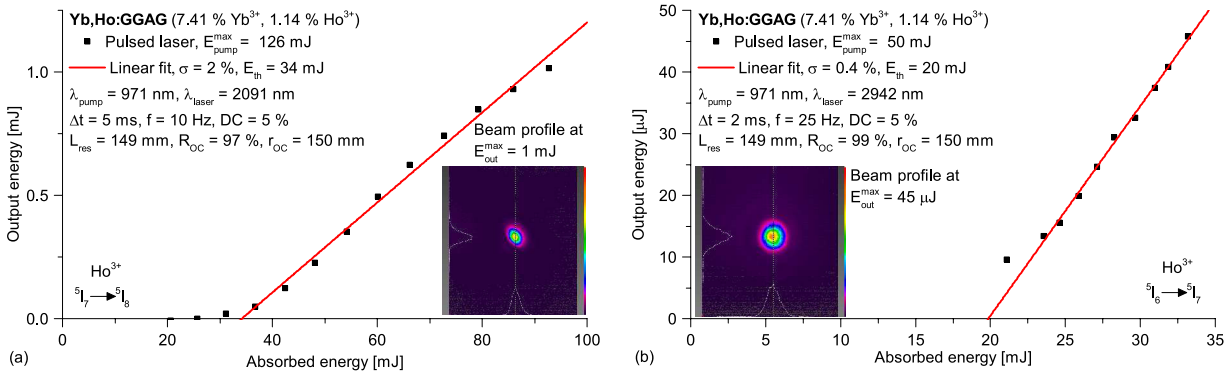

Figure 6. Laser output characteristics of Yb,Ho:GGAG at 2 μm and 3 μm; σ—slope efficiency, E_{th}—laser threshold, λ_{pump}—pumping wavelength, λ_{laser}—laser wavelength, Δt—pumping pulse width, f—frequency, DC—duty cycle, E_{pump}^{max}—maximal pumping energy, L_{res}—resonator length, R_{OC} and r_{OC}—output coupler reflectivity and radius, E_{out}^{max}—maximal output energy.

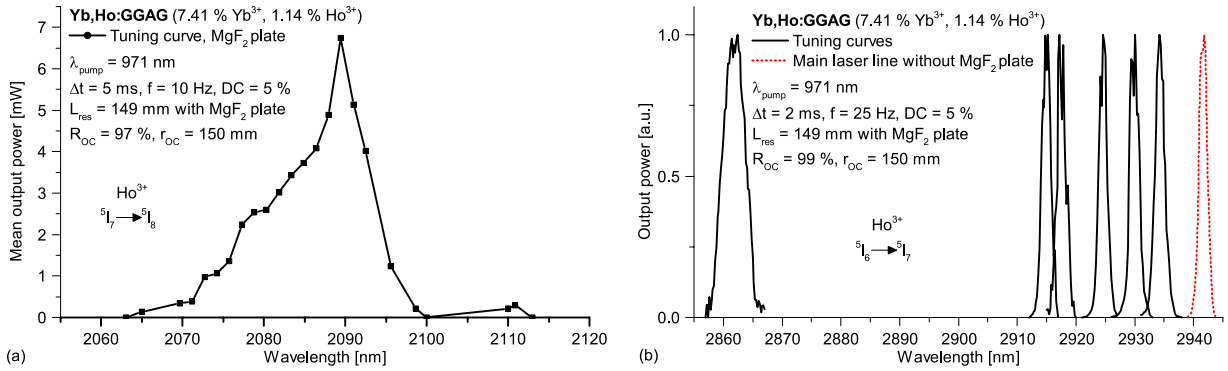

Figure 7. Tuning curves of Yb,Ho:GGAG measured for maximal pumping; λ_{pump}—pumping wavelength, Δt—pumping pulse width, f—frequency, L_{res}—resonator length, R_{OC} and r_{OC}—output coupler reflectivity and radius.

was shifted. In figure 7 the results for the laser wavelength tuning are presented. One can see that from 2063 nm to 2113 nm (measured at zero of the output power) the laser can be continuously tuned within a spectral range of 50 nm. Also, several laser lines were obtained in the spectral range from 2860 nm to 2942 nm which is presented in figure 7. In comparison with Er:GGAG [4], Yb,Ho:GGAG covers a wider spectral range from 2912 nm to 2942 nm, which is probably given by broader fluorescence spectrum.

4. Conclusion

From the results presented above it can be seen that the diode-pumped Yb,Ho:GGAG active medium is able to lase at 2091 nm ($^5I_7 \rightarrow {}^5I_8$) and 2942 nm ($^5I_6 \rightarrow {}^5I_7$). Moreover, at both wavelengths it is possible to tune the emitted laser wavelength in a wide spectral range. The main advantage of this Yb,Ho-doped crystal is the possibility to generate both 2.1 μm and 2.94 μm laser wavelength under diode pumping ($\sim$970 nm) at the same time. The low slope efficiency and output energies are mainly given by the crystal quality and by non-optimized Yb/Ho doping ratio. In our future work we will optimize both the crystal quality and dopant concentrations to improve the mentioned characteristics further. Also, the CW laser regime should be reachable if smaller samples are used to ensure better cooling. The CW regime was not tested to prevent the destruction of the crystal. Moreover, similarly to erbium [4], if cascade lasing is used the lower laser level ($^5I_7$) of $\sim$3 μm transition can be bleached, which rapidly changes the ratio between the population inversion of the upper $^5I_6$ and lower $^5I_7$ laser level. This effect can also help to improve lasing in the mid-infrared spectral region.

In conclusion, we presented the spectroscopic and laser properties of Yb,Ho:GGAG as a new laser active medium. In the pulse regime the Yb,Ho:GGAG laser emitted laser radiation at 2091 nm or at 2942 nm with maximal output energy 1 mJ or 45 μJ with slope efficiency 2% or 0.4%, respectively. From the wavelength tunability measurements, it follows that the Yb,Ho:GGAG laser was continuously tunable from 2063 nm to 2113 nm and line-tunable from 2860 nm to 2942 nm. The obtained results show that laser matrices based on multicomponent garnets such as GGAG, with broadband absorption and emission spectral lines, are a prospective option to achieve broadly tunable lasers and generate short pulses at 3 μm.

Acknowledgments

This research was supported by the Czech Science Foundation, *Optimization of the solid-state laser active materials for spectral range from near-up to mid-infrared*, project no. 18-11954S. The work was partially supported by the Operational Programme Research, Development and Education financed by European Structural and Investment

Funds and the Czech Ministry of Education, Youth and Sports (project no. SOLID21 CZ.02.1.01/0.0/0.0/16_019/0000760).

References

[1] Jelínková H (ed) 2013 *Lasers for Medical Applications Diagnostics, Therapy and Surgery* 1st edn (Philadelphia, PA: Woodhead)
[2] Fedorov V V *et al* 2006 *IEEE J. Quantum Electron.* **42** 907–17
[3] Mirov S B, Fedorov V V, Martyshkin D, Moskalev I S, Mirov M and Vasilyev S 2015 *IEEE J. Sel. Top. Quantum Electron.* **21** 292–310
[4] Švejkar R, Šulc J, Němec M, Boháček P, Jelínková H, Trunda B, Havlák L, Nikl M and Jurek K 2018 *Opt. Lett.* **43** 3309–12
[5] Weber M J (ed) 1996 *Handbook of Laser Wavelength* (Boca Raton, FL: CRC Press)
[6] Diening A and Kück S 2000 *J. Appl. Phys.* **87** 4063–8
[7] Wang Y, Li J, Zhu Z, You Z, Xu J and Tu C 2013 *Opt. Lett.* **38** 3988–90
[8] Rothacher T, Lthy T and Weber H 1998 *Opt. Commun.* **155** 68–72
[9] Zavartsev Y D, Osiko V V, Semenkov S G, Studenikin P A and Umyskov A F 1993 *Quantum Electron.* **23** 312–6
[10] Weber M J (ed) 2003 *Handbook of Optical Materials* (Boca Raton, FL: CRC Press)
[11] You Z, Wang Y, Xu J, Zhu Z, Li J and Tu C 2014 *IEEE Photon. Technol. Lett.* **26** 667–70
[12] Henderson B and Bartram R H 2000 *Crystal-Field Engineering of Solid-State Laser Materials* (*Cambridge Studies in Modern Optics*) (Cambridge: Cambridge University Press)
[13] Nejezchleb K, Kubát J, Šulc J and Jelínková H 2017 Yb:YAG disc for high energy laser systems *Proc. SPIE Solid State Lasers XXVI: Technology and Devices* **10082** 100820H
[14] Stehlík M, Šulc J, Boháček P, Jelínková H, Nejezchleb K, Trunda B, Havlák L, Nikl M and Jurek K 2018 *Laser Phys.* **28** 105802
[15] Jelínek M, Kubeček V, Ma W, Zhao B, Jiang D and Su L 2016 *Laser Phys. Lett.* **13** 065004
[16] Moulton P F 1992 Tunable solid-state lasers *Proc. IEEE* **80** 348–64